



The
University
Of
Sheffield.

Hydrogen Bonding Effects on Reactivity

The University of Sheffield

Department of Chemistry

Fatma Ahmed Aburass

October 2019

Supervisor: Prof. Nicholas H. Williams

Submitted to The University of Sheffield in part- fulfilment of the requirements for the degree of Doctor of Philosophy.

Declaration

The work described herein was undertaken at the Chemistry Department, University of Sheffield between October 2015 and October 2019 under the supervision of Professor N. H. Williams. This thesis and the data presented within it was completed solely by the author and has not previously been submitted for any degree at this or any other institution.

Fatma Ahmed Aburass

October 2019

Acknowledgements

First and foremost, I would like to thank God Almighty for giving me the opportunity to study in the pioneer research institution (Sheffield university) and giving me the power ability to undertake this research and do not stop working until complete it.

During the four years of my PhD, I have found many people around me, who I cannot forget their help and support, and without them this thesis did not complete.

First of all, I would like to thank my supervisor, Prof. Nicholas H. Williams, who provided me support like I can never imagine. I cannot forget his patient guidance, encouragement and advice, and also his care about my work. I consider myself lucky to have him as a supervisor. I would also like to thank all my colleagues of Prof. Nick Williams's group for exchanges of knowledge, skills, helps and advice, which helped me in the lab and writing this thesis. I would also thank them for sharing the snacks and chocolate. I will always remember these days. I would also like to thank all the members of staff at Sheffield University who helped me in my study, directly and indirectly.

Thanks to my beloved family, my dad, my mum, my sister and my brothers, who were the source of my strength. I would express my gratitude to my husband, Husni, for his endless love, kindness, continued support, encouragement and help he has shown during the past four years. Deep thanks to my happiness source and light of my life, my son Ramadan and my daughter Ragad. Without their patience and love, this work would not have been possible. I cannot forget to thank my friends, who always support me in the difficult times.

This thesis dedicated to my family who would be very proud of this achievement.

Abstract

Hydrogen bonds play a crucial role in the catalytic activity of biological systems. In this thesis, the effect of hydrogen bonds on the reactivity of phosphate triesters is studied, particularly towards hydrolysis and the attack of hydroxylamine.

The synthesis of methyl 8-hydroxy-1, 9-anthryl cyclic phosphate 46 and its reaction with water and nucleophiles are investigated. These reactions are accelerated by the presence of the hydroxyl group through hydrogen bonding, with a rate acceleration of about 30 and 173 fold (~ 9 and 13 kJ mol^{-1} , respectively) in comparison to the hydrolysis of methyl 1,9-anthryl cyclic phosphate and methyl 1,8-naphthyl cyclic phosphate. It is concluded that the presence of hydroxyl group plays a significant catalytic role in increasing the rate of P-O cleavage through hydrogen bond catalysis in a system where both the hydrogen bond donor and reacting group are held in a fixed relationship.

The catalytic role of hydrogen bond are also evaluated on the reaction of acyclic phosphate triesters with hydroxylamine. The hydrolysis of diethyl 8-hydroxy-1-naphthyl phosphate was studied. The rate of hydrolysis was enhanced almost 500 fold compared with diethyl 1-naphthyl phosphate and diethyl 2'-hydroxy-2-biphenyl phosphate. The rotational freedom of biphenyl rings leads to less effective hydrogen bond interaction between the hydroxyl group and leaving group oxygen.

An attempt was made to study the effect of multiple hydrogen bonds on phenyl triesters. Diethyl 1,2- and 1,3-dihydroxy phenyl phosphate were synthesised and their hydrolysis studied in the presence of hydroxylamine. The rate of the reaction was a similar to that of diethyl 1-hydroxy phenyl phosphate. The reaction of these triesters is catalysed by the ionised hydroxyl group with a mechanism involving intramolecular nucleophilic catalysis instead of hydrogen bond enhanced departure of the aryloxy group. The reaction is stereospecific for displacement of alkoxide anion. It is concluded that the hydroxyl group in these structures is more effective

as a nucleophile than hydrogen bond donor when an *exo*-alkyl group is present. The rate of reaction of diethyl phenyl phosphate was too slow to measure accurately under these conditions, and so any hydrogen bond enhanced cleavage may be too inefficient to be observed in the presence of the cyclisation pathway. Attempts to create models with multiple hydrogen bond donors acting on the leaving group using an anthracene scaffold are carried out, but were not successful in creating the desired targets.

Abbreviations

Nu:	Nucleophile	kJ mol^{-1}	Kilojoule per mole
<i>I</i>	Ionic strength	NMR	Nuclear magnetic resonance
R	Correlation coefficient	MS	Mass spectrometry
EPPS	4-(2-Hydroxyethyl)piperazine-1-propanesulfonic acid	mM	Milimolar
Abs	Absorbance	DMSO	Dimethyl sulfoxide
pTsOH	Para toluenesulfonic acid	MES	4-Morpholineethanesulfonic acid
NH ₂ OH	Hydroxylamine	MOPS	4-Morpholinepropanesulfonic acid
TFA	Trifluoroacetic acid	HEPES	4-(2-Hydroxyethyl)piperazine-1-ethanesulfonic acid
HPLC	High performance liquid chromatography	CHES	2-(Cyclohexylamino)ethanesulfonic acid
THF	Tetrahydrofuran	CAPS	3-(Cyclohexylamino)-1-propanesulfonic acid
TEA	Triethylamine	NaCl	Sodium chloride
SnCl ₂	Tin chloride	PhLi	phenyllithium
EtOAc	Ethyl acetate	iPrOH	Isopropanol
TLC	Thin layer chromatography	PivCl	Pivaloyl chloride 2,2-Dimethylpropanoyl chloride
R.t.	Retention time	(MeO) ₂ PCl	Methyl dichloro phosphate
AcCl	Acetylchloride	TMSCl	Trimethylsilyl chloride
AcOH	Acetic acid	k_{obs}	The observed rate constant
PhCH ₂ Cl	Benzyl chloride	k_2	The second-order rate constant

Contents

Declaration	i
Acknowledgements.....	ii
Abstract	iv
Abbreviations	vi
Contents	vii
List of Figures.....	x
List of Schemes	xiv
Chapter one: Introduction.....	1
1.1. General introduction	2
1.1.1. Hydrogen bonds	3
1.1.2. Enzyme Catalysis by hydrogen bonding	4
1.1.3. Low-barrier hydrogen bond (LBHB)	5
1.1.4. Hydrogen bond network	6
1.2. Previous work.....	7
1.2.1. The effect of hydrogen bond network on acidity	7
1.2.2. The effect of hydrogen bond network on binding.....	12
1.2.3. The effect of intramolecular hydrogen bonds on reactivity.....	13
1.3. The reaction of hydroxylamine with phosphate esters	25
1.4. Phosphate ester hydrolysis as a model reaction	28
1.5. The aim of the project	31
Chapter Two: Cyclic Aryl Phosphate Triesters	33
2.1 Introduction	34
2.2 Aim	35
2.3 Result and discussion.....	37
2.3.1 Synthesis of Methyl 8-hydroxy-1, 9-anthryl cyclic phosphate 46.....	37
2.3.2 Synthesis of Methyl 1, 9-anthryl cyclic phosphate 47	37
2.3.3 Synthesis of cyclic phosphate triester 48	38
2.3.4 Synthesis of cyclic phosphate triester 49	39
2.3.5 Kinetic study.....	39
2.4 Conclusion.....	71
Chapter Three: Acyclic Triester Phosphate with One Hydrogen Bond Donor	73
3.1. Introduction	74
3.2. Result and discussion.....	77
3.2.1. Synthesis of acyclic aryl triesters	77
3.3. Kinetic study.....	81
3.3.1. The reaction of diethyl 8-hydroxy 1-naphthyl phosphate 69 and diethyl 1-naphthyl phosphate 70 with hydroxylamine.....	81
3.3.2. The reaction of diethyl 2-hydroxy biphenyl phosphate 71 and diethyl biphenyl phosphate 72 with hydroxylamine	86
3.3.3. Influence of the hydroxylamine concentration on diethyl 2-hydroxy biphenyl phosphate 71 degradation.....	91
3.4. Conclusion.....	93
Chapter Four: Multiple Hydrogen Bonds Effect (Phenyl System)	95
4.1. Introduction	96
4.2. Results and discussion	98
4.2.1. Synthesis of acyclic phenyl triester 84-86:.....	98
4.2.2. Synthesis of acyclic phenyl triester 82 and 83:.....	98
4.2.3. Attempts to separate the mixture of 82 and 83	101

4.2.4.	Hydroxylamine reaction with triesters 82 and 83	102
4.2.5.	Product analysis of triesters 82 and 83	105
4.2.6.	Hydrolysis of phenyl phosphate triesters 84-86.....	107
4.2.7.	Additional notes on HPLC chromatogram: P-O bond cleavage reaction.....	110
4.2.8.	Possibility of Intramolecular nucleophilic catalytic reaction.....	111
4.3.	Conclusion.....	115
Chapter Five: Multiple Hydrogen Bonds (Anthracene System)	116
6.1.	Introduction	117
6.1.	Result and discussion.....	119
5..1.	Attempts to synthesis of diethyl 1, 8-diamines anthracene-9-phosphate	119
5..2.	Attempt to synthesis diethyl 1-piperidine 9-anthryl phosphate 125	129
5..3.	Synthesis of diethyl 1,8-dihydroxy anthracene-9-phosphate	130
6.1.	Conclusion.....	135
Chapter Six: Future Work	137
6.1.	Suggestions for future work	138
Chapter Seven: Experimental Chapter	141
7.1.	General material and instruments	142
7.2.	Synthesis of 1,8-dihydroxyanthracen-9(10 H)-one 51.....	142
7.3.	Synthesis of 1-hydroxyanthracen-9(10 H)-one 53	143
7.4.	Methyl 8-hydroxy-1,9-anthryl cyclic phosphate 46	143
7.5.	Methyl 1,9-anthryl cyclic phosphate 47.....	144
7.6.	Methyl naphthyl 1,8-cyclic phosphate 48	145
7.7.	Ethyl naphthyl 1,8-cyclic phosphate 49.....	146
7.8.	Synthesis of Ethyl 2,2'-biphenyl cyclic phosphate 80.....	146
7.9.	Synthesis of Diethyl 2- hydroxyl-2'-biphenyl phosphate 71	148
7.10.	Synthesis of Diethyl 1-naphthyl phosphate 70	149
7.11.	Synthesis of Diethyl 1,2-dimethoxy-3-phenyl phosphate 85	150
7.12.	Synthesis of Diethyl phenyl phosphate 86	151
7.13.	Synthesis of diethyl 2-hydroxy-1-phenyl phosphate 84.....	152
7.14.	Synthesis of 2-Methoxybenzo[1,3]dioxol-4-ol 91	152
7.15.	Synthesis of diethyl 2-methoxybenzo[1,3]dioxol-4- phosphate 92	153
7.16.	Synthesis of Diethyl 1, 3-dihydroxy-2-phenyl phosphate and diethyl 1, 2-hydroxy-3-phenyl phosphate 82 and 83.....	154
7.17.	Synthesis of 10-phenyl, 1,8,10-trihydroxy-9- anthrone 134	155
7.18.	Preparation of 1,8-dihydroxy-10-phenyl-9- anthrone 135	156
7.19.	Synthesis of 1,8-dipiperidine anthraquinone 103	156
7.20.	Synthesis of 1-piperidine anthraquinone 109	157
7.21.	Synthesis of 1,8-dipiperidine-10-hydroxy-10-phenyl-9- anthrone 119	158
7.22.	Synthesis of 1, 8-diamino anthraquinone 112	159
7.23.	Synthesis of 1,8-dichloro- -9- anthrone 107.....	160
7.24.	Synthesis of 1,8-dichloro-10-bromo-9- anthrone 122.....	161
7.25.	Synthesis of 1,8-dipivaloyl-10-phenyl-9- anthrone 136	162
7.26.	Synthesis of 1,8-dipivaloyl-9- anthrone 133	163
7.27.	Kinetic experiments	164
7.27.1.	Hydrolysis of phosphate triesters 46, 47 and 48	164
7.27.2.	The reaction of 46, 47 and 48 with hydroxylamine.....	164
7.27.3.	The effect of hydroxylamine concentration on 46, 47 and 48 degradation	165
7.27.4.	The reaction of 46 with nucleophiles.....	165
7.27.5.	Product analysis for the hydrolysis of phosphate triesters 46, 47, 48 and 49 by ³¹ P NMR	165
7.27.6.	The effect of DMSO on the degradation of triesters 46.	165

7.27.7.	Product analysis for the hydrolysis of ethyl biphenyl cyclic phosphate by ^{31}P NMR.....	166
7.27.8.	The reaction of diethyl 8-hydroxy-1-naphthyl phosphate 69 with hydroxylamine	166
7.27.9.	Effect of hydroxylamine concentrations on diethyl 8-hydroxy-1-naphthyl phosphate 69.....	166
7.27.10.	The reaction of hydroxylamine with phosphate triesters 70, 71 and 72 using HPLC.....	167
7.27.10.1.	Hydrolysis of phosphate triesters 70-72.....	167
7.27.10.2.	Hydrolysis of phosphate triesters 82-84.....	169
References	172
A.	Appendix: Chapter Two.....	179
B.	Appendix: Chapter Three.....	186
C.	Appendix: Chapter Four.....	187

List of Figures

Figure (1-1): Diagram of a catalytic reaction showing difference in activation energy in an uncatalysed and catalysed reaction.....	2
Figure (1-2): General aspects of an ordinary hydrogen bond (HB), a low-barrier hydrogen bond (LBHB) and single-well H-B between oxygen heteroatoms.	4
Figure (1-3): Oxyanion hole in active site of a serine protease.....	7
Figure (1-4): Compounds studied by Shokri et al.....	9
Figure (1-5): Adamantane triols and pKas in DMSO.....	11
Figure (1-6): Flexible system studied by Samet et al.....	11
Figure (1-7): Hydrogen-bonding between the complexation of tri-n-butyl phosphine oxide and phenolic system with different number of hydrogen bonds, (Terminal H-bond labelled).	13
Figure (1-8):Structures of carbonate esters studied by Tillett and Wiggins.....	13
Figure (1-9): Two mechanisms suggested for the hydrolysis of carboxylic ester 4	14
Figure (1-10): pH-Rate profile for the alkaline hydrolysis of carbonate esters 14 , 15 and 16 in NaOH at 25 °C, ionic strength at 1.0 (KCl).	15
Figure (1-11): Variation of the first-order rate constant (k_{obs}) for hydrolysis of 1-acetoxy-8-hydroxy naphthalene with hydroxide concentration.	16
Figure (1-12): The structure of model system studied by Hibbert <i>et al</i>	18
Figure (1-13): Compounds studied by Bender and <i>et al</i>	18
Figure (1-14): Compounds studied by Williams <i>et al</i>	19
Figure (1-15): The structure of bis-2-carboxyphenyl phosphate and diphenyl phosphate.....	20
Figure (1-16): Structure of phosphate diesters 29 ⁺ , 27 ⁺ and 28 ⁺	22
Figure (1-17): pH rate profile for hydrolysis of mono- , di- and triester (30 , 31 and 32). The points are derived experimentally and the curves are best fit for the reactions of the different ion forms.	24
Figure (1-18): Compounds have been studied by Williams <i>et al</i>	25
Figure (1-19): Target model compounds (System 1 and 2) proposed for this research.....	32
Figure (2-1): Structures of phosphate triesters studied previously.	35
Figure (2-2): Structures of cyclic triester phosphate in this work.	36

Figure (2-3): compounds formed of pyrogallol oxidation.....	38
Figure (2-4): Time-dependent spectral changes observed upon the hydrolysis of triester 46 at pH 7. Overall time = 1h and 30 min	40
Figure (2-5): Time-dependent spectral changes observed upon the hydrolysis of triester 47 at pH 7. Overall time = 28 h.....	41
Figure (2-6): Time-dependent spectral changes observed upon the hydrolysis of triester 48 at pH 7.3. Overall time = 40 h.....	41
Figure (2-7): Following the hydrolysis of cyclic anthryl phosphate triester 46 using ^{31}P NMR at pH = 6 in DMSO.....	42
Figure (2-8): Following the hydrolysis of cyclic anthryl phosphate triester 47 using ^{31}P NMR at pH = 6 in DMSO.....	44
Figure (2-9): Following the reaction of naphthyl methyl phosphate cyclic triester 48 with 0.5 M hydroxylamine by ^{31}P NMR in DMSO at pH 7 and 25 °C.	46
Figure (2-10): Following the reaction of naphthyl ethyl phosphate cyclic triester 49 with hydroxylamine by ^{31}P NMR in DMSO, at 25 °C and pH 7.....	48
Figure (2-11): Buffer catalysis of 46 ; MES buffer pH = 6 & 7 \pm 0.04; 25 °C, 1 M NaCl. The linear correlation was fitted to equation (2-1).	49
Figure (2-12): Kinetic profile according to pH for the hydrolysis of triester 46 (red), 47 (green) and 48 (blue) at 25°C and ionic strength of 1 M. The curves correspond to the fit given by equation (2-2) for triester 46 and equation (2-3) for triesters 47 and 48	50
Figure (2-13): Structures of cyclic phosphate studied here with relative rate constants of spontaneous hydrolysis.....	51
Figure (2-14): Structures of anthrols with their pK _a s.	53
Figure (2-15): Phenols and aryl anilinium ions with their pK _a s in aqueous solution (pK _a for 9-ammonioanthracene reported from ref 72).	53
Figure (2-16): Naphthalene 54 ion with its pK _a and anthracene 53 ion with expected pK _a	55
Figure (2-17): Structures of phenyl phosphate diester 67 , and naphthyl phosphate diester. 68	57
Figure (2-18): Series of triester phosphate studied previously.....	58
Figure (2-19): Expected free energy profile of the hydrolysis of phosphate triesters 46 , 47 and 48 in water (red), (green) and (blue), respectively.....	58
Figure (2-20): The structure of transition states involved in the spontaneous hydrolysis of phosphate triester 46 , 47 and 48	59
Figure (2-21): ^{31}P NMR analysis data of 46 ; pH = 6 & 9 \pm 0.04 (blue and red line, respectively); 25 °C, ionic strength 1 M NaCl in DMSO.....	60

Figure (2-22): Kinetic profile according to pH for the hydrolysis of triester 46 (red), 47 (green) and 48 (blue) at 25°C and ionic strength of 1 M.	61
Figure (2-23): ¹ H NMR of the complete hydrolysis of cyclic phosphate triester 46 at pH = 6 in DMSO.	62
Figure (2-24): ³¹ P NMR of the hydrolysis of cyclic anthryl phosphate triester 46 after 4 days at pH = 6 in DMSO.	62
Figure (2-25): Kinetic profile according to pH for the reaction of 0.5M hydroxylamine with triester 46 (blue), triester 47 (green) and triester 48 (red) at 25°C and <i>I</i> = 1 M. The curves correspond to the fit by equation (2-4).	64
Figure (2-26): Kinetic profile according to the reaction of phosphate triester 46 with NH ₂ OH at pH 6 & 7, 25°C and ionic strength of 1 M. The curves correspond to the fit given by Equation (2-5).	66
Figure (2-27): Kinetic profile according to the reaction of phosphate triester 47 with NH ₂ OH at pH 7, 25°C and ionic strength of 1 M. The curves correspond to the fit given by Equation (2-5).	67
Figure (2-28): Kinetic profile according to the reaction of phosphate triester 48 with NH ₂ OH at pH 7, 25°C and ionic strength of 1 M. The curves correspond to the fit given by Equation (2-5).	67
Figure (2-29): Kinetic profile according to the reaction of 46 with nucleophiles (and hydroxylamine for comparison), at pH 6, 25°C and ionic strength of 1 M.	70
Figure (2-30): Brønsted plot comparing second-order rate constants for the reactions of 46 with NH ₂ OH, MeONH ₂ , acetate and fluoride.	71
Figure (3-1): Cyclic triesters 46 and 47 with relative rates of their spontaneous hydrolysis reaction with hydroxylamine.	74
Figure (3-2): Structures of acyclic phosphate triesters studied in this chapter.	75
Figure (3-3): The hydrolysis of diethyl 8-hydroxy naphthyl phosphate triester 69 , monitored by ³¹ P NMR, in 0.5 M NH ₂ OH in D ₂ O.	79
Figure (3-4): Plot of <i>k</i> _{obs} as a function of pH for reactions with triester 69 at 60 °C <i>I</i> = 1.0 M (NaCl).	82
Figure (3-5): Plot of <i>k</i> _{obs} as a function of hydroxylamine concentration for reactions with triester 69 at 60.0 °C, pH = 7.3 and <i>I</i> = 1.0 M (NaCl).	83
Figure (3-6): Plot of <i>k</i> _{obs} as a function of hydroxylamine concentration for reactions with triester 70 at 60 °C, pH = 7.3 and <i>I</i> = 1.0 M (NaCl).	83
Figure (3-7): Expected free energy profile of the reactions of phosphate triesters 69 and 70 with hydroxylamine (blue) and (red) respectively.	85
Figure (3-8): Structure of phenyl phosphate diester 67 , and naphthyl phosphate diester 68	86

Figure (3-9): Representative HPLC chromatogram of the hydrolysis of 71 in the presence of hydroxylamine at different times (1=0 h, 2=20 h, 3= 40 h, 4=50 h). (30 % DMSO, pH 7.3 and 60 °C.).....	87
Figure (3-10): The hydrolysis of diethyl 2-hydroxy biphenyl-2`-phosphate triester 71 , monitored by ³¹ P NMR, in 0.5 M NH ₂ OH in D ₂ O at pH 7.3 and 60 °C.....	88
Figure (3-11): Monitoring the hydrolysis of ethyl biphenyl cyclic phosphate triester 80 by ³¹ P NMR, 0.5 M NH ₂ OH in D ₂ O at pH 7.3.	91
Figure (3-12): Plot of <i>k</i> _{obs} as a function of hydroxylamine concentration for reactions with triester 71 at 60.0 °C, pH = 7.3 and <i>I</i> = 1.0 M (NaCl).	92
Figure (4-1): Structures of acyclic triester phosphates with different number of hydroxyl groups.	96
Figure (4-2): The mechanism of hydrogen bond catalysis.	97
Figure (4-3): Transition states for the cleavage of triesters 82 and 83	97
Figure (4-4): General base and intramolecular nucleophilic catalysis mechanisms.....	98
Figure (4-5): A mixture of 82 and 83 representing by ³¹ P NMR (A), ¹ H NMR (B) and HPLC chromatogram (C)..	100
Figure (4-6): Triesters 82 and 83 after separation using HPLC as presented by ³¹ P NMR.	101
Figure (4-7): Triesters 82 and 83 after separation using HPLC as presented by ¹ H NMR.	102
Figure (4-8): Plot of <i>k</i> _{obs} as a function of hydroxylamine concentration for reactions with triester 82 (red) and 83 (blue) at 25.0 °C, pH = 7.3 and <i>I</i> = 1.0 M (NaCl).....	103
Figure (4-9): pH-rate profiles for the reactions of TPP 82 (●) and 83 () with 0.5 M NH ₂ OH, at 25 °C and <i>I</i> = 1.0 (NaCl).	104
Figure (4-10): Representative HPLC chromatogram of the hydrolysis reaction of 82 and 83 in the presence of hydroxylamine at different time (1 = 10 min, 2 = 18 h).	105
Figure (4-11): Monitoring the hydrolysis of phosphate triester 82 and 83 using ³¹ P NMR in D ₂ O.	106
Figure (4-12): Plot of <i>k</i> _{obs} as a function of hydroxylamine concentration for reaction of triester 84 at 25.0 °C, pH = 7.3 and <i>I</i> = 1.0 M (NaCl).	107
Figure (4-13): ³¹ P NMR spectra of the hydrolysis products of phosphate triesters 84 (at 25 °C) in D ₂ O.	108
Figure (4-14): ³¹ P NMR spectra of the hydrolysis products of phosphate triesters 85 and 86 (at 60 °C) in D ₂ O.	109
Figure (5-1): Structure of phosphate triesters 82 , 83 , 69 and 46	117
Figure (5-2): Phosphate triesters proposed to be synthesised in this chapter.	118

Figure (5-3): Difference between Hydrogen bonding and general acid mechanisms.....	119
Figure (6-1): structures of sulfate di- and monoester.....	138
Figure (6-2): structure of naphthyl phosphate with different substituent.....	139
Figure (6-3): structure of phenyl phosphate mono ester with two hydrogen bond donors	139

List of Schemes

Scheme (1-1): The deprotonation of salicylic acid and related compounds (1 and 3).....	8
Scheme (1-2): The aminolysis reaction of styrene oxide with aniline.....	12
Scheme (1-3): Proposed mechanisms involving in the hydrolysis of 17 ; general acid (blue) and general base (red) catalysis.....	15
Scheme (1-4): Hydrolysis of salicyl phosphate.....	17
Scheme (1-5): Aryl 2-carboxyphenyl phosphate anions studied Kirby <i>et al.</i>	19
Scheme (1-6): Hydrolysis of aryl 2-carboxyphenyl phosphate anions studied Kirby <i>et al.</i>	20
Scheme (1-7): Hydrolysis of bis (2-(1-methyl-1H-imidazolyl) phenyl) phosphate 27[±] by two imidazole.....	22
Scheme (1-8): The hydrolysis of 8-dimethylammonium-naphthyl-1-phosphate monoanion.....	23
Scheme (1-9): The hydrolysis of methyl 8-dimethylamino-1-naphthyl phosphate.....	23
Scheme (1-10): Hydrolysis of diethyl 8-dimethylamino-1-naphthyl phosphate.....	24
Scheme (1-11): Equilibria for hydroxylamine and its known ionic species and pK_a values for hydroxylamine and its derivatives in aqueous solution at 25 °C; Experimental values (pK_{a1} and pK_{a2}), and Computed values (pK_{a3} , pK_{a4} and pK_{a5}).....	26
Scheme (1-12): The hydroxylamine-phosphate products of mono-, di- and triesters.....	27
Scheme (1-13): Suggested mechanism for the decomposition of hydroxylamine-O-phosphate 40 in the presence of an excess of hydroxylamine.....	27
Scheme (1-14): The reactions of protonated and anionic aspirin with hydroxylamine at 25.0 °C and ionic strength = 1.0 M (KCl).....	28
Scheme (1-15): Possibly ways of phosphate hydrolysis.....	29
Scheme (2-1): The hydrolysis of phosphate-ester dinucleotides by RNase A by general base and acid catalysis assisted by hydrogen bond.....	34
Scheme (2-2): Synthesis of cyclic methyl 8-hydroxy-1,9-anthryl phosphate triester 46	37
Scheme (2-3): Synthesis of cyclic methyl 8-hydroxy-1,9-anthryl phosphate triester 47	38
Scheme (2-4): Synthesis of yield cyclic methyl 1, 9-naphthyl phosphate triester 48	38
Scheme (2-5): Synthesis of yield cyclic ethyl 1, 9-naphthyl phosphate triester 49	39
Scheme (2-6): The proposed route of hydrolysis of phosphate triester 46	43

Scheme (2-7): Proposed reaction mechanism for the opening the ring (route A) of triester 46 under neutral pH conditions.	43
Scheme (2-8): The proposed route of hydrolysis of cyclic phosphate triester 47	45
Scheme (2-9): The route proposed for hydrolysis of phosphate cyclic triester 48	47
Scheme (2-10): The route proposed for cyclic phosphate triester 49 reaction with hydroxylamine.	48
Scheme (2-11): Buffer catalysis mechanism involved in hydrolysis of phosphate triester 46.	50
Scheme (2-12): The proposed route of hydrolysis of cyclic phosphate triester 46	52
Scheme (2-13): The mechanism involving Prior or simultaneous protonation of the phospho- diester (P=O unit) with nucleophilic attack leads to a monoanionic phosphorane intermediate that can react further by cleavage or migration.	56
Scheme (2-14): The mechanism proposed for hydrolysis of phosphate triester 46.	63
Scheme (2-15): Two-step mechanism for the reaction of hydroxylamine with phosphate triester 46 , by the zwitterionic form. In first step the water or hydroxylamine can act as a general base in the first step.	68
Scheme (2-16): Mechanism of the reaction of phosphate triesters with hydroxylamine, showing hydrolysis of the intermediate by second molecule of hydroxylamine.	69
Scheme (3-1): The mechanism proposed for hydrolysis of diethyl 8-hydroxy-1-naphthyl phosphate 69	75
Scheme (3-2): Possible transition states involved in hydrolysis of triester 71	76
Scheme (3-3): Synthesis of diethyl aryl phosphate triesters 69-72	77
Scheme (3-4): Possible route for formation of ethyl naphthyl cyclic phosphate 49	78
Scheme (3-5): Hydrolysis of diethyl-8-hydroxy naphthyl phosphate 69	79
Scheme (3-6): The proposed route for hydrolysis of diethyl-8-hydroxy naphthyl phosphate 69 . .	80
Scheme (3-7): The proposed mechanisms of cleavage of diethyl 2-hydroxy biphenyl-2`-phosphate triester 71 , 0.5 M NH ₂ OH in D ₂ O, Hydrogen bond catalysis (red), intramolecular nucleophilic catalysis (black) and intermolecular nucleophilic catalysis (blue).	89
Scheme (3-8): Synthesis of ethyl cyclic biphenyl phosphate triester 80	90
Scheme (3-9): The proposed mechanism of hydrolysis of ethyl 2,2`-biphenyl cyclic triester 80 , where the nucleophile is the hydroxylamine.	90
Scheme (4-1): Synthesis of diethyl acyclic phenyl phosphate triesters 84-87	98

Scheme (4-2): Synthesis of diethyl acyclic phenyl phosphate triesters 82 and 83	99
Scheme (4-3): Expected route for hydrolysis of diethyl phenyl phosphate triesters 82 and 83	105
Scheme (4-4): Hydrolysis of diethyl acyclic phenyl phosphate triesters 82 and 83	106
Scheme (4-5): Hydrolysis of diethyl acyclic phenyl phosphate triesters 84-86	110
Scheme (4-6): The reaction of diethyl-2-hydroxy-phenyl phosphate 84 with hydroxylamine at pH 7.3 and 25 °C.	111
Scheme (4-7): The hydrolysis of dimethyl 5'-O- methyluridine 2'-phosphate.	112
Scheme (4-8): The hydrolysis of dialkyl 2-carboxyphenyl phosphate.	113
Scheme (4-9): Proposed possible routes for hydrolysis of diethyl acyclic phenyl phosphate triesters studied here.	113
Scheme (4-10): Proposed routes for the hydrolysis of the diethyl acyclic phenyl phosphate triesters studied here.	114
Scheme (5-1): The proposed synthesis of 105	120
Scheme (5-2): The reduction C-10 position of 106	121
Scheme (5-3): The reaction of 107 with piperidine.	121
Scheme (5-4): The proposed synthesis route of 110	122
Scheme (5-5): The proposed synthetic route to 115.	123
Scheme (5-6): The routes of decomposition of dithranol.	124
Scheme (5-7): The proposed protection route of 117	126
Scheme (5-8): Proposed reduction of 116 by borohydride.	127
Scheme (5-9): The proposed synthesis route of the intermediate 121	128
Scheme (5-10): The proposed synthesis of 117 by bromination of 107	129
Scheme (5-11): The proposed synthesis route of 125	130
Scheme (5-12): The proposed synthesis route of 128 and 129 from anthraquinone 126	131
Scheme (5-13): A protection attempt of 127	131
Scheme (5-14): A protection attempt of 127 by trimethylorthoformate.	132
Scheme (5-15): Acylation reaction of dithranol 127 and proposed phosphate reaction.	133

Scheme (5-16): The oxidation route of 1,8-divaloyl-9-anthrone.....	134
Scheme (5-17): Protection of C-10 position of 126	134
Scheme (5-18): Protection of 1,8-O- positions of 135	135

List of Tables

Table (1-1): Acid-Catalyzed Aminolysis of Styrene Oxide with Aniline.....	12
Table (2-1): Rate constants for the reaction of water (k_0) and hydroxylamine (k_2). (a) The rate was estimated from fitting the curve to equation (2-4), based on the same reactivity of hydroxylamine at this pH region.....	65
Table (2-2): the second order rate constants of the reaction of hydroxylamine with triesters 46, 47 and 47 at pH 7 and 25 °C.....	67
Table (3-1): The second order rate constants, k_2 and the relative rate constants, k_{rel} for the reactions of various phosphate triesters with NH_2OH	84
Table (7-1): The Solvent system used in HPLC analysis to follow the hydrolysis of triesters studied here.	167
Table (7-2): Structure and retention time of triester 71 and the corresponding products of hydrolysis.	168
Table (7-3): Structure and retention time of triester 72 , and the corresponding products of hydrolysis.	168
Table (7-4): Structure and retention time of triester 70 , and the corresponding products of hydrolysis.	169
Table (7-5): Structure and retention time of triesters 82 and 83 and the corresponding products of hydrolysis.	170
Table (7-6): Structure and retention time of triester 84 and the corresponding products of hydrolysis.	170
Table (A-1): First-order rate constants for buffer catalysis of the hydrolysis of triester 46 , at 25 °C and ionic strength 1.0 M.....	179
Table (A-2): First-order rate constants for hydrolysis of triester 46 , at 25 °C and ionic strength 1.0 M.	179
Table (A-3): First-order rate constants for the effect of DMSO on the hydrolysis of triester 46 , at pH 6, 25 °C and ionic strength 1.0 M.....	180
Table (A-4): First-order rate constants for hydrolysis of triester 47 , at 25 °C and ionic strength 1.0 M.	180
Table (A-5): First-order rate constants for hydrolysis of triester 48 , at 25 °C and ionic strength 1.0 M.	181
Table (A-6): First-order rate constants for the reaction of triester 46 with hydroxylamine, at 25 °C and ionic strength 1.0 M.....	181
Table (A-7): First-order rate constants for the reaction of triester 47 with hydroxylamine, at 25 °C and ionic strength 1.0 M.....	182

Table (A-8): First-order rate constants for the reaction of triester 48 with hydroxylamine, at 25 °C and ionic strength 1.0 M.....	182
Table (A-9): First-order rate constants for the reaction of triester 46 with vary concentration of hydroxylamine, at 25 °C and ionic strength 1.0 M.	183
Table (A-10): First-order rate constants for the reaction of triester 47 with vary concentration of hydroxylamine, at 25 °C and ionic strength 1.0 M at pH 7.....	183
Table (A-11): First-order rate constants for the reaction of triester 48 with vary concentration of hydroxylamine, at 25 °C and ionic strength 1.0 M at pH 7.....	184
Table (A-12): First-order rate constants for the reaction of triester 46 with nucleophiles, at 25 °C and ionic strength 1.0 M at pH 6.	184
Table (A-13): First order rate constants for the reaction of triester 46 with nucleophiles, at 25 °C and ionic strength 1.0 M at pH 6.	185
Table (B-1): First-order rate constants for the hydrolysis of triester 69 at 60 °C and ionic strength 1.0 M.	186
Table (B-2): First-order rate constants for the reaction of triester 69 , 70 and 71 with vary concentrations of hydroxylamine, at pH 7.3, 60 °C and ionic strength 1.0 M.	186
Table (C-1): First-order rate constants for the hydrolysis of triester 82 and 83 at pH 7.3, 25 °C and ionic strength 1.0 M.....	187
Table (C-2): First-order rate constants for the reaction of triester 82 , 83 and 84 with vary concentrations of hydroxylamine, at pH 7.3, 25 °C and ionic strength 1.0 M.	187

Chapter one: Introduction

1.1. General introduction

In living cells, huge numbers of chemical reactions occur leading to growth, reproduction and movement. Most of these biochemical reactions are not spontaneous but are accelerated by biochemical catalysts called enzymes. The catalytic effect of enzymes results in the reactions becoming more faster within a biological system. The most widely accepted explanation of enzyme activity advanced by Pauling focuses on noncovalent factors. Pauling proposed the modern notion of how enzymes obtain their extraordinary catalytic ability in 1948; “enzymes are complementary in structure to the activated complexes (transition state) of the reactions that they catalyse”.¹ A large number of complementary noncovalent interactions form between the substrate and the active site of the enzyme, including hydrogen bonds, ionic bonds, and hydrophobic interactions that extend along the active site.² The enzyme binds to the transition state more strongly than it binds to the ground state of the substrate. This results in relatively greater stabilisation of the transition state, thus lowering the activation energy compared to that of the uncatalyzed process, Figure (1-1).³

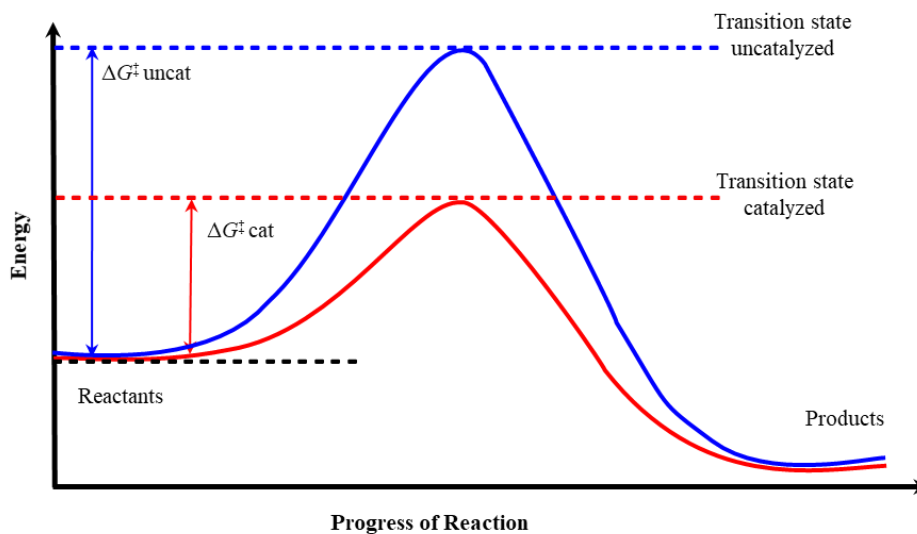


Figure (1-1): Diagram of a catalytic reaction showing difference in activation energy in an uncatalysed and catalysed reaction.⁴

Recently, Houk *et al.* studied the binding affinities in a wide variety of enzyme-inhibitors, enzyme-transition-states, and antibody-antigens and found that the highest average binding affinity observed was in the case of enzyme-transition-states. They proposed that this high enzyme proficiency (over 10^{11} M^{-1}) and binding energy (more than 62 kJ mol^{-1}) is achieved by full or partial covalent bond formation to the substrate in the transition state, which could involve proton transfer (general acid-base catalysis and low-barrier hydrogen bonds) and metal ion coordination (Mg^{2+} , Zn^{2+} , etc.) or cofactors such as pyridoxal.³

It can be seen that the hydrogen bond is one of the fundamental interactions in enzyme catalysed reactions, and thus considerable attentions have been devoted to provide insight into how their contribution affects reactions and how much the power of using hydrogen bonds to perform catalysis is. Therefore, designing model systems establishing intramolecular hydrogen bonds can be useful to investigate their role in catalysing reactions, such as biological processes catalysed by enzymes.

1.1.1. Hydrogen bonds

Hydrogen bonds are important in nature and life, because of their crucial role in various chemical processes. They affect physical and chemical properties of molecules. For example, hydrogen bonding is responsible for water's unique solvent capabilities, such as being liquid instead of gas and having a high boiling point for its mass. In biological systems, hydrogen bonds hold complementary strands of DNA together, and they are responsible for determining the three-dimensional structure of folded proteins including enzymes and antibodies.

As a definition, “*The hydrogen bond is an attractive interaction between a hydrogen atom from a molecule or a molecular fragment X–H in which X is more electronegative than H, and an atom or a group of atoms in the same or a different molecule, in which there is evidence of bond formation*”.⁵ There are three types of hydrogen bonds depending on the strength: weak

hydrogen bonds have energies ($< 20 \text{ kJ mol}^{-1}$), hydrogen bonds of moderate strength have energies between ($20\text{-}60 \text{ kJ mol}^{-1}$), and strong hydrogen bonds have energies ($60\text{-}100 \text{ kJ mol}^{-1}$). Commonly, the proton in a hydrogen bond exists in a double-well potential; as the length of the hydrogen bond becomes shorter the barrier separating the two wells becomes lower (low-barrier hydrogen bond) or a single-well (very strong hydrogen bond), Figure (1-2).⁶⁻⁷

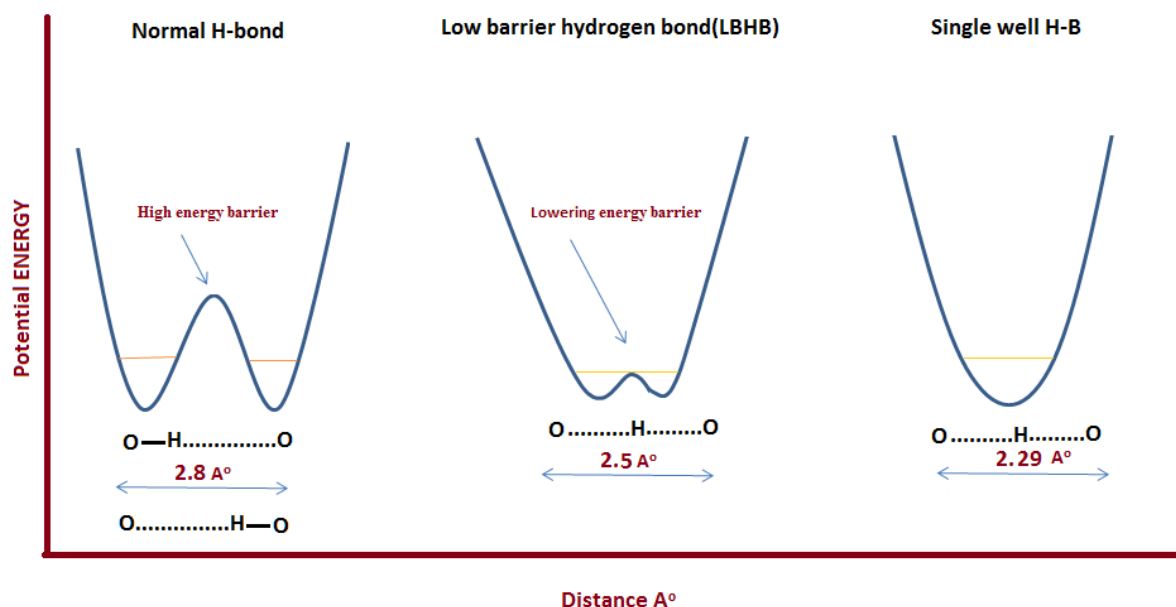


Figure (1-2): General aspects of an ordinary hydrogen bond (HB), a low-barrier hydrogen bond (LBHB) and single-well H-B between oxygen heteroatoms.⁸

Weak and medium hydrogen bonds can be considered as electrostatic interactions, whereas strong hydrogen bonds are proposed to have some features of covalent bonding. Based on their nature, hydrogen bonds are classified as a strong non-covalent interaction, but still weaker than covalent or ionic bonds.

1.1.2. Enzyme Catalysis by hydrogen bonding

Enzyme active sites frequently use hydrogen bonds to help catalyse transformations of the main functional groups involved in metabolic processes. However, although hydrogen bonds between active site of enzymes and substrates were proposed to be essential for the catalytic function and specificity of enzymes, the contribution from the variation in strength of normal hydrogen bonds in enzyme-catalyzed reactions has been perceived by some workers not to be

of sufficient magnitude. To explain the contribution of hydrogen bonds in enzyme catalysis, two hypotheses has been invoked and investigated; low barrier hydrogen bond and hydrogen bond networks.

1.1.3. Low-barrier hydrogen bond (LBHB)

Low-barrier hydrogen bonds which are partially covalent have been proposed to play a role in enzyme catalysis. It is likely that when the pK_a s of the catalytic group and reactant become equal, normal hydrogen bonds in the ground state convert to shorter and stronger ones (low-barrier hydrogen bonds) at the transition state in reactions involving general acid-base catalysis.^{3, 9} For example, Cleland *et al.* have proposed that hydrogen bonds with perfect pK_a matching between proton donor and acceptor are remarkably short or even single –well hydrogen bonds.¹⁰

Although, the role of hydrogen bonding in catalytic processes has been investigated extensively, the involvement of low-barrier hydrogen bonds or unique short strong hydrogen bonds in this process is still not clear.^{11, 6} Most studies on low-barrier hydrogen bonds rely on removing or replacing the specific residue on the enzyme that is thought to be involved in forming a key hydrogen bond. For example, Gerlt and Gassman suggested that stabilisation of the transition state in reactions catalysed by chymotrypsin and other serine protease involves LBHB in the oxyanion hole of the enzyme.¹² Bryan *et al.* use site-specific mutagenesis to study the role of hydrogen bonding in the oxyanion hole in subtilisin and found that loss of one of the hydrogen-bonding groups (Asn155 changed to Leu155) decreased k_{cat} by 300 fold. In a study of the effect of phenolic pK_a on hydrogen bonds in substituted salicylamides, Mock and Chua suggested that the loss of one hydrogen bond should reduce the rate by about 30-fold. It is clear that the point mutation results with subtilisin lead to large variation in estimating the H-bonding factor by an order of magnitude (ca. 330-fold versus 30-fold). Therefore, Mock and

Chua state that “involving LBHB in enzyme catalysis needs more evidence before being a likely explanation of the kinetic acceleration in the active site”.¹³

However, LBHB have some evidence experimentally, such as high ¹H NMR chemical shifts, a low deuterium fractionation factor, a broad continuum absorption and short heavy atom – heavy atom distances.¹¹ Birgit *et al.* have investigated the electronic nature of low-barrier hydrogen bonds using low temperature neutron and X-ray diffraction experiments and high level ab initio calculations. They concluded that the low-barrier hydrogen bond involved in proton transfer contains a double-well potential with a small barrier. An analysis of the electron density of this bond indicates that there is partial charge on oxygen atoms bonded to hydrogen, but this feature has changed to include a covalent bond character, and thus the stabilisation can be related to both electrostatic interactions and a partially covalent bond. They concluded that “all short-strong and LBHB systems possess similar electronic features of the hydrogen-bonded region, namely polar covalent bonds between the hydrogen atom and both heteroatoms in question”.¹⁴

In spite of enzymatic model studies, the mutagenesis data from enzymes suggest that the contribution of LBHB could be significantly large, but there is still conflict on the required energy provided by LBHB. Thus, the existence of a short strong hydrogen bond is a contentious issue. Alternatively, it has been suggested that a significant magnitude of the catalytic power of an enzyme can be provided by using multiple hydrogen bond interactions instead of a single interaction.¹⁵

1.1.4. Hydrogen bond network

The use of hydrogen-bonding network (HBN) was proposed as an alternative to LBHB. Here, it is suggested that an array of hydrogen bonds can work cooperatively to provide the stabilisation energy for enzyme catalysed reactions. A well-known example of using multiple hydrogen bonding in enzymatic catalysis is the oxyanion hole of serine protease,

Figure (1-3), which is an arrangement of hydrogen bond donors that stabilise the transition state by hydrogen bonding to a forming tetrahedral intermediate, which becomes a stronger hydrogen acceptor as it forms. As shown in Figure (1-3), the serine -OH group is a nucleophile that attacks the carbonyl carbon of the scissile peptide bond of a substrate. The nitrogen electron pair of histidine accepts the hydrogen from the serine OH-group forming a hydrogen bond; they make a coordinated attack on the peptide bond. Moving electrons onto oxygen increases the electron density around C=O oxygen. The carboxyl group on the aspartic acid forms a hydrogen bond with the histidine, making the histidine nitrogen much more electronegative, thus increasing the strength of the hydrogen bond between histidine and serine. The oxyanion hole formed by two hydrogen bond donors from the amino acid of Ser195 and Gly193 that stabilize the transition state and tetrahedral intermediate shows a contribution in catalytic hydrolytic activity with a reaction rate 1000-fold higher than that for the uncatalysed hydrolysis.¹⁶⁻¹⁸

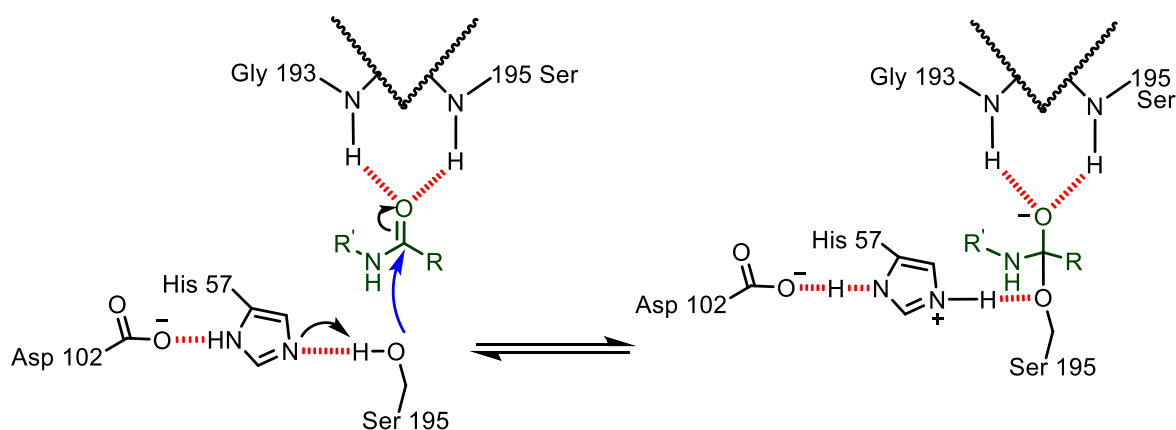


Figure (1-3): Oxyanion hole in active site of a serine protease.¹⁹

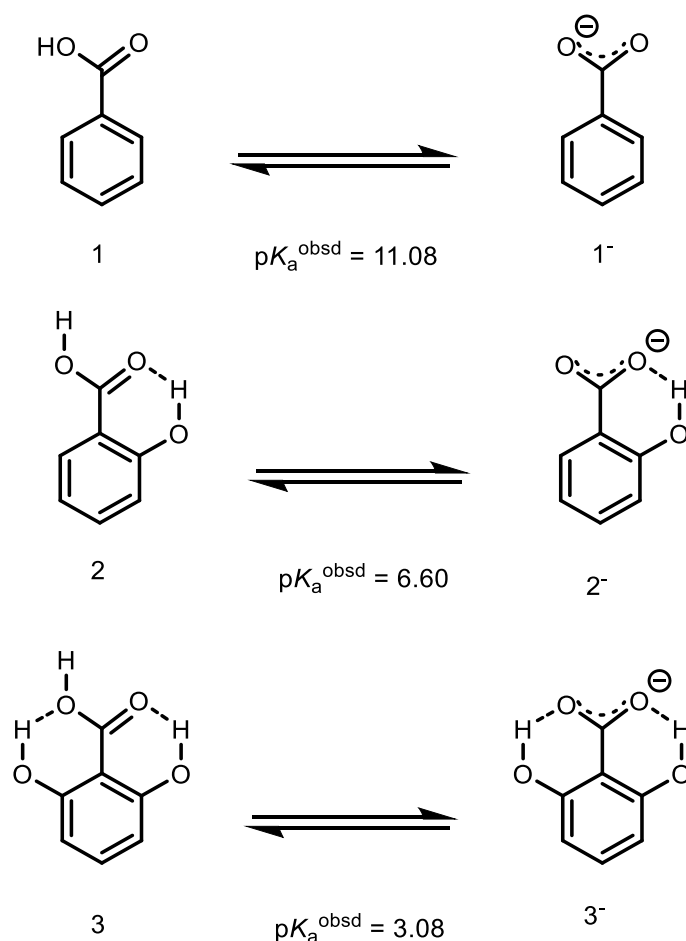
1.2. Previous work

Over many years, numerous investigations have been carried out on the catalytic role of hydrogen bonding on binding and reactivity, and key examples, which are relevant to this research, are described here.

1.2.1. The effect of hydrogen bond network on acidity

Multiple hydrogen bonds can provide greater catalytic power and increase acidities. The deprotonation of benzoic acid and related compounds can mimic charge relocalizations occurring at active sites of enzymes. For example, Shan and Herschlag have studied the deprotonation of the benzoic acid systems (**1**, **2** and **3**) with one or two hydroxyl groups adjacent to the carboxylic acid in the *ortho* positions to reveal whether the existence of more than one hydrogen bond donor would enhance the acidity,

Scheme (1-1).¹⁵ They found that the pK_{a} s of these acids in DMSO decreased with increasing number of hydroxyl groups for compounds **1** – **3**, where pK_{a} is 11.08, 6.6 and 3.08, respectively. The result reveals that the formation of two direct hydrogen bonds to the carboxylate anion centre in the conjugate base increases the acidity of the benzoic acid by up to 8.0 pK_{a} units (*i.e.* 45.6 kJ mol^{-1}). The larger value of the pK_{a} value of **1** (11.08) is due to the lack of intermolecular hydrogen bonding and the resulting oxygen anion centre is not stabilised. Thus, deprotonation of a carboxylic acid can be preferred when an adjacent hydroxyl proton forms an intramolecular hydrogen bond with carboxyl oxygen in the acid form, and then this bond is strengthened upon deprotonation of the carboxylic acid, providing specific stabilisation of the monoanion relative to the acid form of the compound.²⁰



Scheme (1-1): The deprotonation of salicylic acid and related compounds (**1** and **3**).¹⁵

Shokri *et al.* have investigated using arrays of hydrogen bonds with different lengths to assess whether they provide the required energy for enzyme-catalysed transformations. Simple model polyhydroxyl alcohols were studied, Figure (1-4), where different types of hydroxyl groups (1° and 2°) and their acidities (pK_a s) were measured in DMSO and the gas phase.²¹ The conjugate bases can be stabilised by hydrogen bond networks. Primary (1°) hydrogen bonds, those between a charged centre and a donor or acceptor group, should be the strongest. Secondary (2°) and tertiary (3°) hydrogen bonds, involving noncharged groups, should be weaker.²¹

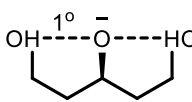
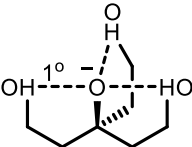
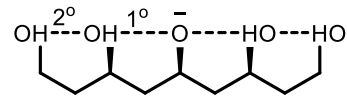
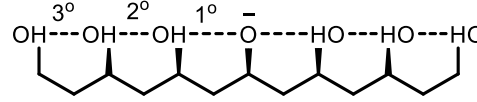
	 4	 5	 6
pK_a (DMSO - M062X)	17.3		14.5
pK_a (Benzene - M062X)	11.1		5.5
pK_a (DMSO experimental values)	19.7	16.1	14.7
	 7		
pK_a (DMSO - M062X)	13.4		
pK_a (Benzene - M062X)	3.3		

Figure (1-4): Compounds studied by Shokri et al.²¹

Experimental and computational results show that the presence of hydrogen bonds to a negatively charged centre and those that are one solvent shell further away (i.e., 1° and 2° hydrogen bonds, respectively) provide a significant amount of stabilisation of their conjugate bases, providing a significant acidity enhancement. By comparing the pK_a 's of **4** and **5**, the alcohol **4** is 3.5 pK_a units (20 kJ mol^{-1}) more acid than alcohol **5**. In going from **4** to **6**, each of the secondary 2° hydrogen bonds afforded further stabilisation of the conjugate base of **6**: the differences in the pK_a s are 2.5 units (14 kJmol^{-1}) per hydrogen bond in DMSO. These secondary hydrogen bonds are weaker, thus they do not stabilise the anion to the same degree as the primary hydrogen bond, but their effect is noticeable in comparison with a 3° hydrogen bond.²¹ However, the 3° hydrogen bonds in **7**, which are even further removed from the charged centre and even weaker, still provide ~ 0.6 pK_a unit (~ 3.4 kJmol^{-1}) in DMSO per hydrogen bond stabilisation. These results indicate that multiple hydrogen bonds in a hydrogen bond network can provide considerable energetic stabilisation and enhanced Brønsted acidities.²¹

Hydrogen bond networks and inductive effects have been used in designing efficient catalysts. Inductive effects can be transmitted over long distances through a chain of hydrogen bonds, increasing H-bond acidity. Electron-withdrawing groups serve to increase the alcohol hydrogen bond donating ability and result in stronger Brønsted acids. However, the inductive effects along the hydrogen bonding network fall off rapidly with distance.²¹

More recently, a study by Samet *et al.* has exploited hydrogen bond networks and an inductive effect on enhancement of the rate of a reaction. They proposed that in a rigid structure such as adamantane, triols (**8-11**) can be utilised as effective catalysts, Figure (1-5). The acidities of a series of adamantane like triols (**8-11**) were measured in DMSO, and reactivity in some reactions was studied. These triols have electron-withdrawing groups in combination with hydrogen bonds.

The results revealed that the incorporation of a first and second trifluoromethyl group (CF₃) enhances the acidity by 4.1 and 4.0 pK_a units (23.4 and 23 kJmol⁻¹), and third CF₃ group by 2.2 pK_a units (12.5 kJmol⁻¹), since the electron-withdrawing effect of CF₃ promotes ionisation. The effect provided by the second and third CF₃ substituents is not much different from that of the first CF₃ substituent.²² However, it might be that the latter two CF₃ groups have some effects due to enhancing the acidity of the hydroxyl groups and their effect can be transmitted through the hydrogen bond network similar to resonance stabilization in π -electron systems.

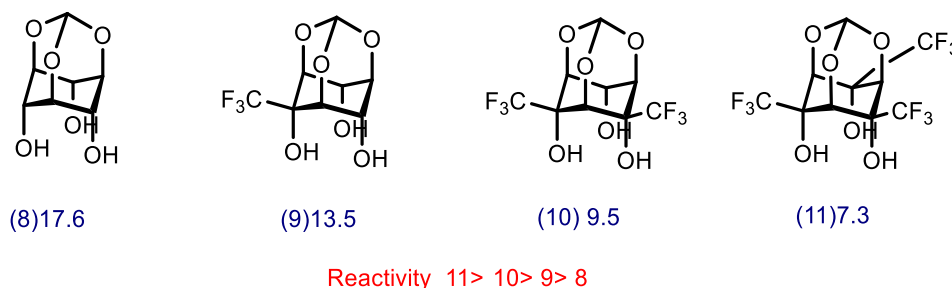


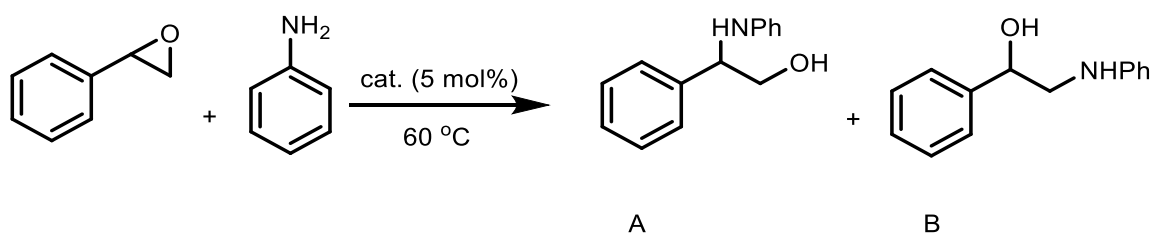
Figure (1-5): Adamantane triols and pK_as in DMSO.²²

Comparing the rigid structure of triol **11** with **12** and **13** revealed that **11** has the same acidity as **13** and is less acidic than diol **12**, Figure (1-6).

	12	13	11
pKa(DMSO)	4.8	7.1	7.3
pKa(gas phase)	302.8	309.6	301.5

Figure (1-6): Flexible system studied by Samet et al.²²

The benefit of the rigidity can be seen when comparing the reactivity of triols **8-11** with **13** and **12**. The catalytic abilities of this triol series has been examined in catalysing the aminolysis of styrene oxide with aniline at 60 °C under solvent-free conditions, Scheme (1-2). In the presence of **11** the reaction was faster (1 h) compared with (3.5 h) for triols **8-10**, and the greater selectivity for the addition product was at the more hindered position (i.e., A).²² Comparing the rigid triols with flexible systems **12** and **13**, the rigid triol **11** enhances the rate of reaction up to 1.5 times over flexible system **13**, and slower than **12**. However, triol **11** is more selectivity than **12**, Table (1-1). In polar environment, the activity was found to correlate to DMSO acidity. However, this was not the same in non-polar environment, the rigid triol was found to enhance the reactions up to 100 fold over flexible acyclic analogues, and the reactivity followed the gas phase acidity. The reactivity enhancement of the rigid structure over the flexible acyclic structure was proposed to be due to an entropic effect.²² This indicates that the oxyanions of triols (**8-11**) are extensively stabilized due to the hydrogen bond networks and presence of the electron withdrawing groups.²²



Scheme (1-2): The aminolysis reaction of styrene oxide with aniline.²²

Table (1-1): Acid-Catalyzed Aminolysis of Styrene Oxide with Aniline.²²

Catalyst	Time (h)	Conversion (%)	k_{rel}	Product ratio (%)	
				Product (A)	Product (B)
No Catalyst	3.5	4.0	1.0	35	65
8	3.5	11	3.0	54	46
9	3.5	58	33	75	25
10	3.5	90	220	84	16
11	1.0	96	580	91	9
13	0.5	69	370	81	19
12	0.25	68	710	88	12

1.2.2. The effect of hydrogen bond network on binding

Chains of hydrogen bonds can enhance the hydrogen bonding properties of the terminal donor. The strength of the terminal H-bonding between donor and acceptor can increase with the length of the hydrogen bond chain.²³ Cockroft and coworkers have investigated the effect of an array of hydrogen bonds on the strength of the H-bonding interactions between a series of phenols and tri-*n*-butylphosphineoxide in solution, Figure (1-7). They found that as the number of OH groups increase, the binding energies became more favorable. The presence of second H-bond made significant energy contributions, which almost doubled the strength of the terminal H bond, but further increasing the length had little additional effect.²³

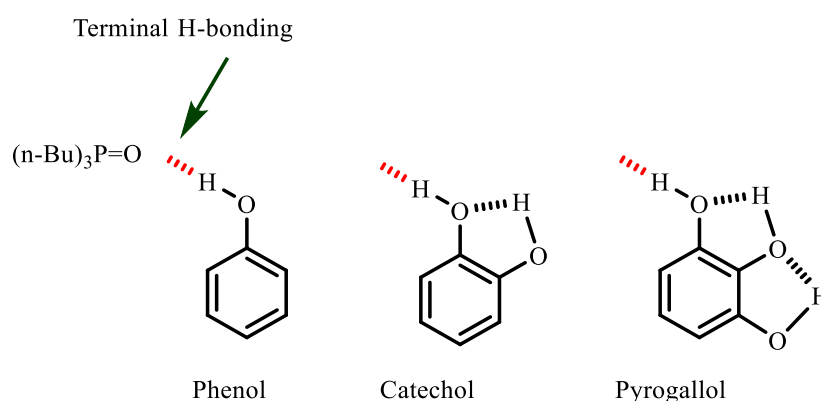


Figure (1-7): Hydrogen-bonding between the complexation of tri-*n*-butyl phosphine oxide and phenolic system with different number of hydrogen bonds, (Terminal H-bond labelled).²³

1.2.3. The effect of intramolecular hydrogen bonds on reactivity

For many years, the mechanisms of systems by which neighbouring groups can catalyse reactions has been of interest. The effect of intramolecular catalysis has been investigated with hydrogen-bonded leaving groups in the hydrolysis of phosphate esters, carbonate, acetoxy and acetal groups. For example, Tillett and Wiggins have reported the intramolecular catalysis by a neighbouring hydroxyl group of the hydrolysis of carboxylic ester **14**, Figure (1-8).²⁴

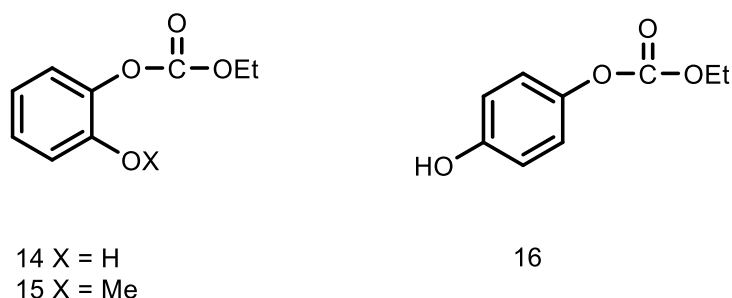


Figure (1-8): Structures of carbonate esters studied by Tillett and Wiggins.²⁴

A plateau region is reached at lower pHs, corresponding to spontaneous hydrolysis. In this region, carbonate **14** hydrolysed **10** times faster than **15**, which suggested that the hydroxyl group has direct involvement in the hydrolysis. They suggested two kinetically indistinguishable mechanisms of intramolecular catalysis could be involved: intramolecular general acid or general base catalysis as shown in Figure (1-9). General acids can catalyse the attack of a nucleophile through hydrogen bonding to the carbonyl and/or leaving group, so it should catalyse the reaction with other general bases.

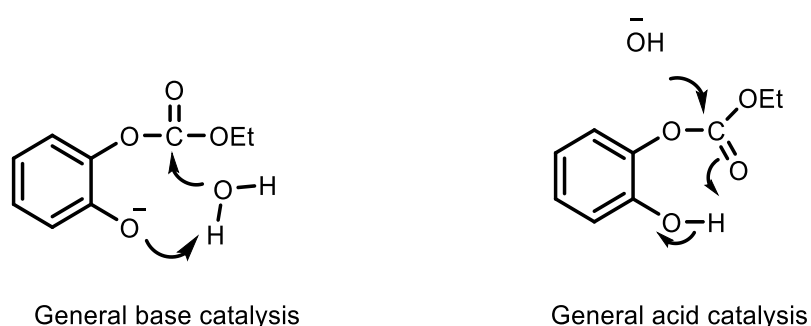


Figure (1-9): Two mechanisms suggested for the hydrolysis of carboxylic ester **4**.²⁴

In the neutral region, $k_{\text{H}_2\text{O}} = 2.04 \times 10^{-5} \text{ M}^{-1} \text{ s}^{-1}$ at 35 °C in the absence of acetate, and $2.20 \times 10^{-5} \text{ M}^{-1} \text{ s}^{-1}$ in the presence of acetate, which has a similar effect on the hydrolysis of ethyl 2-methoxyphenyl carbonate (1.70 and $1.80 \times 10^{-6} \text{ M}^{-1} \text{ s}^{-1}$, respectively). Thus, general acid catalysis could be ruled out as there was no difference in the rate of the reaction with hydroxide ion or acetate.²⁴ However, from the pH profile, Figure (1-10), the plateau region was observed at pH 10 to 11. In this region, if most all of the carbonate was in its ionised form, the dissociated hydroxyl group would be involved in general base or nucleophilic catalysis.²⁴ Nucleophilic attack by the hydroxyl group in the neutral hydrolysis of **14** was ruled out based on the entropy of activation value of $-167.36 \text{ J K}^{-1} \text{ mol}^{-1}$, which was interpreted as showing the involvement of solvent on the hydrolysis of acyl compounds in water by comparison with other related reactions *e.g.* alkyl trifluoroacetates ($-209 \text{ J K}^{-1} \text{ mol}^{-1}$) and acetic anhydride ($-167.36 \text{ J K}^{-1} \text{ mol}^{-1}$).²⁴

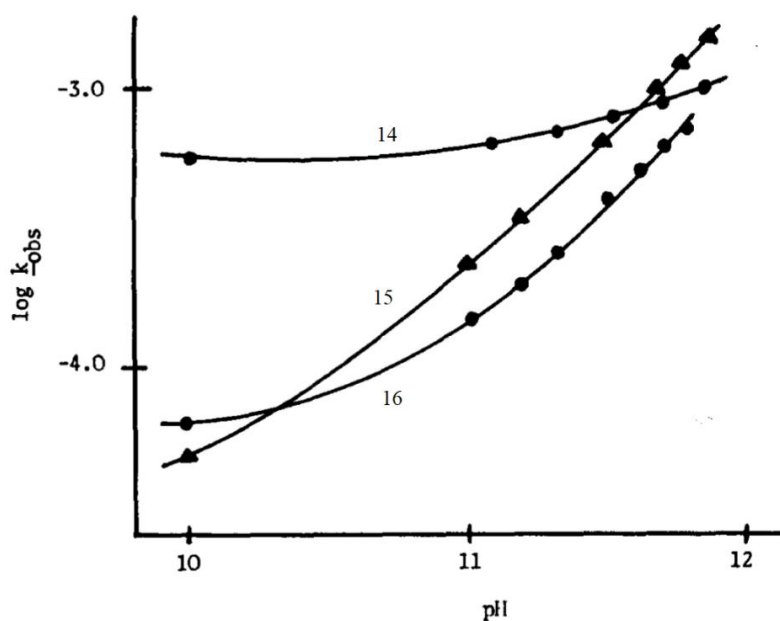
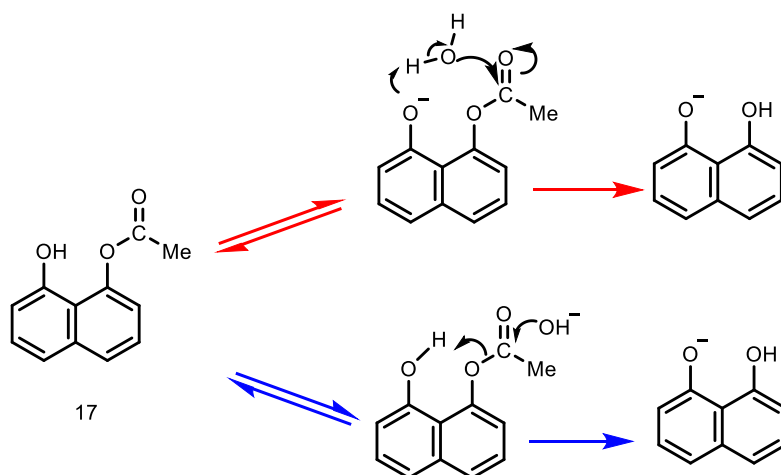


Figure (1-10): pH-Rate profile for the alkaline hydrolysis of carbonate esters **14**, **15** and **16** in NaOH at 25 °C, ionic strength at 1.0 (KCl).²⁴ [Original citation] – Reproduced with permission of Elsevier.

Hibbert and Spiers have reported the hydrolysis of 1-acetoxy-8-hydroxy-naphthalene **17**, in which the hydroxyl group can play a role either as an intramolecular general acid or base catalyst, Scheme (1-3).



Scheme (1-3): Proposed mechanisms involving in the hydrolysis of **17**; general acid (blue) and general base (red) catalysis.²⁵

The linear dependence of rate constant on $[\text{OH}^-]$ is attributed to reaction of the ionised form with OH^- , whereas the curved dependence at low $[\text{OH}^-]$ is due to the reaction of ionised 1-acetoxy-8-hydroxy-naphthalene with solvent, Figure (1-11).²⁵

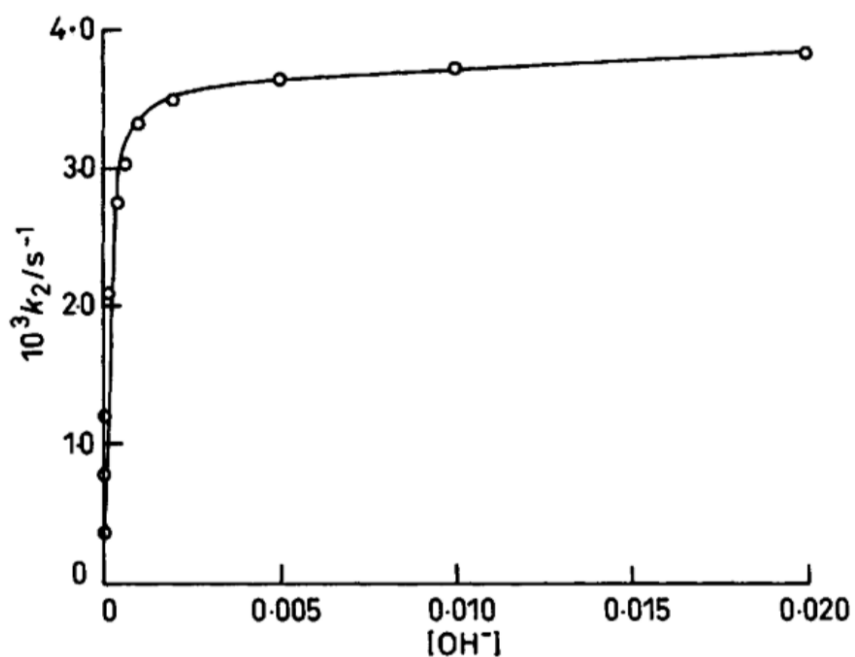
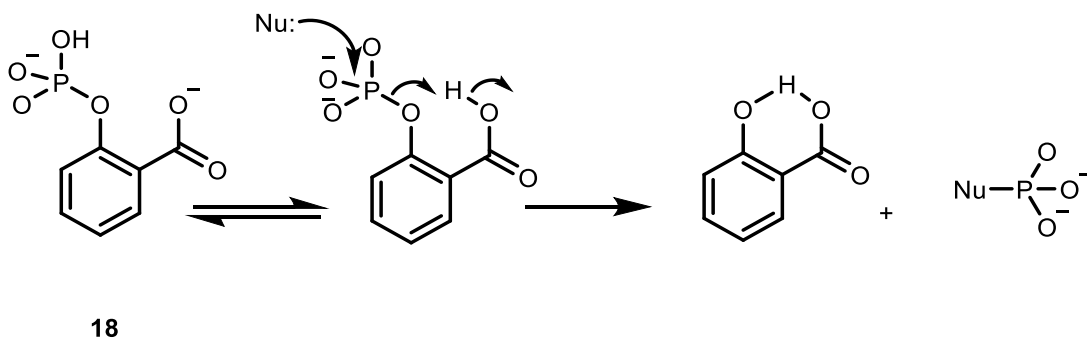


Figure (1-11): Variation of the first-order rate constant (k_{obs}) for hydrolysis of 1-acetoxy-8-hydroxy naphthalene with hydroxide concentration.²⁵ [Original citation] – Reproduced with permission of The Royal Society of Chemistry.

In the latter case the value of the rate coefficient (k_2 $3.7 \pm 0.4 \times 10^{-3} \text{ s}^{-1}$) for this reaction, in comparison with the value for the reaction of 1-acetoxy-naphthalene **17** with water, estimated as $7 \times 10^{-8} \text{ s}^{-1}$, brings about a 5×10^4 fold increase in the rate of spontaneous hydrolysis. This

effect could be explained either by the intramolecular general base catalysis by the ionised hydroxyl group on the attack of water, or due to the hydroxyl group acting as an intramolecular acid catalyst to assist the reaction with OH^- , Scheme (1-3). However, a solvent kinetic isotope effect value of 2.2 was measured, which is consistent with other reactions involving general base catalysis by the hydroxyl group assisting the water attack.²⁵

Bromilow and Kirby studied the phosphate transfer of salicyl phosphate 18 and showed the rate of hydrolysis is enhanced up to 10^8 fold. A solvent kinetic isotope effect was not observed, which was used to rule out the general base catalysis by carboxylate ion. This enhancement was attributed to the mechanism involving the carboxyl group as a general acid catalyst, Scheme (1-4).²⁶



Scheme (1-4): Hydrolysis of salicyl phosphate.²⁶

Hibbert *et al* have studied 1-methoxymethoxy 8-substituted naphthalene, Figure (1-12), and found that the efficiencies of the intramolecular catalytic groups; OH, COOH and Me_2NH^+ on the rate of the spontaneous hydrolysis of 1-methoxymethoxynaphthalenes were different. Using an estimated k_0 of $4 \times 10^{-9} \text{ s}^{-1}$ for 1-methoxy methoxy naphthalene, the dimethyl ammonium Me_2NH^+ increases the rate by 1900 fold, while hydroxyl and carboxyl groups show an effect of 40 fold and 1000 fold, respectively. This enhancement of the rates accounts for a significant effect of an intramolecular hydrogen bond donor. The strength of the intramolecular hydrogen bond increased going from the ground state to the transition state, which can stabilise the negative charge developing on the leaving group during progress of the reaction. The intramolecular hydrogen bond becomes stronger for Me_2NH^+ , and decreases in strength from

COOH to OH, respectively. This difference was attributed to the ability of the substituent to participate in an intramolecular hydrogen bond. However, the high enhancement of the rate by dimethyl ammonium group compared with COOH to OH could not just be related to the formation of hydrogen bond, but also to participation of proton transfer (general acid catalysis), particularly for Me_2NH^+ .²⁷ All three systems give products involving such a hydrogen bond, with the most efficient Me_2NH^+ system having the strongest product intramolecular H-bonds, and 1-methoxymethoxy-8-hydroxy naphthalene **21** is less efficient than COOH and Me_2NH^+ naphthalene system, **19** and **20**. In the case of the hydroxyl group, the general acid catalysis can be ruled out based on the libido rule suggested by Jencks; “*General acid catalysis will occur when a thermodynamically unfavourable proton transfer in the ground state is converted to a thermodynamically favourable transfer in the transition state*”.⁷ This means that the leaving group must be less basic in the ground state than the general acid, but becomes more basic in the product. In acetal **21** the leaving group and the general acid are identical, thus there is no proton transfer favourable. Kirby has suggested that the key factor for general acid catalysis to play a significant catalytic role in systems such as in these acetals is the strong intramolecular hydrogen bond, which involves the catalytic proton, in the products of reaction. This hydrogen bond has been proposed to be too weak or absent in the ground states for there to be an increase in strength and catalysis to occur.²⁸

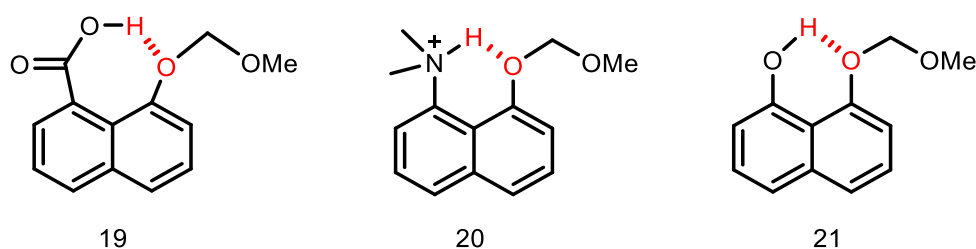


Figure (1-12): The structure of model system studied by Hibbert *et al.*²⁷

For instance, Bender *et al.* studied the hydrolysis of the dianion of 8-hydroxy-1-naphthyl dihydrogen phosphate **23**, Figure (1-13).

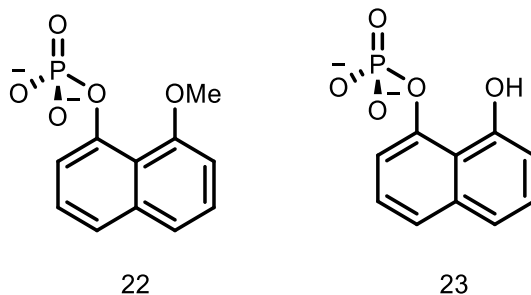


Figure (1-13): Compounds studied by Bender and *et al.*²⁹

About a 10 fold rate enhancement is provided by the hydroxyl group over the dianion of the 8-methoxy ester **22**.²⁹ The rate enhancement is much higher when a metal ion is combined with the dianion, Figure (1-14). Williams *et al.* have reported a rate acceleration of about 5000 and 50000 fold by the adjacent OH group comparing with the hydrogen atom and methoxy group, respectively. The rate increase resulted from cooperation between intramolecular hydrogen bond catalysis and metal ion based catalysis.³⁰ The hydrogen atom and methoxy group are unable to form hydrogen bonds to the leaving group oxygen, thus they have no effect or even a destabilising effect on the transition state. The very low rate in the presence of the methoxy group might be due to the orientation of the oxygen lone pair to an unfavoured position near the leaving group, resulting in destabilisation of the negative charge developed on the leaving group oxygen. Based on libido rule, the product of hydrolysis of the hydroxyl complex has a leaving group with pK_a identical to the general acid, thus the 50000 fold acceleration in the rate which about 21 kJ mol⁻¹ is provided by hydrogen bond catalysis and not general acid catalysis.

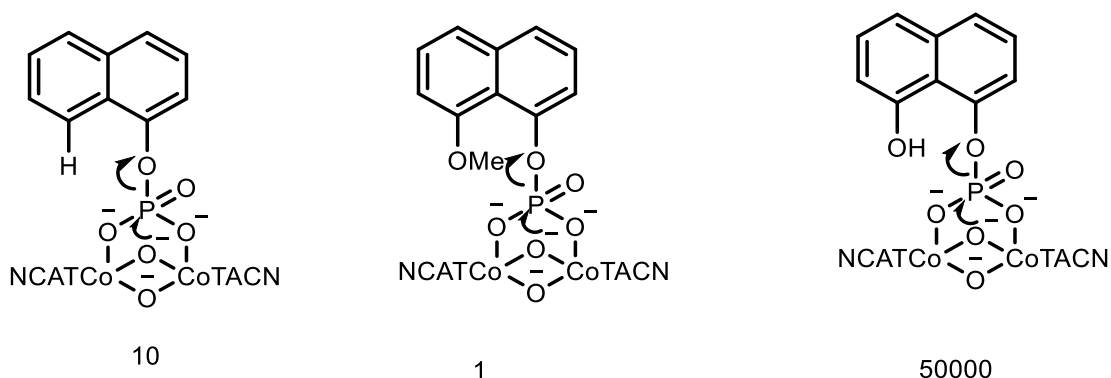
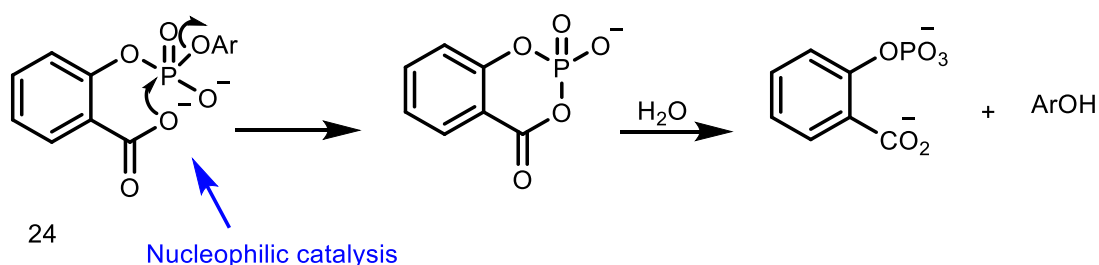


Figure (1-14): Compounds studied by Williams *et al.*³⁰

Kirby *et al.* determined a rate enhancement of 10^7 - 10^8 for the hydrolysis of aryl 2-carboxyphenyl phosphate anions **24** by the ionised carboxy-group *o*-COO⁻, Scheme (1-5). The mechanism of the reaction involves breakdown of a pentacoordinate-intermediate formed by addition of COO⁻ of one salicyl group to the phosphorus atom.³¹ This leads to the departure of the *exo*-aryl group. It was suggested that carboxylate ion is more efficient as a nucleophile when an *exo*-aryl group is present.



Scheme (1-5): Aryl 2-carboxyphenyl phosphate anions studied Kirby *et al.*³¹

Kirby *et al.* observed that the hydrolysis of the diester bis-2-carboxyphenyl phosphate **25** shows bifunctional catalysis by the ionised carboxy-group *o*-COO⁻ and *o*-CO₂H group, Figure (1-15), when two carboxyl groups are present. The reaction was faster than diphenyl phosphate **26** by 10^{10} fold with a half-life of 10.2 min at 39 °C. The reaction is accounted for in terms of intramolecular nucleophilic catalysis by the COO⁻, and intramolecular general acid catalysis by the ortho-COOH, Scheme (1-6). The general acid catalysis is unexpectedly inefficient. However, nucleophile catalysis is limited by COOH as a general acid due to COOH being deprotonated at pH 3.76.²⁶ To follow the reaction of phosphate transfer, which involves a general acid catalysis, needs model systems active above pH 4 and near pH 7 to mimic biological system.

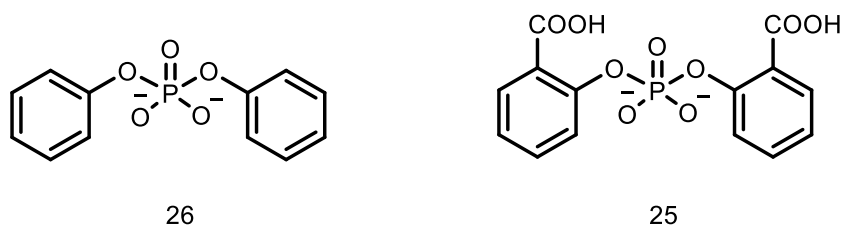
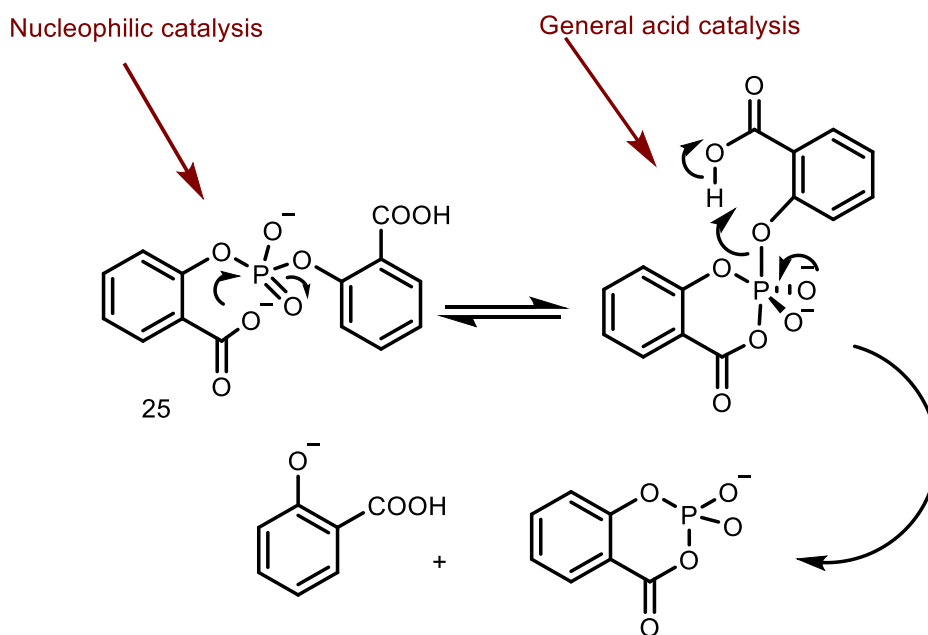


Figure (1-15): The structure of bis-2-carboxyphenyl phosphate and diphenyl phosphate.³²



Scheme (1-6): Hydrolysis of aryl 2-carboxyphenyl phosphate anions studied Kirby *et al.*³²

Recently, Orth *et al.*³³ have studied the role of two imidazole groups in the hydrolysis of phosphodiester, in which these two groups can mimic two histidine imidazoles in enzymes of the phospholipase D superfamily³⁴ and Ribonuclease (RNase A).³⁵ The protonated imidazole group of histidine can act as a general acid while the free imidazole was thought to act either as a nucleophile³⁴ or a general base.³⁵ They found that the hydrolysis of bis (2-(1-methyl-1H-imidazolyl) phenyl) phosphate **27[±]** is catalysed by two imidazole groups. In considering the experimental data and computational results, the mechanism shown in Scheme (1-7) has been suggested. This suggests that bifunctional catalysis of the zwitterionic species **27[±]** occurs through efficient intramolecular nucleophilic catalysis by neutral imidazole and general acid catalysis by the imidazolium group to assist the departure of the leaving group. Because of the absence of imidazole groups, the hydrolysis of biphenyl phosphate is slower than **27[±]** by a factor of about 10^7 . Comparing the hydrolysis rate constants (k_{obs} for **28⁺** = 5.83×10^{-6} , **29⁺** = 3.65×10^{-6} and k_{obs} = 1.98×10^{-3} for BMIPP[±] **27[±]**, Figure (1-16), shows that the hydrolysis of **29⁺** is appreciably slower, by a factor of up to 540, than that of the corresponding diester **27[±]**.

In addition, diester 27^{\pm} is found to be more reactive than 27^{+} , hydrolysing about 100 times faster. These results support the role of neutral imidazole as either a general base or nucleophile. The hydrolysis of diester 28^{+} is observed to be approximately 8 times faster than hydrolysis of monoester 27^{+} . This reduced reactivity could be attributed to the steric effect of the methyl group in 27^{+} . In addition, the difference in the reactivity between 28^{+} and 29^{+} is two-fold. This is presumably due to the effect of the N-methyl group on the planarity of the system, thus, decreasing the catalytic efficiency of the imidazolium general acid. In conclusion, based on the detection of a short-lived intermediate, it was proposed that the neutral imidazole group is involved in concerted intramolecular nucleophilic catalysis, although IGBC mechanism by the free imidazole group cannot be completely ruled out.³⁶⁻³⁸

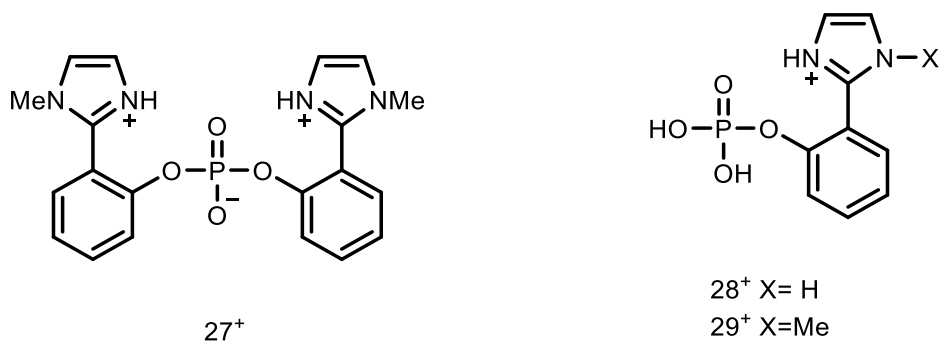
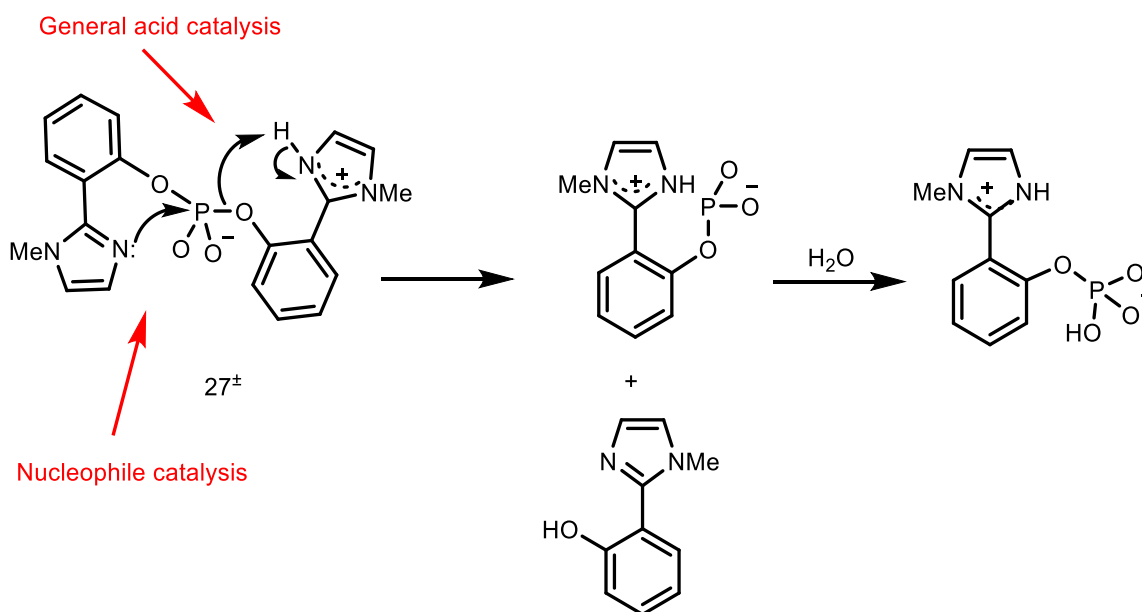
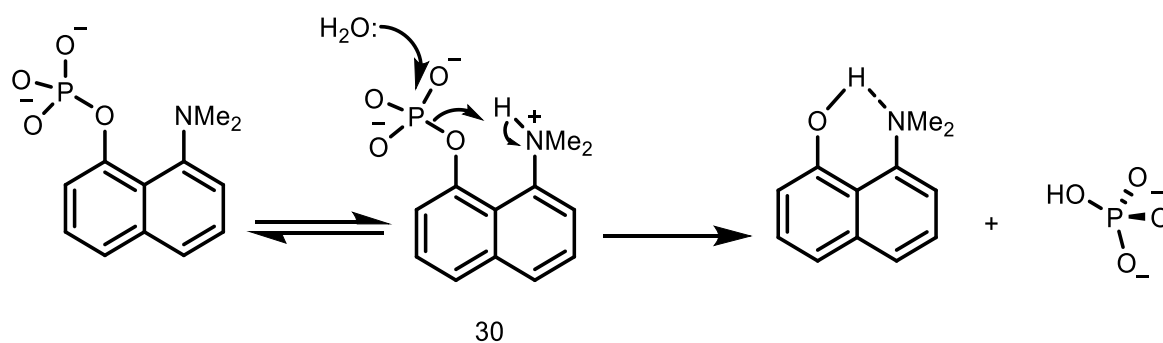


Figure (1-16): Structure of phosphate diesters 29^{+} , 27^{+} and 28^{+} .³⁶

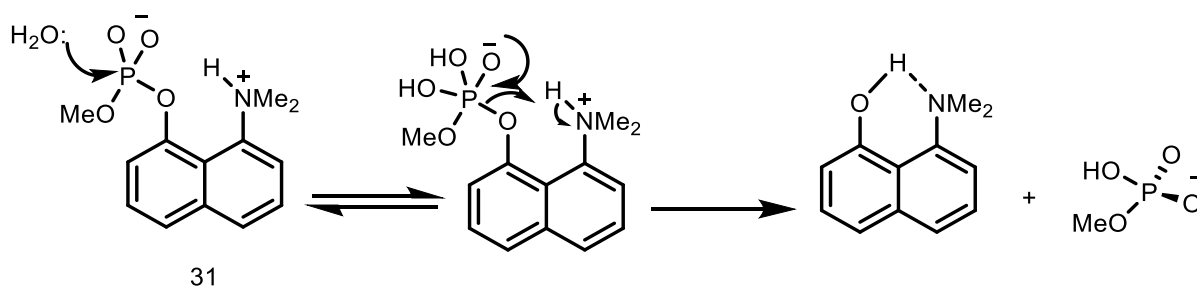


Scheme (1-7): Hydrolysis of bis(2-(1-methyl-1H-imidazolyl)phenyl) phosphate 27^{\pm} by two imidazole.³⁶

The cleavage of the conjugate acids of 8-dimethylammonium-naphthyl-1-phosphate esters mono, di and triesters, was studied to probe the effect of the neighbouring Me_2NH^+ group on the hydrolysis and the reaction with nucleophiles. The hydrolysis of the monoanion **30** was found to be catalysed by dimethyl ammonium Me_2NH^+ through a strong hydrogen bond with a 10^6 rate acceleration comparing with diethyl naphthyl-1-phosphate. The corresponding diester, methyl 8-dimethylamino-1-naphthyl phosphate **31**, has also showed the same effect of dimethyl ammonium Me_2NH^+ on the hydrolysis and nucleophilic attack of oxyanions; intramolecular hydrogen bonding is involved and considered the key of the general acid catalysis, Scheme (1-8) and Scheme (1-9). The strong hydrogen bond is present in the product, and in the ground state.³⁹⁻⁴⁰



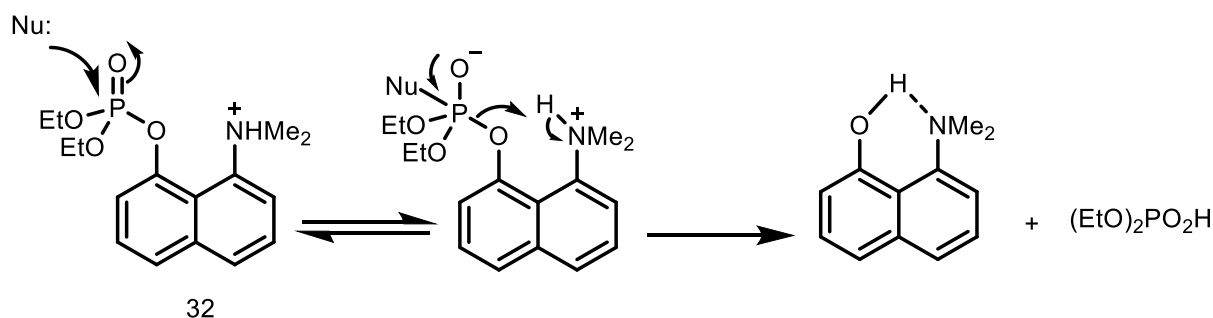
Scheme (1-8): The hydrolysis of 8-dimethylammonium-naphthyl-1-phosphate monoanion.³⁹



Scheme (1-9): The hydrolysis of methyl 8-dimethylamino-1-naphthyl phosphate.⁴⁰

The hydrolysis of the corresponding triester (3H^+) **32**, diethyl 8-dimethylaminonaphthyl-1-phosphate Scheme (1-10), is catalysed efficiently by the neighbouring Me_2NH^+ group. The key to efficient intramolecular proton-transfer catalysis appears to be an intramolecular hydrogen

bond between the ammonium Me_2NH^+ general acid and the leaving-group oxygen, which is strong in the product and transition states, but weak or absent in the ground state. It shows more efficient general acid catalysis than other compounds such as acetal 8-dimethyl-1-methoxymethoxynaphthalene²⁷ and esters **30** and **31**. Kirby et al. found that the hydrolysis of triester **32** is catalysed by dimethyl ammonium Me_2NH^+ through strong intramolecular hydrogen bond. The rate acceleration of diethyl 8-dimethylaminonaphthyl-1-phosphate is 10^6 compared with diethyl naphthyl-1-phosphate.²⁸



Scheme (1-10): Hydrolysis of diethyl 8-dimethylamino-1-naphthyl phosphate.²⁸

The pK_a of the triester is 4.63, which is different to that of monoester **30** and diester **31** which have pK_a s of 9.31 and 7.06, respectively. It was suggested that this variation depends on the strength of hydrogen bond between the NH^+ and the leaving group oxygen. In triester **32**, the strong hydrogen bond is present in the transition state and the product, but little or absent in the reactant. The proton sponge geometry, which is known to have a strong hydrogen bond ($\text{N}\cdots\text{H}\cdots\text{N}$), leads to a stabilisation of these systems. From the pH profile, Figure (1-17), the rate constant of hydrolysis at pHs above the pK_a of the ester was found to decrease. The neutral amine is unreactive, due to the absence of intramolecular hydrogen bond and destabilisation of the negative charge developing on the leaving group in the transition state.³⁹⁻⁴⁰

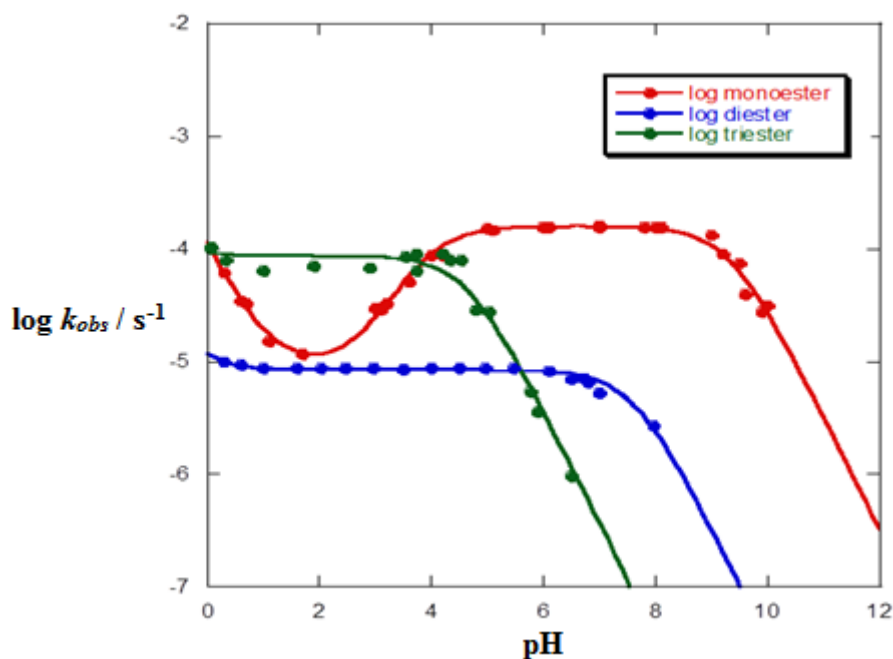


Figure (1-17): pH rate profile for hydrolysis of mono-, di- and triester (**30**, **31** and **32**). The points are derived experimentally and the curves are best fit for the reactions of the different ion forms.^{28, 39-40}

In a further study, Williams *et al.* have studied how changing the ability of a proton donor affects the rate of hydrolysis. They altered the methylation of amine in triester **32** as shown in Figure (1-18), but found no significant effect on the rate of P-O cleavage. This reflected that the effect of methylation of the amine on the rate of P-O cleavage in the triester is not an important factor.⁴¹

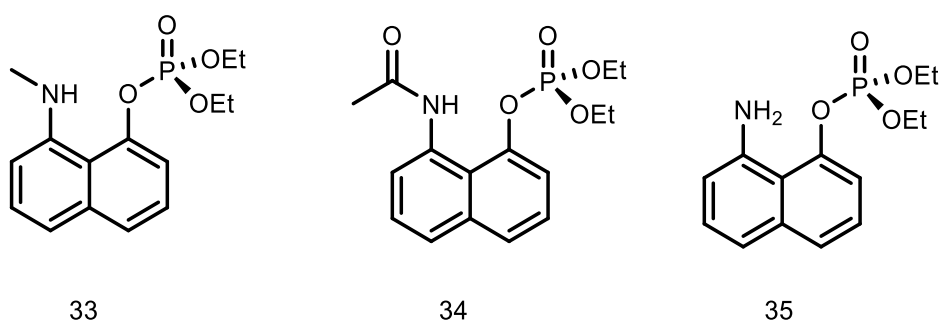
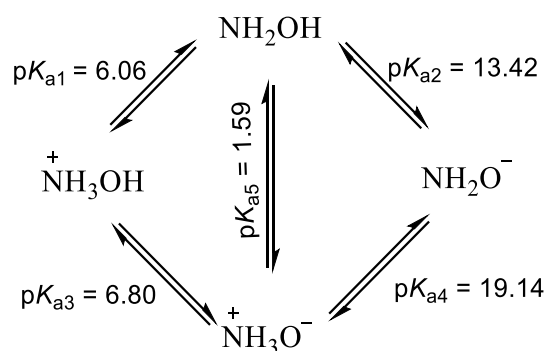


Figure (1-18): Compounds have been studied by Williams *et al.*⁴¹

Although many studies of phosphate ester hydrolysis have investigated efficient general acid catalysis in phosphate transfer reactions in water and with many nucleophiles, distinguishing between hydrogen-bond catalysis and general acid catalysis is often difficult.

1.3. The reaction of hydroxylamine with phosphate esters

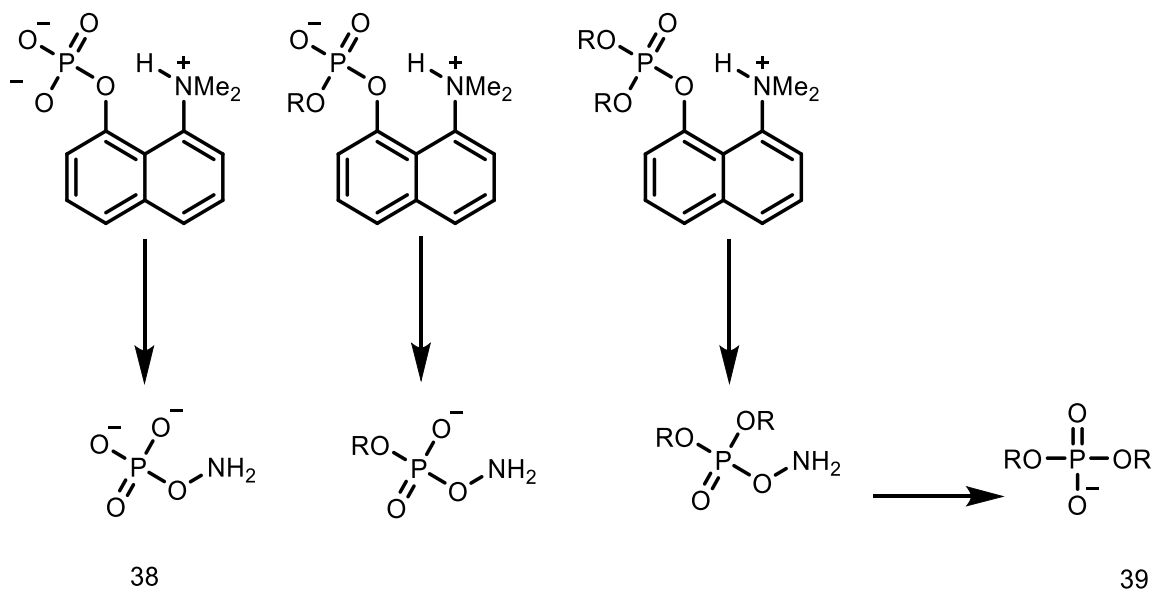
Hydroxylamine is known to be a useful, powerful nucleophile that can be employed in the conversions of phosphoryl groups of phosphate esters and in nucleophilic substitutions of carboxylate esters.^{40, 42-44} Extensive computational and experimental studies of reactions involving hydroxylamine have been discussed in the literature due to its remarkably high reactivity in nucleophilic substitutions. Hydroxylamine can be alkylated on nitrogen, or acylated and phosphorylated on oxygen.⁴⁵ Hydroxylamine can be present in various forms in three distinct regions of pH: acid, neutral and alkaline region, Scheme (1-11). It was shown that the reaction through oxygen is via its ammonia oxide tautomer $\text{H}_3\text{N}^+\text{O}^-$, in which state almost 20% of hydroxylamine exists in water and this reactivity appears in the neutral pH region because the pK_a of hydroxylamine is 6.06 at 25 °C⁴³⁻⁴⁴, and reported to be (5.96 at 25 °C)⁴⁶. At high pH 13.4 and above, hydroxylamine is mainly present in its anionic form, which is the responsible for the reactivity in this pH region.⁴³



Scheme (1-11): Equilibria for hydroxylamine and its known ionic species and pK_a values for hydroxylamine and its derivatives in aqueous solution at 25 °C; Experimental values ($\text{p}K_{a1}$ and $\text{p}K_{a2}$)⁴³, and Computed values ($\text{p}K_{a3}$, $\text{p}K_{a4}$ and $\text{p}K_{a5}$)⁴⁶.

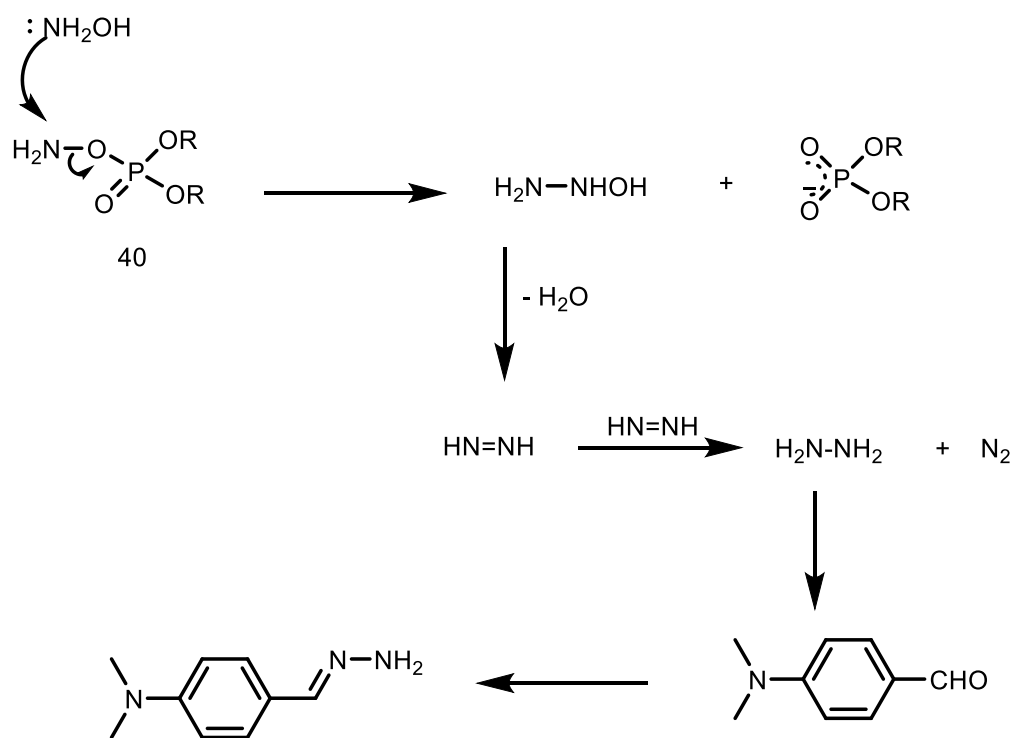
Kirby *et al.* have reported studies of the reactions of hydroxylamine with 8-dimethylamino-1-naphthyl phosphate esters **30-32**. Hydroxylamine shows higher reactivity than the spontaneous hydrolysis, which is attributed to the reactivity of the zwitterionic tautomer ammonia oxide, $^+\text{H}_3\text{N}-\text{O}^-$, as the active nucleophile. Notably, the hydroxylamine reaction with 1-naphthyl phosphate esters was found to be slower than 8-dimethylamino-1-naphthyl phosphate esters

30-32. This can be attributed to the formation of a hydrogen bond between Me_2NH^+ and leaving group oxygen, which stabilises the developing negative charge in the transition state. Therefore, it is clear that this enhancement relies on breaking and forming bonds in the transition state; more bond formation to the nucleophile (NH_2OH) leads to the generation of negative charge on the leaving group. Interestingly, the product of hydroxylamine reaction with phosphate triester was not the simple substitution product, which might be expected. Only one phosphorus-containing product (diethyl phosphate **39**) was formed as detected by ^{31}P NMR, whereas the products of the reaction with phosphate mono- and diesters are the hydroxylamine-O-phosphate, Scheme (1-12). This result poses the question: what is the mechanism for the reaction of the triester with hydroxylamine?



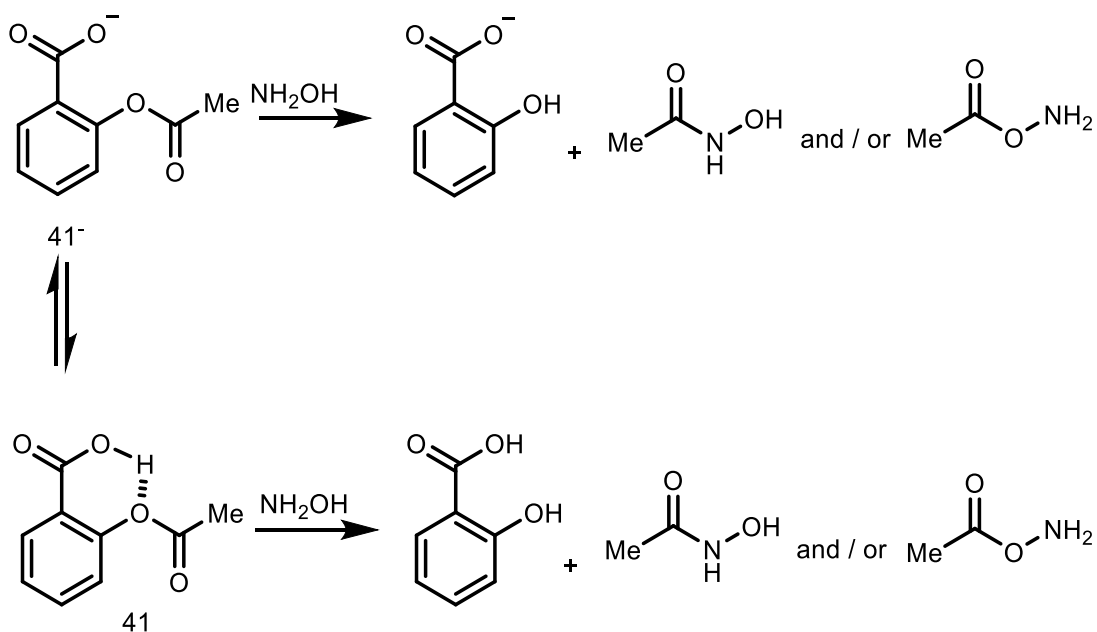
Scheme (1-12): The hydroxylamine-phosphate products of mono-, di- and triesters.

Analysis of the products of the reaction revealed the formation of nitrogen and hydrazine. The latter was detected by formation of the hydrazone derivative of p-dimethyl amino benzaldehyde. The generation of hydrazine was suggested to occur by the attack of a second hydroxylamine molecule on ammonia diethyl phosphate, Scheme (1-13).



Scheme (1-13): Suggested mechanism for the decomposition of hydroxylamine-O-phosphate 40 in the presence of an excess of hydroxylamine.^{44, 47}

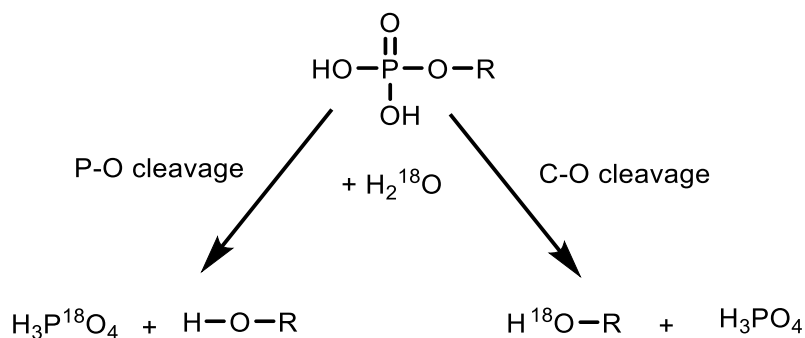
In a further study, Kirby *et al.* also studied the reaction of hydroxylamine with aspirin. The reaction was found to proceed predominantly through ammonia oxide, $^+\text{H}_3\text{N}-\text{O}^-$, to give O-acetyl hydroxylamine as the initial product, Scheme (1-14). Enhancement of the rate up to 10^4 -fold was observed in the presence of 0.3 M hydroxylamine. The pH profile showed an increase in the rate with increasing of pH, which involves both CO_2^- and CO_2H forms of aspirin, **41**⁻ and **41** respectively. However, the reaction of hydroxylamine with the CO_2H form of the substituted aspirins was found to be faster than that for reaction with the anionic form, 2.65×10^{-1} and $2.18 \times 10^{-2} \text{ M}^{-1} \text{ s}^{-1}$, respectively. This can be due to the suggested leaving group stabilisation, by intramolecular proton transfer from the carboxylic acid moiety through an intramolecular hydrogen bond by the CO_2H group, similar to the transition state defined in the intramolecular general acid catalysis mechanism favoured by Kirby for phosphate esters.⁴⁸



Scheme (1-14): The reactions of protonated and anionic aspirin with hydroxylamine at 25.0 °C and ionic strength = 1.0 M (KCl).⁴⁸

1.4. Phosphate ester hydrolysis as a model reaction

Phosphate hydrolysis is a simple reaction and may occur in one of two possible ways, which involve P–O cleavage or C–O cleavage depending on the site of attack of a nucleophile, Scheme (1-15). As an example of this, the uncatalyzed hydrolysis of dimethyl phosphate, proceeds by at least 99 % C-O bond cleavage at 25 °C, and so with an upper limit of $1 \times 10^{-15} \text{ s}^{-1}$ for the rate of spontaneous P–O cleavage.⁴⁹⁻⁵⁰



Scheme (1-15): Possibly ways of phosphate hydrolysis.⁴⁹

Phosphate esters are extremely stable bonds, and resistant to cleavage under mild aqueous solutions without efficient catalysts. The hydrolysis of phosphate mono-, di- and triesters can be accelerated by specific or general acid base-catalysis, and/or metal ion-catalysis.⁵¹

In biological systems, reactions involving phosphoryl transfer are ubiquitous, including phosphorylation and dephosphorylation, which are accelerated by different enzymes, kinase and phosphatase, respectively. Kinase enzymes catalyse the transfer of phosphoryl groups from nucleoside triphosphates such as ATP to various organic compounds, and phosphatases transfer phosphoryl groups from organic compounds to water, which is a hydrolysis reaction. As an example, the spontaneous hydrolysis half-life of phosphodiester DNA is 31 million years. In contrast, spectacular rates are achieved in catalysed hydrolysis by enzymes: for example, *staphylococcus* diesterase accelerates phosphate anion hydrolysis up to 6×10^{14} , and a rate enhancement of 2×10^{16} is achieved for the phenyl phosphate dianion cleavage by *Yarsinia* monoesterase.^{49, 50}

For many kinases and phosphatases, the hydrolysis of phosphate mono and diesters involves cooperation of metal ions and functional groups as general acids, bases, or nucleophiles, resulting in high catalytic efficiency. However, many of these enzymes involve hydrogen bonding. Since the enzyme's structure is much more complicated, it is difficult to study the natural mechanisms of hydrolysis in these esters, so it is often useful to work with simpler artificial models. A reactive system with a good and convenient leaving group rather than a poor leaving group can simulate the active site of the enzyme, and elucidate the mechanisms by which phosphate ester hydrolysis is activated by hydrogen bonding. Breaking the P-O bond in phosphate esters is known to be slow and needs catalysis of correspondingly high efficiency to achieve biologically useful rates such as found in enzymes.

Importance of phosphate triesters: We chose a phosphate triester model as substrate of the hydrolysis reaction of phosphate esters. Phosphate triesters do not occur naturally in biological

systems as mono and diesters do, and thus their importance in biological systems seems to be ignored. Their importance comes from the industrial field as huge quantities of organophosphorus compounds were made, and some of them showed toxic activities such as warfare agents,⁵²⁻⁵⁴ pesticides and insecticides. For examples, triesters such as methyl-paraoxon, a phosphate-based toxic pesticides and Sarin phosphate-based chemical warfare agents, are capable of disrupting biological functions. Thus, there are attempts to overcome stockpiles of toxic organophosphorus pesticides, nerve gases as well as herbicides. These attempts run into challenges such as employing enzymes that are capable of hydrolyzing and detoxifying such agents and convert them into nontoxic and safely species; for example bacterial enzyme capable of hydrolyzing the lethal organophosphate nerve agents.⁵⁴ Nature has evolved enzymes in response to this challenge. A new class of enzyme showed high phosphotriesterase activity that seems to be due to the high use of these toxic materials.⁵⁵ Phosphotriesterase enzymes, which are a group of organophosphate hydrolysis enzymes (OPHs), are classified under the aryl-dialkyl-phosphatase family. These enzymes can hydrolyse the phosphotriesters, thiophosphotriesters, and phosphorothiolesters to become nontoxic agents. Usually the products of the hydrolysis catalysed by these enzymes are derived from cleavage of the P-O bond where the aryloxy group is a leaving group. However, the unique phosphotriesterase from *Sphingobium* sp. TCM1 (Sb-PTE) shows a different selectivity towards the cleavage of phosphate triesters. It has an ability to cleave an alkyl group as well as the phenyl group from the central phosphorus. Bigley *et al.* have studied different diethyl phenyl triesters and found that this enzyme can hydrolyse the substituted aryl and alkyl of the same substrate. For example diethyl phenyl phosphate is hydrolysed by Sb-PTE to give only 23% cleavage of the phenyl group, in addition to ethyl group cleavage.⁵⁶

Thus, there has been intensive work done in studying enzymes, proteins, and small molecules, which are capable to cleave phosphate-ester efficiently, particularly on nitro-phenol containing

pesticides/nerve-agent simulants to enhance phosphate transfer to water, to convert the active triester agent to an unreactive diester i.e. catalysing the hydrolysis using different strategies.⁵⁵

1.5. The aim of the project

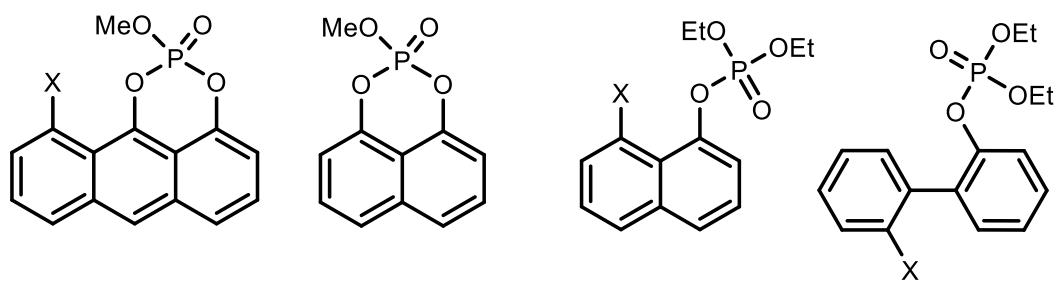
Intramolecular hydrogen bond catalysis has been reported in the literature, but how much this affects reactivity is still a contentious issue. Therefore, the main aim of this research is to investigate the effect of intramolecular hydrogen bonding on the rate of hydrolysis of phosphate triesters. Thus, models with different numbers of intramolecular hydrogen bond donors were designed, synthesised and studied, Figure (1-19).

The substrates for the first model have a single hydrogen bond donor, which could form a hydrogen bond to the oxygen of the leaving group. This should give stabilisation to the negative charge developing on the oxygen in the transition state. These structures will probe the effects of varying the geometry on any effect the hydrogen bonds have on the reaction rate.

Secondly, we will explore multiple hydrogen bonds in systems with two neighbouring groups. Each group can provide a hydrogen bond, which may work cooperatively to provide greater stabilisation to transition state than the statistical sum of the individual hydrogen bonds.

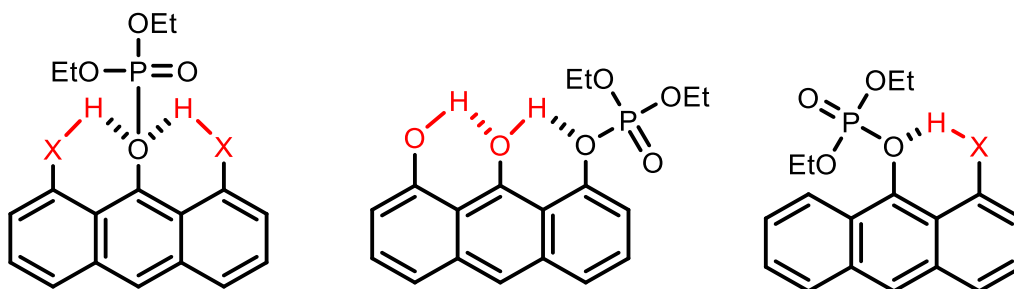
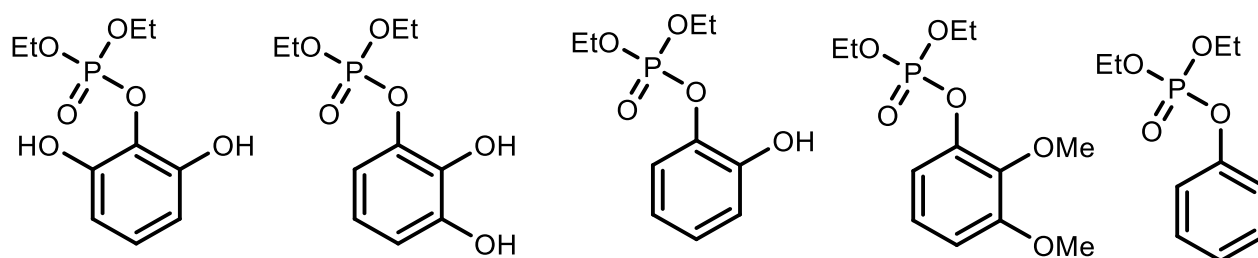
As neighbouring groups could be involved in general acid and /or hydrogen bond catalysis,^{26, 28, 30} a kinetic study of model system **2**, where X is an amino group, will distinguish whether the formation of a hydrogen bond is important or if general acid catalysis is essential for efficient reaction. If the hydrogen bond plays the major role in catalysis, the rate will increase according to the additional energetic benefit. If the general acid is the reason of catalysis, the rate will increase statistically.

Model system 1



X = H / OH

Model system 2



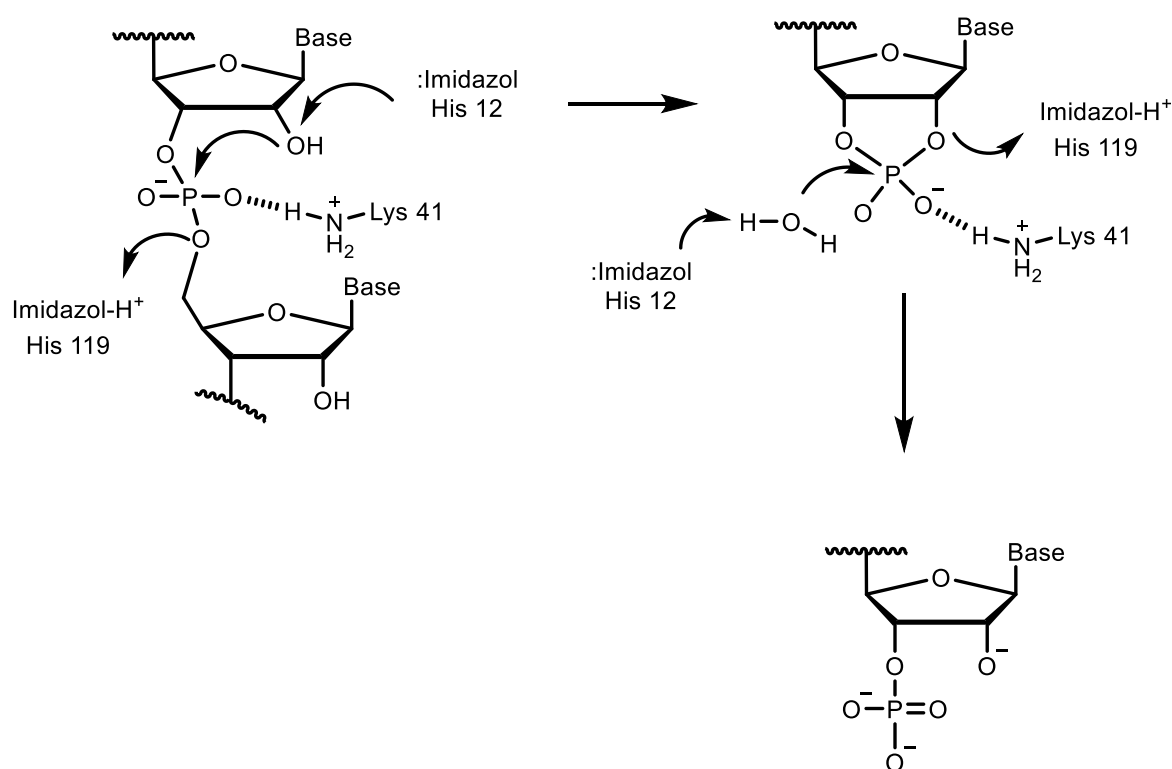
X = OH
NR₂
NH₂

Figure (1-19): Target model compounds (System 1 and 2) proposed for this research.

2 Chapter Two: Cyclic Aryl Phosphate Triesters

2.1 Introduction

Cyclic phosphate ester is known to be an intermediate in some biological processes such as the hydrolysis of phosphate-ester linkages in single-stranded RNA by Bovine pancreatic ribonuclease A (RNase A). For the next step this intermediate undergoes hydrolysis by intermolecular attack from water. The active site of this enzyme applies three kinds of catalysis general base and acid catalysis by His-119, His-12 residues and hydrogen bond catalysis by Lys-41. It was suggested that the hydrogen bond plays a role in stabilising the intermediate, which hydrolyses to monoester phosphate in the second step, Scheme (2-1).⁵⁷



Scheme (2-1): The hydrolysis of phosphate-ester dinucleotides by RNase A by general base and acid catalysis assisted by hydrogen bond.⁵⁷

Hydrolysis of cyclic phosphate esters has been studied. These compounds were found to hydrolyse orders of magnitude faster than the acyclic analogues. Westheimer and Haake showed that cyclic ethylene and methylene phosphate is hydrolysed 10^7 times faster than acyclic phosphate analogues in aqueous solution.⁵⁸ The large enhancement in the rate is attributed to ring strain in the cyclic ester. Cyclic phosphate esters become interesting to

investigate, not just due to their reactivity but also due to the chemical and biochemical activities, such as using cyclic phosphates as potential means for prodrugs delivery.⁵⁹ In addition, some of the cyclic phosphorus esters are toxic compounds such as cyclic phosphorus esters of saligenin which are known to be very strong antiesterase agents and have toxic activity as well. Therefore, efforts are made to study enzymes, proteins, and small molecules aiming to perform phosphate-ester hydrolysis on such agents.⁶⁰

Hydrolysis reactions of phosphate monoesters, diesters, and triesters are different and complex, which made their study to understanding their mechanism of interest over the years. However, most of the relevant work of hydrolysis of cyclic phosphate esters has been done previously with relatively reactive systems in absence of intramolecular catalysis. This includes di and triester, such as shown in Figure (2-1).⁶¹⁻⁶²

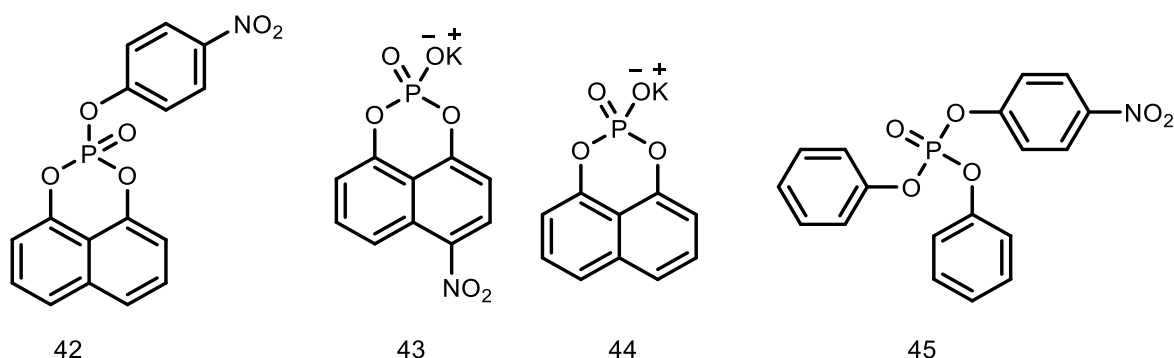


Figure (2-1): Structures of phosphate triesters studied previously.⁶¹⁻⁶²

2.2 Aim

Hydrogen bond catalysis is found to take an important role in phosphate hydrolysis as seen in introduction chapter. Therefore, in this chapter, hydrolysis of aryl cyclic phosphate system, Figure (2-2), with intramolecular hydrogen bond donor is investigated to probe the effect of hydrogen bond to catalyse the reaction. It is thought that a neighbouring hydroxyl group in the precise position on anthracene system would provide an enhancement on the rate compared with no hydroxyl group present. The presence of adjacent catalytic groups, such as hydrogen

bond donors, to the leaving group has been shown to catalyse the hydrolysis reaction. For example, dimethyl ammonium group of methyl 8-dimethylamino-1-naphthyl phosphate showed a high reactivity to enhance the rate of the reaction as general acid catalysis through hydrogen bond (presented in the introduction chapter).^{28, 40, 63} In similar but could not be the same, hydroxyl group should show high reactivity probably as hydrogen bond donor. It is not clear if the reaction would involve general acid catalysis but it is not expected. This prediction is based on the Jencks proposal of the libido rule. The general acid catalysis can be involved in the reaction if only the basicity of leaving group is less than the general acid in the ground state, but become more basic in the product.⁶⁴ In the model used here; 8-hydroxy cyclic anthryl phosphate **46**, the hydroxyl group could play a role as general acid if the pK_a of the leaving group changes during the course of the reaction; become higher than the pK_a of hydroxyl group on position 8. However, if the pK_a s of the leaving group and hydroxyl group are identical, the reaction would involve hydrogen bonding catalysis. Thus, there would be change in the reactivity in presence of the hydroxyl group on triester **46** compared with **47** with the change depending on the activation energy provided by hydrogen bond.

In a second aim, the reactions of a series of nucleophiles, including hydroxylamine, methoxy amine, acetate, and fluoride, with the model **46** are investigated allowing convenient reaction rate to be determined.

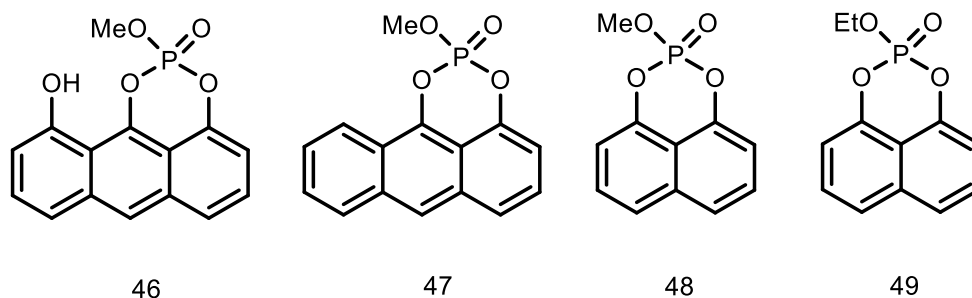


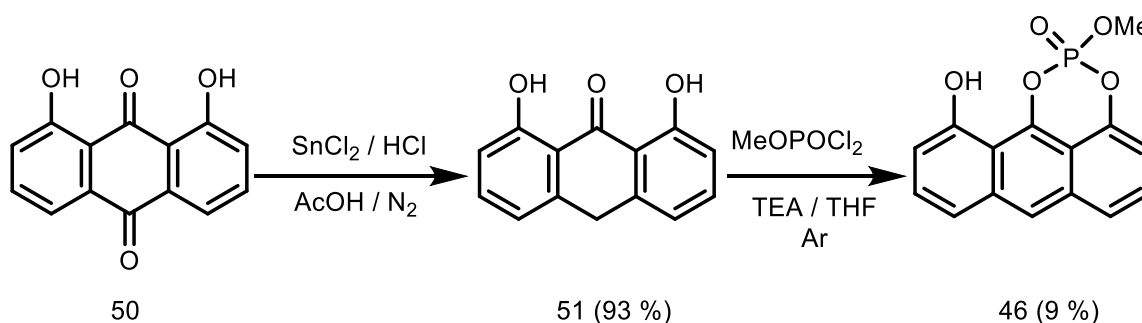
Figure (2-2): Structures of cyclic triester phosphate in this work.

2.3 Result and discussion

2.3.1 Synthesis of Methyl 8-hydroxy-1, 9-anthryl cyclic phosphate 46

Compound **46** was synthesised as shown in Scheme (2-2), using 1, 9-dihydroxy anthraquinone **50**, as the starting material, which is reduced to anthrone **51**. The anthrone reacted with methyl dichlorophosphate to yield cyclic methyl 8-hydroxy-1, 9-anthryl phosphate triester **46**.

The reaction was a challenging as in achieving sufficient quantity and purity for kinetic experiments was difficult. The main issues encountered were instability and the purification of compound **46**, which make the yield of compound low. The reaction was performed under inert and dry condition using N₂ or Ar and THF as a dry solvent. Although using column chromatography failed to yield pure compound with high yield, it was the best method for purification giving a pure sample. ¹H, ³¹P, ¹³C NMR and mass spectrum confirmed the structure. ¹H NMR did not show OH⁻ proton, but was confirmed by IR; IR 3500(OH) cm⁻¹.

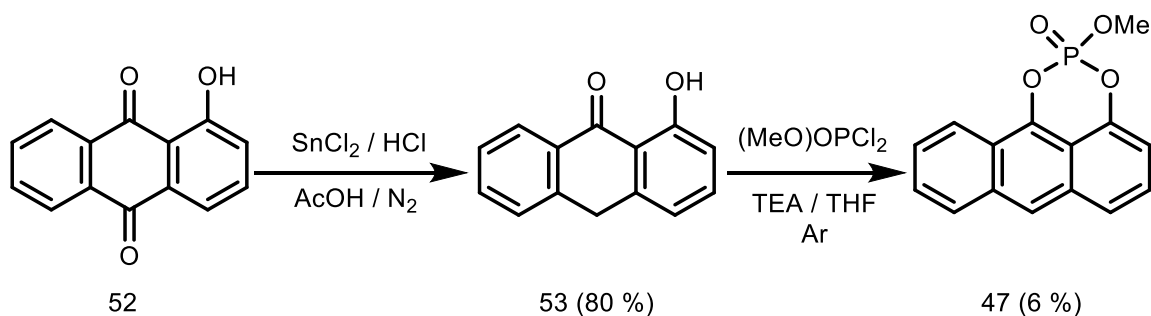


Scheme (2-2): Synthesis of cyclic methyl 8-hydroxy-1,9-anthryl phosphate triester **46**.

2.3.2 Synthesis of Methyl 1, 9-anthryl cyclic phosphate 47

Compound **47** was synthesised as shown in Scheme (2-3) using 1-hydroxy anthraquinone **52**, as starting material in this procedure, which is reduced to anthrone **53**. The anthrone reacted with methyl dichlorophosphate to yield cyclic methyl 1, 9-anthryl phosphate triester **47**. The reaction was performed under dry condition, using Ar and THF. Purification was by column chromatography to yield the pure compound. ¹H, ³¹P, ¹³C NMR and mass spectrum confirmed the structure. However, similar to compound **46**, the synthetic challenge of cyclic methyl 1, 9-

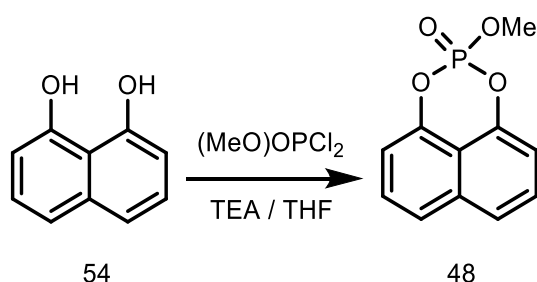
anthryl phosphate triester **47** was found, and the yield was not good, but a sufficient quantity a pure enough for kinetic experiments was obtained.



Scheme (2-3): Synthesis of cyclic methyl 8-hydroxy-1,9-anthryl phosphate triester **47**

2.3.3 Synthesis of cyclic phosphate triester **48**

Compound **48** was synthesised as shown in Scheme (2-4). Triethylamine was added to 1, 9-naphthyldiol **54** with the methyl dichlorophosphate to yield cyclic methyl 1, 9-naphthyl phosphate triester.



Scheme (2-4): Synthesis of yield cyclic methyl 1, 9-naphthyl phosphate triester **48**

Although, the procedure looks simple, the yield was not quantitative, due to the decomposing of the starting material (1, 9-naphthyldiol). Pyrogallol is known to oxidize in alkaline solutions to produce oxidation species such as purpurogallin via quinone, Figure (2-3).⁶⁵

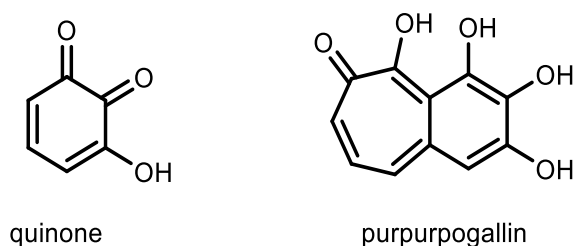
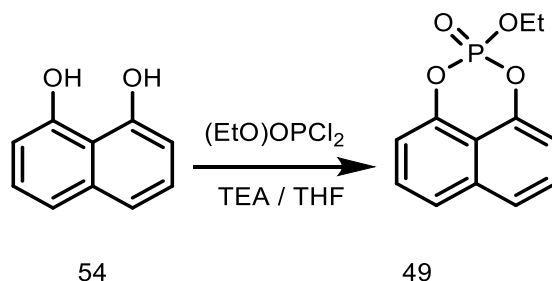


Figure (2-3): compounds formed of pyrogallol oxidation.

2.3.4 Synthesis of cyclic phosphate triester 49

Compound 49 was synthesised as shown in Scheme (2-5). Triethylamine was added to 1, 9-naphthyldiol 54 with the ethyl dichlorophosphate to form cyclic ethyl 1,9-naphthyl phosphate triester.



Scheme (2-5): Synthesis of yield cyclic ethyl 1, 9-naphthyl phosphate triester 49.

2.3.5 Kinetic study

2.3.5.1 The change of absorbance for hydrolysis of triester 46, 47 and 48

Phosphate triesters **46**, **47** and **48** were studied by UV/VIS spectrophotometry, thus scans of the reactions were carried out to determine the wavelength, where the absorbance undergoes maximum change during the reaction.

UV scans of hydrolysis of triesters **46** were taken for different pH 3-7 over a range of 200-800 nm, and after the reaction completed the pH was measured. Figure (2-4), the change of absorbance gave a good isosbestic point, which is the same case for the rest of pH in this range. Scans of the reaction of phosphate triesters **47** and **48** were also carried out as shown in Figure (2-5) and Figure (2-6). From the spectra, changing absorbance of substrates and the appearance of products are observed with good isosbestic points.

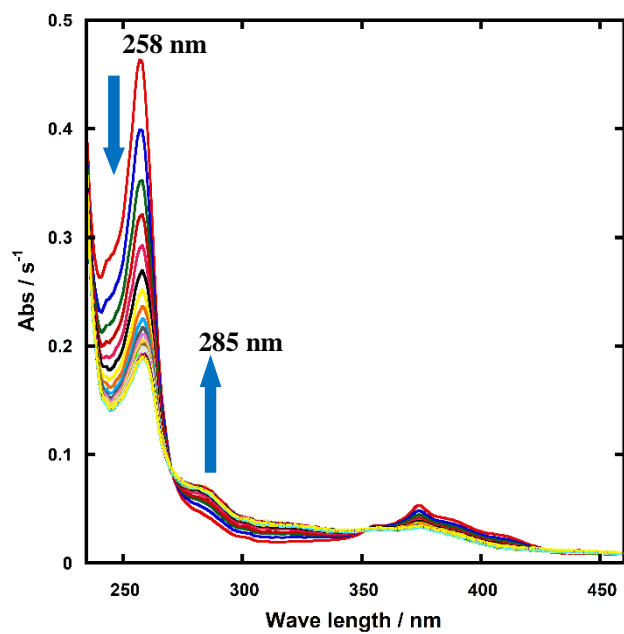


Figure (2-4): Time-dependent spectral changes observed upon the hydrolysis of triester **46** at pH 7. Overall time = 1h and 30 min

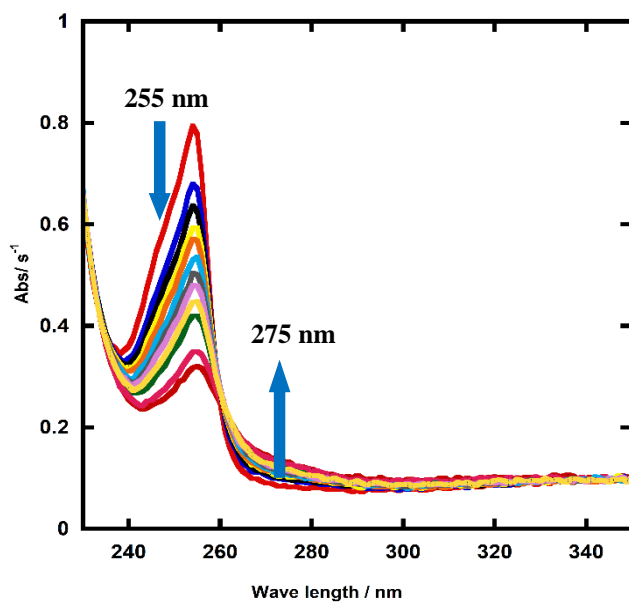


Figure (2-5): Time-dependent spectral changes observed upon the hydrolysis of triester **47** at pH 7. Overall time = 28 h

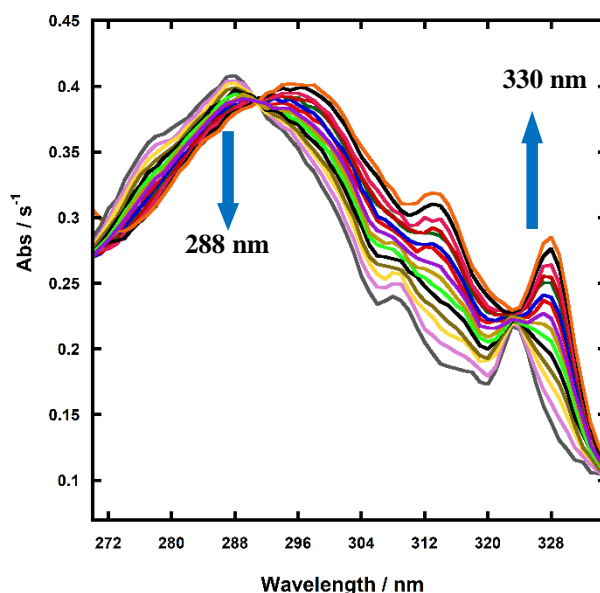


Figure (2-6): Time-dependent spectral changes observed upon the hydrolysis of triester **48** at pH 7.3. Overall
time = 40 h

2.3.5.2 Product analysis of methyl 8-hydroxy 1, 9-anthryl cyclic phosphate **46**

In order to check the products of the hydrolysis of phosphate triester **46**,³ the reaction was monitored by ³¹P NMR at pH = 6. The ³¹P NMR spectrum shows two new peaks at -4.38, -5.23 ppm, which were assigned to diesters **55** and **56** and another peak at -16.12 ppm assigned to cyclic phosphate **57**, Figure (2-7).

Two different hydrolysis routes were proposed, happening by P-O bond cleavage from the ring opening (path **A** and **B**, leading to two degradation products, phosphate diesters (**55** and **56**), Scheme (2-6). It could be that the peak shift at -16.12, which was assigned to cyclic phosphate diester **57**, can be formed either from intramolecular nucleophilic attack by the adjacent hydroxyl group leading to cleaving the P-O bond to replace methoxy group or by intermolecular attack from water on the methyl carbon resulting in C-O bond cleavage. Both reactions have been seen in such hydrolysis reactions of organophosphate esters,⁶⁶⁻⁶⁷ thus both reactions can happen at the same time.

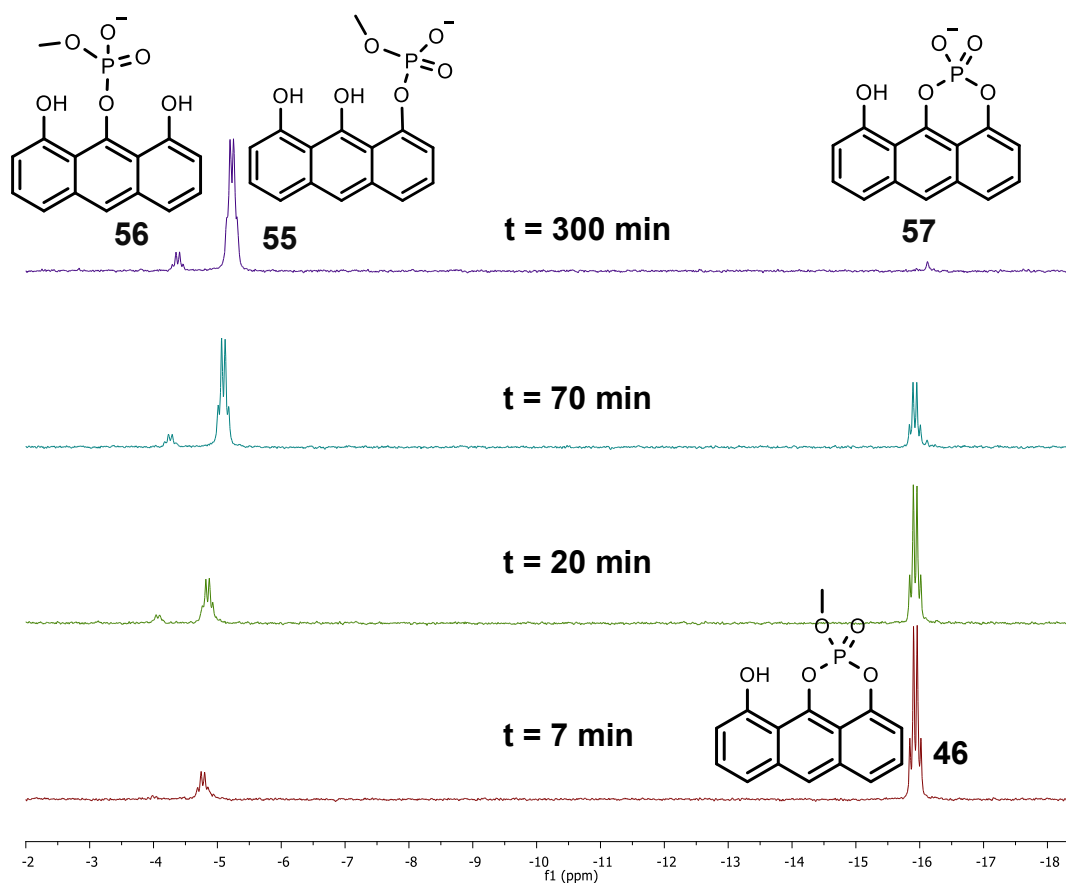
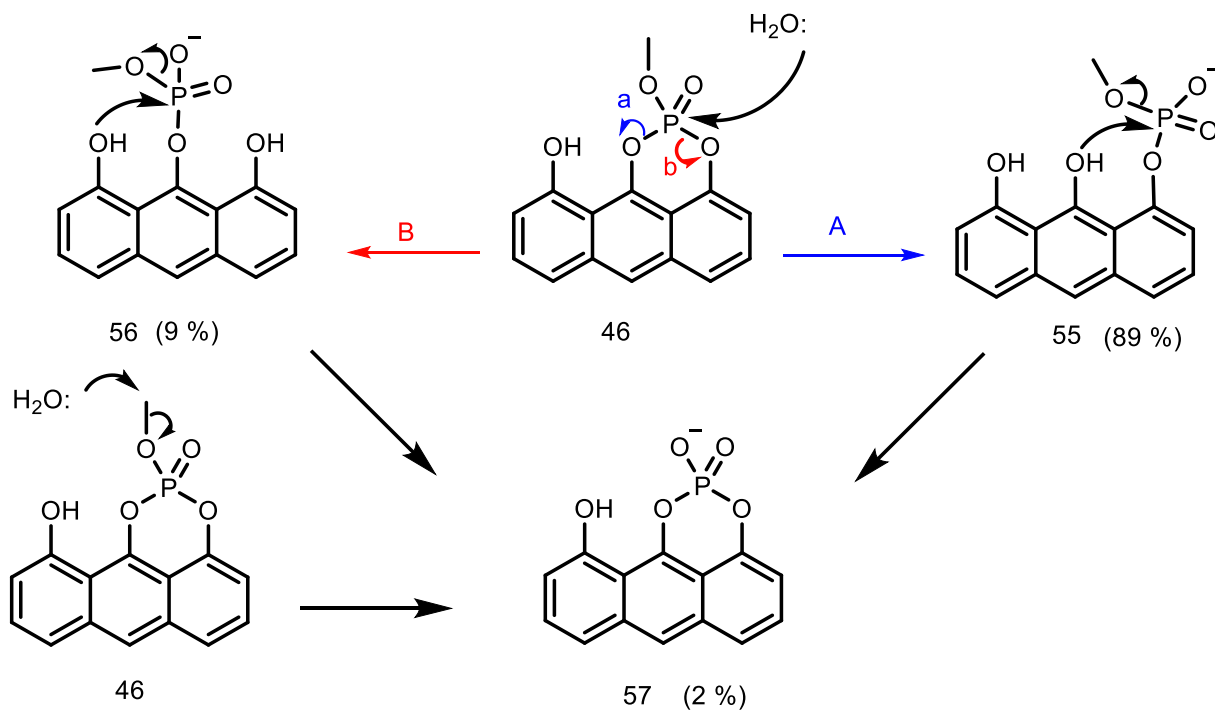
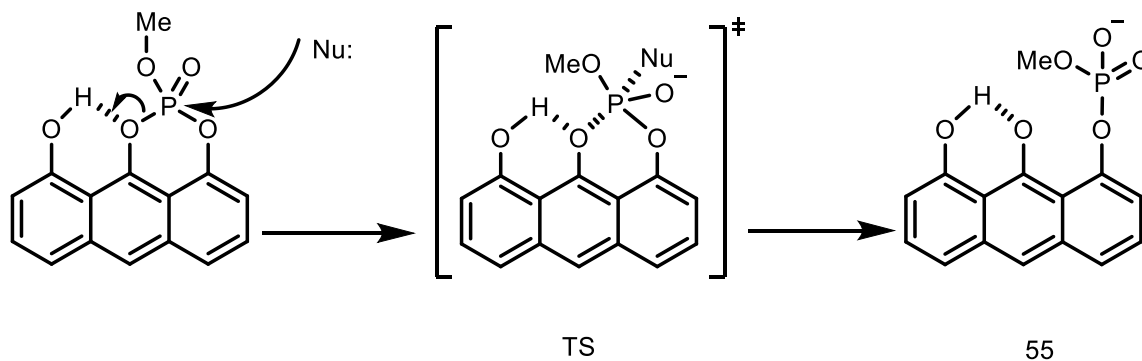


Figure (2-7): Following the hydrolysis of cyclic anthryl phosphate triester **46** using ^{31}P NMR at pH = 6 in DMSO.



Scheme (2-6): The proposed route of hydrolysis of phosphate triester **46**.

It was expected that the P-O cleavage would undergo the way A as the only or the majority cleavage if the adjacent hydroxyl group on anthryl ring could provide significant stabilising effect to the transition state compared to route B, Scheme (2-7).



Scheme (2-7): Proposed reaction mechanism for the opening the ring (route A) of triester **46** under neutral pH conditions.

2.3.5.3 Product analysis of methyl 1, 9-anthryl cyclic phosphate **47**

Hydrolysis of methyl anthryl phosphate triester **47** was followed by ^{31}P NMR at pH = 7 at 25 °C using ^{31}P NMR. Due to the solubility problem in water as the reaction performed in aqueous buffer, DMSO was used as a co-solvent in 50 % volume. ^{31}P NMR spectrum shows three peaks at -4.11, -1.94 and -13.58 ppm, which are assigned to diesters **58**, **59** and **60**, Figure (2-8). The reaction mixture was analysed by mass spectroscopy to investigate the products of the reaction. In corresponding to the information available of the mass spectrum, the products should be diesters **58** and / or **59**, and **60**.

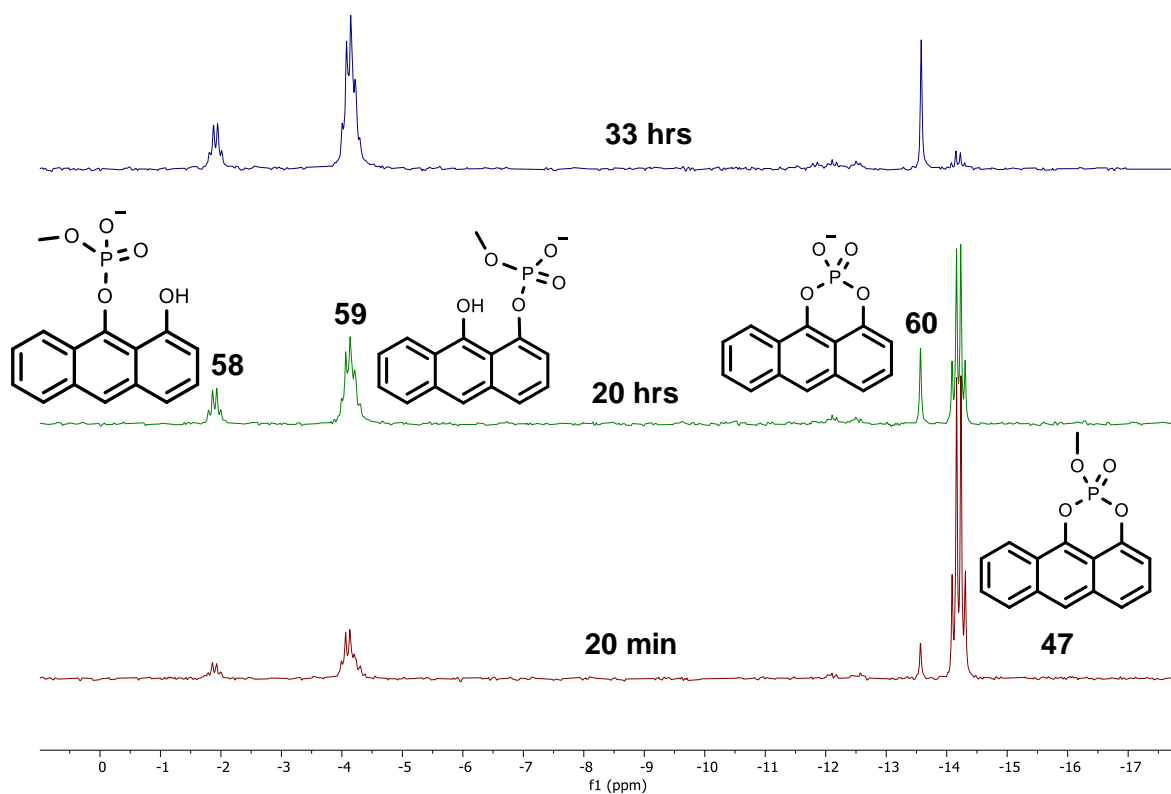
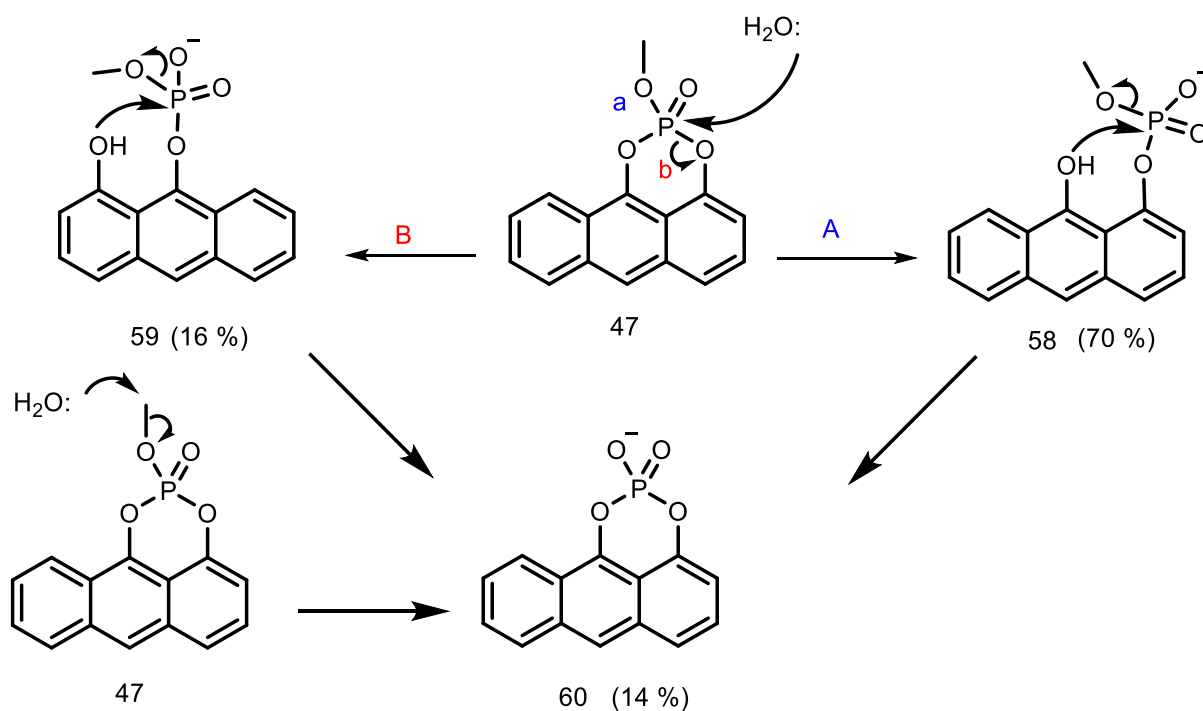


Figure (2-8): Following the hydrolysis of cyclic anthryl phosphate triester **47** using ^{31}P NMR at pH = 6 in DMSO.

In combination of initial analysis from mass spectrum and ^{31}P NMR, phosphate triester **47** could undergo hydrolysis according to proposed route summarised in Scheme (2-8). This route can be explained as following points:

The hydrolysis could happen through P-O bond cleavage from the ring opening (path A and B, leading to a two degradation products, methyl anthryl phosphate (**58** and **59**), which would undergo intramolecular nucleophilic attack by deprotonated hydroxyl group to displace methoxy group resulting in cyclic diester **60** as shown in Scheme (2-8).



Scheme (2-8): The proposed route of hydrolysis of cyclic phosphate triester **47**.

2.3.5.4 Product analysis of hydrolysis of methyl naphthyl cyclic phosphate **48**

The hydroxylamine reaction with cyclic phosphate **48** were monitored by ^{31}P NMR at 25 °C using DMSO in 50 % of total volume. Interestingly, the reactions were not exclusively P—O cleavage of opening ring, as expected. As the ^{31}P NMR spectra showed, there are two products with shifting, singlet peaks at -13.63 ppm and (quartet peak) -4.30 ppm, indicating for cyclic diester **61** and acyclic diester **62**, respectively. This result was confirmed by mass spectrum after the reaction finished. The question here is whether the cyclic ester **61** formed from diester **62** as result from intramolecular nucleophilic attack or direct from cyclic triester **48**, Scheme (2-9). Two possible ways could be the result of this case: (i) an intermolecular nucleophile attack on methyl carbon of triester **48** lead to C-O bond cleavage to give cyclic ester **61** (ii) an intramolecular nucleophile attack of deprotonated OH-group leading to methoxy groups as a leaving group. However, the $\text{p}K_{\text{a}}$ of methoxy groups is about -13.63, which turns out that displacement of the ethoxy groups unlikely to compete with the reaction of interest (the $\text{p}K_{\text{a}}$ is about 9 for first OH of naphthyl ring). Thus, the reaction was monitored for a longer time after

disappearing of starting material. As could be seen from Figure (2-9), after the disappearance of starting material, the formation of cyclic phosphate **61** did not increase and there was no significant decrease of acyclic diester **62**. Both cyclic and acyclic diesters were formed in 50:50. After two days, the percentage of these products had not changed significantly, which confirmed that the formation of cyclic ester **61** is exclusively from C—O cleavage of triester **48**. Products of the water reaction was also investigated and found to be the same as the hydroxylamine reaction, where both cyclic and acyclic diesters were formed.

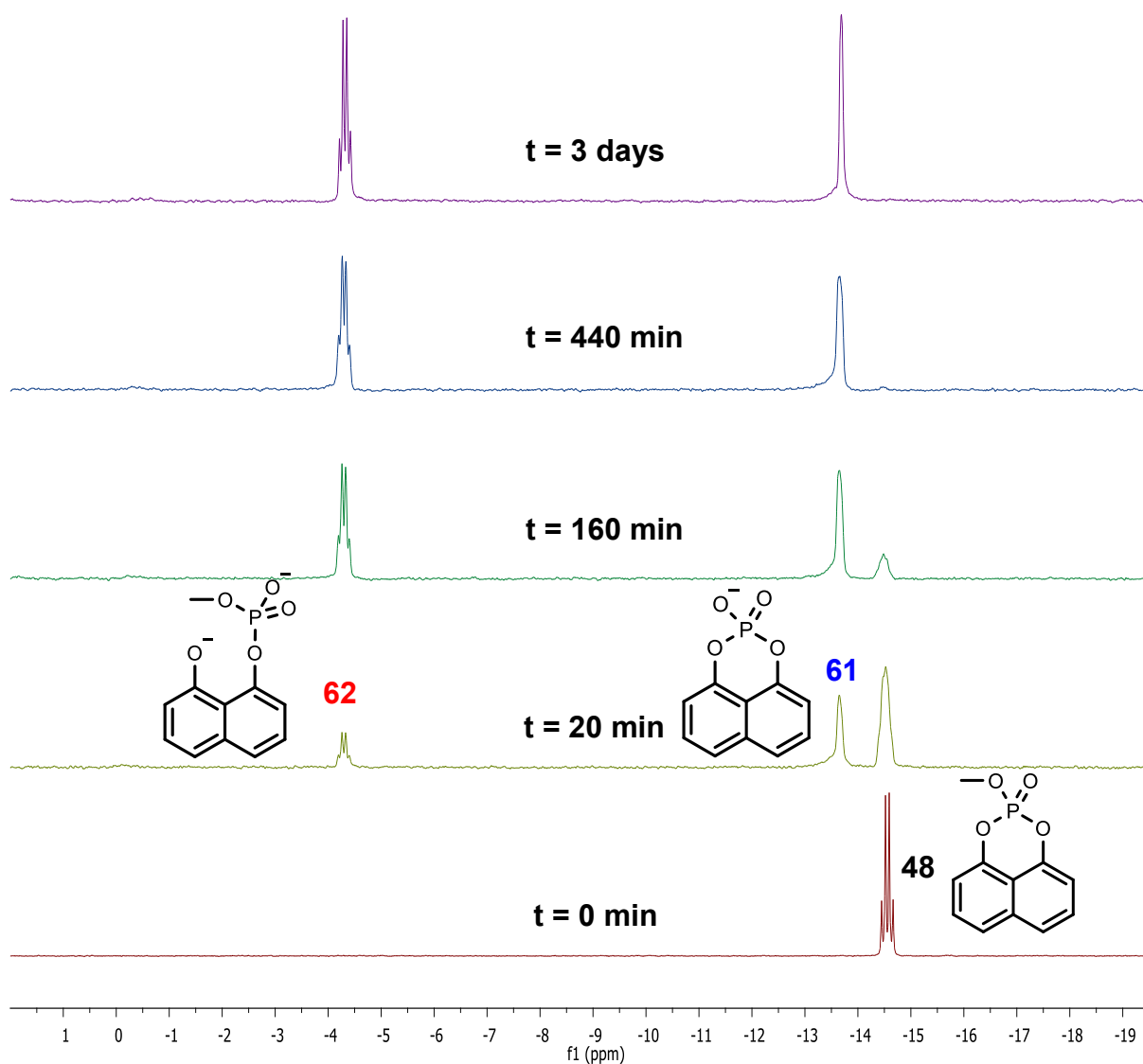
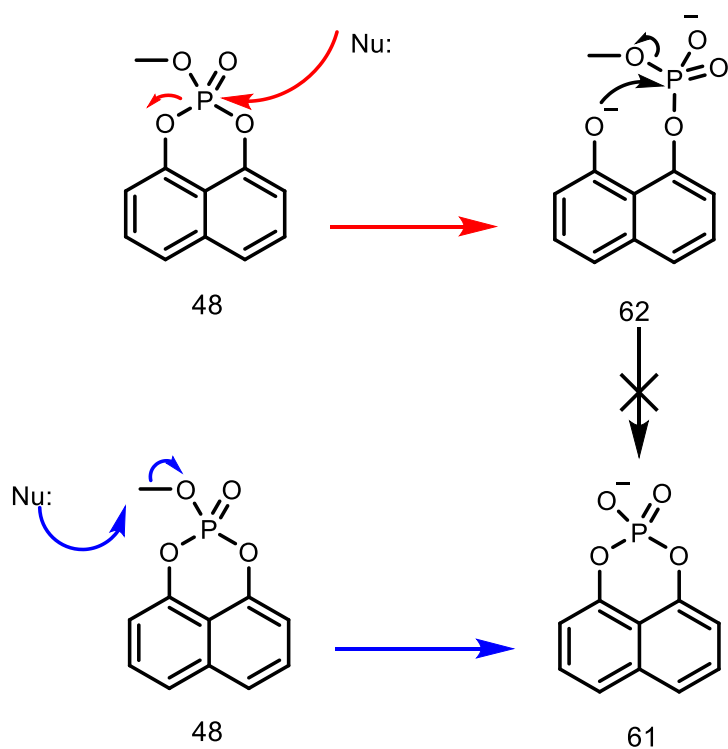


Figure (2-9): Following the reaction of naphthyl methyl phosphate cyclic triester **48** with 0.5 M hydroxylamine by ^{31}P NMR in DMSO at pH 7 and 25 °C.



Scheme (2-9): The route proposed for hydrolysis of phosphate cyclic triester **48**.

On the other hand, to investigate if this case specific for methyl group, ethyl cyclic phosphate ester **49** was prepared and its reaction with hydroxylamine was investigated under similar condition to phosphate ester **48**. A different result was observed and the only product formed was diester **63** of opening ring, Scheme (2-10). It turns out that the difference could be related to the steric effect of alkyl group to the attack on carbon and prevents the C-O bond cleavage, and thus the attack of the nucleophile; hydroxylamine is more accessible for carbon of methyl than ethyl group.

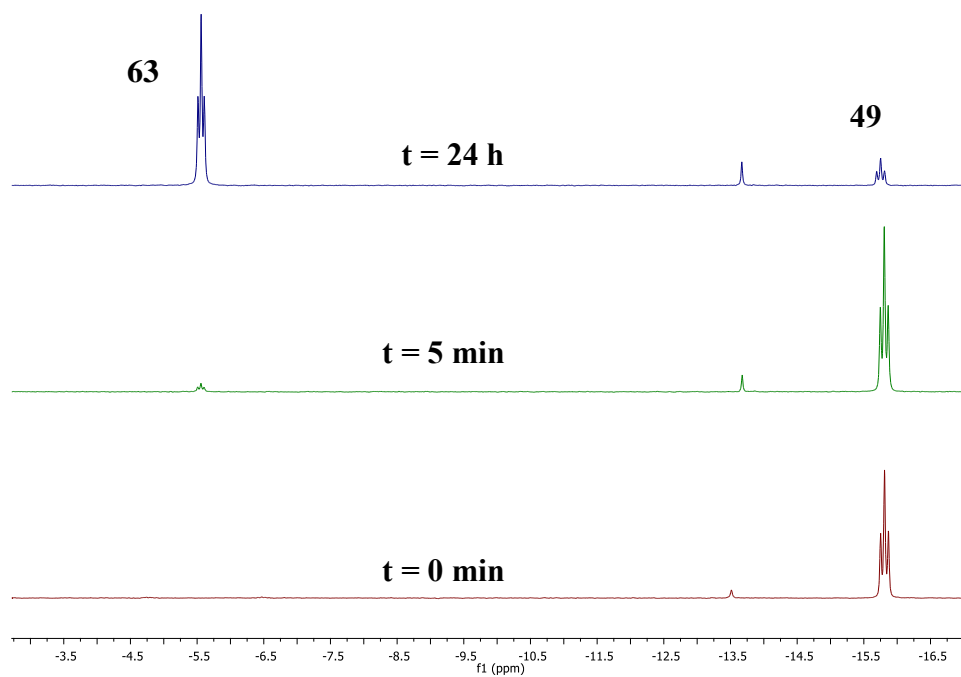
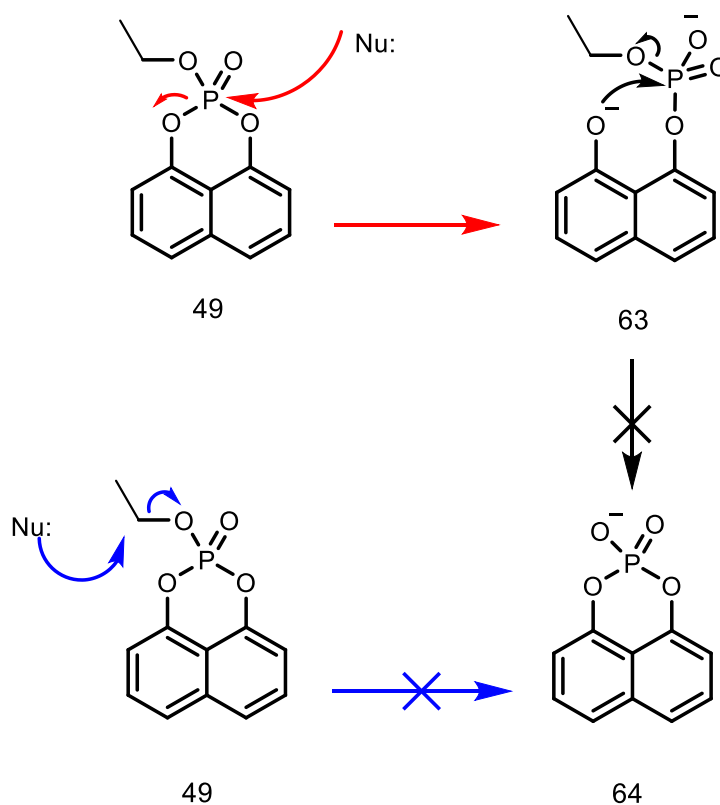


Figure (2-10): Following the reaction of naphthyl ethyl phosphate cyclic triester **49** with hydroxylamine by ^{31}P NMR in DMSO, at 25 °C and pH 7.



Scheme (2-10): The route proposed for cyclic phosphate triester **49** reaction with hydroxylamine.

2.3.5.5 Influence of pH on the chemical degradation of triester **46**, **47** and **48**

The hydrolysis of cyclic phosphates **46**, **47** and **48** have been studied in the range pH 3-10 at 25 ± 0.1 °C and 1 M NaCl using UV-VIS. The reactions were monitored at 258 nm for **46**, and 255 nm for **47**, and 330 nm for **48**. The pH of the reactions was maintained using buffer solutions including MES, EPPS, CHES, CAPS, formic acid and acetic acid. The presence of buffer catalysis was tested for the three phosphates. Unlike cyclic triesters **47** and **48**, hydrolysis of triester **46** showed slight buffer catalysis. Thus, the hydrolysis of triester **46** was performed by varying the concentrations of buffer at the same pH and temperature. Kinetic measurements of compound **46** using buffer catalyst were extrapolated to zero buffer catalyst by plotting the pseudo first order rate constants against the concentration of the buffer, which allowed k_0 to be evaluated for the pH profile. First order rate constants were observed with all buffers used here, and the second order rate constants of the buffer catalysed reaction were obtained by plotting k_{obs} values against the concentration of the buffer. For example, Figure (2-11) showed that the hydrolysis of **46** at pH 6 and 7 (MES buffer) undergoes buffer catalysis. Thus, the buffer is likely to be involved in the reaction as a base to assist the water addition as shown in Scheme (2-11).

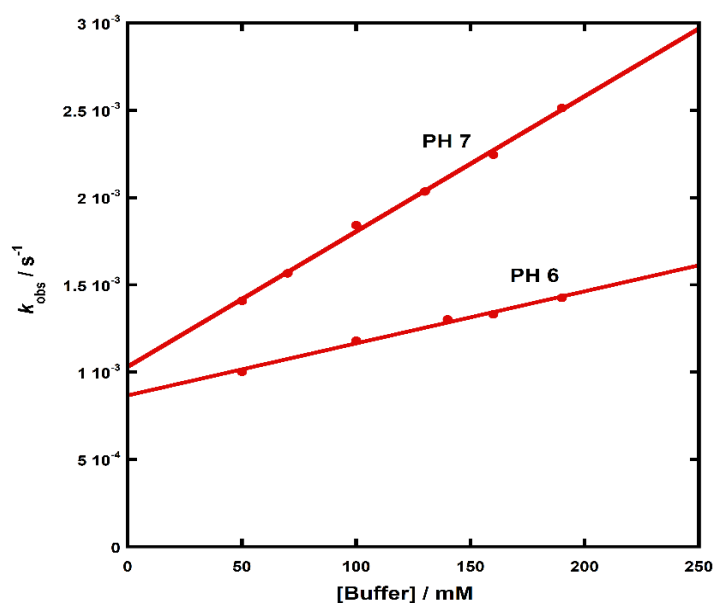
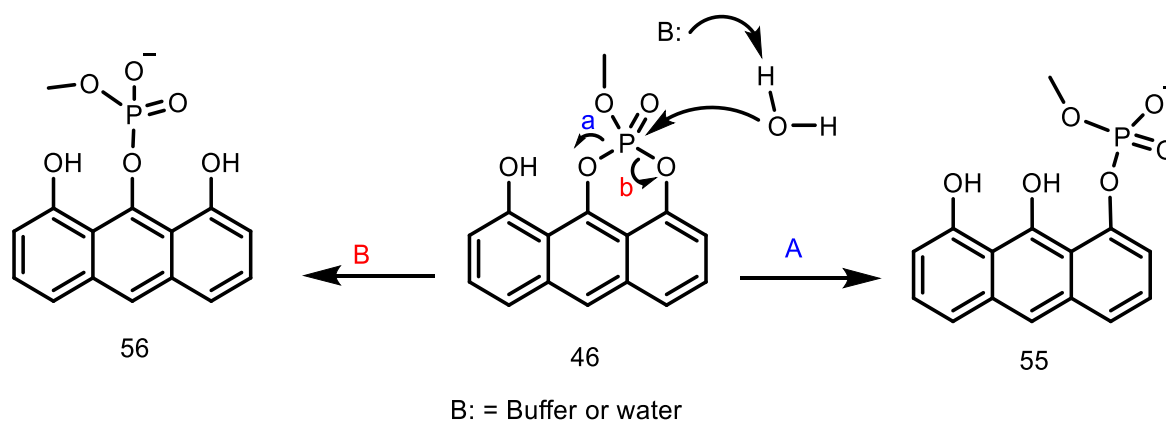


Figure (2-11): Buffer catalysis of **46**; MES buffer pH = 6 & 7 ± 0.04 ; 25 °C, 1 M NaCl. The linear correlation was fitted to equation (2-1).

$$k_{\text{obs}} = k_0 + k_2 [\text{buffer}]$$

$$\text{Equation (2-1)}$$



Scheme (2-11): Buffer catalysis mechanism involved in hydrolysis of phosphate triester 46.

The k_{obs} or k_0 values for cyclic esters **47** and **48** as well as k_0 **46** were plotted as a function of pH as shown in Figure (2-12). Equation (2-2) was fitted to the experimental points for triester **46** and equation (2-3) for triesters **47** and **48**.

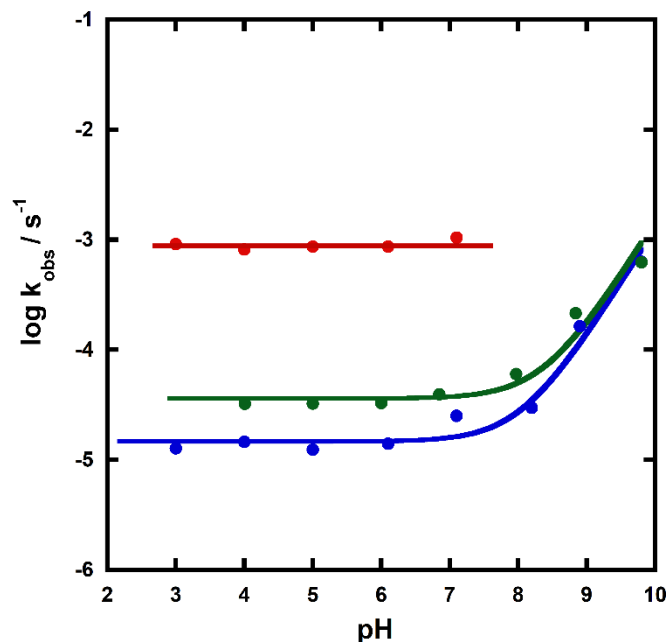


Figure (2-12): Kinetic profile according to pH for the hydrolysis of triester **46** (red), **47** (green) and **48** (blue) at 25°C and ionic strength of 1 M. The curves correspond to the fit given by equation (2-2) for triester 46 and equation (2-3) for triesters **47** and **48**.

$$\log k_{\text{obs}} = \log(k_0)$$

$$\text{Equation (2-2)}$$

$$\log k_{\text{obs}} = \log(k_0 + k_{\text{OH}^-} [\text{OH}^-])$$

$$\text{Equation (2-3)}$$

As shown in Figure (2-12), the pH rate profile for the hydrolysis of **46**, **47** and **48** shows a plateau between pH 3 and 7. This plateau region corresponds to the pH-independent neutral reaction involving water. The values of k_{obs} for triester **46**, **47** and **48** are $8.0 \pm 0.3 \times 10^{-4} \text{ s}^{-1}$, $2.5 \pm 0.4 \times 10^{-5} \text{ s}^{-1}$ and $1.1 \pm 0.1 \times 10^{-5} \text{ s}^{-1}$, respectively, giving the relative rate as summarised in Figure (2-13). The hydrolysis of cyclic phosphate **47** and **48** at higher pH showed slightly increasing of rate above pH 8, which is attributed to the alkaline hydrolysis by hydroxide ion, OH^- .

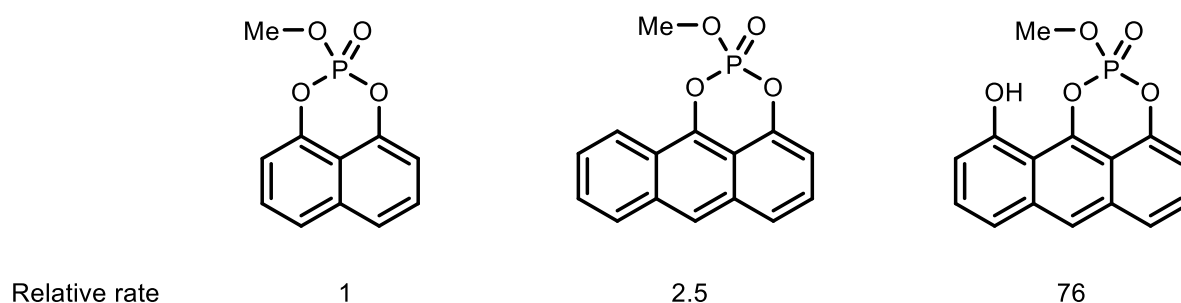


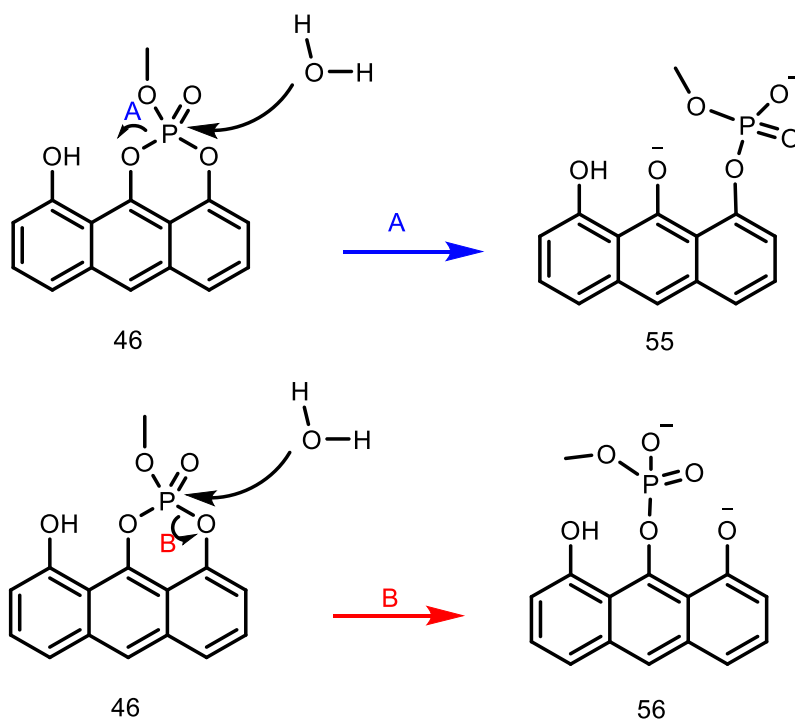
Figure (2-13): Structures of cyclic phosphate studied here with relative rate constants of spontaneous hydrolysis.

2.3.5.6 Analysis the difference in the rates

The effect of $\text{p}K_{\text{a}}$ of the leaving group

From the values of the rate constants obtained above, the rate of cleavage of triester **46** is enhanced in the presence of the hydroxyl group compared with **47** and **48**, which could indicate a catalytic role for the hydroxyl group on the rate. On the other hand, this enhancement could be due to a change in the intrinsic properties of the leaving group as well.

In cyclic naphthyl ester **48**, the leaving groups for ring opening on both sides are identical, but are not identical in cyclic anthryl triester **46**. Thus, if there is no difference in the $\text{p}K_{\text{a}}$ s of leaving groups of ring opening in triester **46** as those in cyclic naphthyl ester **48**, then both reactions (A and B routes) would happen at similar rates, Scheme (2-12). However, this was not the case, where the main product was the diester with leaving group of 9-position (route A).



Scheme (2-12): The proposed route of hydrolysis of cyclic phosphate triester **46**.

On the other hand, if the leaving groups pK_a s are not identical, the better leaving group will leave more readily, and this needs to be considered along with other factors such as hydrogen bond catalysis by the hydroxyl group.

A direct measurement of the pK_a of these leaving groups is not available in the literature. Thus, it is necessary to estimate the pK_a of the leaving group oxygens (*i.e.* the pK_a of ArOH for the cleavage of a P–O bond in path A and B) using similar structures. Limited data are available for measuring or calculating pK_a s of anthrol derivatives (**51**, **53**, **65** and **66**), Figure (2-14). These data could allow for indirect comparison of the leaving groups in the compound of interest **46**.

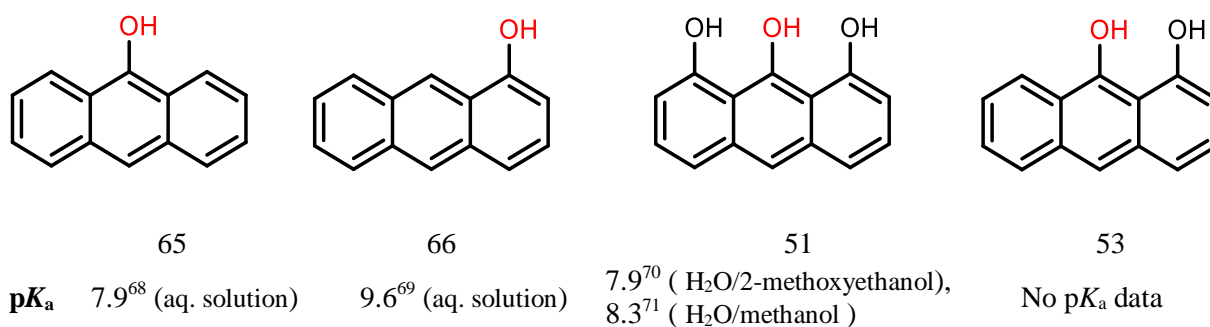


Figure (2-14): Structures of anthrols with their pK_a s.

Comparing with 1-anthrol, 9-anthrol is more acidic. The pK_a of 1-anthrol (**66**) is about 1.7 unit larger than 9-anthrol (**65**) which is about 9.7 kJ mol⁻¹ stabilisation for 9-anthrol relative to 1-anthrol. In addition, 9-anthrol is more acidic than for phenol ($pK_a = 10.0$) and α -naphthol ($pK_a = 9.4$). Thus, the structure of the ring system has a significant effect on the pK_a of the superficially similar aromatic leaving groups, Figure (2-15). This suggested that there is extra stabilisation due to a resonance effect by a strong interaction between a lone pair of electrons on the oxygen and the π -electron system of the central anthracene ring. Thus, the difference in the rate about 2.5 fold (~ 2.3 kJ mol⁻¹) between **47** and **48**, can be attributed to this resonance effect. If **47** only reacts to cleave the bond to the O attached to the central ring, then this reaction is 5 fold faster than breaking either one of the bonds in **48** due to the statistical factor involved.

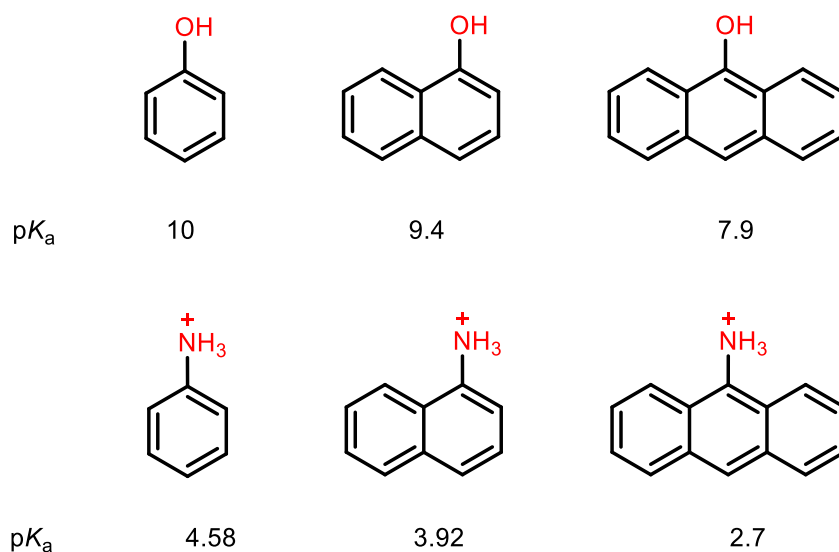


Figure (2-15): Phenols and aryl anilinium ions with their pK_a s in aqueous solution (pK_a for 9-ammonioanthracene reported from ref 72).^{68, 72-73}

In cyclic phosphate ester **47**, both the possible leaving groups are comparable to those of triester **46** as far as the core aromatic ring system is concerned, thus any difference in the rate between these two esters should be account for simply by catalysis by the hydroxyl group (*i.e.* In stabilisation of the product **58** or the transition state in route A, Scheme (2-12). Thus, the P-O cleavage would undergo pathway (A) as the only or the majority cleavage if the adjacent hydroxyl group on anthryl ring could provide a stabilising effect through hydrogen bonding to the developing negative charge in the transition state compared to route (B). This is expected to assist the opening ring from this side, insofar as this hydrogen bond has developed in the transition state for P–O cleavage, Scheme (2-12).

In addition, the presence of an adjacent hydroxyl group (*i.e.* the pK_a of conjugate base in a structure such as **51** and **53**) would be expected to reduce the pK_a of the leaving group by hydrogen bonding stabilisation, which is absent in anthrols **65** and **66**. This stabilisation to the conjugate base providing by hydrogen bonding has been shown previously with networks of hydrogen bonds (discussed in chapter 1).⁷⁴⁻⁷⁵ The value of the pK_a for the ionisation of **51** to its anthrolate anion is found to be vary due to using different co-solvents in each case to overcome the limited solubility of anthraline in aqueous solution. For example, the value of 7.9 was measure using a stock solution in DMSO and a mixture of 1:2 (v/v) buffer: ME (ME, 2-methoxyethanol) and the value of 8.3 was measure using stock solution in methylene chloride and a mixture of 1:1 (v/v) buffer: methanol. The pK_a for anthrol **65** was measured in aqueous buffer. Thus, it is difficult to make the comparison between the structures as the differing solvent effects cannot be predicted accurately. Usually, pK_a s measured in alcohol are higher than in aqueous solution, and so the pK_a of **51** is likely to be lower than for **65** despite the apparent similarity. For example, the pK_a of phenol is 10.8 in 50% aqueous methanol, 11.1 in 50% aqueous ethanol and 9.99 in water.⁷⁶⁻⁷⁷

In a different way, 1, 8-dihydroxy naphthalene could be a useful system to estimate the pK_a of the 9-anthrone with an adjacent hydroxyl group. Ignoring the effect of the third ring of the anthracene system and noting that the highlighted part of anthrone **53** is similar to the naphthalene system, the pK_a of the hydroxyl group on position 9 should be same or less than that of the naphthalene system.

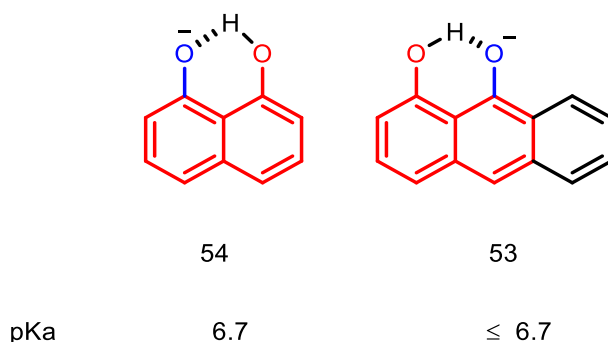
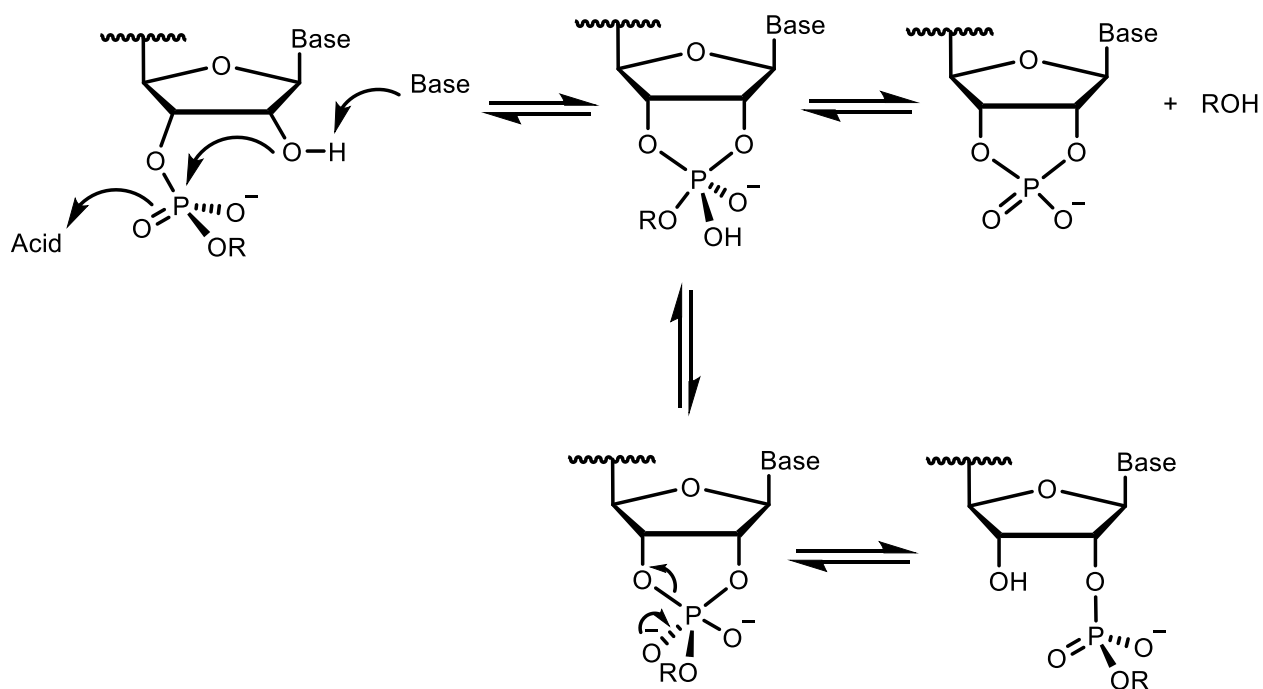


Figure (2-16): Naphthalene **54** ion with its pK_a and anthracene **53** ion with expected pK_a

Thus, there is a 32-fold rate acceleration by the intramolecular hydroxyl group of triester **46** ($\sim 8.8 \text{ kJ mol}^{-1}$) compared with triester **47**. If the pK_a of 9-anthrolate is similar to the naphthalene ion **54** (the products of hydrolysis of triester **46**), the pK_a value of the 1-anthrolate **56** is more basic (about 2 units, 11.7 kJ mol^{-1}) than the leaving group 9-anthrolate **55**. Thus, the libido rule is not obeyed and the intramolecular OH group can only contribute to catalysis by hydrogen-bond formation in the transition state.

Furthermore, a hydrolysis mechanism involving protonation of P=O unit to give a pentacoordinate intermediate has been proposed in RNA transesterification, Scheme (2-13).⁷⁸ Thus, it is possible to invoke this in the hydrolysis of phosphate triester **46**. However, this possibility mechanism of catalysis can be ruled out based on two reasons. The geometry of the P=O unit is not favourable for an interaction with the hydroxyl group through hydrogen bonding due to the rigidity of cyclic phosphate preventing the rotation of P=O unit to approach the OH group.



Scheme (2-13): The mechanism involving Prior or simultaneous protonation of the phospho- diester (P=O unit) with nucleophilic attack leads to a monoanionic phosphorane intermediate that can react further by cleavage or migration.⁷⁸

On the other hand, the spontaneous hydrolysis rate of fully protonated phosphate diester **67** at 25 °C, Figure (2-17), $k_{\text{obs}} = 3.0 \pm 0.3 \times 10^{-5} \text{ s}^{-1}$,⁷⁹ is the same within experimental error as the spontaneous reaction of phosphate triester **47**, and slower than phosphate triester **46**, which suggests that the enhancement in the rate is not due to the protonation of P=O unit by hydroxyl group. Detailed study on phosphate esters complexes by Williams and Forconi has showed a rate acceleration of hydrolysis of phosphate diester **68** of about **60** fold compared with phosphate diester **67**. This is consistent with the analysis that the hydroxyl group does not catalyse the reactions by P=O protonation.⁸⁰

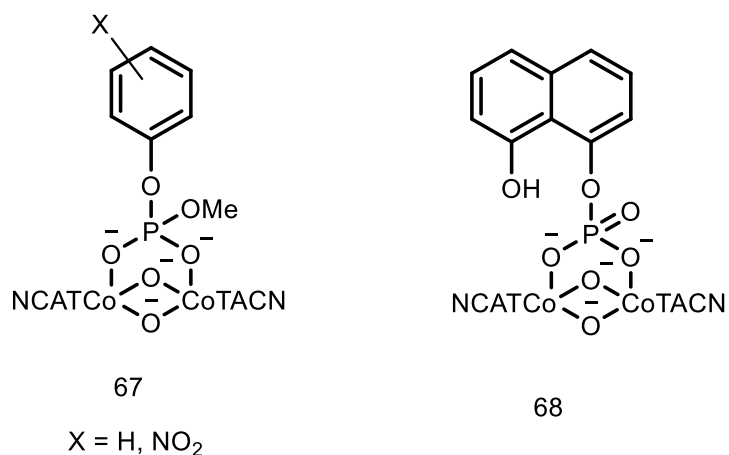


Figure (2-17): Structures of phenyl phosphate diester 67,⁷⁹ and naphthyl phosphate diester. 68.⁸⁰

Recently, triester *tris*-2-pyridyl phosphate (pK_a of phenol = 9.09) is hydrolysed at a surprisingly high spontaneous rate ($k_0 = 2.4 \pm 0.3 \times 10^{-5} \text{ s}^{-1}$ at 25 °C) in water, which was reported to involve intramolecular general-base (GB) catalysis.⁸¹⁻⁸² A similar hydrolysis rate ($k_0 = 1.93 \times 10^{-5} \text{ s}^{-1}$ at 25 °C in water) has been reported for *tris*-3-chlorophenyl phosphate (pK_a of phenol=9.02) which is attributed to the electronic effects of the non-leaving groups, and suggests that efficient intramolecular base catalysis was not a factor after all, Figure (2-18).⁸¹ These rates are the same within experimental error as the water reaction observed for cyclic phosphate **47** ($k_0 = 2.51 \pm 0.36 \times 10^{-5} \text{ s}^{-1}$), which has no potential catalytic functionality. On the other hand, cyclic aryl triester with a good leaving group such as 4-nitrophenol and 2,4-dinitrophenol ($pK_a = 7.14$ and 4.1) hydrolyse at much slower rates ($k_0 = 8.8 \times 10^{-9}$ and $8.3 \times 10^{-6} \text{ s}^{-1}$ at 39 °C in water), respectively.⁸³ Since the cyclic phosphate triester **46** has no potential catalytic functionality except the hydroxyl group, the enhancement in the rate of hydrolysis of triester **46** compared with that for the corresponding triester **47** must be attributed to the catalytic effect by the adjacent hydroxyl group through hydrogen bonding catalysis.

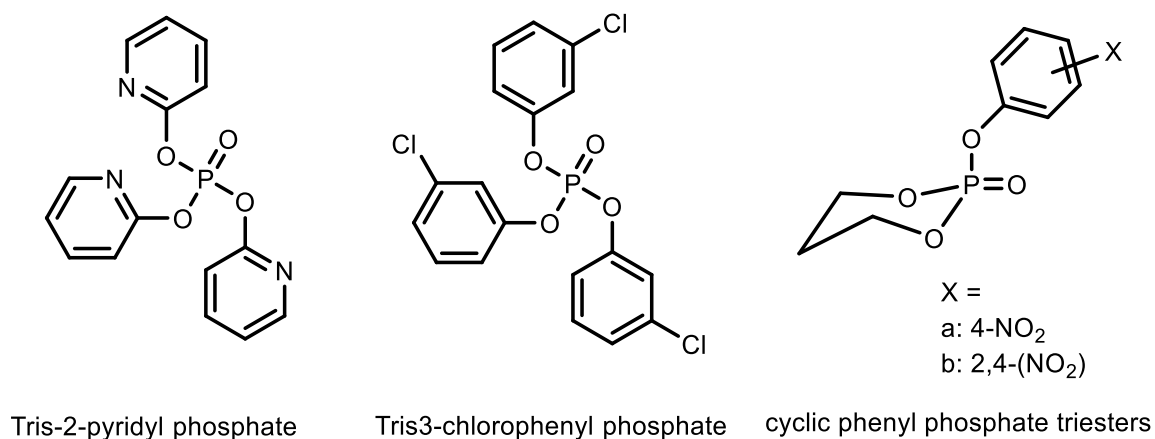


Figure (2-18): Series of triester phosphate studied previously.⁸¹⁻⁸³

Clearly, the hydrolysis of phosphate triester **46** involves a transition state (TS3) with a lower energy by 8.8 and 10.9 kJ mol⁻¹ than that for phosphate triesters **47** and **48** (TS1 and TS2), respectively, which have similar barriers, Figure (2-19) and Figure (2-20). However, some of the stabilisation could be provided by hydrogen bond in product **55** by the adjacent OH⁻ group on the position 1 of anthryl ring. Products **58** and **64** do not have such stability. Thus, it is expected that these two products have a similar energy.

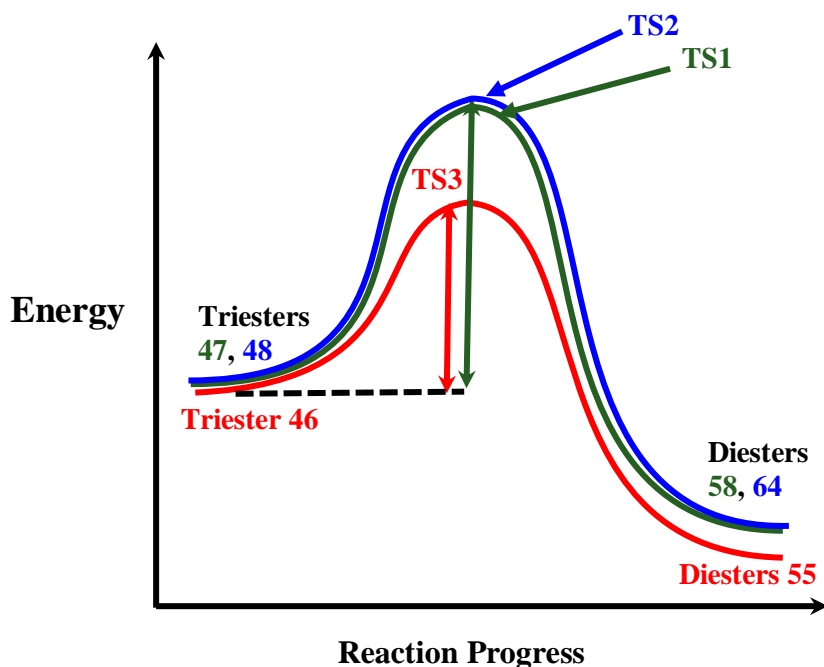


Figure (2-19): Expected free energy profile of the hydrolysis of phosphate triesters **46**, **47** and **48** in water (red), (green) and (blue), respectively.

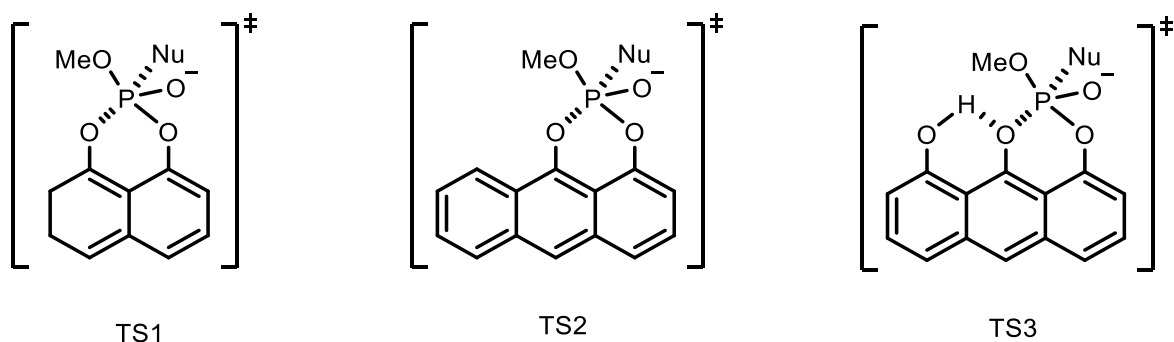


Figure (2-20): The structure of transition states involved in the spontaneous hydrolysis of phosphate triester **46**, **47** and **48**.

2.3.5.7 Investigation of the hydrolysis of **46** at high pH

The hydrolysis of cyclic phosphate **46** was studied at higher pH, and appeared to be slower than at $\text{pH} \leq 7$. The absorbance of starting material at wavelength 258 nm decreased slowly and did not reach the minimum absorbance at ~ 0.2 expected from previous reactions at lower pH. Thus, further investigation for the reaction in this pH region by ^{31}P NMR analysis was carried out.

^{31}P NMR analysis was used to follow the reaction at pH 6 and 9 at 25 °C and ionic strength 1 M, Figure (2-21). DMSO was used as co-solvent to help with the solubility problems found with phosphate triester **46**. The rates of the hydrolysis of **46** was measured at pH 9 and 6, and the result showed no significant difference in the reaction rates, $k_{\text{obs}} = 2.8 \pm 0.2 \times 10^{-4} \text{ s}^{-1}$ and $k_{\text{obs}} = 2.03 \pm 0.05 \times 10^{-4} \text{ s}^{-1}$ for pH 9 and 6, respectively. Repeating the reaction under same conditions as the NMR experiment and following the reaction by UV/Vis spectroscopy showed that the rate of reaction pH 6 is same as the NMR rate, $k_{\text{obs}} = 2.59 \pm 0.01 \times 10^{-4} \text{ s}^{-1}$.

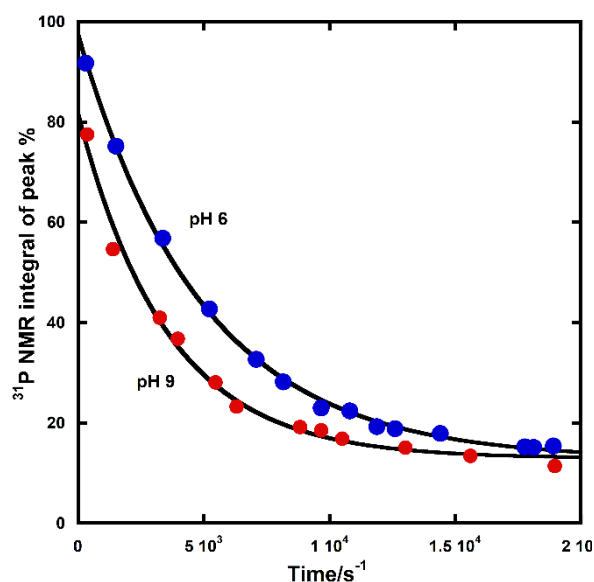


Figure (2-21): ³¹P NMR analysis data of **46**; pH = 6 & 9 ± 0.04 (blue and red line, respectively); 25 °C, ionic strength 1 M NaCl in DMSO.

Based on the NMR data, the rate constant at pH 9 is 1.4 times greater than at pH 6. Using this value and the rate constant under aqueous conditions at pH 6 from pH profile, $k_{\text{obs}} = 8.13 \times 10^{-4} \text{ s}^{-1}$, gave an estimated rate for pH 9 under the same conditions of $k_{\text{obs}} = 1.14 \times 10^{-3} \text{ s}^{-1}$, which provided a prediction for the pH profile as shown in Figure (2-22). Over this pH-independent region (pH 3-9), it is believed that the reaction is for the spontaneous reaction and the rate acceleration is probably due to intramolecular catalysis by neighbouring hydroxyl group. The reaction with OH⁻ ion is not significant up to pH 9.

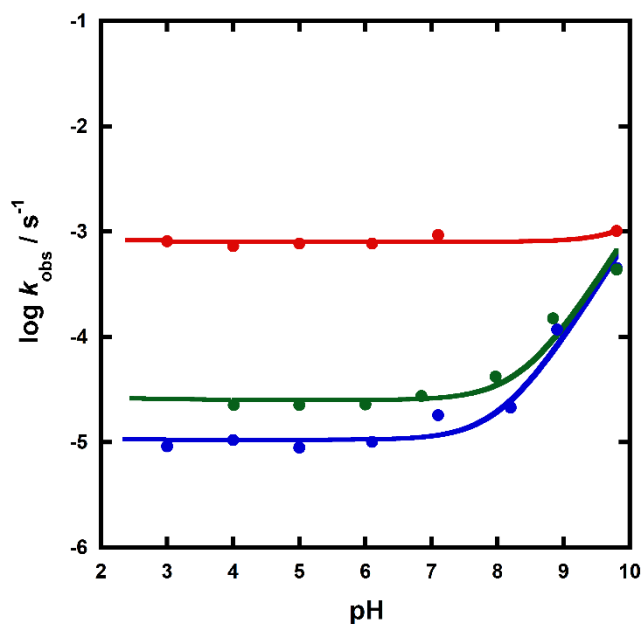


Figure (2-22): Kinetic profile according to pH for the hydrolysis of triester **46** (red), **47** (green) and **48** (blue) at 25°C and ionic strength of 1 M.

2.3.5.8 Mechanism proposed

The proposed mechanism of phosphate triester **46** is shown in Scheme (2-14). Over the pH range studied here, the water attacks the phosphorus centre and the negative charge develops on the leaving group. The presence of the rigidly positioned hydroxyl group in position 8 facilitates a hydrogen bond to the leaving group. This stabilises the negative charge, and then cleavage of the bond, in two different ways. This intramolecular catalysis is converting ester **46** to a mixture of two diesters, and one of these products was the majority of the mixture as shown by the ³¹P NMR investigations and by the ¹H NMR for the complete reaction at pH 6, Figure (2-23) and Figure (2-24). This indicates that this product is diester **55**, where the aryl proton peaks show asymmetric spectra, Figure (2-23). Intermediate has been seen in ³¹P NMR experiment and the UV spectrum showed a very clear isosbestic point.

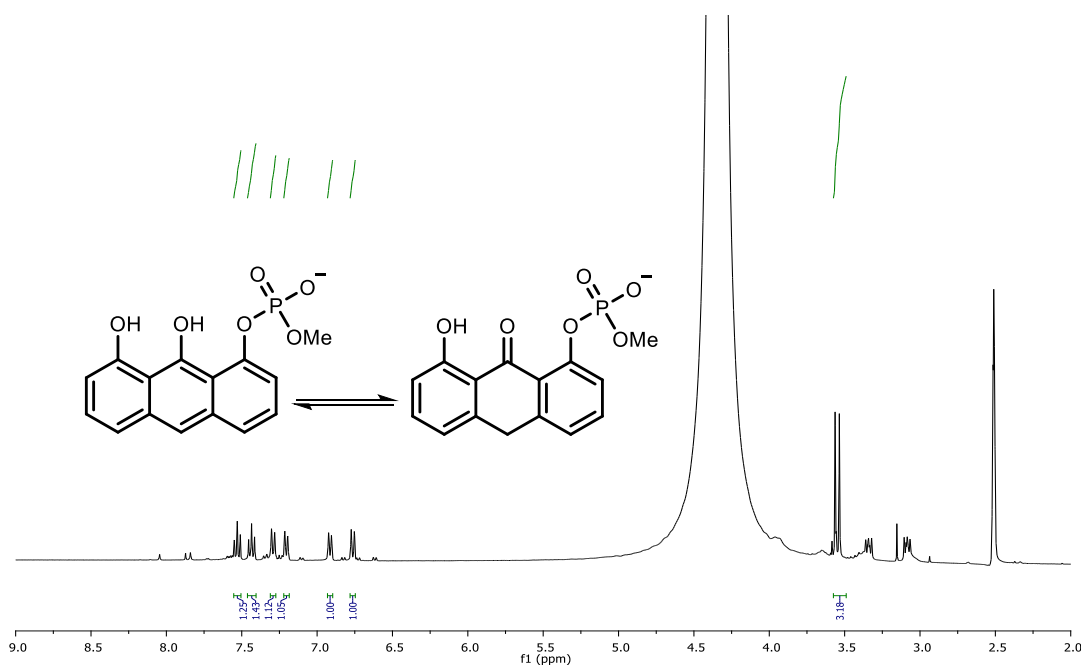


Figure (2-23): ^1H NMR of the complete hydrolysis of cyclic phosphate triester **46** at pH = 6 in DMSO.

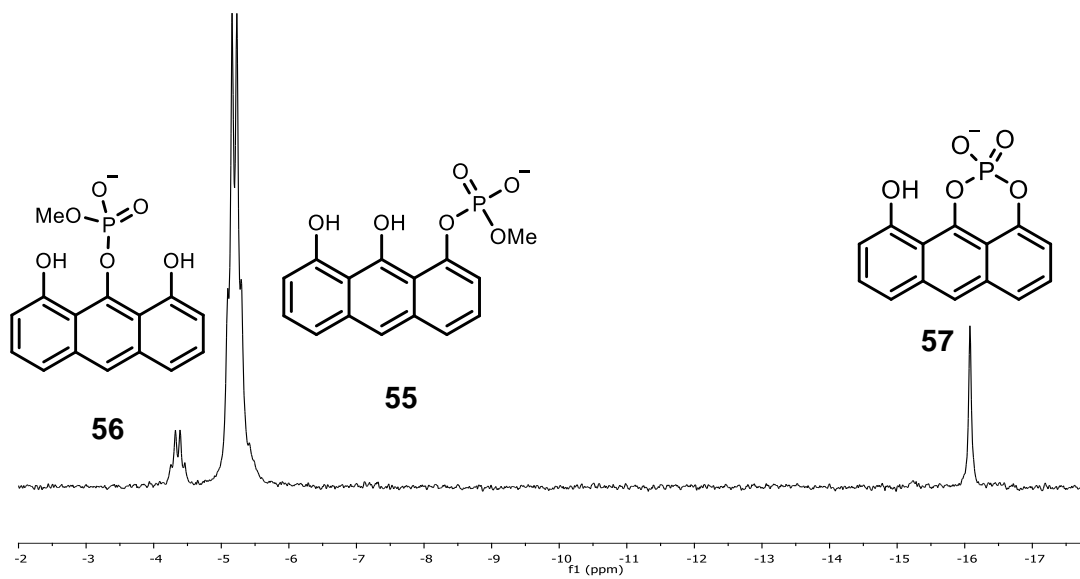
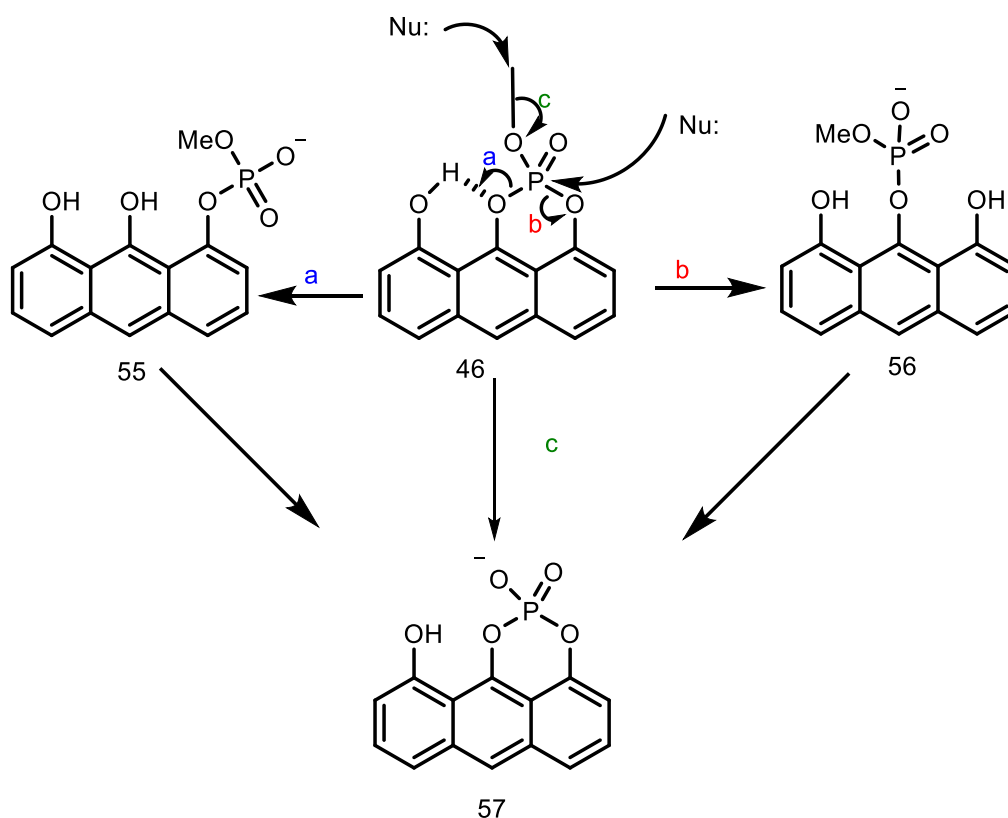


Figure (2-24): ^{31}P NMR of the hydrolysis of cyclic anthryl phosphate triester **46** after 4 days at pH = 6 in DMSO.



Scheme (2-14): The mechanism proposed for hydrolysis of phosphate triester 46.

2.3.5.9 The effect of nucleophiles on hydrolysis of phosphate ester 46

Over many years, the reactions of phosphate esters have been studied, and show differing reactivity dependencies on nucleophile and leaving group capabilities and also, in the cases of tri- and diesters, on the "spectator group" or groups. A wide range of data has been reported for the nucleophilic substitution reactions of phosphate mono-, di- and triesters.^{40, 42-43, 63} Hydroxylamine was of interesting due to its remarkably high reactivity in cleaving phosphate esters as discussed in chapter 1.

A study of the reactions of hydroxylamine and nucleophiles with the cyclic phosphate ester **46** was carried out to identify the reactive nucleophile(s) and if there is a difference in the mechanism involved.

2.3.5.10 Reaction with hydroxylamine

The reactions of cyclic triesters **46**, **47** and **48** with 0.5 M hydroxylamine was studied over the pH range 3-9 at 25 °C and ionic strength 1.0 M (NaCl), using an excess of hydroxylamine to ensure that reactions were pseudo-first order with respect to the substrate. Reactions were followed spectrophotometrically by monitoring the disappearance of the esters **46** and **47** at 258 nm and 255 nm, respectively, and for triester **48** by monitoring the product at 330 nm. The reactions were found to follow first order kinetic behaviour, and the logarithm of observed first order rate constants were plotted against pH, Figure (2-25). Equation (2-4) was used to fit the data for phosphate triester **46**, **47** and **48**. The water and hydroxylamine reactions rates are given in Table (2-1).

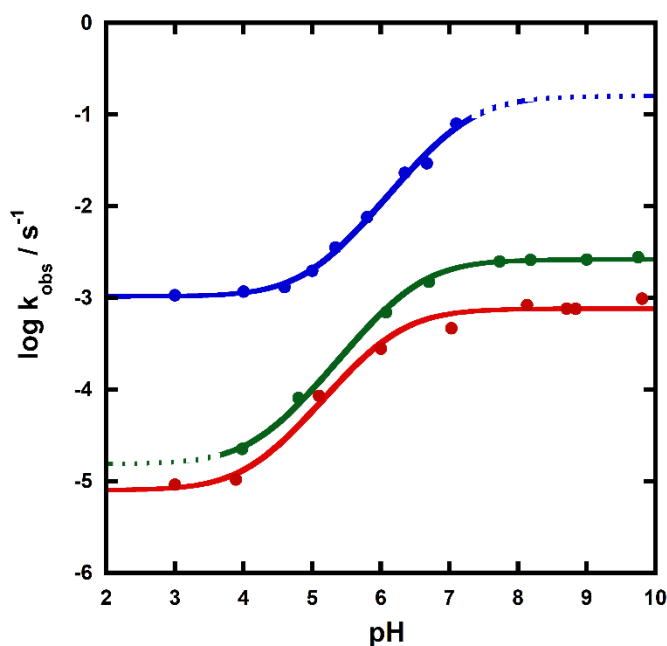


Figure (2-25): Kinetic profile according to pH for the reaction of 0.5M hydroxylamine with triester **46** (blue), triester **47** (green) and triester **48** (red) at 25°C and $I = 1$ M. The curves correspond to the fit by equation (2-4).

$$\log k_{\text{obs}} = \log (k_0 + k_2[\text{NH}_2\text{OH}]_{\text{total}} (K_a / (K_a + [\text{H}^+]))) \quad \text{Equation (2-4)}$$

where K_a is the dissociation constant of N-hydroxylammonium.

Table (2-1): Rate constants for the reaction of water (k_0) and hydroxylamine (k_2). (a) The rate was estimated from fitting the curve to equation (2-4), based on the same reactivity of hydroxylamine at this pH region.

Cyclic phosphate triester	k_0 / s^{-1}	$k_2 / \text{M}^{-1} \text{s}^{-1}$	k_2 / k_0	$\text{p}K_a(\text{NH}_2\text{OH})$
46	$1.04 \pm 0.09 \times 10^{-3}$	$1.6 \pm 0.5 \times 10^{-1(\text{a})}$	1.54×10^2	7.18 ± 0.17
47	$1.5 \pm 0.3 \times 10^{-5}$	$2.6 \pm 0.1 \times 10^{-3}$	1.73×10^2	6.47 ± 0.05
48	$8 \pm 2 \times 10^{-6}$	$7.5 \pm 0.8 \times 10^{-4}$	9.38×10^1	6.14 ± 0.11

The $\text{p}K_a$ of hydroxylamine was obtained from the pH profile as shown in the table (2-1). The value of 6.14 ± 0.11 for triester **48** is in an agreement with the previous value reported by Kirby *et al.* within the experimental error (6.06 at 25°C)⁴³. The values 7.18 ± 0.17 and 6.47 ± 0.05 for triesters **46** and **47**, respectively, which are 16 % and 6 % increase in $\text{p}K_a$ obtained based on the estimated extended curve (dashed curve). Increases of 16 % and 6 % compared with the $\text{p}K_a$ reported in the literature could be due to the high reactivity of the reaction for anthryl systems **47** and **46** above pH equal to $\text{p}K_a$ of hydroxylamine, which lead to an increase of $\text{p}K_a$ of hydroxylamine.

It can be seen from the curves that the reaction is dependent on hydroxylamine concentration as well as pH. A plateau is reached from pH 6 to 9 for triester **47** and **48**, which is consistent with the reaction with hydroxylamine in its neutral form ($\text{NH}_2\text{OH} \rightleftharpoons \text{H}_3\text{N}^+-\text{O}^-$). There is no significant difference in the rate between phosphate esters **47** and **48**, where the reaction of triester **47** is about 2.5 times faster than **48**.

For phosphate triester **46**, the reaction is enhanced in the presence of hydroxylamine as well. The reaction did not measured at a pH higher than 7, for the same reason discussed above for the reaction with water. However, it was expected that the reaction would reach the plateau at same range of pH as this depends on the $\text{p}K_a$ of N-hydroxylammonium.

2.3.5.11 Dependence of the reaction on the concentration of hydroxylamine

To evaluate the influence of hydroxylamine on the degradation of triesters **46**, **47** and **48**, reactions were followed at pH 3-7 for triester **46** with varying concentrations of hydroxylamine, and at pH 7 for triesters **47** and **48**. The k_{obs} was plotted against hydroxylamine concentration, and the data were fitted to Equation (2-5), where k_0 and k_2 are the rate constants for the spontaneous hydrolysis and the first order reaction with hydroxylamine, respectively. Values of k_2 at pH 7 with relative rate for the reactions are given in Table (2-2). A plot of k_{obs} vs hydroxylamine concentration shows linear and curvature behaviour at very low and higher concentrations of the nucleophile, evidence for a reaction first and second order in low and high hydroxylamine concentrations, respectively, Figure (2-26), Figure (2-27) and Figure (2-28). Such behaviour has been observed previously for the reaction of phosphate triesters, such as tri-2-pyridyl phosphate hydrolysis with hydroxylamine.⁴³

$$k_{\text{obs}} = k_0 + k_1 [\text{NH}_2\text{OH}] + k_2 [\text{NH}_2\text{OH}]^2$$

Equation (2-5)

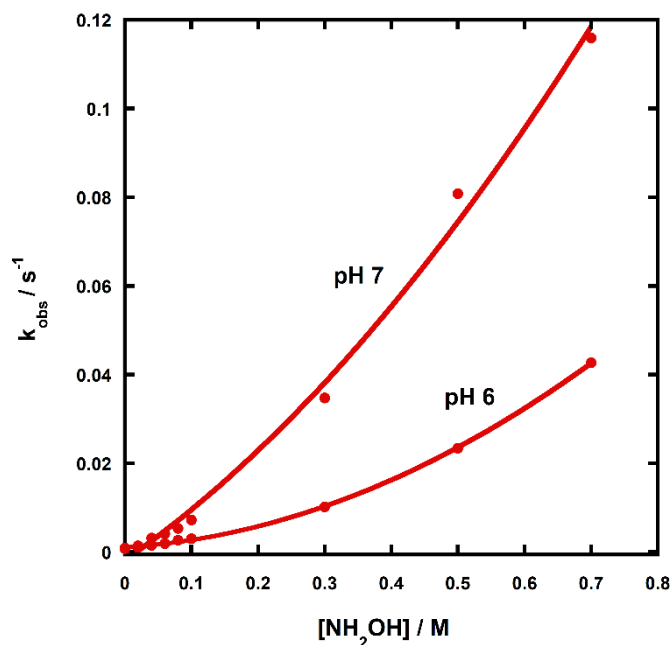


Figure (2-26): Kinetic profile according to the reaction of phosphate triester **46** with NH_2OH at pH 6 & 7, 25°C and ionic strength of 1 M. The curves correspond to the fit given by Equation (2-5).

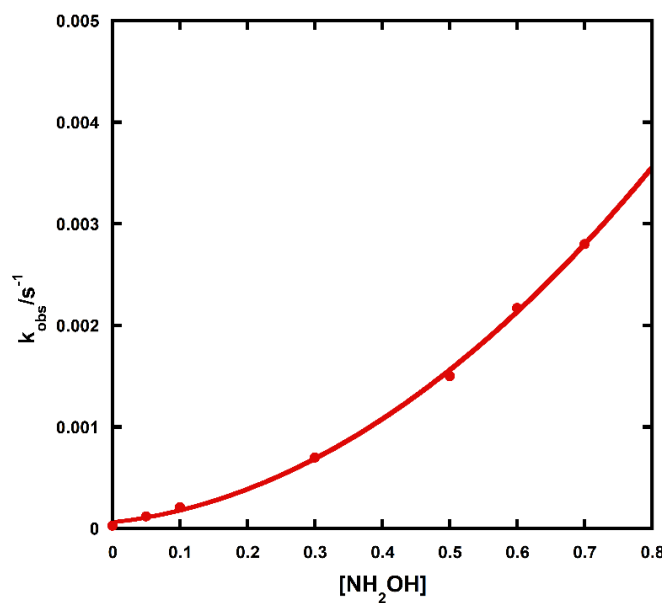


Figure (2-27): Kinetic profile according to the reaction of phosphate triester **47** with NH_2OH at pH 7, 25°C and ionic strength of 1 M. The curves correspond to the fit given by Equation (2-5).

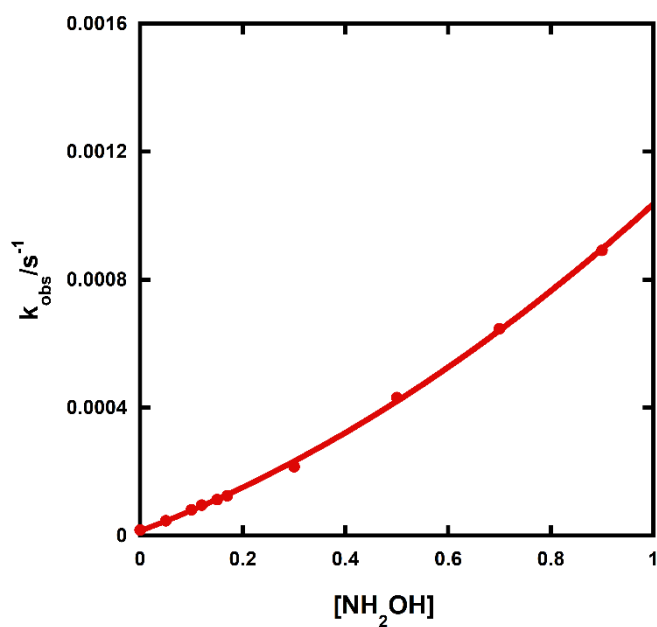
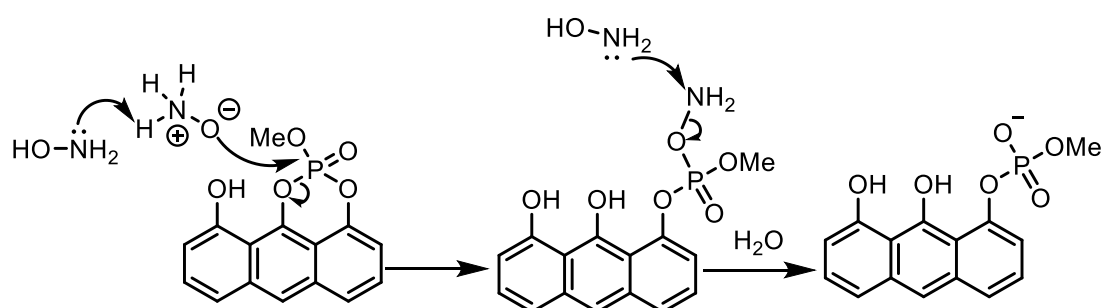


Figure (2-28): Kinetic profile according to the reaction of phosphate triester **48** with NH_2OH at pH 7, 25°C and ionic strength of 1 M. The curves correspond to the fit given by Equation (2-5).

Table (2-2): the second order rate constants of the reaction of hydroxylamine with triesters 46, 47 and 47 at pH 7 and 25 °C.

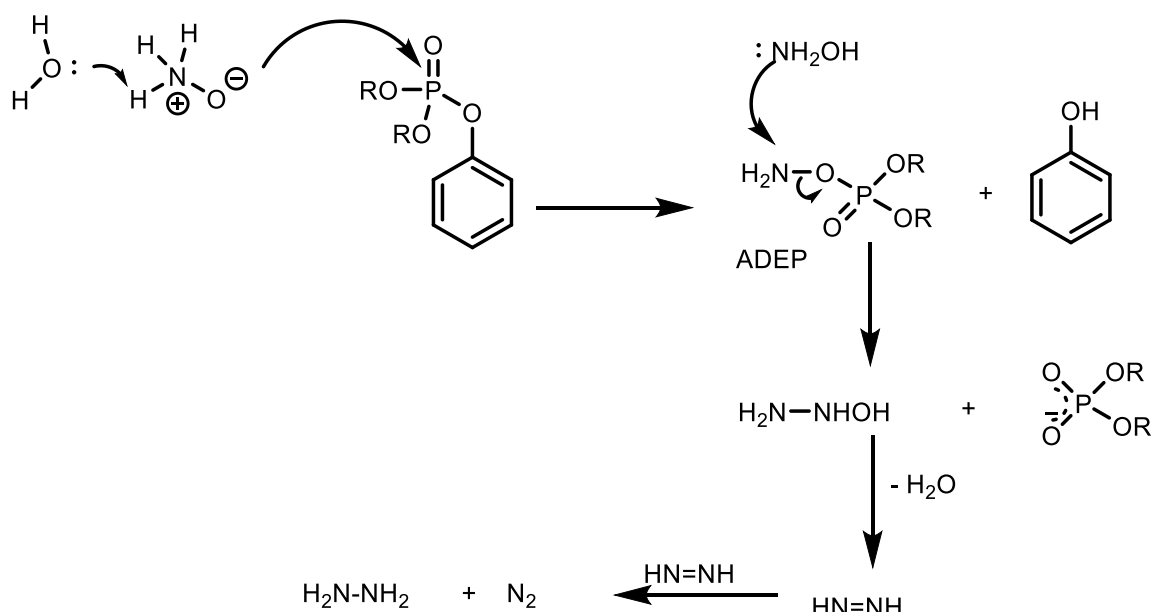
Cyclic phosphate triester	Triester 46	Triester 47	Triester 48
$k_2 / \text{M}^{-1} \text{s}^{-1}$	$1.04 \pm 0.2 \times 10^{-1}$	$7.1 \pm 0.2 \times 10^{-4}$	$6.0 \pm 0.4 \times 10^{-4}$
Relative rate	173	1	1

The rate of hydrolysis of phosphate triester **46** is enhanced in the presence of hydroxylamine compared with triester **47** and **48**. Cyclic phosphate triester **46** hydrolysed with a rate constant of $1.0 \pm 0.2 \times 10^{-1} \text{ M}^{-1} \text{ s}^{-1}$, which indicates that the value of k_2 ($1.6 \pm 0.5 \times 10^{-1}$) from the pH profile is reliable within the error of the experimental. The second order reaction of hydroxylamine at high concentration is consistent with a reaction involving two molecules of hydroxylamine in the reaction. One molecule can attack as a nucleophile and the second molecule acts as a general base facilitating nucleophilic attack or is involved in the second step of a reaction involving an intermediate, Scheme (2-15).



Scheme (2-15): Two-step mechanism for the reaction of hydroxylamine with phosphate triester **46**, by the zwitterionic form. In first step the water or hydroxylamine can act as a general base in the first step.

This mechanism involving the hydroxylamine in this step of hydrolysis of phosphate triesters has been proposed before. For example, Kirby has studied the hydrolysis of diethyl 8-dimethyl amine 1-naphthyl phosphate with hydroxylamine. The product of the reaction was not the intermediate ammonia diester phosphate (ADEP), but instead, hydrazine and nitrogen along with diethyl phosphate were formed. They proposed that the second hydroxylamine attacks the intermediate according to the mechanism in Scheme (2-16).^{42, 84}



Scheme (2-16): Mechanism of the reaction of phosphate triesters with hydroxylamine, showing hydrolysis of the intermediate by second molecule of hydroxylamine.⁸⁴

The cleavage of cyclic phosphate triester **46** in the presence of hydroxylamine compared with phosphate esters **47** and **48** indicates a catalytic role for the hydroxyl group to assist the attack of hydroxylamine. The rate acceleration of 145 to 175 fold equates to $\sim 12.6 \text{ kJ mol}^{-1}$ stabilisation of the negative charge in the transition state by the hydrogen bond, indicating that the bond forming with the nucleophile and breaking of the leaving group are well advanced in the transition state. Although this value of the activation energy falls in the range of the weak hydrogen bond, it reveals a kinetic catalytic role of the hydroxyl group in the structure.

2.3.5.12 Reactions of phosphate triester **46** with other nucleophiles

Reactions involving nucleophilic attack on phosphorus can sometimes show different enhanced reactivity. To investigate that, the reaction of phosphate triester **46** with different nucleophiles was followed at varying concentrations of a range of nucleophiles (i.e. MeONH_2 , acetate and fluoride). Methoxy amine cannot react through its oxygen in contrast to hydroxylamine. A plot of $\log k_{\text{obs}}$ vs. nucleophile concentration, Figure (2-29), shows linear behaviour providing evidence for a reaction pathway that is first order in nucleophile (i.e. MeONH_2 , acetate and fluoride). The points are the experimental data, and the lines correspond to the fit given by

Equation (2-6). The addition of sodium acetate at pH 6 and constant ionic strength (1 M) has $k_2 = 1.06 \pm 0.02 \times 10^{-2} \text{ M}^{-1} \text{ s}^{-1}$, which indicates that sodium acetate has a catalytic effect on the reaction either as a general base or nucleophile.

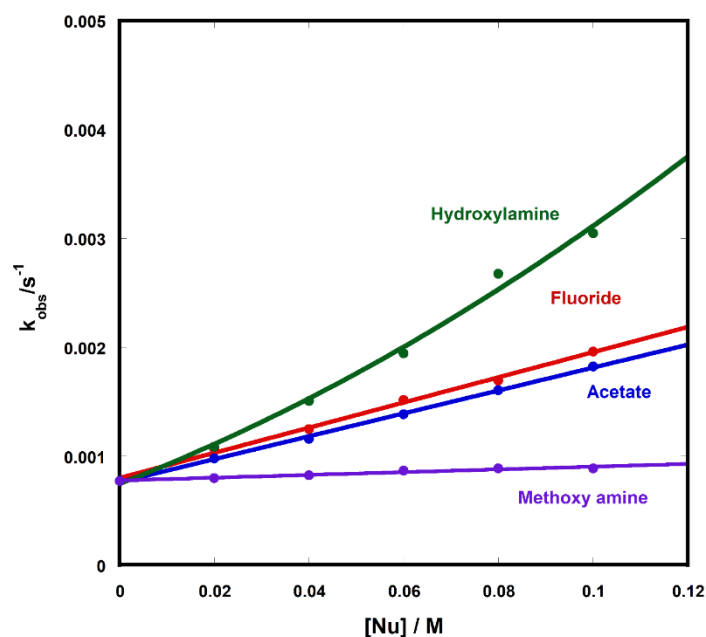


Figure (2-29): Kinetic profile according to the reaction of **46** with nucleophiles (and hydroxylamine for comparison), at pH 6, 25°C and ionic strength of 1 M.

$$k_{\text{obs}} = k_0 + k_2[\text{Nu}]$$

Equation (2-6)

Less basic hydroxylamines as expected to react more slowly with phosphate esters than hydroxylamine.⁴⁴ The reaction of phosphate triester **46** with O-methyl hydroxylamine derivative is already 13 times slower than with hydroxylamine itself, $k_2 = 1.3 \pm 0.1 \times 10^{-3} \text{ M}^{-1} \text{ s}^{-1}$ and $k_2 = 1.7 \pm 0.4 \times 10^{-2} \text{ M}^{-1} \text{ s}^{-1}$, for methoxy amine and hydroxylamine, respectively. This behaviour is preceded,⁴⁴ and consistent with the involvement of N–OH group acting as oxygen nucleophiles in their reactions with phosphate triester **46**, via the zwitterion tautomer $^+\text{NH}_3\text{O}^-$. The fluoride anion, which is a significantly stronger nucleophile compared with an oxyanion of the same $\text{p}K_a$, showed enhanced reactivity similar to that of acetate anion, $k_2 = 1.16 \pm 0.03 \times 10^{-2} \text{ M}^{-1} \text{ s}^{-1}$. From the Brønsted plot for different types of nucleophile, Figure (2-30), the lack of correlation provides evidence that the reactions concerned involves nucleophilic rather than general base catalysis.

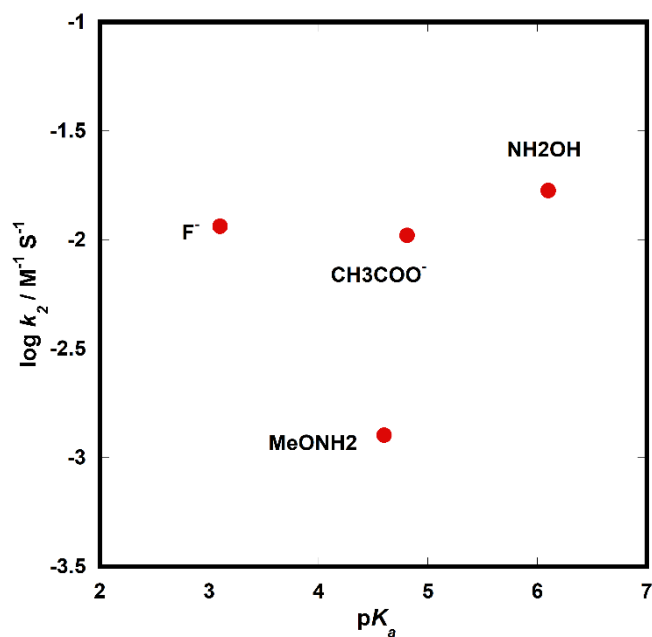


Figure (2-30): Brønsted plot comparing second-order rate constants for the reactions of **46** with NH₂OH, MeONH₂, acetate and fluoride.

2.4 Conclusion

The reactivity of phosphate triesters with a neighbouring hydroxyl group as a catalytic group has not been investigated before, and so data is not available in the literature to be compared with. Therefore, to study the effect of hydroxyl group on the cleavage of cyclic phosphate triesters, three methyl cyclic phosphate triesters have been successfully synthesised and the result of their reaction with water and hydroxyl amine were studied, giving evidence of the role of hydroxyl group effect on the reactions. In this research the presence of a hydroxyl group in a specific position of phosphate triester **46** showed an acceleration of more than 25 fold compared with the absence of this group in ester **47**. Ring opening was not the only reaction observed for esters **47** and **48**, but subsequent nucleophilic cyclisation leading to the departure of methyl group was also observed. The ring opening became more favourable in phosphate triester **46**, indicating the importance of the adjacent catalytic hydroxyl group to enhance such reactions of phosphate esters and other species.

In addition, the reaction of hydroxylamine with phosphate triester **46** was faster than the reaction with phosphate triester **47** and **48**, up to 173 fold. This enhancement is attributed to

stabilisation by the hydrogen bond in the transition state. Although this hydrogen bond is not strong, it still contributes about 13 kJ mol^{-1} stabilisation. In biological system such these energy contribution has been shown previously with values of $2\text{-}8 \text{ kJ mol}^{-1}$ by removal of the hydrogen bonding interaction in the specific place of interest.⁸⁵

**Chapter Three: Acyclic Triester
Phosphate with One Hydrogen Bond
Donor**

3.1. Introduction

As has been illustrated in chapter two, the presence of a neighbouring hydroxyl group which is able to make an intramolecular hydrogen bond with a leaving group makes a significant difference on the reaction rate of cyclic phosphate esters. The reaction of methyl 1-hydroxy anthryl phosphate **46** with water and hydroxylamine was accelerated 32 and 173 fold compared with the control compound anthryl phosphate **47**, Figure (3-1). This chapter will look at the effect of hydroxyl groups on the hydrolysis of acyclic phosphate triesters to investigate the difference that the presence of an intramolecular hydrogen bond can make.

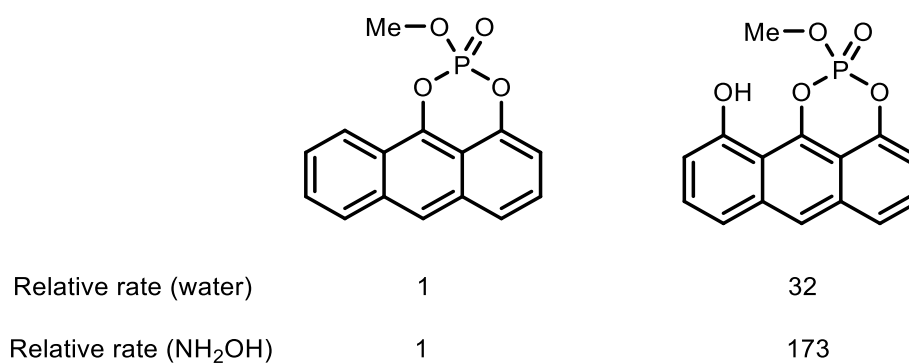


Figure (3-1): Cyclic triesters **46** and **47** with relative rates of their spontaneous hydrolysis reaction with hydroxylamine.

Four initial targets of acyclic phosphate triesters with and without hydroxyl groups were chosen to be synthesised and studied, Figure (3-2). The hydroxyl group in structures **69** and **71** are different in the geometry and rigidity. In triesters **69** and **71**, the rates would be expected to be greater than the unsubstituted controls **70** and **72**, respectively.

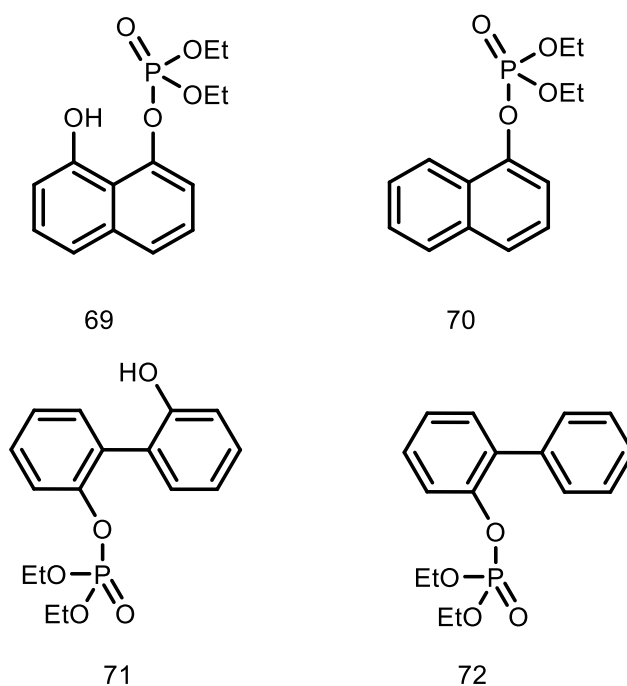
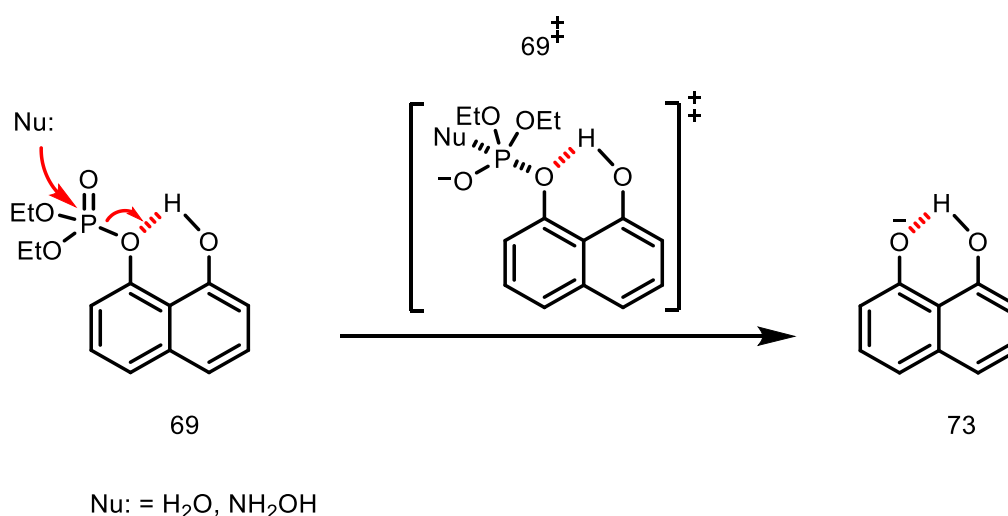


Figure (3-2): Structures of acyclic phosphate triesters studied in this chapter.

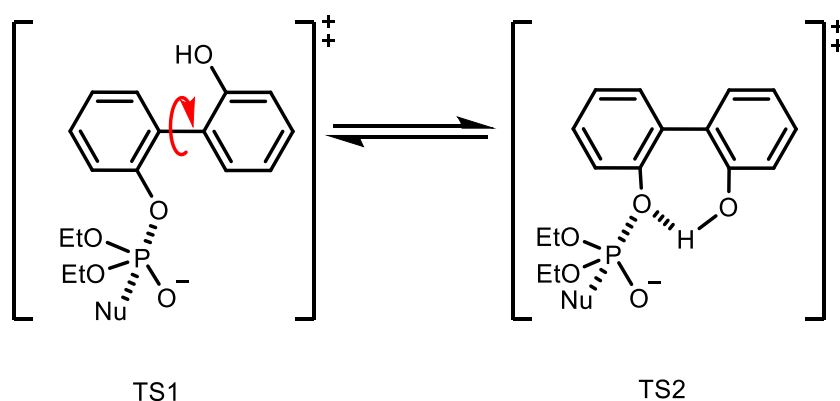
The mechanism shown in Scheme (3-1), which was proposed by Kirby *et al.* for the hydrolysis of diethyl 8-dimethylamine-1-naphthyl phosphate catalysed by dimethylammonium group, might be observed for phosphate triesters **69** and **71**. Similar to the Kirby model,^{28, 42} the naphthyl ester **69** is a model with a hydrogen bond donor held rigidly in close proximity to the leaving group. Using the naphthalene scaffold with a hydrogen bond donor as a model **69** is of interest in that the hydrogen bond donor directed to the oxygen of O-Ar bond (leaving group). Thus, intramolecular stabilisation of transition state **69[‡]** could be achieved.



Scheme (3-1): The mechanism proposed for hydrolysis of diethyl 8-hydroxy-1-naphthyl phosphate **69**.

Phosphate triester **71** has an OH-group with more conformational freedom due to rotation around the C-C bond between the phenyl rings. Hence, the hydroxyl group is not held rigidly in close proximity to the triester as in **69**. Thus, the possibility of the hydrogen bond to the leaving group should be less significant than in **69**. Two transition states could be possible in this case, TS1 and TS2, Scheme (3-2). In transition state TS1, the hydroxyl group is positioned away from the phosphate group. Thus, it is unable to form a hydrogen bond to the leaving group oxygen atom to help the cleavage of the P-O bond. By rotation around C-C bond, the hydroxyl group becomes closer to the oxygen atom as shown in TS2. In the latter case, the position of the hydroxyl group becomes more favourable for forming an intramolecular hydrogen bond to the leaving group and thus stabilisation can be achieved, although it might not be as effective as in the case of triester **69**.

Compounds **70** and **72** act as control compounds, where the hydroxyl group is replaced by a hydrogen atom. Thus, the formation of the hydrogen bond with the leaving group oxygen is not available, and as a result, there is no specific stabilising effect in the transition state to be observed in these systems.

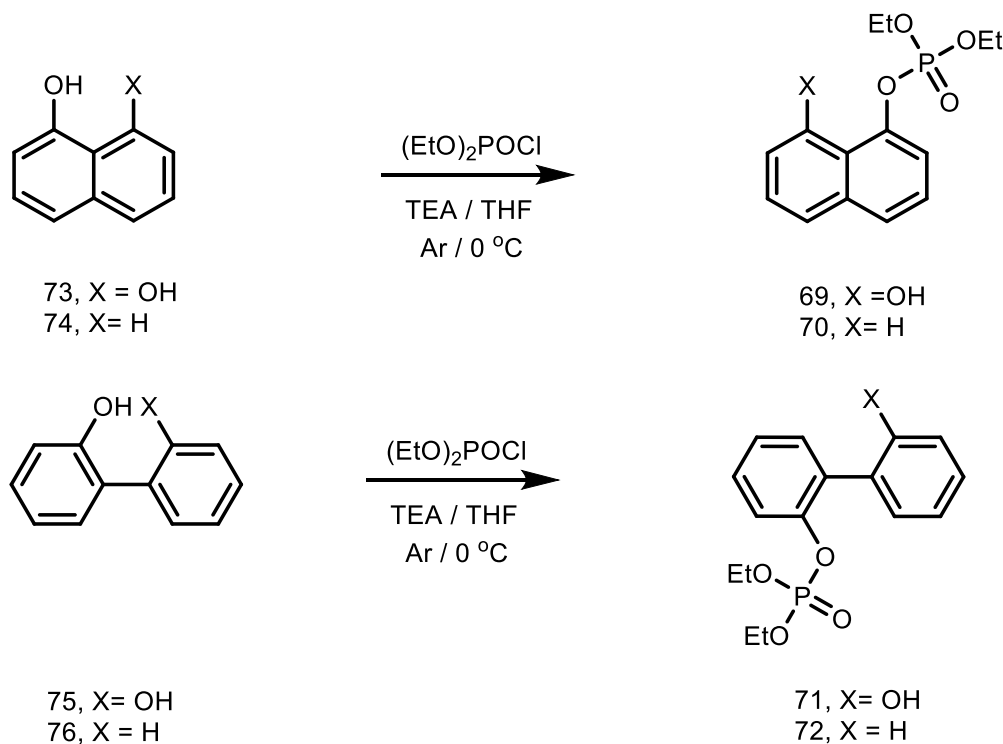


Scheme (3-2): Possible transition states involved in hydrolysis of triester **71**.

3.2. Result and discussion

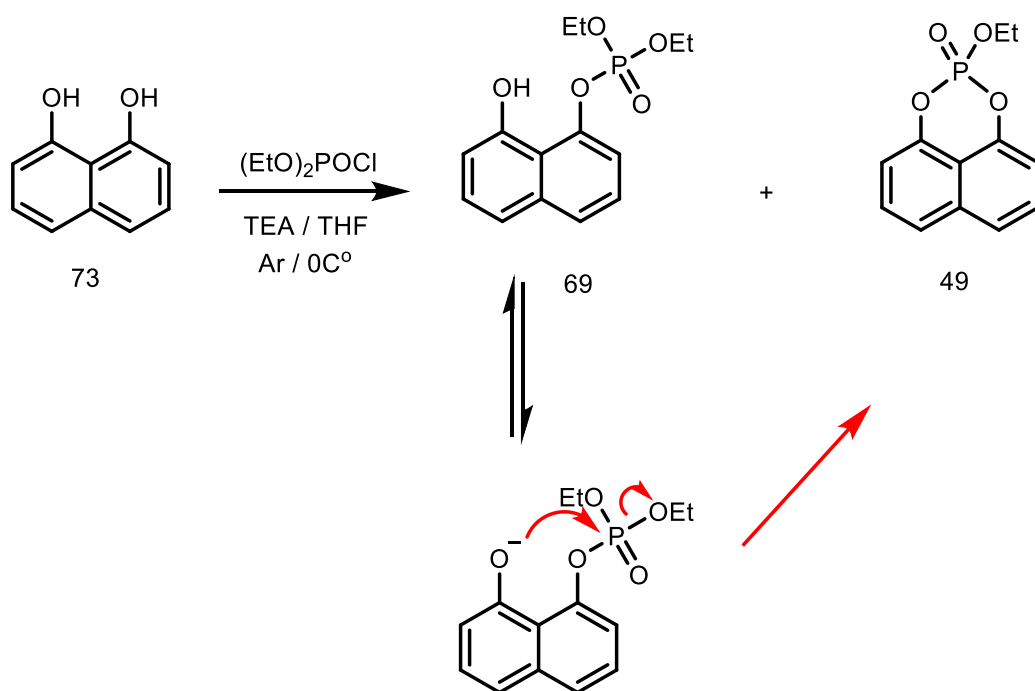
3.2.1. Synthesis of acyclic aryl triesters

Phosphate triesters **69**, **70**, **71** and **72** were synthesised from the commercially available phenols **73-76** in one-step as shown in Scheme (3-3).



Scheme (3-3): Synthesis of diethyl aryl phosphate triesters **69-72**.

When synthesising phosphate triester **69**, both acyclic and cyclic phosphate triester, **69** and **49** were formed in a ratio that varied with time, Scheme (3-4). Leaving the reaction overnight resulted in cyclic phosphate **49** as the dominate product with a low yield of the acyclic triester **69**. However, after approximately an hour, acyclic phosphate **69** was the dominant product and isolated in better yield than when the reaction left for more longer time, even though the reaction had not proceeded to completion. The formation of cyclic phosphate **49** can be attributed to the intramolecular nucleophilic attack by the hydroxyl group on the phosphorus centre, which results in expelling the ethoxy group. Thus, the reaction time for synthesising **69** should take into account the need to avoid formation of the side product **49**.

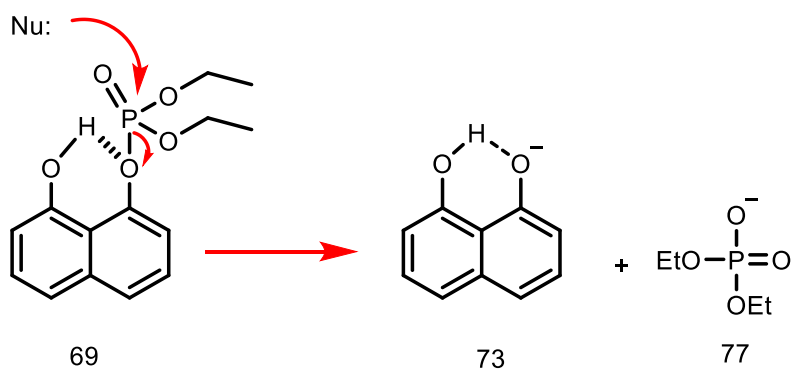


Scheme (3-4): Possible route for formation of ethyl naphthyl cyclic phosphate **49**.

Products of the reaction of triester **1** with hydroxylamine

The hydrolysis of hydroxyl naphthyl phosphate **69** was found to be too slow to follow, thus its degradation was studied in presence of hydroxylamine as this nucleophile is of interest because of its remarkably high reactivity.

Monitoring the progress of the reaction of triester **69** by UV spectroscopy showed a change in the UV spectrum. The wavelength 343 nm was chosen as the anionic form of **73** absorbed at this wavelength, which indicates that the product is 1,8-dihydroxy naphthalene **73**, as expected for P-O cleavage, Scheme (3-6). In chapter two, loss of an alkoxy group was also observed with triesters **46**, **47** and **48**. Hydrolysis of phosphates **69** and **70** were followed by ^{31}P NMR in D_2O at 60°C under the same conditions, Figure (3-3).



Scheme (3-5): Hydrolysis of diethyl-8-hydroxy naphthyl phosphate **69**

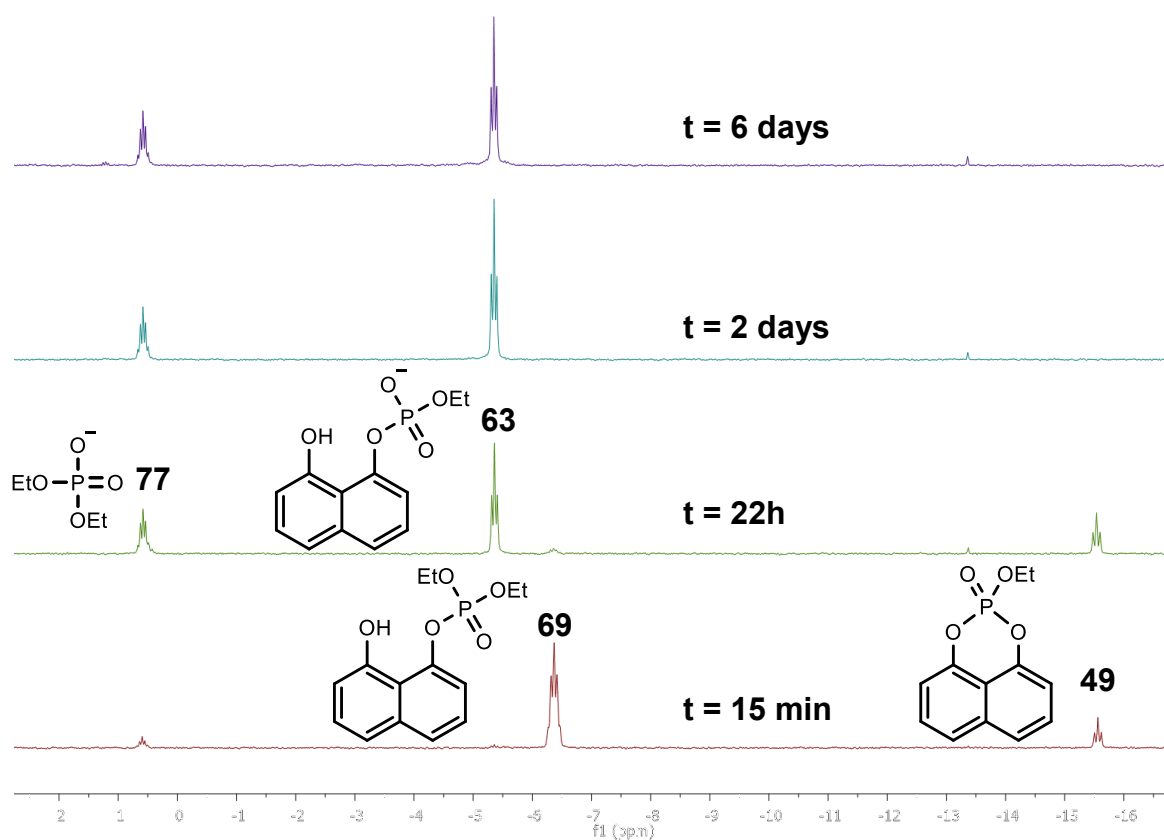
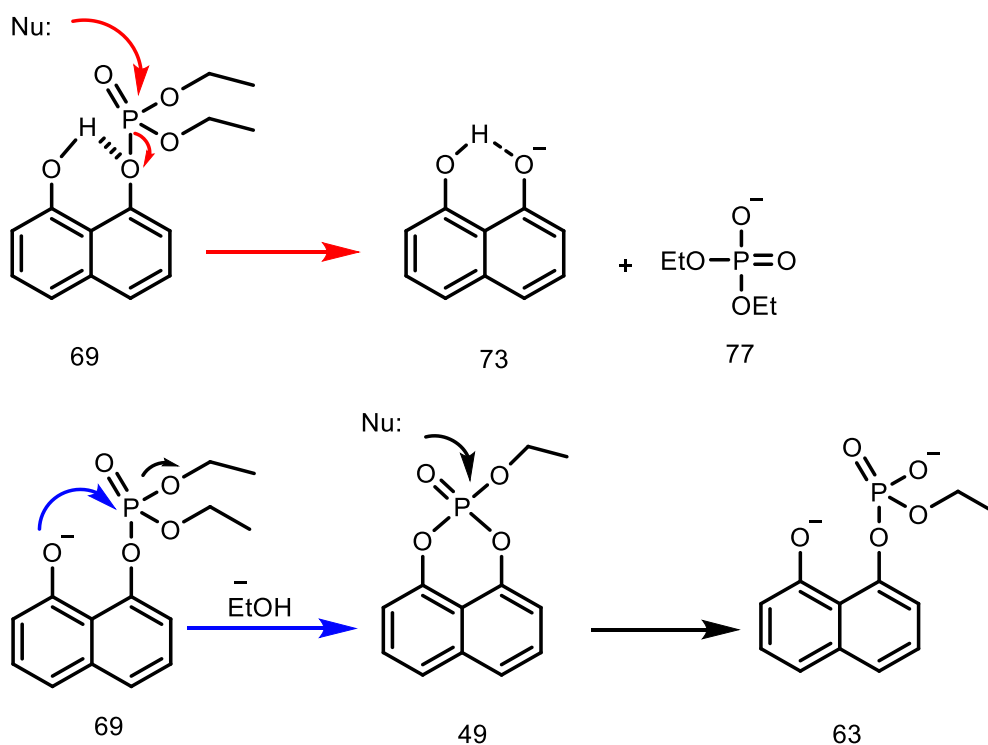


Figure (3-3): The hydrolysis of diethyl 8-hydroxy naphthyl phosphate triester **69**, monitored by ^{31}P NMR, in 0.5 M NH_2OH in D_2O .

^{31}P NMR spectroscopies revealed two phosphorus compounds as final products, which were assigned as phosphate diesters **63** and **77**, Scheme (3-6). One of these products at 0.56 ppm is diethyl phosphate as expected from the reaction of a triester with hydroxylamine, but the other product at -5.36 ppm is an aryl diester, which is most likely formed from the cyclic phosphate **49**, which was assigned at -13.37 ppm. Cyclic phosphate **49** could be formed as an intermediate

from intramolecular nucleophilic attack and reacts further with hydroxylamine to open the ring. By following the whole reaction, cyclic ester **49** was found to be produced gradually and disappeared when starting material finished. In addition, the hydrolysis of cyclic ester **49** was investigated in chapter two, and revealed that the main product was formed from an opening ring reaction. It is possible that the reaction involves C-O bond cleavage of ethyl group by an intermolecular nucleophilic reaction, but this may not be a significant contribution. From figure (3-3), it can be seen that as cyclic phosphate ester **49** was formed it is hydrolysed to phosphate ester **63**. On the other hand, considering in-line that the displacement of the ethyl group $pK_a = \sim 50$ (poor leaving compared with naphthalenediol group, $pK_a = 6.7$ from P-O cleavage) is unlikely to compete with the reaction of interest (the displacement of the naphthalenediol group **73**). Thus the scene is set for intramolecular nucleophilic reaction by deprotonated hydroxyl group as the main reaction path. This type of intramolecular catalysis by a neighbouring group has been observed in phosphate esters previously.⁸⁶⁻⁹⁰



Scheme (3-6): The proposed route for hydrolysis of diethyl-8-hydroxy naphthyl phosphate **69**.

3.3. Kinetic study

3.3.1. The reaction of diethyl 8-hydroxy 1-naphthyl phosphate **69** and diethyl 1-naphthyl phosphate **70** with hydroxylamine

As mentioned above, the hydrolysis occurred inconveniently slowly in water, thus it was necessary to use a reactive nucleophile for the kinetic study of the degradation of compound **69**.

The reaction with hydroxylamine at 60 °C was studied initially. The reaction of 0.5 M hydroxylamine with phosphate triester **69** was investigated over a pH range from 5 to 10, where the neutral form of hydroxylamine is the dominant species. The reaction was followed by monitoring the appearance of the product naphthalene-1,8-diol at 343 nm, using an excess of hydroxylamine to ensure that reactions were pseudo-first order with respect to the substrate. The k_{obs} values were plotted as a function of pH as shown in Figure (3-4). The experimental points were fitted to Equation (3-1), where k_2 is the second order rate constant for reaction of triester **69** with neutral hydroxylamine and pK_a is the dissociation constant for hydroxyl amine.

The pH profile of the reaction with hydroxylamine showed the usual form for a reaction where the deprotonation of one of the reactants is required for reaction. A plateau region at pH 7-10 is consistent with neutral hydroxylamine ($\text{NH}_2\text{OH} \rightleftharpoons \text{HONH}_3^+ - \text{O}^-$) as the dominant reactive species. The pK_a of acid dissociation of HONH_3^+ obtained from the pH profile has a value of 5.8 ± 0.2 , consistent within experimental error with the reported of 5.96^{91} and 6.06^{43} at 25 °C.

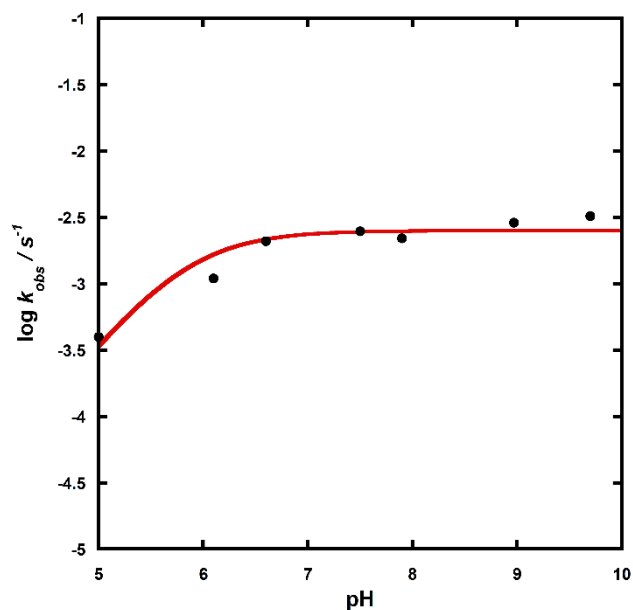


Figure (3-4): Plot of k_{obs} as a function of pH for reactions with triester **69** at 60 °C $I = 1.0$ M (NaCl).

$$\log k_{obs} = \log (k_2[\text{NH}_2\text{OH}]_{\text{total}}(K_a / (K_a + [\text{H}]^+))) \quad \text{Equation (3- 1)}$$

The dependence of the reaction on the concentration of hydroxylamine was also evaluated. The reaction of hydroxylamine with triester **69** was investigated at pH 7.3, where almost all of the substrate is in its neutral form and hydroxylamine is present almost entirely in the neutral form: the k_{obs} values obtained are plotted in Figure (3-5) as a function of $[\text{NH}_2\text{OH}]$ concentration. The data were fitted to Equation (3-2), where k_0 is the rate constant for the spontaneous hydrolysis and k_2 is the second order rate constant for reaction of the triester with neutral hydroxylamine. From the fitting data of Figure (3-5), using Equation (3-2), the hydroxylamine reaction hydrolysis constant could be estimated as $k_2 = 4.1 \pm 0.2 \times 10^{-3} \text{ M}^{-1} \text{ s}^{-1}$, whereas the hydrolysis in water did not happened spontaneously (too slow). For control compound **70**, the reaction with hydroxylamine at different concentrations was also investigated at pH 7.3 and 60 °C: k_{obs} values are plotted against $[\text{NH}_2\text{OH}]$ concentrations as shown in Figure (3-6), and the data was fitted to Equation (3-2).

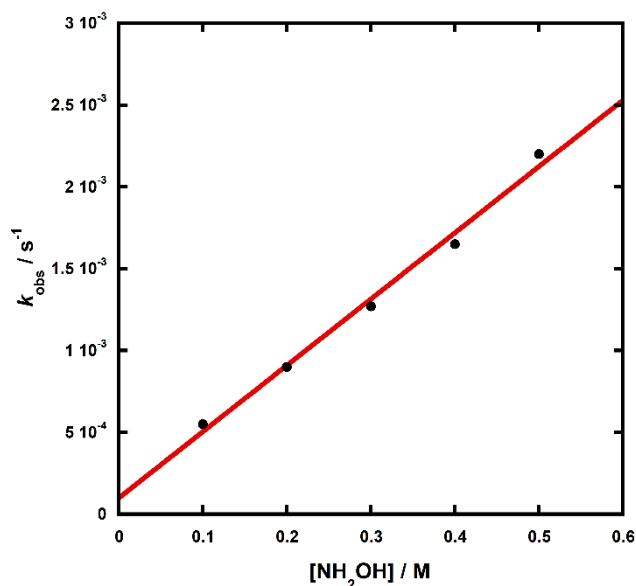


Figure (3-5): Plot of k_{obs} as a function of hydroxylamine concentration for reactions with triester **69** at 60.0 °C, pH = 7.3 and $I = 1.0$ M (NaCl).

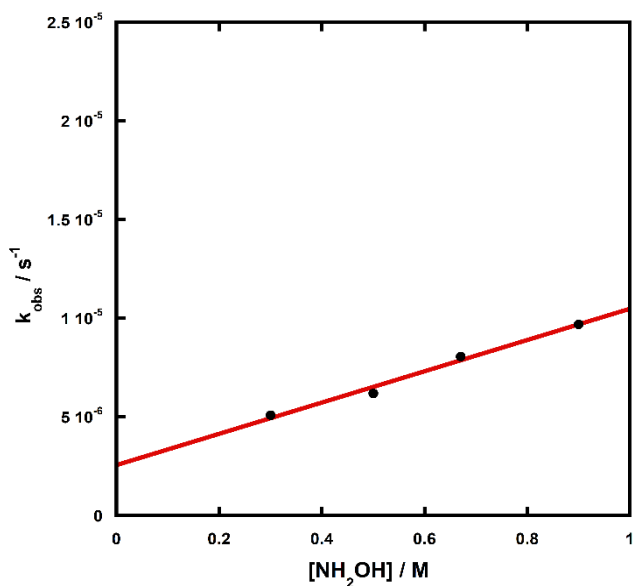


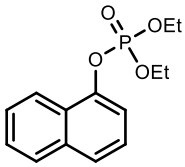
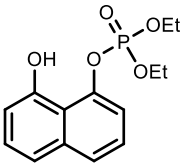
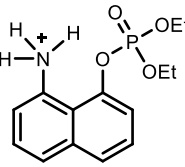
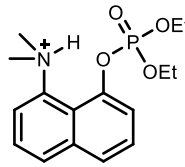
Figure (3-6): Plot of k_{obs} as a function of hydroxylamine concentration for reactions with triester **70** at 60 °C, pH = 7.3 and $I = 1.0$ M (NaCl).

$$k_{\text{obs}} = k_0 + k_2[\text{NH}_2\text{OH}]$$

Equation (3- 2)

The second-order rate constants so derived are given in Table (3-1), together with the values for related compounds already reported. The value of k_2 for hydroxylamine reacting with triester **70** showed that the reaction rate of **69** is 500 fold higher. This remarkable increase in the rate indicates that effective catalysis of the degradation of **69** by the hydroxyl group through intramolecular hydrogen bond to the leaving group can be achieved.

Table (3-1): The second order rate constants, k_2 and the relative rate constants, k_{rel} for the reactions of various phosphate triesters with NH_2OH .

Triester				
$k_2 / \text{M}^{-1} \text{s}^{-1}$	$7.9 \pm 0.7 \times 10^{-6}$	$4.1 \pm 0.2 \times 10^{-3}$	$5.5 \pm 0.7 \times 10^{-2}$ (41)	$1.32^{(42)}$
k_{rel}	1	500	7 000	170 000

The most reactive system showed a rate acceleration of 10^6 for the diethyl 8-dimethylamino phosphate triester by general acid catalysis by ammonium group. In this system the hydrogen bond has been suggested to assist the general acid catalysis, where this hydrogen bond is assumed to be weak or absent in the ground state. Considering that it is the same case in triester **69**, thus as the nucleophile attack the phosphorus centre, the hydrogen bond must be developed or become stronger in the transition state (TS1), and then bond formation to the nucleophile would be advanced. In the transition state for the reaction of **70**, there is no intramolecular hydrogen bond due to the absence of a hydroxyl group, so the stability of negative charge that developed on the leaving group oxygen was not possible. The acceleration of 500 fold by hydroxyl group of hydrolysis of phosphate naphthyl triester **69** indicates a stabilisation of about 17 kJ mol^{-1} in transition state (TS1), and thus lowers the energy barrier for the reaction compared with **70**.

However, some of the stabilisation could be provided by hydrogen bonds in the product. The effect of hydroxyl group in the product anion (the first pK_a of 1,8-naphthalenediol is 6.6, 2.8 units lower than 1-naphthol corresponding to about 16 kJ mol^{-1}).⁸⁰ It has been reported in the literature that the effect of the hydroxyl group that has similar pK_a value to the leaving group can provide approximately 10-40 fold rate acceleration (in carboxylic ester hydrolysis, phosphate monoester hydrolysis⁸⁰, phosphate triester hydrolysis⁹² and acetal²⁷ hydrolysis).

Thus, the almost of 500 fold acceleration can be attributed to stabilisation of the transition state by hydrogen bonding. Based on this initial analysis, it is clear that the transition state for the intramolecular catalysed reaction of **69** is significantly different from that for triester **70** as can be illustrated in Figure (3-7).

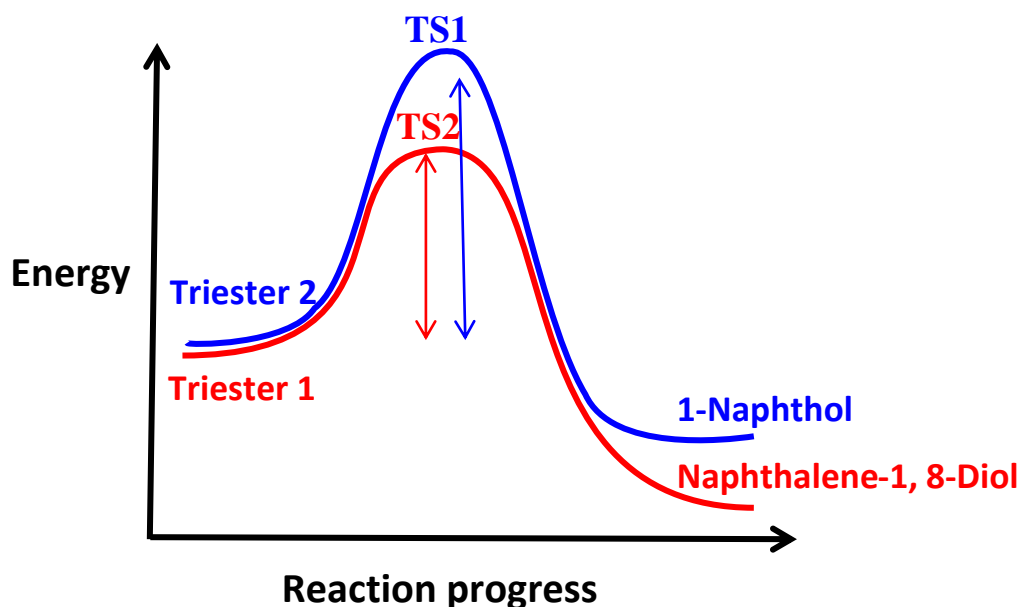


Figure (3-7): Expected free energy profile of the reactions of phosphate triesters **69** and **70** with hydroxylamine (blue) and (red) respectively.

The rate of cleavage of diethyl 8-dimethylamine 1-naphthyl phosphate is 325-fold faster than the reaction of phosphate triester **69**, showing that the dimethylammonium group has a considerably higher catalytic effect than the hydroxyl group. Kirby *et al.* have explained this reactivity due to the general acid catalysis (GAC) assisted by hydrogen bonding, where the general acid catalysis is absent in hydroxyl compound **69** based on the libido rule (explained early in introduction chapter). Thus, during progress of the reaction of Kirby model, transferring the proton from acid to leaving group becomes more effective to catalyse the reaction. In the case of phosphate triester **69**, the general acid and the leaving group in the product have the same pK_a value, thus the contribution of the hydrogen bond by a hydroxyl group can only be observed to catalyse the reaction, and the proton transfer will not be involved thus the rule is not obeyed in naphthalene system **69**.

Protonation of the P=O unit by the hydroxyl group to catalyse the reaction was ignored in hydrolysis of cyclic phosphate **46** (chapter two), due to geometry as discussed in chapter two. In the case of phosphate triester **69** the phosphate unit has more flexibility to be rotated into hydroxyl group side, making protonation of the P=O unit more plausible. However, it is not possible to use the comparison with full protonated diester **67** (studied at 25 °C)⁷⁹ and phosphate triester **69** (studied at 60 °C) due to different conditions. Thus, it is possible to use the comparison between hydrolysis of phosphate diester **67** with phosphate diester **68**, Figure (3-8), which have been studied previously at the same conditions, to evaluate the catalytic role of hydroxyl group by protonating the P=O unit to catalyse reactions. A detailed study on phosphate ester complexes by Williams and Forconi has shown a rate acceleration for the hydroxide-catalysed reaction of phosphate diester **68** of about 60 fold compared with phosphate diester **67**.⁸⁰ This is consistent with the view that the hydroxyl group does not catalyse the reactions by P=O protonation. In considering that the effect of the hydroxyl group on the similar structure of phosphate triesters would be the same, it is accepted that the OH group of naphthyl phosphate triester **69** is not accelerating the reaction by protonating the P=O unit.

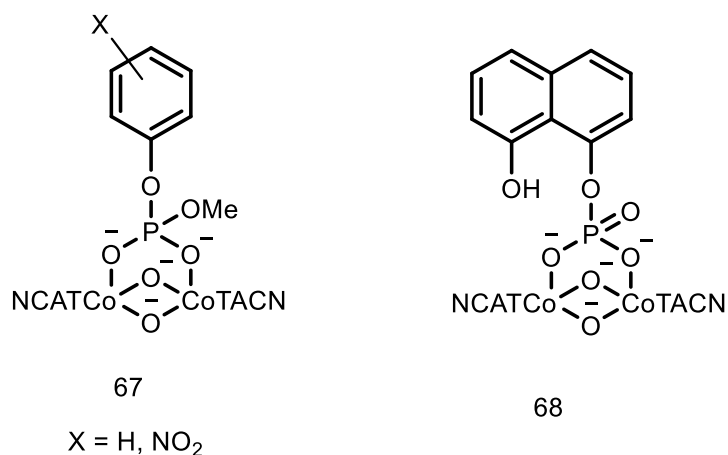


Figure (3-8): Structure of phenyl phosphate diester **67**,⁷⁹ and naphthyl phosphate diester **68**.⁸⁰

3.3.2. The reaction of diethyl 2-hydroxy biphenyl phosphate **71** and diethyl biphenyl phosphate **72** with hydroxylamine

The reaction of **71** at different concentrations of hydroxylamine was studied at pH 7.3 and 60 °C, monitoring the reaction by HPLC, Figure (3-9). Two new products were observed in the

HPLC chromatogram of the product mixture from **71**: the expected product of P-O cleavage, 2,2'-dihydroxy biphenyl at 17.5 min, **75**, and another product with a retention time of 12.5 min. The reaction of **71** was also monitored by ^{31}P NMR analysis under the same conditions, which revealed that the second product at -4.87 ppm is plausibly assigned as the ethyl 2-hydroxy biphenyl phosphate diester, **78**, Figure (3-10).

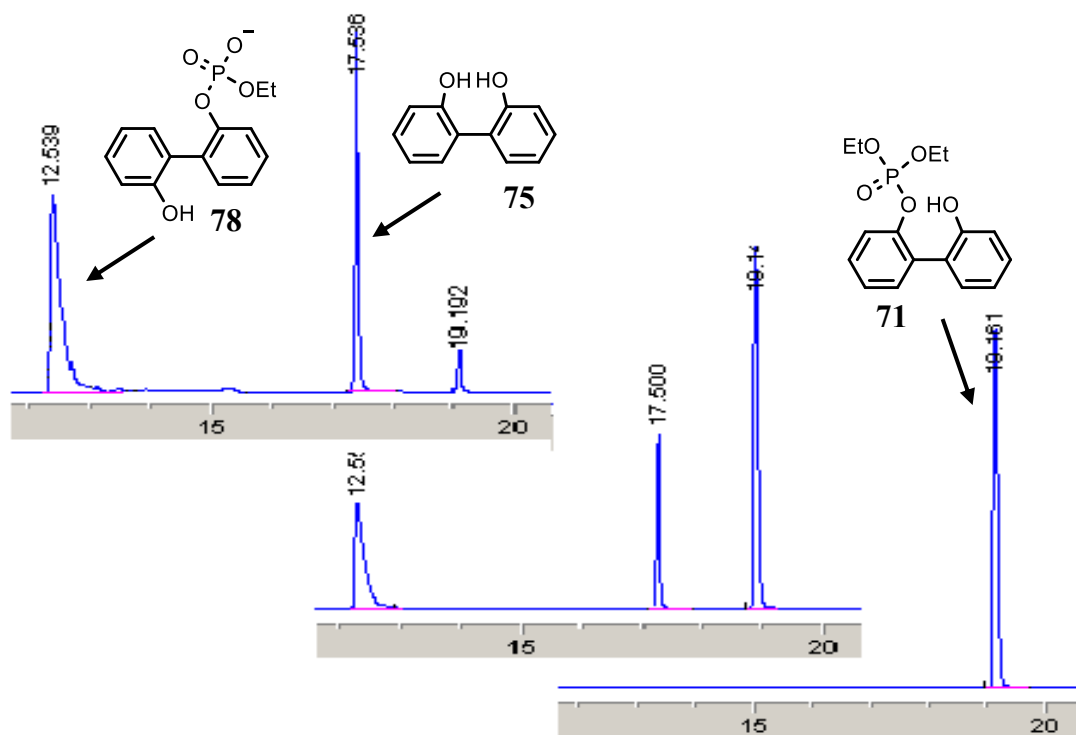


Figure (3-9): Representative HPLC chromatogram of the hydrolysis of **71** in the presence of hydroxylamine at different times (1=0 h, 2=20 h, 3= 40 h, 4=50 h). (30 % DMSO, pH 7.3 and 60 °C.).

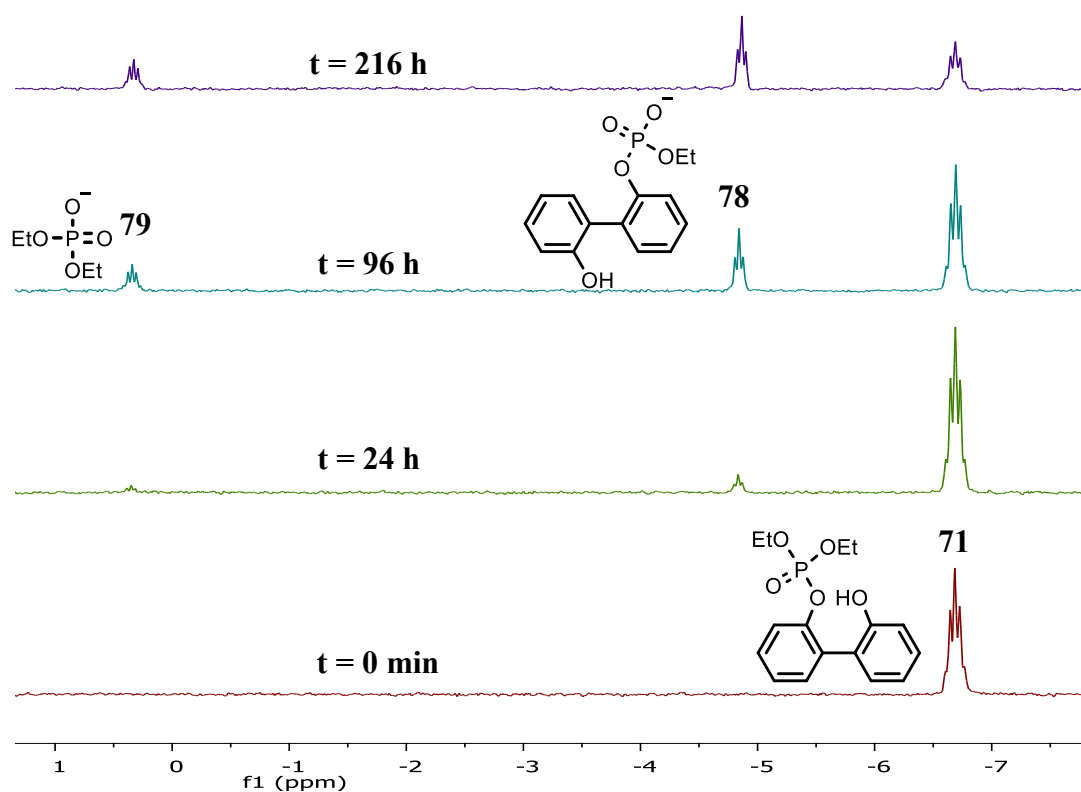
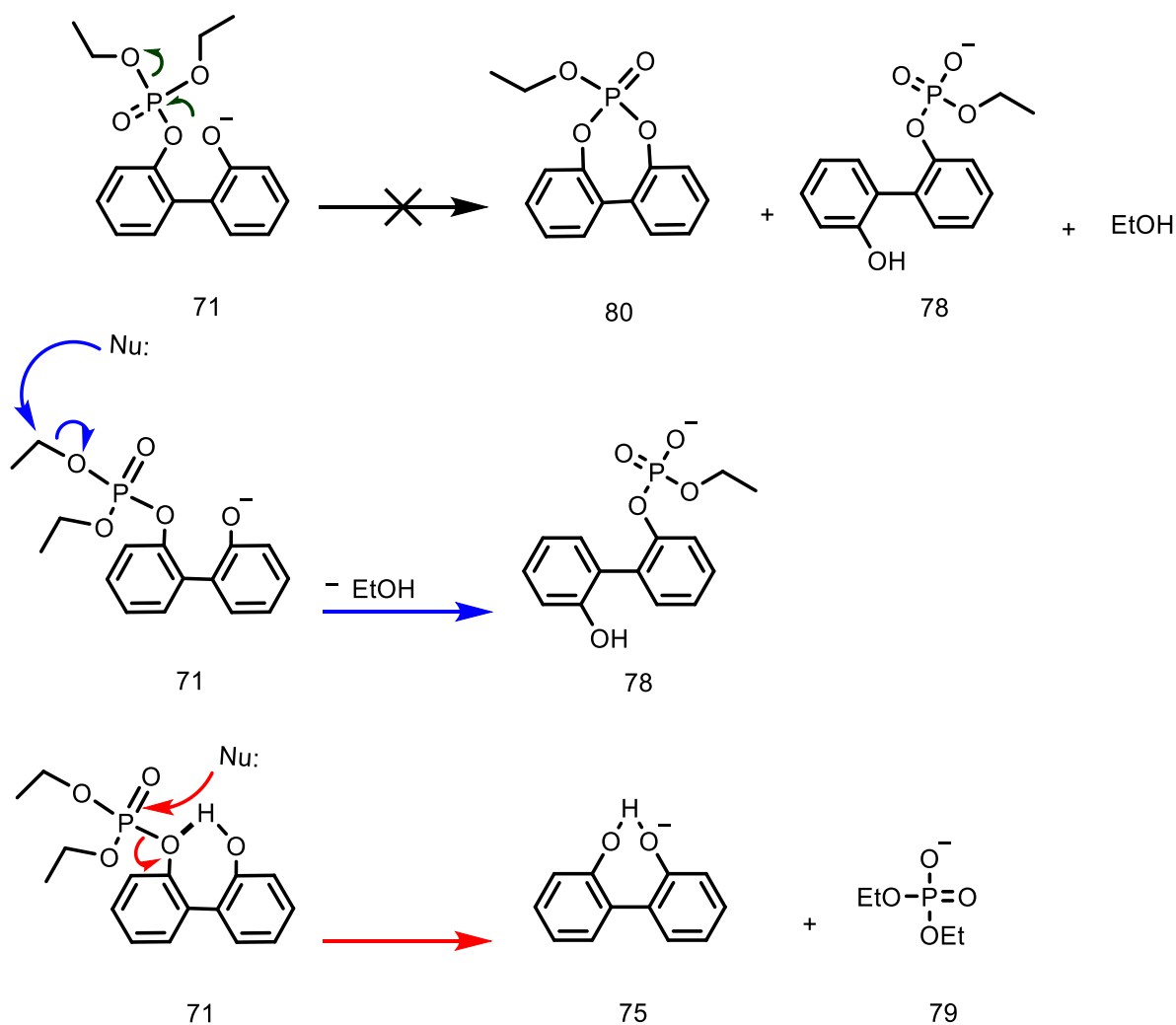


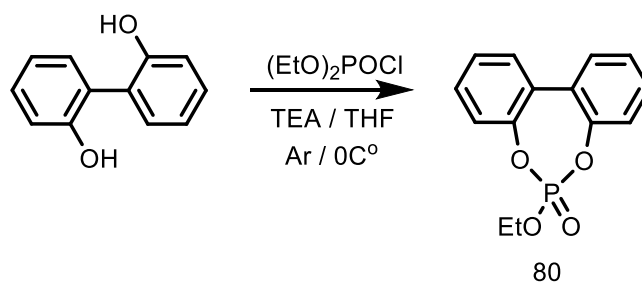
Figure (3-10): The hydrolysis of diethyl 2-hydroxy biphenyl-2'-phosphate triester **71**, monitored by ^{31}P NMR, in 0.5 M NH_2OH in D_2O at pH 7.3 and 60°C .

It was expected that this ester could form from intramolecular nucleophilic attack by the deprotonated hydroxyl group, forming an intermediate cyclic phosphate diester **80**. A similar reaction was observed in naphthalene model **60**, however, ^{31}P NMR did not detect this intermediate **80**, Scheme (3-7).



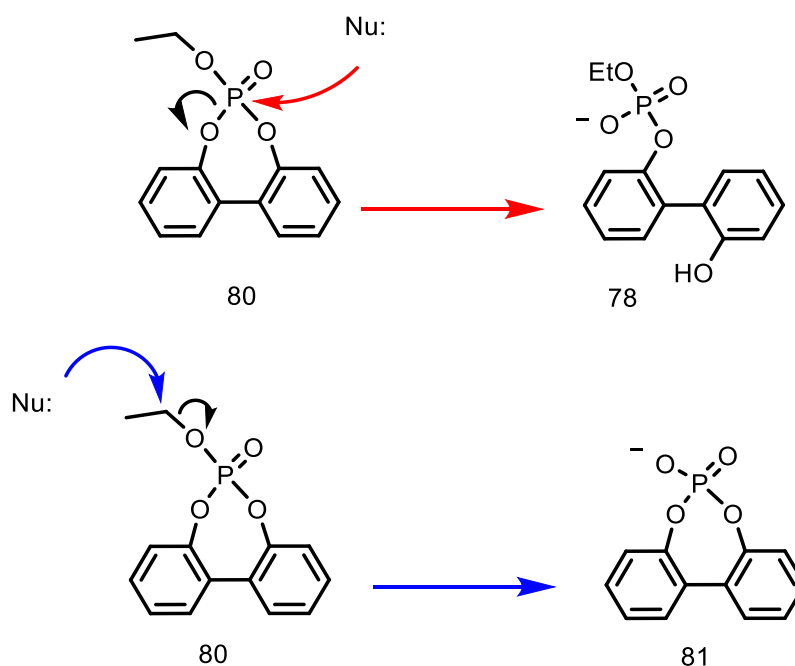
Scheme (3-7): The proposed mechanisms of cleavage of diethyl 2-hydroxy biphenyl-2'-phosphate triester **71**, 0.5 M NH_2OH in D_2O , Hydrogen bond catalysis (red), intramolecular nucleophilic catalysis (black) and intermolecular nucleophilic catalysis (blue).

The cyclic ester **80** could be a reactive species and hydrolyse rapidly as soon as it is formed to give diester **78**. To test this hypothesis it was decided to synthesize the cyclic phosphate intermediate **80** to observe its hydrolytic behaviour. Compound **80** was prepared as shown in Scheme (3-8) from 2,2'-dihydroxy biphenyl, with triethylamine added to the diethyl dichlorophosphate to yield cyclic diethyl phosphate triester.



Scheme (3-8): Synthesis of ethyl cyclic biphenyl phosphate triester **80**.

The hydrolysis of **80** was carried out under same conditions as used for the reaction of triester **71**, by following the reaction by ^{31}P NMR in D_2O and 60°C . The ^{31}P NMR spectrum, Figure (3-11), showed the disappearance of starting material **80**, and two new products forming at 5.4 ppm and -4.52 ppm in agreement with HPLC data. One of these peaks at 5.4 ppm was assigned as cyclic phosphate monoester **81** as the main product of reaction, with ethyl biphenyl phosphate **78** as minor product, Scheme (3-9). Clearly, the hydrolysis of cyclic phosphate triester **80** was slow enough for this intermediate to be observed if it were formed in hydrolysis route of phosphate triester **71**. Thus, the conclusion on hydrolysis of phosphate triester **71** confirms that diester **78** was formed directly of intermolecular nucleophilic attack by the nucleophile (hydroxylamine).



Scheme (3-9): The proposed mechanism of hydrolysis of ethyl 2,2'-biphenyl cyclic triester **80**, where the nucleophile is the hydroxylamine.

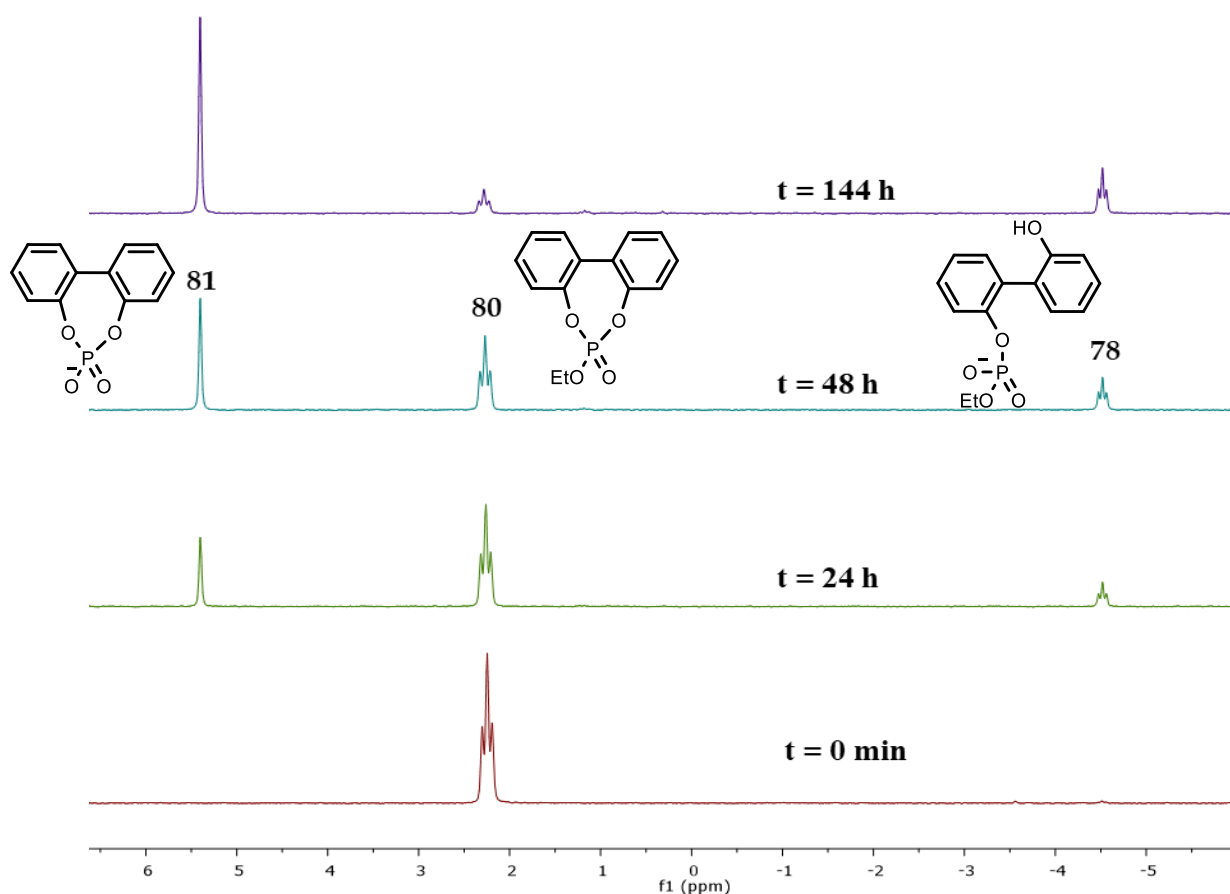


Figure (3-11): Monitoring the hydrolysis of ethyl biphenyl cyclic phosphate triester **80** by ^{31}P NMR, 0.5 M NH_2OH in D_2O at pH 7.3.

3.3.3. Influence of the hydroxylamine concentration on diethyl 2-hydroxy biphenyl phosphate **71** degradation

The degradation of phosphate triester **71** was studied in different concentrations of hydroxylamine at pH 6.3, Figure (3-12). The second order constant, $k_2 = 7.82 \pm 0.44 \times 10^{-6} \text{ M}^{-1} \text{ s}^{-1}$. This value is about 500-fold lower than for naphthalene model **69**, and similar to naphthalene model **70**. This difference and similarity with **69** and **70**, respectively, can be attributed to the degree of rotational freedom in **71**, which makes the formation of hydrogen bond less favourable. Compound **72**, which has no hydroxyl group, was found to be more stable than **71**. The rate constant in the presence of 0.5 M hydroxylamine with phosphate triester **72** at pH 7.3, $k_{\text{obs}} = 2.5 \pm 0.5 \times 10^{-7} \text{ s}^{-1}$, and for biphenyl phosphate **71** ($k_{\text{obs}} = 6.7 \pm 0.3 \times 10^{-6} \text{ s}^{-1}$) showed a difference in the rate of 27 times. Thus, the reaction of phosphate triester **71** with hydroxylamine involves a transition state with a smaller energy barrier than phosphate triester

72, by $\sim 6 \text{ kJ mol}^{-1}$. This difference is a small but makes a noticeable effect on the rate of reaction of **71**, which can be attributed to some contribution from the hydroxyl group through formation of a hydrogen bond. This hydrogen bond must be weak and remarkably inefficient when compared with triester **69**. These results were not very accurate because of experimental difficulties related to solubility problems especially of phosphate triester **72**, despite using 50% of a co-solvent to help the solubility.

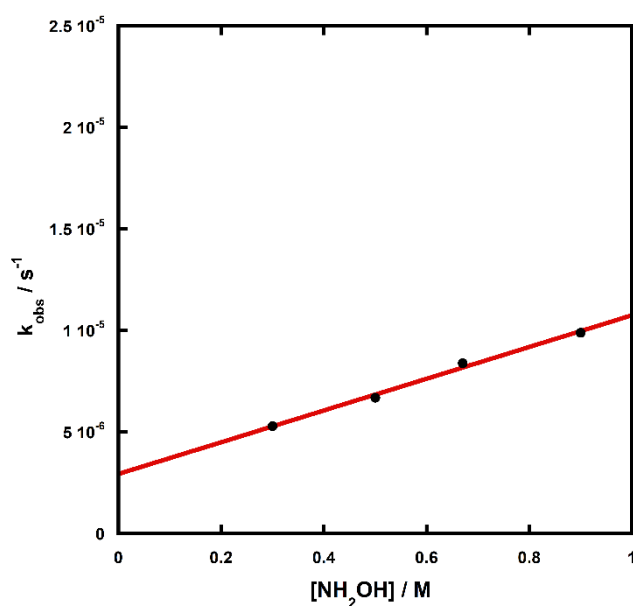


Figure (3-12): Plot of k_{obs} as a function of hydroxylamine concentration for reactions with triester **71** at 60.0 °C, pH = 7.3 and $I = 1.0 \text{ M}$ (NaCl).

In summary: The observations made here revealed that the presence of a hydroxyl group in triester **69** provides a significant acceleration in the reaction rate, although the effect is 325 fold less than for a dimethylammonium group held in the same geometry. The difference between reaction rates resulted due to involving of general acid catalysis assisted by hydrogen bonding by dimethylammonium group to leaving group, which drives the reaction thermodynamically by transferring the proton from ammonium group to leaving group during the reaction.

The hydroxyl group showed a rate acceleration of 500 fold, equivalent to about 17 kJ mol^{-1} , compared with triester **70**. This effect should not be attributed to the stability of the hydrogen

bonding in the product as discussed earlier.⁸⁰ The effective catalysis by hydroxyl group should be contributed to hydrogen bonds in the transition state, as has been suggested recently by Williams *et al.*⁸⁰ In addition, the rigidity of the structure was found to play an important role in controlling the reactivity. The reaction of diethyl 2-hydroxy-2'-biphenyl phosphate **71** with hydroxylamine was 500-fold slower than the reaction of diethyl 8-hydroxy-1-naphthyl phosphate **69**. The pK_a of 2,2'-biphenol is 7.5, 0.5 units higher than 1, 8-dihydroxy naphthalene, 6.6. There is no significant difference in the pK_a s, which indicates again that the catalytic reactivity by hydroxyl group in **69** is not due to thermodynamic effect. The activation energy of 17 kJ mol^{-1} is close to data of **71**, this indicates that the enforced proximity (the precise position of OH on scaffold naphthalene) in triester **69** can be an important factor to achieve a hydrogen bond that can have an effect in the transition state.

However, a difference of 27 fold for the reaction of hydroxylamine with **71** and **72** indicates that although there is a degree of rotation and absence of enforced proximity in triester **71**, the hydroxyl group is still able to provide some catalytic effect (27 fold acceleration $\sim 9 \text{ kJmol}^{-1}$). In the product anion (the pK_a of 2-phenyl phenol is 10.0,⁹³ 2.4 units lower than 2, 2'-biphenol (first pK_a is 7.6)⁹⁴ $\sim 14 \text{ kJmol}^{-1}$. This value is higher than the hydroxyl group effect on the transition state, which provides $\sim 9 \text{ kJ mol}^{-1}$. Thus, the reaction of biphenyl phosphate **71** could have a thermodynamic benefit of hydrogen bonding in the product of 2,2'-biphenol, but there is no clear cut evidence of ruling out the contribution of some extra kinetical benefit of formation of a hydrogen bond in the transition state leads to catalyse the reaction. However, the biphenyl rings with ortho substituents favours the two phenyl rings to be in the twisted conformation to avoid the steric effect, and thus less stable hydrogen bond formation.

3.4. Conclusion

The effect of hydrogen bond catalysis has been investigated with hydroxyl group as intramolecular hydrogen bond donor in phosphate triester. Dephosphorylation of diethyl 8-

hydroxy 1-naphthyl phosphate **69** by hydroxylamine has been investigated, and found to be promoted by hydroxyl group as hydrogen bond donor. The hydroxyl group showed a rate acceleration of 500 fold, equivalent to an up to 17 kJ mol^{-1} stabilisation in the transition state, compared with triesters without of this catalytic group diethyl 1-naphthyl phosphate **70**, and with flexible system, diethyl 2-hydroxy-2'-biphenyl phosphate **71**. The sum total of all the above observations indicates that the mechanism of the hydrolysis of naphthyl phosphate triester **69** is the hydrogen bond catalysis, and there is no other suggested mechanism involved in the reaction such as general acid catalysis or catalyse the reaction by protonating the P=O unit of phosphate group.

It is obvious that the hydroxyl group has clearly a great effect in these systems particularly in naphthalene system. Thus, the project aim goes further one hydroxyl group to probe the influence of more than one hydroxyl group on the reactivity.

Chapter Four: Multiple Hydrogen Bonds Effect (Phenyl System)

4.1. Introduction

As described in chapter two and three, even in water a carefully positioned hydroxyl group can provide a significant contribution to promoting the reaction of methyl 1, 9-anthryl cyclic phosphate triester **46** with water and nucleophiles, as well as diethyl 8-hydroxy-1-naphthyl phosphate **69**. As this effect appears to be due to hydrogen bond formation rather than general acid catalysis, it suggests that investigating the effect of multiple hydrogen bond donors would be interesting. In previous studies, intramolecular OH groups can work cooperatively to stabilise a conjugate base⁹⁵ or to increase the binding²³ as discussed in the introduction chapter. The question posed here is: how does a hydrogen bonding network affect the rate of hydrolysis of phosphate esters and will it provide a substantial additional effect compared with single hydrogen bond?

Therefore, this chapter describes studies on two model systems bearing more than one –OH group, triesters **82** and **83**, Figure (4-1).

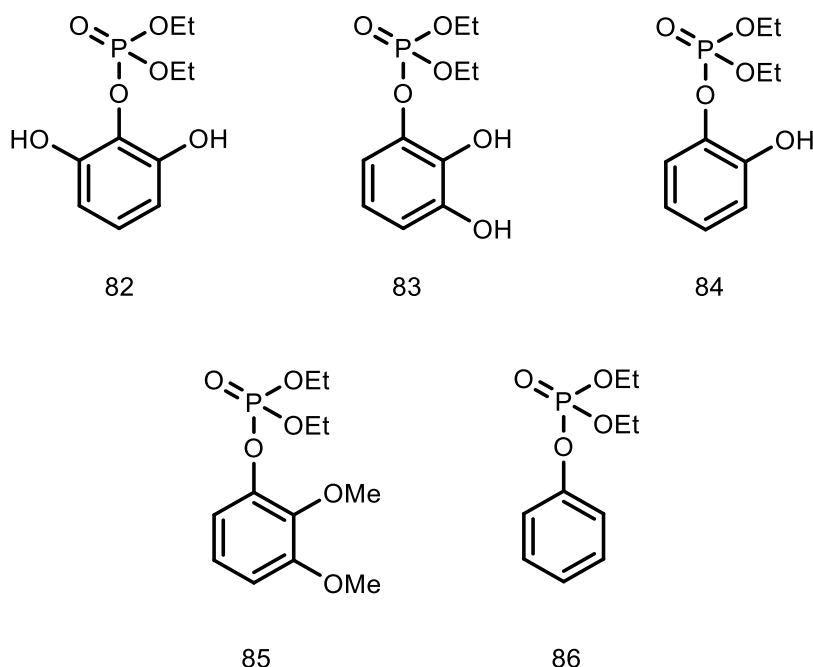


Figure (4-1): Structures of acyclic triester phosphates with different number of hydroxyl groups.

As described in chapter 1, hydrogen bond arrays were also found to stabilise negatively charged centres and thus increase DMSO acidities of a series of polyols⁹⁵, and increase the binding affinity using a phenol system with different number of hydrogen bond donors.²³ Based on findings by Shokri. *et al.*⁹⁵ and Cockroft *et al.*²³ adding a second H-bond donor to structures **82** and **83** could significantly enhance stabilisation to the transition state of the P-O cleavage reaction and add extra catalytic effect, Figure (4-2). The hydroxyl groups in esters **82** are designed to interact simultaneously with a leaving group oxygen, and in **83** a second hydroxyl group is positioned to enhance the effect of terminal hydrogen bond donor that interacts with the leaving group and then increase its strength, Figure (4-3). Triesters **84-86** are control compounds, to establish the effect of a single hydrogen bond donor with this geometry, and to measure the intrinsic reactivity of the systems.

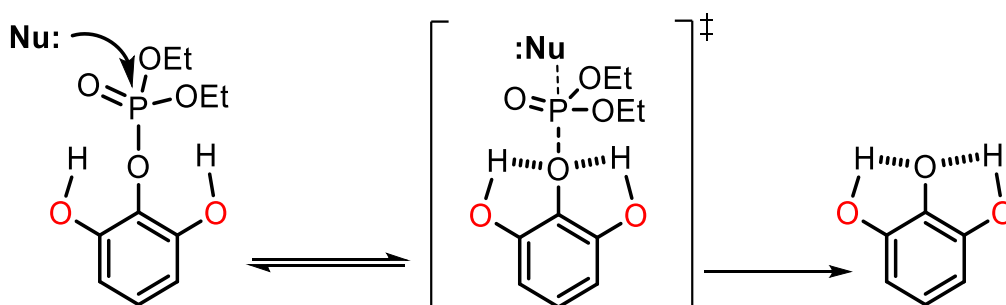


Figure (4-2): The mechanism of hydrogen bond catalysis.

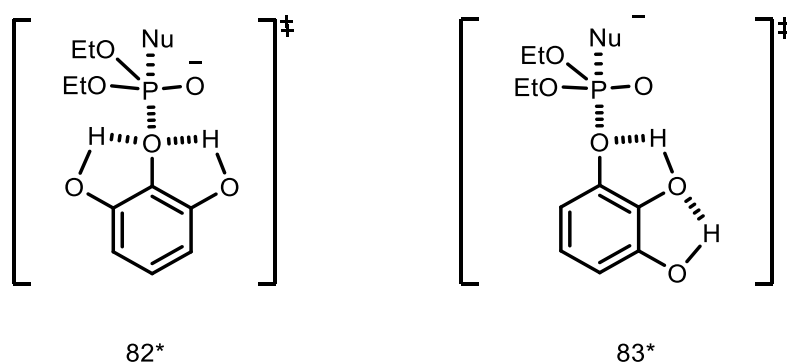


Figure (4-3): Transition states for the cleavage of triesters **82** and **83**.

However, intramolecular catalysis by a neighbouring hydroxyl group in its deprotonated form might also be observed in these cases:²⁴ general base catalysed hydrolysis or nucleophilic attack

could occur and are outlined in Figure (4-4). These are kinetically identical, but give different products.

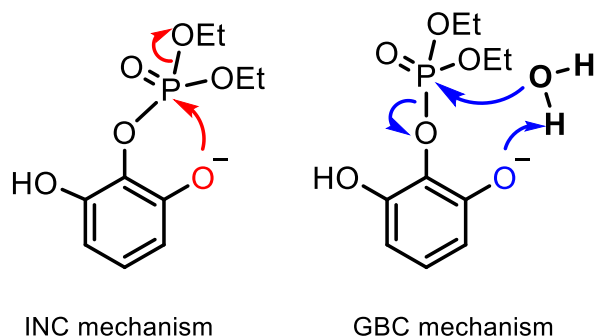
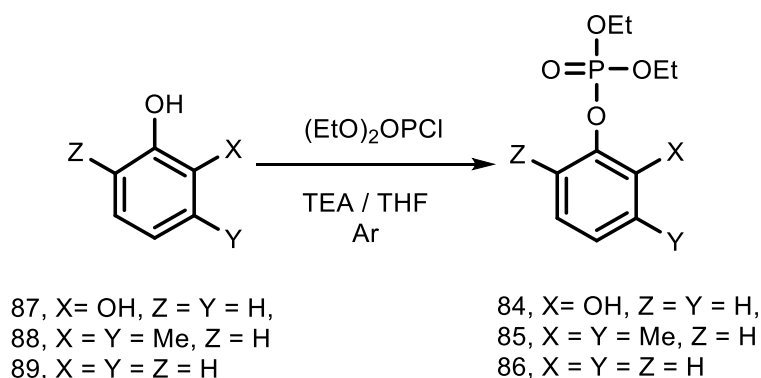


Figure (4-4): General base and intramolecular nucleophilic catalysis mechanisms.

4.2. Results and discussion

4.2.1. Synthesis of acyclic phenyl triester 84-86:

Compounds **84-86** were prepared following Scheme (4-1). The reaction was initiated by adding triethylamine to a mixture of phenol and diethyl chlorophosphate and the desired compound purified by column chromatography.

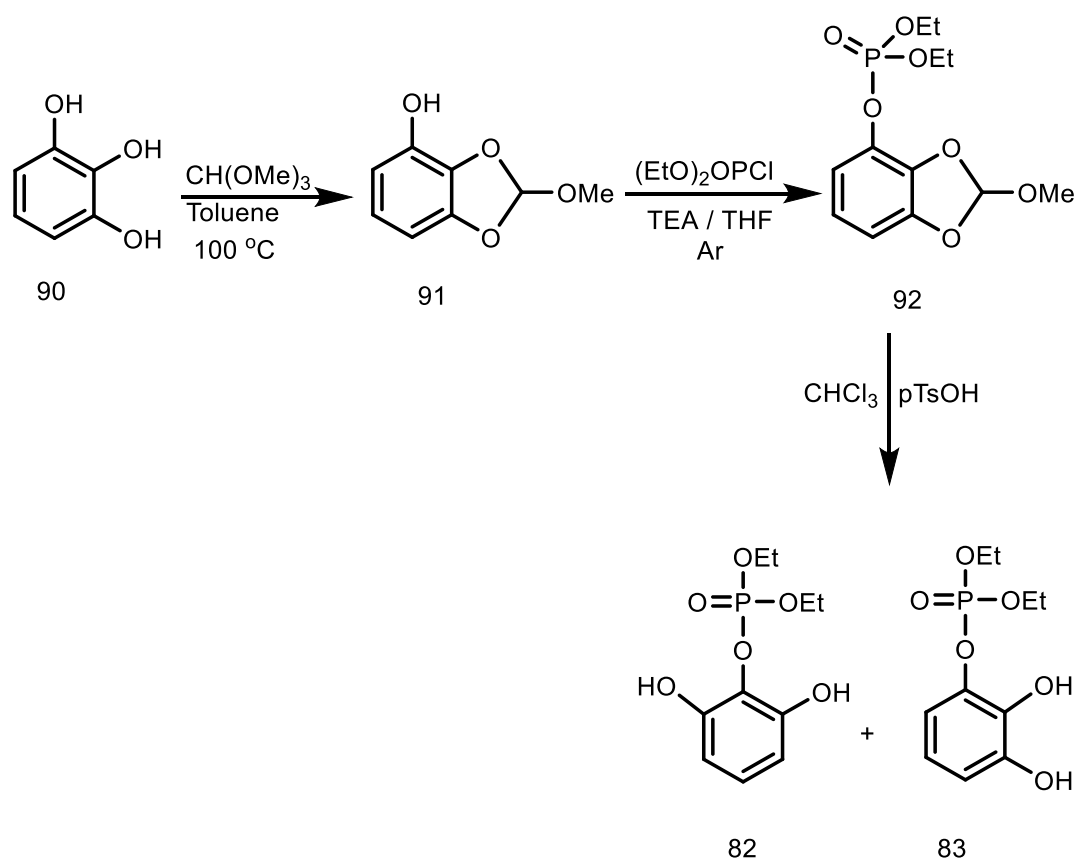


Scheme (4-1): Synthesis of diethyl acyclic phenyl phosphate triesters **84-87**.

4.2.2. Synthesis of acyclic phenyl triester 82 and 83:

The direct phosphorylation of pyrogallol **90** in the specific positions of interest to give triesters **82** and **83** was a challenge. NMR analysis of the reaction mixture always showed multiple P environments in a range -3 to -10, as expected for phosphate triesters. Thus a different synthetic

route for compound **83** was adopted, which involved protection of two of the hydroxyl groups with trimethyl orthoformate to give the intermediate **91**, to prevent multiple phosphorylation of pyrogallol. The next step was phosphorylation of the hydroxyl group to give triester **92** followed by a deprotection step to yield triester **83**. Interestingly, the isolated product was a mixture of triester **82** and **83**, Scheme (4-2). ^{31}P NMR, ^1H NMR and mass spectrum confirmed that a mixture of products form in a ratio of 1:3, Figure (4-5).



Scheme (4-2): Synthesis of diethyl acyclic phenyl phosphate triesters **82** and **83**.

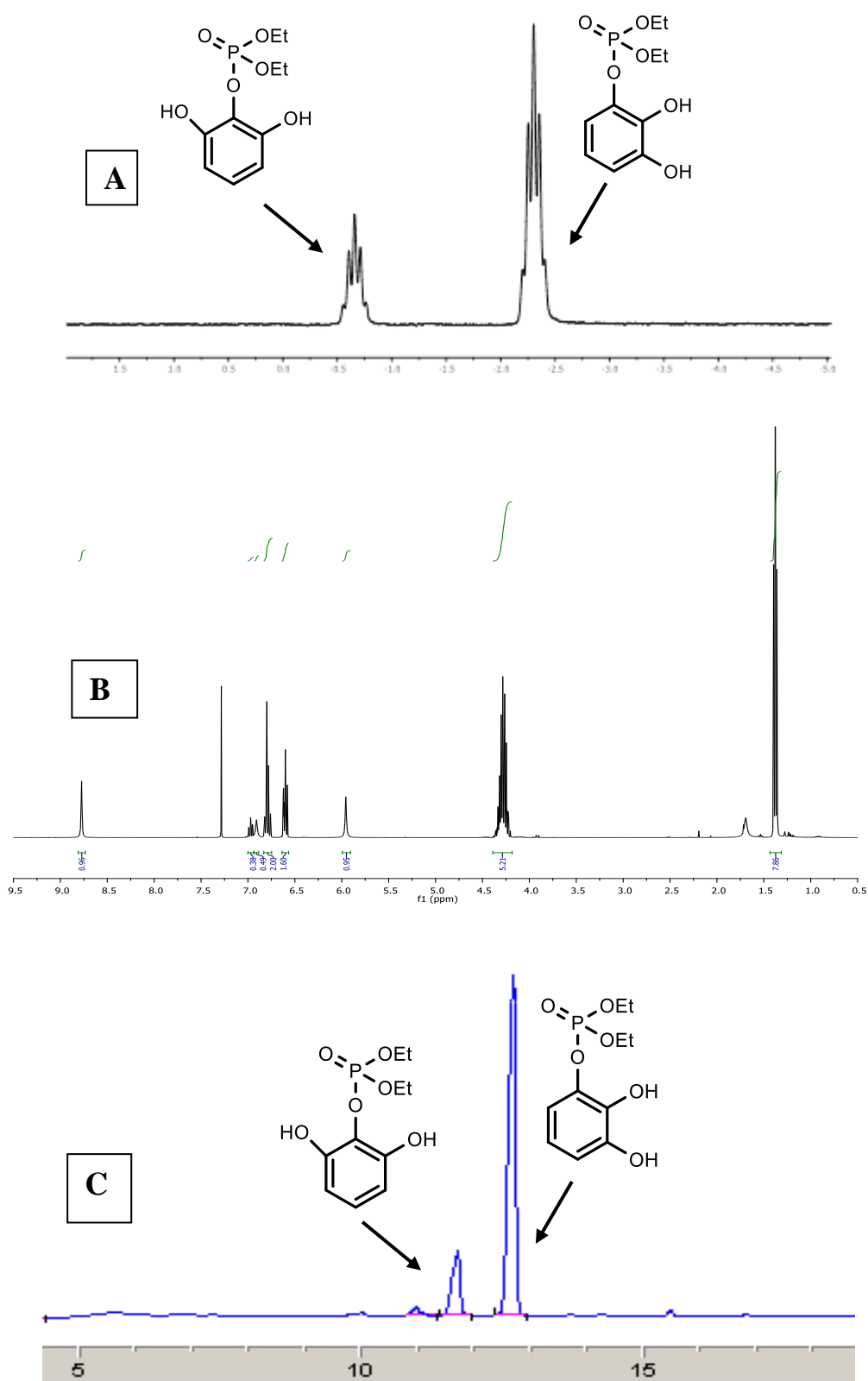


Figure (4-5): A mixture of **82** and **83** representing by ^{31}P NMR (A), ^1H NMR (B) and HPLC chromatogram (C).

4.2.3. Attempts to separate the mixture of **82** and **83**

Separation by column chromatography was not possible due to the similar R_f of both compounds despite testing a range of different solvents. HPLC showed that these triesters **82** and **83** have different retention times (RT 12.1 and 13.08 min respectively). Thus, an attempt was made to separate them by this technique (using water and acetonitrile as an eluent). The separation of these two esters was not quite successful, and ^{31}P NMR and ^1H NMR showed that some of each isomer can be found with the other, to give mixtures with different ratios, as shown in Figure (4-6) and Figure (4-7). However, the sample of fraction 1 (where the majority is triester **82** was found to convert to the same ratio as before separation where the majority of the mixture is triester **83**). Therefore, no more attempts to separate these compounds were carried out, and it was decided to carry out the kinetic study on the mixture using HPLC.

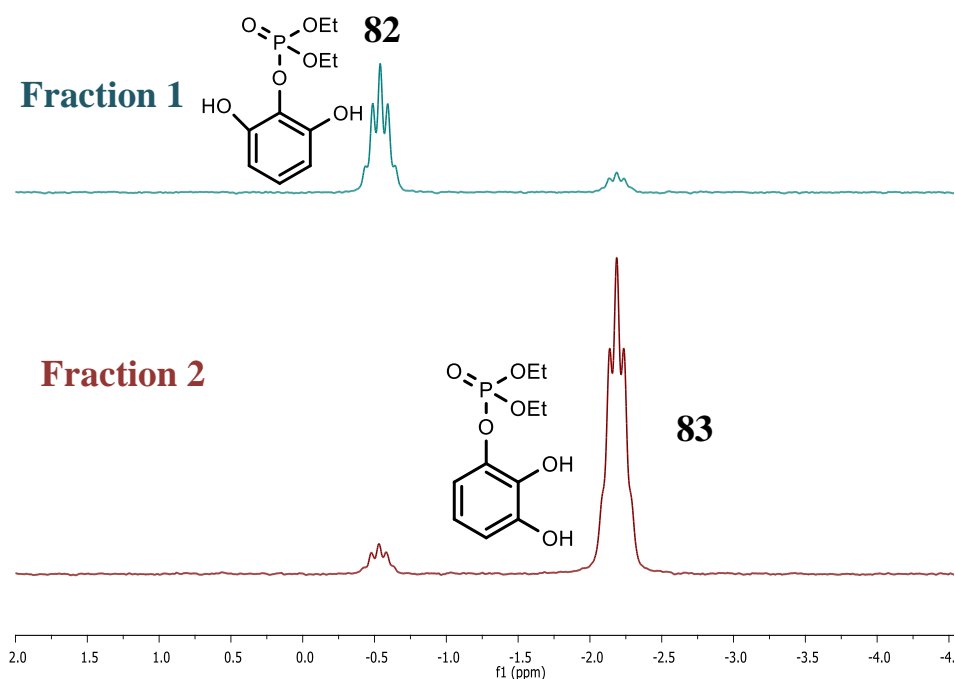


Figure (4-6): Triesters **82** and **83** after separation using HPLC as presented by ^{31}P NMR.

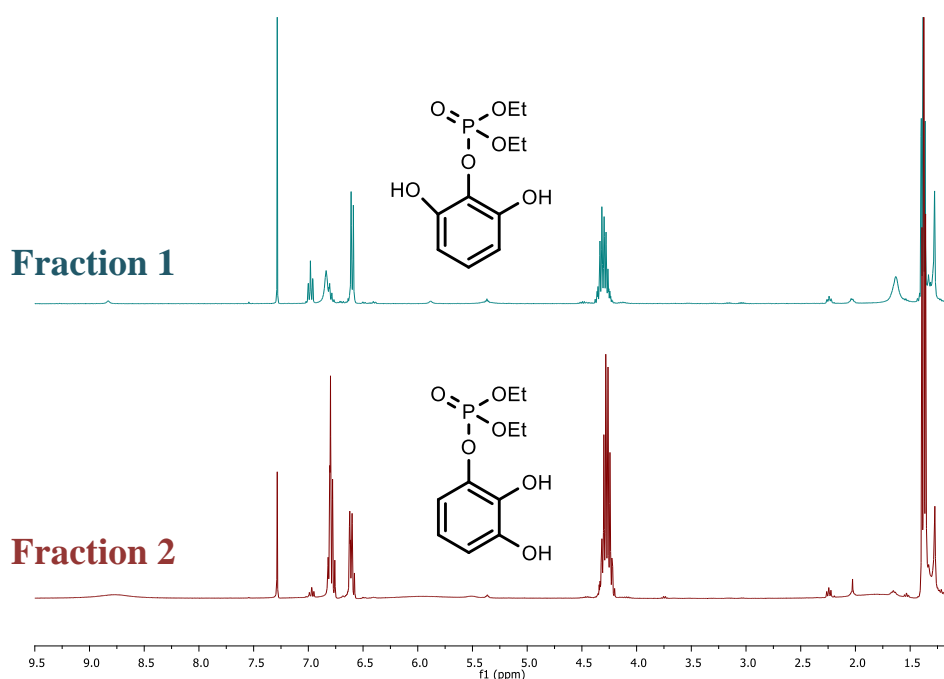


Figure (4-7): Triesters **82** and **83** after separation using HPLC as presented by ^1H NMR.

4.2.4. Hydroxylamine reaction with triesters **82** and **83**

The reaction of compounds **82** and **83** with hydroxylamine was studied at different concentrations (0.1 - 0.7 M) of hydroxylamine, using HPLC at 25 °C, ionic strength 1 M (NaCl), and 4-nitrobenzoic acid as internal standard, at pH 6.9. At this pH, hydroxylamine is in its neutral form (NH_2OH or $^+\text{NH}_3\text{O}^-$). The pseudo first-order reactions of compounds **82** and **83** were obtained by plotting the ratio of area peaks values as a function of the time. The second order rate constants were obtained by plotting the k_{obs} values as a function of neutral $[\text{NH}_2\text{OH}]$ concentration as shown in Figure (4- 1). The data were fitted to equation (4-1), where k_0 is the rate constant for the spontaneous hydrolysis and k_2 is the second order rate constant for reaction of the phosphate ester with hydroxylamine. The second-order rate constants are $k_2 = 7.22 \pm 0.36 \times 10^{-5}$ and $6.94 \pm 0.46 \times 10^{-5} \text{ M}^{-1} \text{ s}^{-1}$ for **82** and **83** respectively. It was possible to estimate the contribution of intramolecular nucleophilic hydrolysis constants for **82** and **83** as $k_0 = 2.66 \pm 1.5 \times 10^{-6} \text{ s}^{-1}$ and $2.45 \pm 1.9 \times 10^{-6} \text{ s}^{-1}$, respectively, from the fitting of the data Figure (4-8) using equation (4-1). The rate of degradation of these triesters is enhanced up to 27 fold in the presence of hydroxylamine, an indication of a small but significant effect.

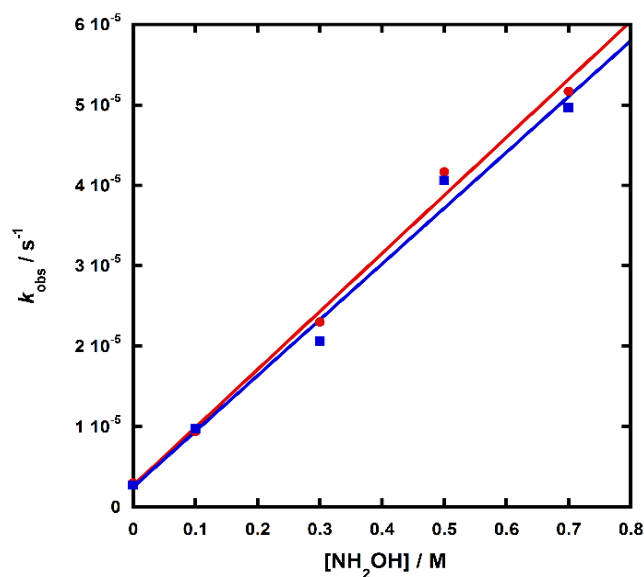


Figure (4-8): Plot of k_{obs} as a function of hydroxylamine concentration for reactions with triester **82** (red) and **83** (blue) at 25.0 °C, pH = 7.3 and I = 1.0 M (NaCl).

$$k_{\text{obs}} = k_0 + k_2[\text{NH}_2\text{OH}]$$

Equation (4- 1)

The pH-dependence of the reaction was also evaluated. The reactions of **82** and **83** with hydroxyl amine (0.5 M) were followed over the pH range 5-10, using HPLC at 25 °C, 1 M (NaCl) ionic strength and 4-nitrobenzoic acid as internal standard in buffered solutions. The reactions were followed by monitoring the disappearing of starting materials **82** and **83**. It was not possible to monitoring the pyrogallol as an expected product of the reaction, due to it decomposing under these conditions during the final analysis. For pH 5-7, self-buffered hydroxylamine was used. The pseudo first-order reactions of compounds **82** and **83** were obtained by plotting the ratio of area peaks values against time. The pH profile data are shown in Figure (4-9), and equation (4-2) was fitted to the data.

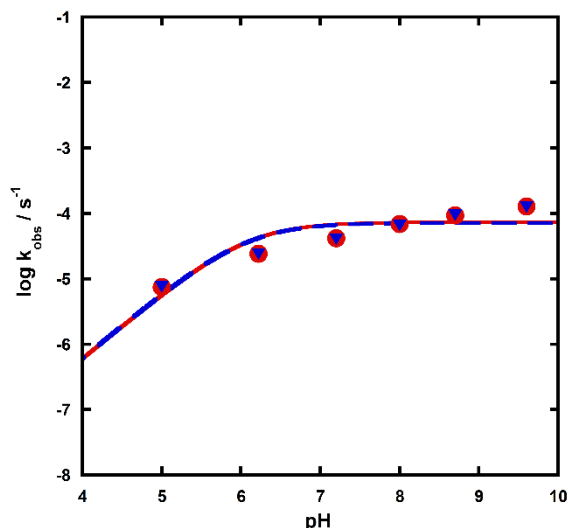
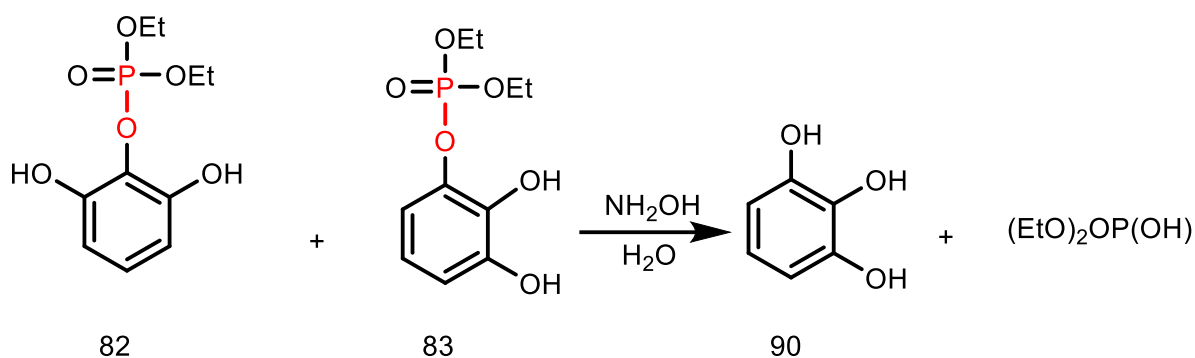


Figure (4-9): pH-rate profiles for the reactions of TPP **82** (●) and **83** (▼) with 0.5 M NH₂OH, at 25 °C and I = 1.0 (NaCl).

$$\log k_{\text{obs}} = \log (k'_2[\text{NH}_2\text{OH}]_{\text{total}}(K_a / (K_a + [\text{H}^+]))) \quad \text{Equation (4-2)}$$

Equation (4-2) include the pK_a value of the hydroxyl amine, and described the correlation between this value and the rate data for each pH value, with $R^2 = 0.99$. The rate constant of hydrolysis of **82** and **83** were estimated for the contribution of hydroxylamine as, $k'_2 = 7.4 \pm 1.8 \times 10^{-5}$ and $7.2 \pm 1.8 \times 10^{-5}$, respectively, which showed an agreement within experimental error with the linear correlation between hydroxylamine concentration and the observed rate constants using Equation (4-1), in terms of $k_2 = k'_2$.

Initially, it seemed of this similarity in the rate between **82** and **83**, that the position of second hydroxyl group did not add different contributions to the catalysis in these structures (*ie.* whether the both hydroxyl groups bonded to the same leaving group or they hydrogen bonded in array manner, the rates were similar). However, HPLC analysis revealed that under these conditions for the spontaneous and hydroxylamine promoted reactions, **82** and **83** are not hydrolysed mainly to the P-O bond cleavage product **90** (RT = 4.9 min), as shown in Scheme (4-3), but other two hydrolysis products are formed as dominant species (peaks at RT = 6.2 and 7.5 min, respectively), Figure (4-10).



Scheme (4-3): Expected route for hydrolysis of diethyl phenyl phosphate triesters **82** and **83**.

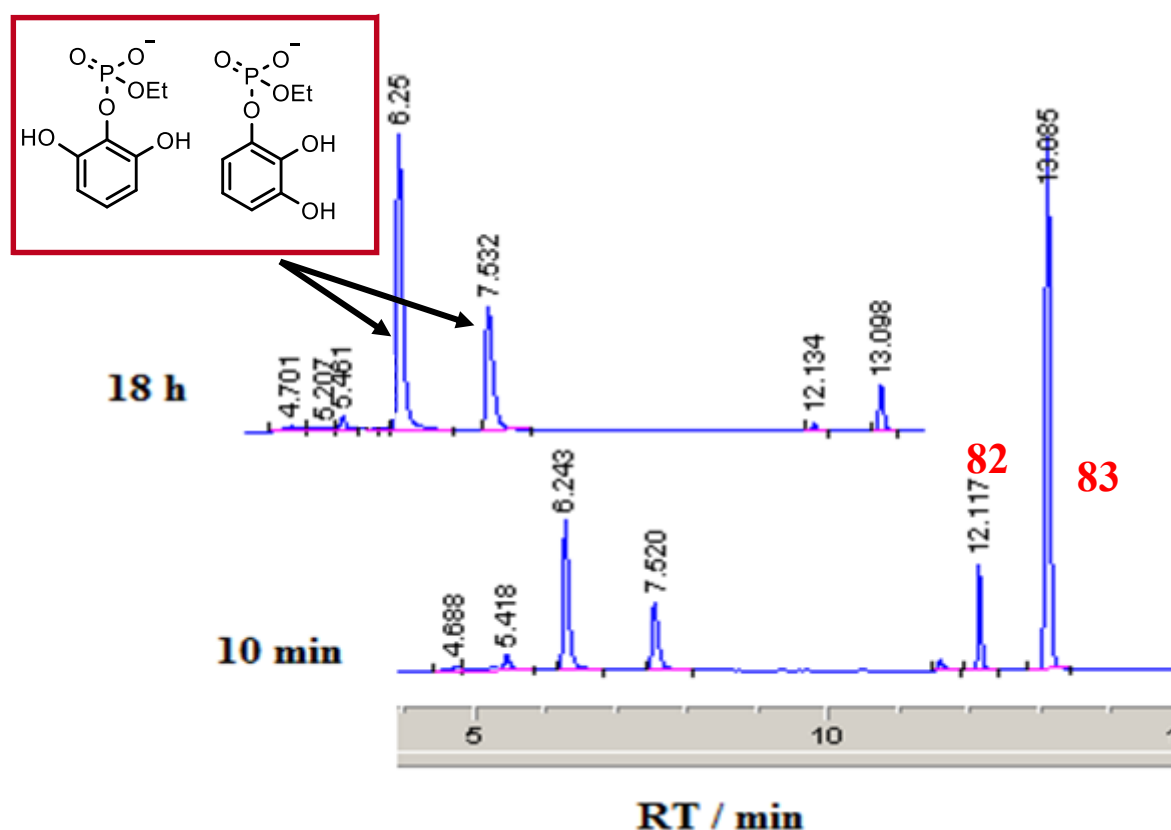


Figure (4-10): Representative HPLC chromatogram of the hydrolysis reaction of **82** and **83** in the presence of hydroxylamine at different time (1 = 10 min, 2 = 18 h).

4.2.5. Product analysis of triesters **82** and **83**

As the HPLC data indicated two different products, ³¹P NMR analysis was carried out in D₂O under the same conditions, Figure (4-11), and revealed that these two products have triplet peaks, which were assigned as phosphate diesters (**93** and **94**), Scheme (4-4). Mass spectrum analysis also indicated the existence of these diesters in the product mixture. These products are most likely formed either from the hydroxyl group acting as intramolecular nucleophile,

which leads to displacement of ethoxy group, or through C-O bond cleavage of the ethyl group by reaction with an intermolecular nucleophile. Both reactions could be operating at the same time, but the question is whether the hydroxyl group can attack as an effective nucleophile, and if it can, which reaction is dominant? Thus, further investigations were carried out on phenyl triesters with and without hydroxyl group. If the reaction proceeds predominantly through intermolecular nucleophilic attack, reaction rates should not be different. If the rates are higher in case of triesters with hydroxyl group in structures, it is likely the dominant reaction does involve hydroxyl group as a nucleophile.

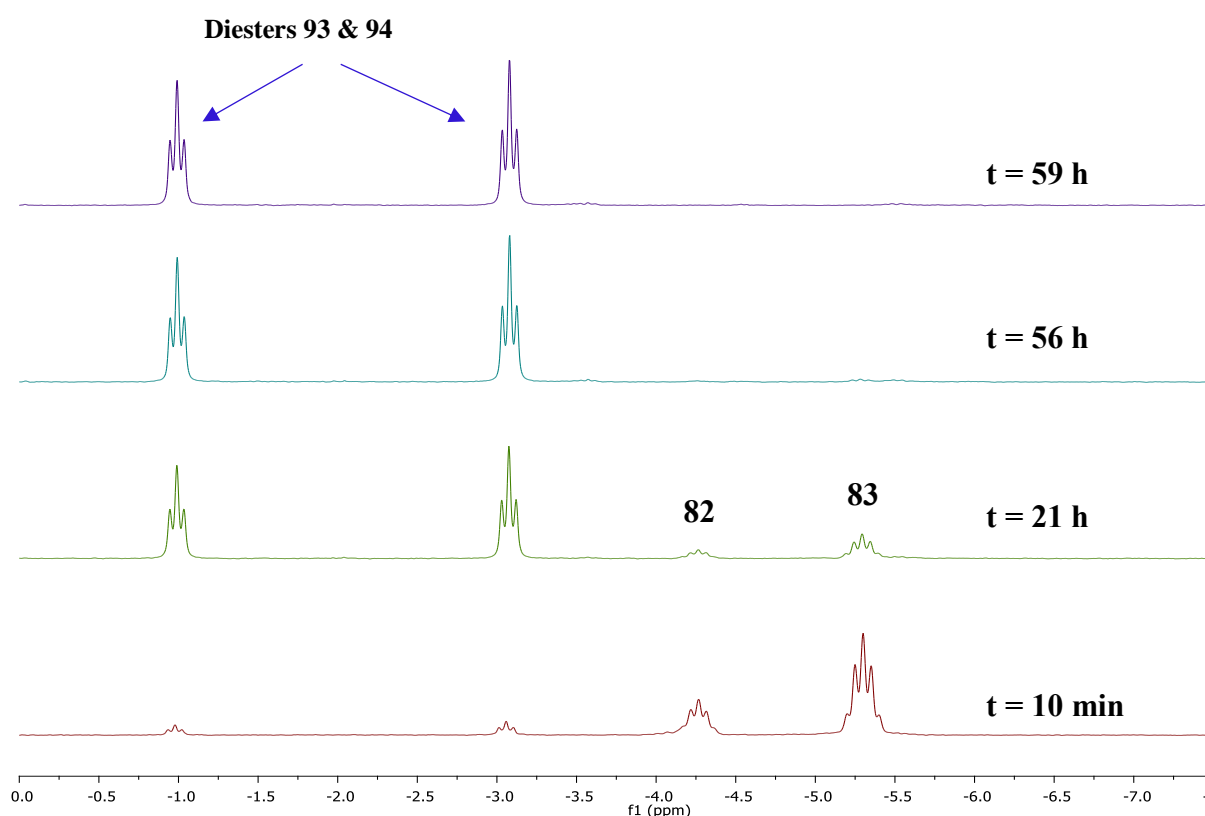
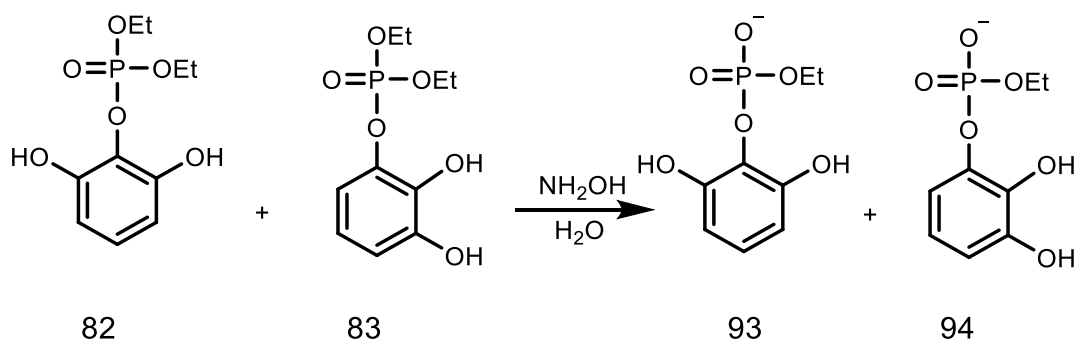


Figure (4-11): Monitoring the hydrolysis of phosphate triester **82** and **83** using ^{31}P NMR in D_2O .



Scheme (4-4): Hydrolysis of diethyl acyclic phenyl phosphate triesters **82** and **83**.

4.2.6. Hydrolysis of phenyl phosphate triesters 84-86

As triester **84** has a hydroxyl group in the same position as **82** and **83**, the reaction of triester **84** with different concentration of hydroxylamine was investigated at pH 7.3, 25 °C and $I = 1.0$ M (NaCl). The reactions were followed by monitoring the disappearance of triester **84** using HPLC. The relative peak areas were calculated between triester **84** and the product formed. The experimental points were fitted to the first order rate Equation (4-1). The second-order rate constants k_2 were calculated by plotting these k_{obs} values against the concentration of hydroxylamine, Figure (4-12). The values of the rate constant for hydroxylamine reaction is $5.27 \pm 0.14 \times 10^{-5}$, whereas k_0 for the reaction with water is too small to be reliably determined.

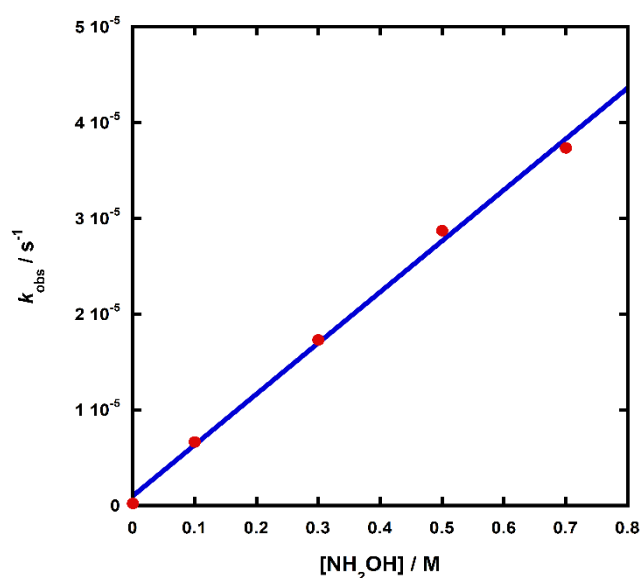


Figure (4-12): Plot of k_{obs} as a function of hydroxylamine concentration for reaction of triester **84** at 25.0 °C, pH = 7.3 and $I = 1.0$ M (NaCl).

$$k_{\text{obs}} = k_0 + k_2 [\text{NH}_2\text{OH}]$$

Equation (4-2)

To confirm that triester **84** hydrolysed mainly to an aryl diester, HPLC was used to show that triester **84** has a retention time at 15.03 min and the catechol a retention time of 8.4 min. However, when the reaction was monitored by HPLC, the product appeared with a retention time of 8.03 min showing that P-O cleavage to form catechol was not occurring. To confirm that this product is not catechol, an investigation was carried out using ³¹P NMR spectroscopy.

^{31}P NMR analysis was carried out in D_2O under the same conditions, and showed disappearance of the triester **84**, and a new product with triplet peak was formed as shown in Figure (4-13).

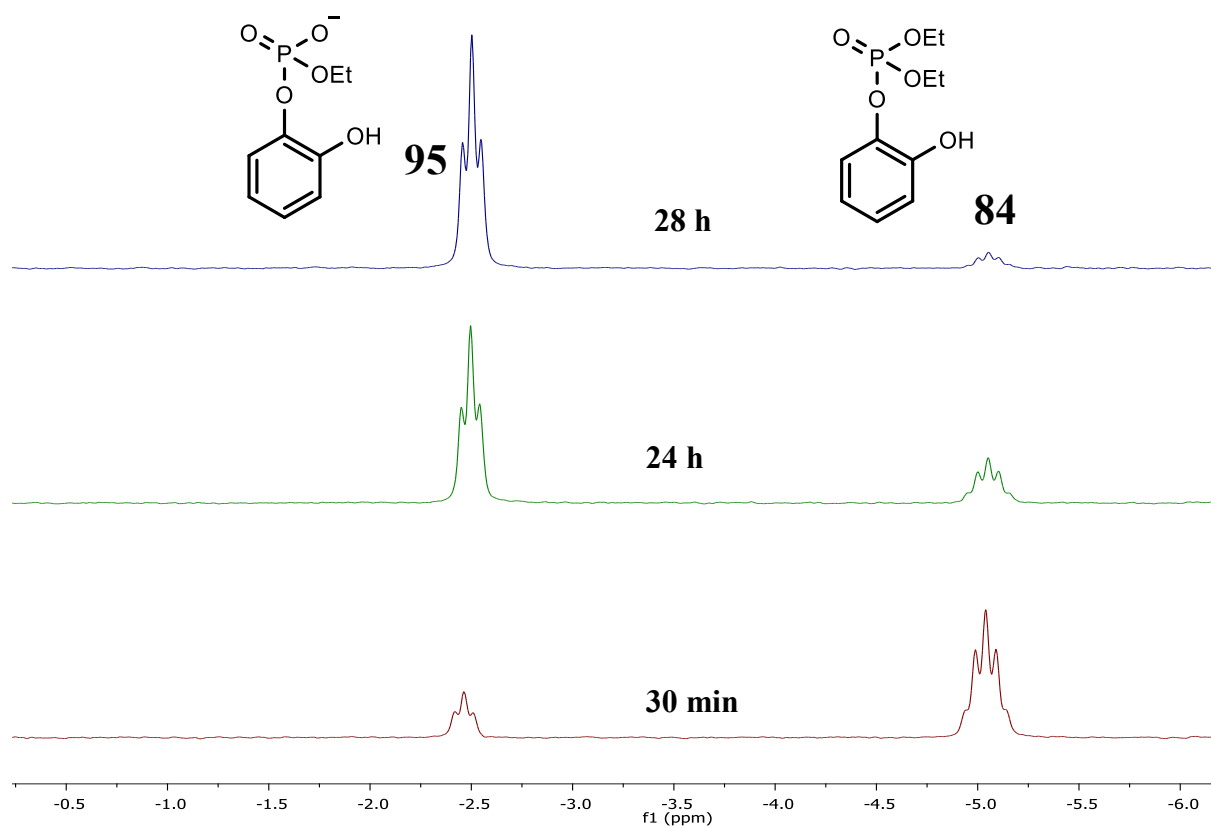


Figure (4-13): ^{31}P NMR spectra of the hydrolysis products of phosphate triesters **84** (at $25\text{ }^\circ\text{C}$) in D_2O .

In the same way, for triesters **85** and **86**, the reactions were very slow at this temperature, thus kinetic experiments were not carried out, and only the reaction products of the reactions were investigated by ^{31}P NMR at $60\text{ }^\circ\text{C}$. Again new peaks were observed, which were assigned as diesters **96** and **97**, respectively, Figure (4-14).

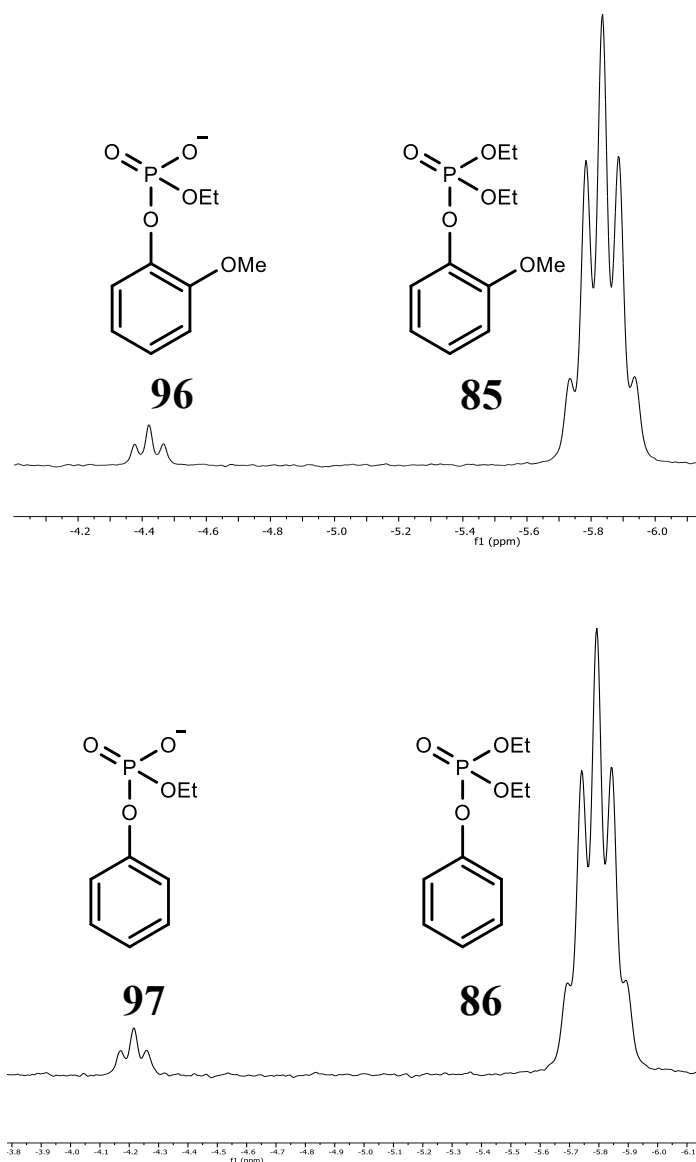
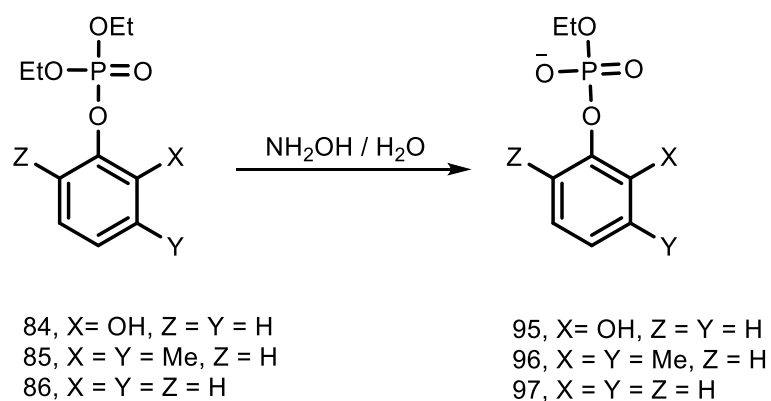


Figure (4-14): ^{31}P NMR spectra of the hydrolysis products of phosphate triesters **85** and **86** (at 60 °C) in D_2O .

The new peaks were assigned as phosphate diesters **95**, **96** and **97** for reactions of **84**, **85** and **86**, respectively, Scheme (4-5). Mass spectrum analysis also indicated the existence of this diester in the product mixture as the main product.

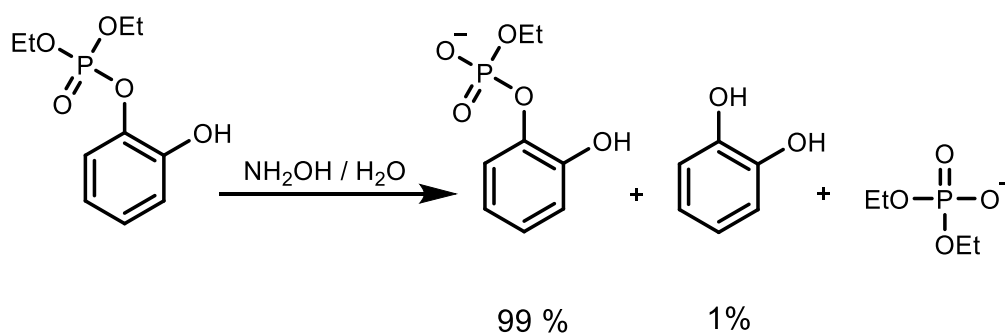


Scheme (4-5): Hydrolysis of diethyl acyclic phenyl phosphate triesters **84-86**

4.2.7. Additional notes on HPLC chromatogram: P-O bond cleavage reaction

The initial observation from ^{31}P NMR analysis of the reactions of phosphate triesters **82** and **83** did not show P-O cleavage to give the parent phenol. On the other hand, HPLC chromatography showed that there was a small peak with a retention time of 4.7 min, which could be pyrogallol as the result of P-O cleavage in triesters **82** and **83**. This peak was very small and did not increase significantly over time. This small quantity may be below the detection for ^{31}P NMR, thus the formation of diethylphosphate, not observed in ^{31}P NMR spectra, cannot be completely ruled out (although it can only be a minor product). The case was the same for catechol triester **84**: there was a small peak at RT 8.4 min, which corresponds to catechol. In order to confirm these observations, mass spectrometry was used to identify the presence of the phenols and diethylphosphate as additional products of hydrolysis. The reactions with 0.7 M NH_2OH were carried out at room temperature and the products were analysed after the reactions were complete (as determined by disappearance of substrates). Mass spectral results confirmed the presence of pyrogallol, catechol and diethyl phosphate in the reaction mixtures beside the main diaryl ester products **93-95**. In contrast to pyrogallol, catechol was quite stable under these conditions. From HPLC catechol was found to be formed in a 1 % yield, Scheme (4-6). Thus, the rate for this reaction could be estimated approximately. From the results obtained earlier, at pH 7.3, the reaction of **84** with hydroxylamine were found

to proceed with an observed rate constant of $5.27 \pm 0.14 \times 10^{-5} \text{ s}^{-1}$ at 25 °C, corresponding to a half time of 6 hrs. That reaction was found to proceed at least 99% ($5.22 \times 10^{-5} \text{ s}^{-1}$ of the rate constant) by intramolecular and intermolecular nucleophilic reaction through C–O and P–O cleavage respectively, suggesting an upper limit of $5.27 \times 10^{-7} \text{ s}^{-1}$ at 25 °C for the rate constant for P–O cleavage with phenol as the leaving group. However, although the reaction of P–O cleavage of phenolic leaving group appeared to take place, it is clear that the effect of hydrogen bonding to catalyse the reaction is inefficient.



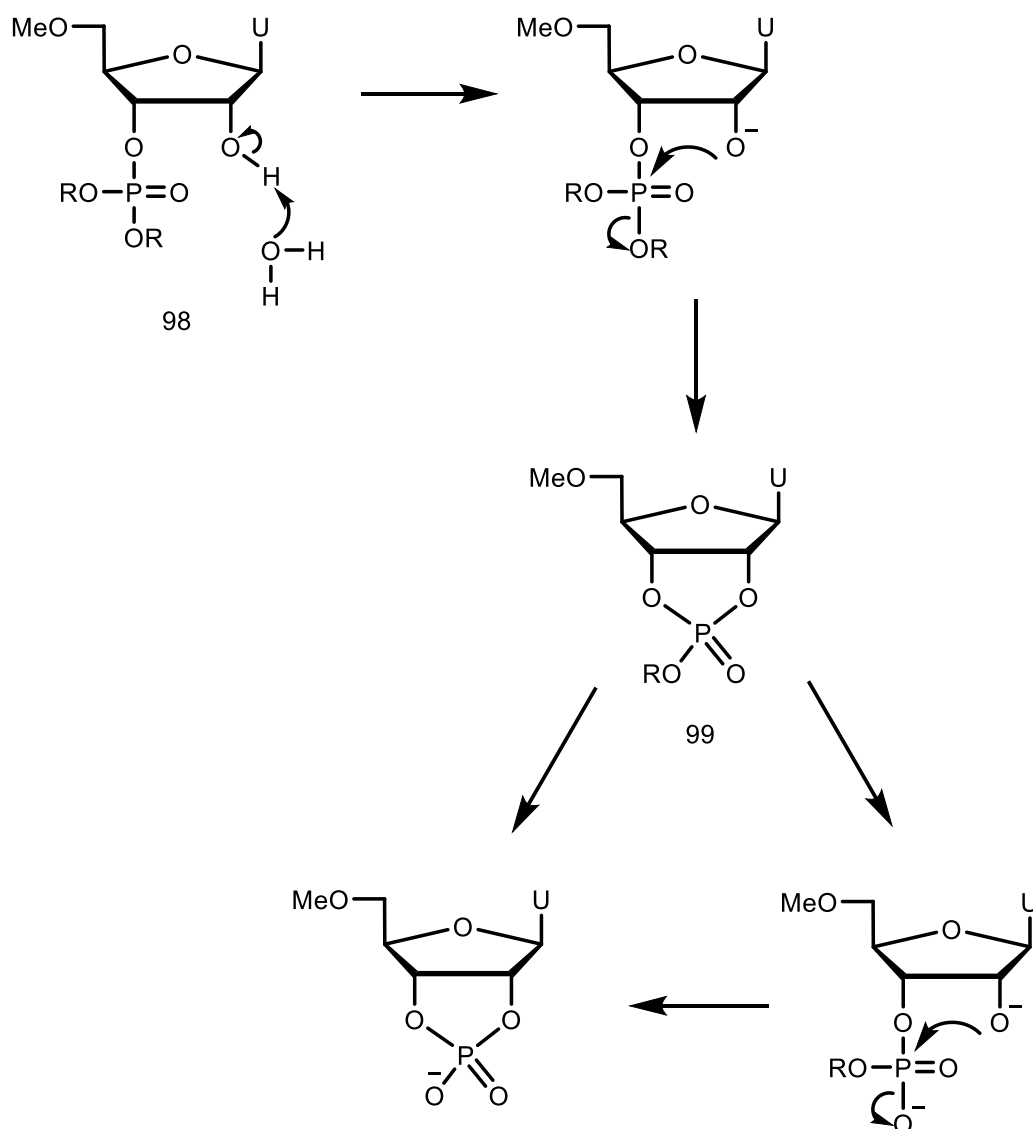
Observed rate constant k_{obs}	$5.21 \times 10^{-5} \text{ s}^{-1}$	$5.27 \times 10^{-7} \text{ s}^{-1}$
---	--------------------------------------	--------------------------------------

Scheme (4-6): The reaction of diethyl-2-hydroxy-phenyl phosphate **84** with hydroxylamine at pH 7.3 and 25 °C.

4.2.8. Possibility of Intramolecular nucleophilic catalytic reaction

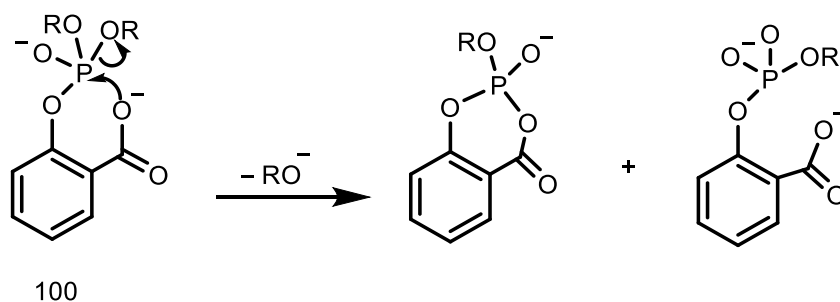
The linear correlation between k_{obs} and hydroxylamine concentration for the decomposition of triesters **82**, **83** and **84** showed a similar second order rate constant k_2 for hydroxylamine reaction with about 27-fold enhancement compared with the reaction in the absence of hydroxyl amine (spontaneous hydrolysis). These rates are higher those that of triesters **85** and **86**, which are still too slow to be observed. The data is consistent with two concurrent mechanisms operating under these conditions. These are intermolecular and intramolecular reactions involving hydroxylamine and an intramolecular phenolic hydroxyl group, respectively. The high reactivity observed for **82-84** compared with **85** and **86** indicated that the reaction proceeds mainly through P–O cleavage by intramolecular nucleophilic attack by a hydroxyl group releasing an ethoxy group. This type of intramolecular catalysis by a

neighbouring group has been observed in phosphate esters previously.⁸⁶⁻⁹⁰ For example, dimethyl phosphate esters **98** were found to undergo hydrolysis according to Scheme (4-7),⁸⁷ where there are two steps involving hydroxyl group as a general base and intramolecular nucleophile in the reaction. The reaction involved the cyclic intermediate **99**, which further hydrolysed to product as shown in Scheme (4-7).



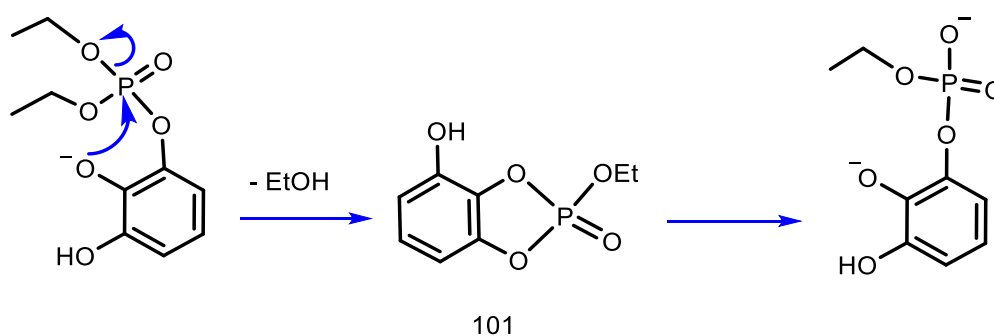
Scheme (4-7): The hydrolysis of dimethyl 5'-O- methyluridine 2'-phosphate.⁸⁷

In another example, dialkyl 2-carboxyphenyl phosphate **100** was found to hydrolyse by the deprotonated neighbouring carboxyl group,⁹⁰ which reacted as an intramolecular nucleophile and showed selectivity for exocyclic displacement of the alkoxy group, Scheme (4-8).⁹⁰



Scheme (4-8): The hydrolysis of dialkyl 2-carboxyphenyl phosphate.⁹⁰

It is clear that the intramolecular nucleophilic attack is the dominant reaction of triesters **82**, **83** and **84**. Thus, this reaction is expected to involve an intermediate **101** as shown in Scheme (4-9).

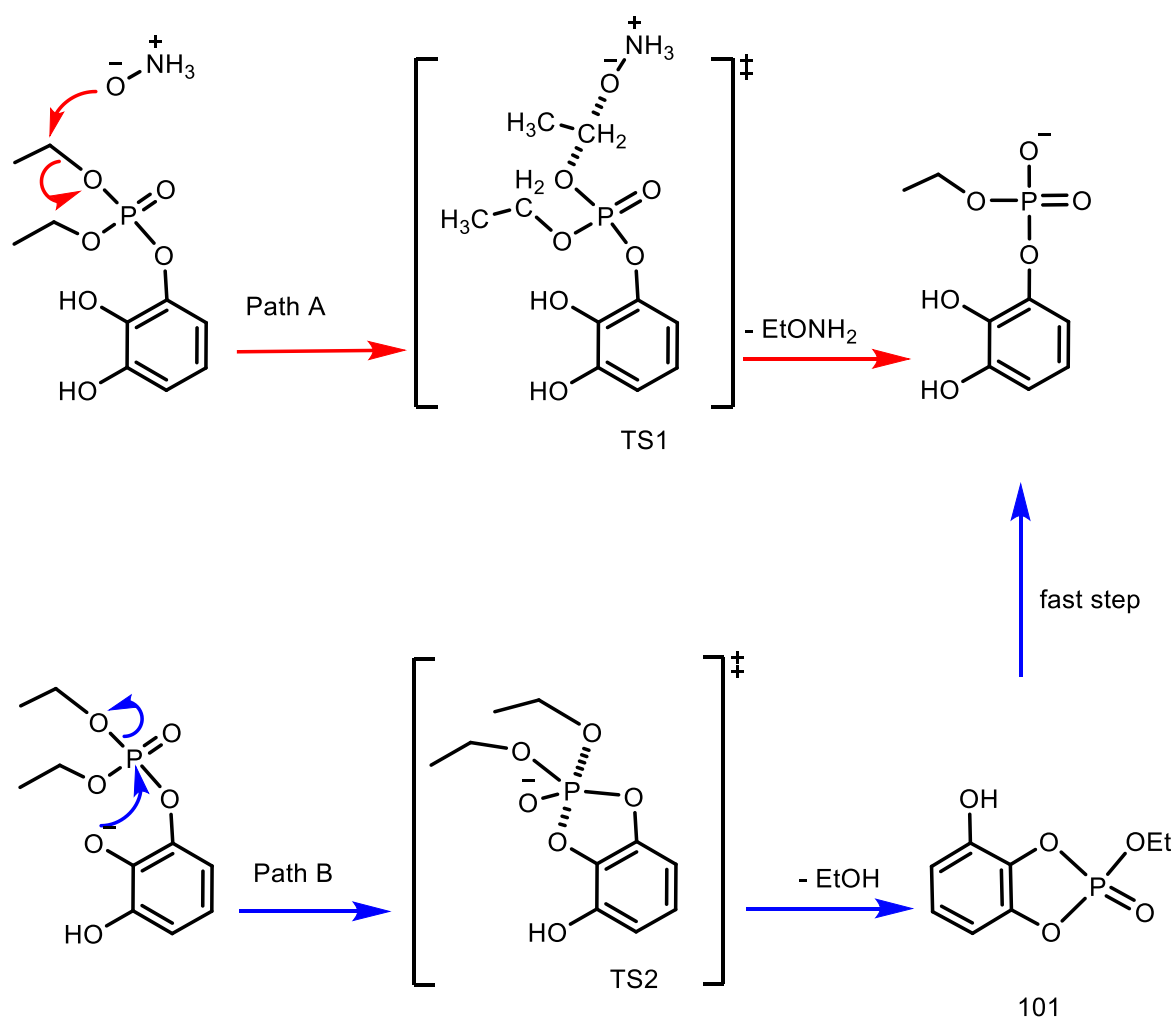


Scheme (4-9): Proposed possible routes for hydrolysis of diethyl acyclic phenyl phosphate triesters studied here.

This intermediate is not observed in our experiments, but has been reported to be highly reactive, especially in alkaline solutions,⁹⁶ and so may not accumulate sufficiently to be observed. Attempts were made to synthesise this intermediate, but unfortunately, the preliminary synthetic experiments showed that the cyclic triester was not present in the crude mixture of the reaction. This can be explained in two ways: (i) the cyclic triester reacted (hydrolysis) too rapidly to be observed by either TLC or by mass spectrometry (ii) another explanation is that the reaction did not involve the formation of this cyclic phosphate, but different side products were formed. Based on ³¹P NMR spectrum of the crude showed multiple P environments between 0 to 10 ppm, which could be related to acyclic mono-, di and triesters, thus no attempt to separate these products was carried out.

Plausible reaction mechanisms

Two reaction mechanisms, Scheme (4-10), can be proposed to explain the observed reaction rates of **82**, **83** and **84** with hydroxylamine and the intramolecular OH group. These involve transition states TS1 and TS2 for the initial step. In the transition state (TS1) on route **A**, the oxygen of hydroxylamine attacks the carbon centre resulting in the production of aryl diester and ethyl hydroxylamine ($\text{CH}_3\text{CH}_2\text{ONH}_2$). The second mechanism (route **B**) involves the phenolate group attacking the phosphorus centre as a nucleophile, resulting in formation of intermediate **101**. The second step involves the rapid hydrolysis of **101** to give the product aryl diester.



Scheme (4-10): Proposed routes for the hydrolysis of the diethyl acyclic phenyl phosphate triesters studied here.

4.3. Conclusion

In conclusion, diethyl hydroxyl phenyl phosphates **82**, **83** and **84** were synthesised successfully and their degradation in the presence of hydroxylamine was studied to investigate the effect of hydrogen bond network on the reactivity. The hydrolysis of these esters seems to involve intramolecular nucleophilic catalysis by hydroxyl group as a dominant reaction. The reaction should involve formation of a reactive five membered cyclic intermediate. In the literature, the observation of large rate enhancements in the similar cases suggests that similar mechanisms are involved.

Enhancements of the rate observed in the anthracene and naphthalene systems due to hydrogen bond catalysis (chapters two and three), suggest that the hydroxyl group is required to be held in a rigid position and brought into close proximity to the leaving group of phosphate ester, thus resulting in intramolecular catalysis by a hydrogen bond. Therefore, it was proposed to use an anthracene ring to design a model with two hydrogen bond donors acting on the leaving group to assess whether hydrogen-bonding networks can act cooperatively to catalyse reactions.

Chapter Five: Multiple Hydrogen Bonds (Anthracene System)

6.1. Introduction

The first substrates **82** and **83**, Figure (5-1), were synthesised and tested to evaluate the impact of two hydrogen bond donors on hydrolytic reactivity and these showed a significant reaction, but this involved the hydroxyl group as an intramolecular nucleophile and no detectable effects as a hydrogen bond donor. On the other hand, the hydrolysis of cyclic phosphate **46** and diethyl naphthyl phosphate **69** showed that when the hydroxyl group is held rigidly in closer proximity to the leaving group a significant catalytic role could be measured.

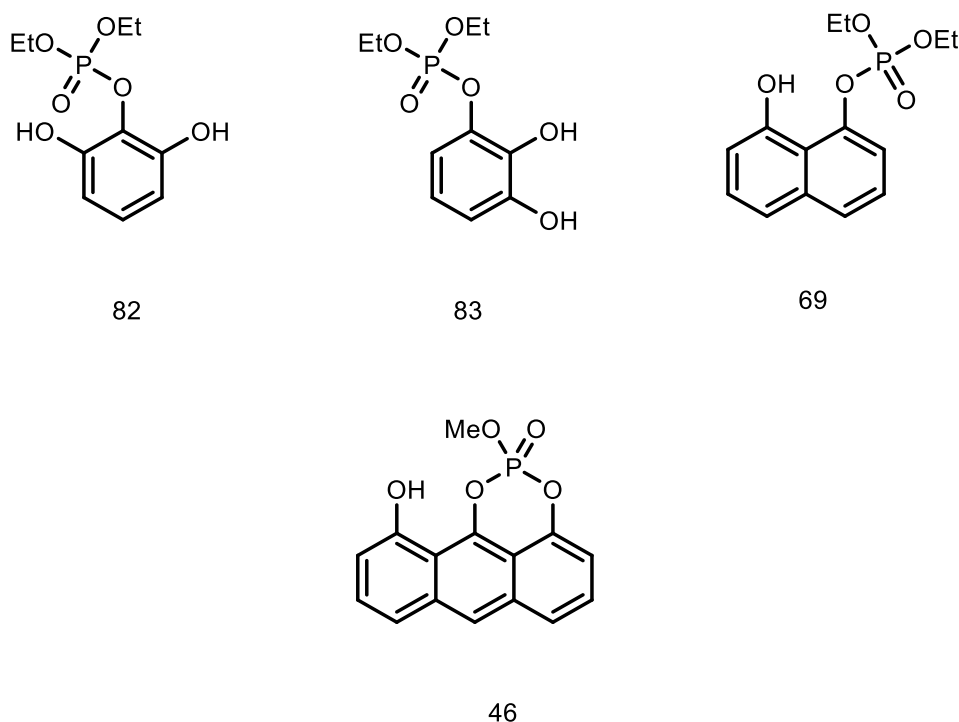


Figure (5-1): Structure of phosphate triesters **82**, **83**, **69** and **46**

Based on these findings, we designed two further model systems based on the anthracene skeleton, system I and II, where one or two proton donors are positioned to form intramolecular hydrogen bonds to the leaving group, Figure (5-2).

The design of molecules a-c is based on the assumption that resulting hydrogen-bonded network would provide a large stabilisation to the transition state that may lead to catalytic rate enhancements greater than those with one hydrogen bond donor in models d-f. Using the anthracene ring allows both two hydroxyl or amine groups and the phosphate ester of the

substrate to be held into close proximity, which enforces the hydrogen bond interaction and delivers the catalytic effect. A similar additive effect can be obtained in system II. The second hydroxyl group can form a hydrogen bond to the terminal hydroxyl group, which should increase the strength of primary hydrogen bond 1° and thus provide more stabilisation to the negative charge developing on the leaving group in the transition state.

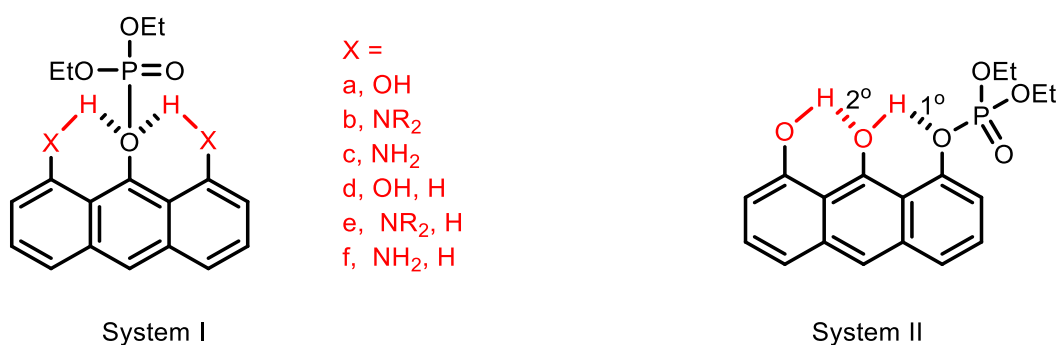


Figure (5-2): Phosphate triesters proposed to be synthesised in this chapter.

However, the adjacent amine groups in several model systems also have been shown to catalyse the reaction by general acid catalysis through an intramolecular hydrogen bond.^{28, 42, 63} The question arises here is which is the most important mechanism in these systems, is it general acid or hydrogen bond catalysis? Thus, kinetic studies of models **b** and **c** will provide information on the two kinds of mechanisms which could be involved in the catalytic reaction, Figure (5-3). If general acid catalysis is the key catalytic process, the rate would be doubled in the presence of a second hydrogen bond donor. If hydrogen bonding is the key to catalysis, then the rate could increase by the square of the rate acceleration for one hydrogen bond donor.

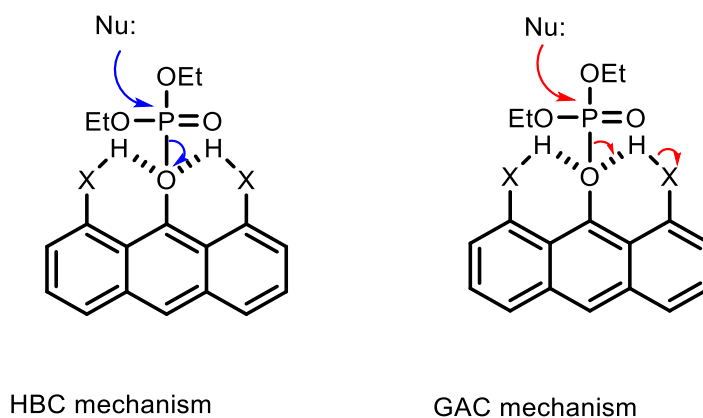


Figure (5-3): Difference between Hydrogen bonding and general acid mechanisms.

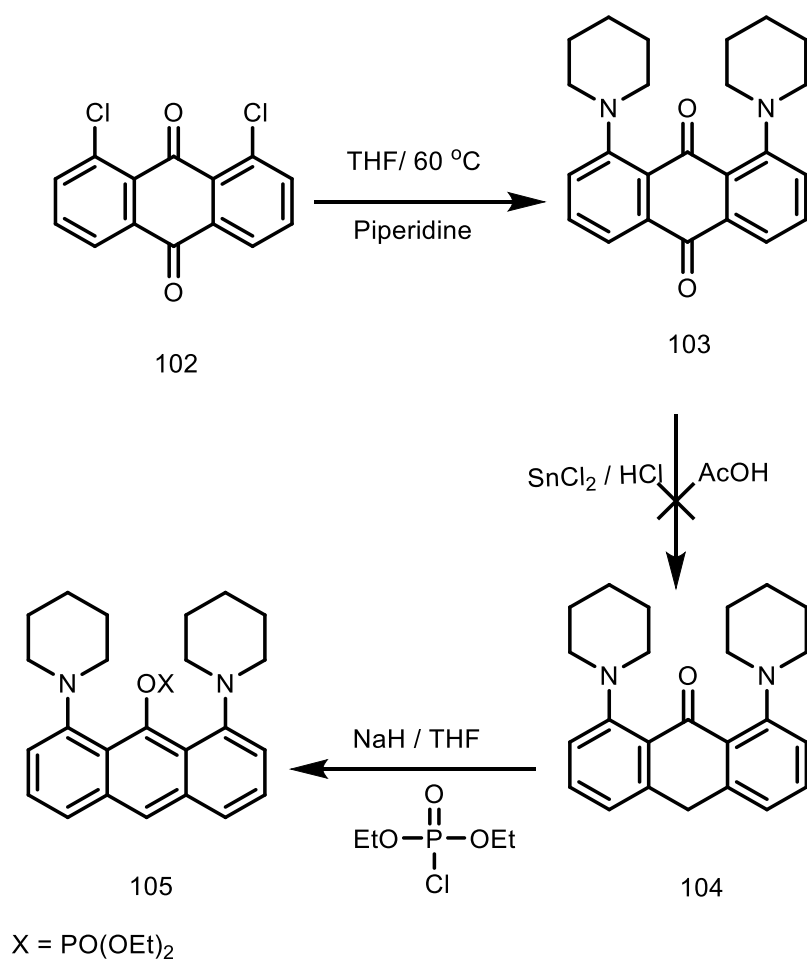
6.1. Result and discussion

5.1. Attempts to synthesis of diethyl 1, 8-diamines anthracene-9-phosphate

5.1.1. Attempt to synthesis of diethyl 1, 8-dipiperidine anthracene-9-phosphate, **105**

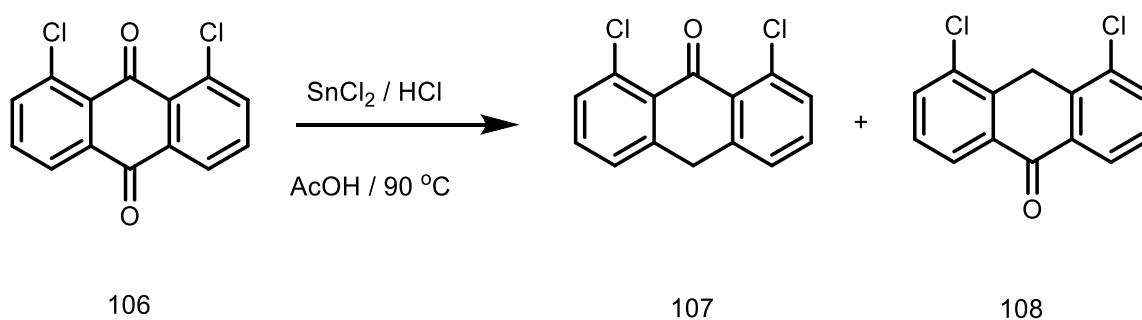
The first proposed route to synthesis compound model **105**, which involves three steps synthesis, is shown in Scheme (5-1). 1,8-dichloroanthraquinone **102** was first converted into 1,8-dipiperidine anthraquinone **103** by adding an excess of the piperidine and heating the reaction overnight. After column chromatography purification, **103** was obtained in 80 % isolated yield. The next step involves a reduction of the carbonyl group in the C-10 position and then phosphorylation on position 9.⁹⁷ The reduction step was carried out with tin chloride SnCl₂/HCl in acetic acid as described in the literature for reduction of 1,8-dihydroxy anthraquinone.⁹⁷ Following the reaction by TLC did not show any progress of the reaction, so analysis by ¹H NMR spectroscopy was used to monitor the reaction progress. However, ¹H NMR of the crude mixture indicates that none of the desired product **104** was formed and only starting material **103** was observed and isolated, which confirms that the observation by TLC. This revealed that the resulting product **104** could be spontaneously oxidised to **103** or the reduction step did not take place at all.

A different reduction agent were tried using zinc in aqueous ammonia.⁹⁸ Unfortunately, reduction of **103** using the same conditions was not succeed and starting material was recovered, thus either anthrone **104** was not formed or spontaneously oxidised.



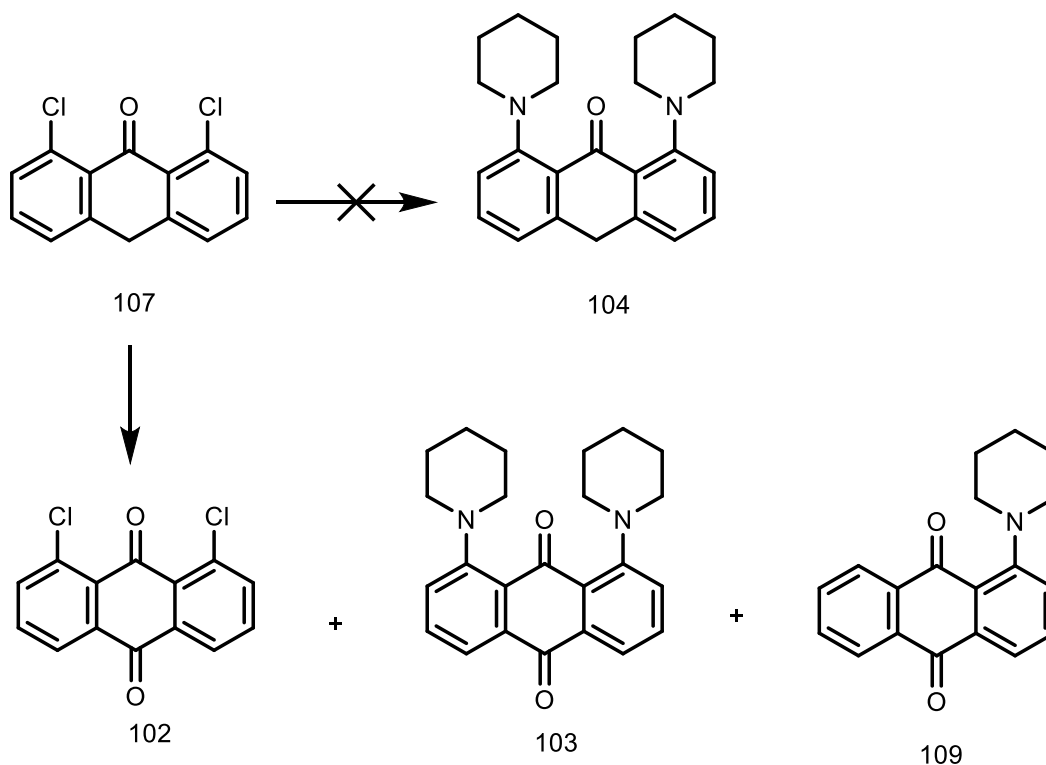
Scheme (5-1): The proposed synthesis of **105**.

Alternatively, anthraquinone, bearing hydroxyl groups (as dithranol) and chlorine atoms (1, 8-dichloroanthraquinone), are reported to undergo reduction at the C-10 position and give relatively stable anthrons.⁹⁹ Thus, due to the failure of the reduction of **103**, attempts to prepare the intermediate **107** was carried out starting with **106** as shown in Scheme (5-2).⁹⁹ Anthraquinone **106** was successfully reduced to give the compounds **107** and **108** in good agreement with literature findings,



Scheme (5-2): The reduction C-10 position of **106**.

The next step was the reaction of compound **107** with piperidine as shown in Scheme (5-3), but the ^1H NMR spectrum of the crude reaction product showed a complicated pattern. Analysis by mass spectrum indicated that the desired compound **104** was not obtained, and instead products **103**, **109** were formed in the mixture. Hence, synthesis of **104** was not continued and a different model was tried.

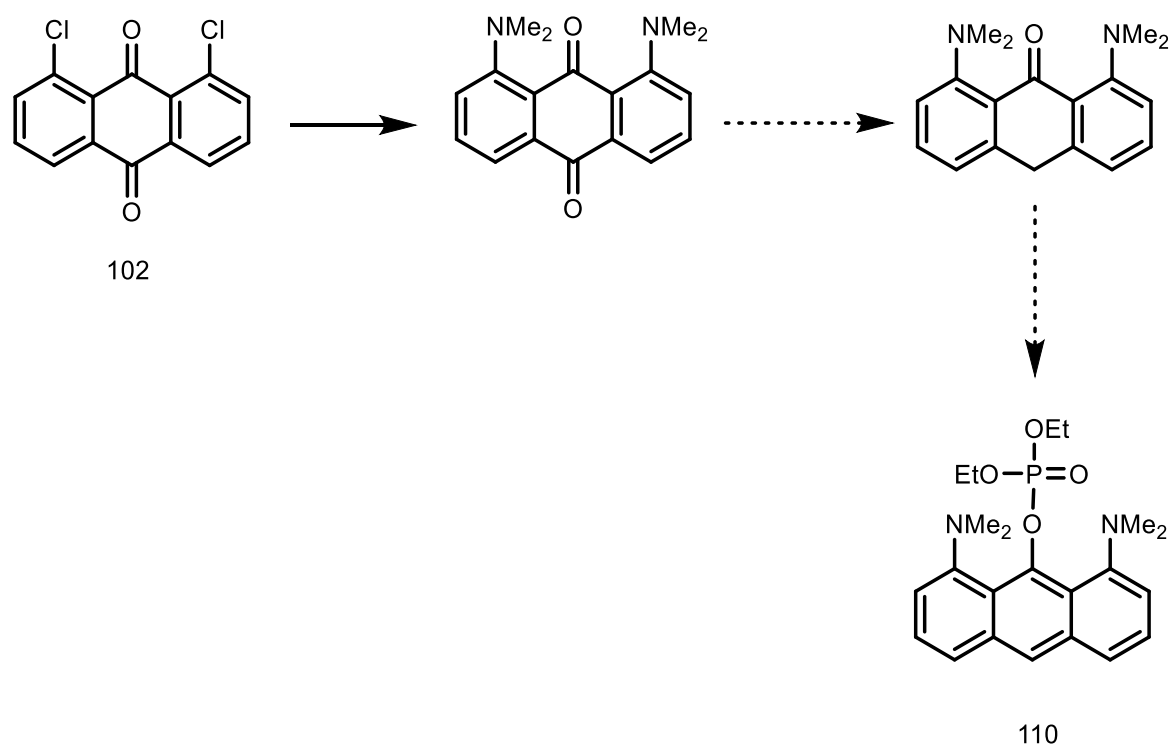


Scheme (5-3): The reaction of **107** with piperidine.

Attempt to synthesis of Diethyl 1,8-bis(dimethylamino) anthracene-9-phosphate, **110**

Compound **108** was chosen as a different model to be prepared as shown in Scheme (5-4). The attempted synthesis of 1,8-bis-(dimethylamino)anthraquinone **110** through condensing an

excess of dimethylamine with commercially available 1,8-dichloro-anthraquinone did not give rise to the desired diamino-anthraquinone **110** in good overall yield. Although the reaction was heated for 3 days, the monoamino-anthraquinone was the most prominent fraction in the product mixture. Repeating the reaction in different solvents (THF, DCM, DMF and toluene) did not improve the reaction, thus no further action was taken to synthesise **110**. However, the substitute amine reaction has been discussed in the literature, leading to the conclusion that it was not likely to be general for simpler substituted anthraquinones from 1,8-dichloroanthraquinone (except when heating in a miniclave is used).¹⁰⁰ In addition, the problem becomes one of separation and purification of products.¹⁰⁰

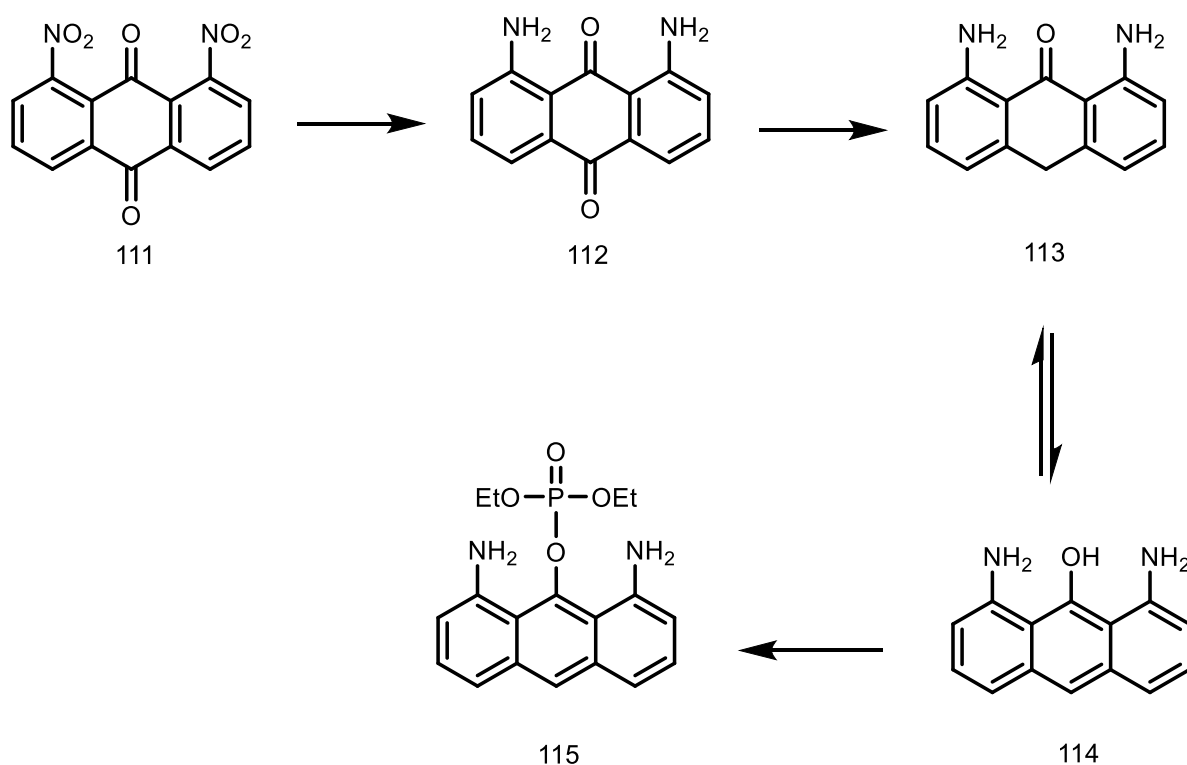


Scheme (5-4): The proposed synthesis route of **110**.

5.1.2. Attempt Synthesis of Diethyl 1,8-bis(diamino) anthracene-9-phosphate, **115**

As direct substitution of 1,8-dichloroanthraquinone did not work, a related amine model was proposed which had the potential to be synthesised by a different method. Phosphate **115** was chosen as the triester and a potential synthesis shown in Scheme (5-5). However, as illustrated in the introduction chapter, Williams *et al.* found that the proton donation ability of the amine

group is not an important factor in increasing the rate of the P-O bond cleavage reaction. Diamino anthraquinone **112** could be prepared from dinitroanthraquinone **111** by the same method described in literature¹⁰¹, and then reduced in aqueous ammonia and zinc dust⁹⁸ to give **113**. Finally, phosphorylation of anthrone **113** was carried out to give phosphate ester **115**. Dinitroanthraquinone **111** was successfully converted to its diamine **112**, and then the later was reduced to anthrone **113** in good yield.



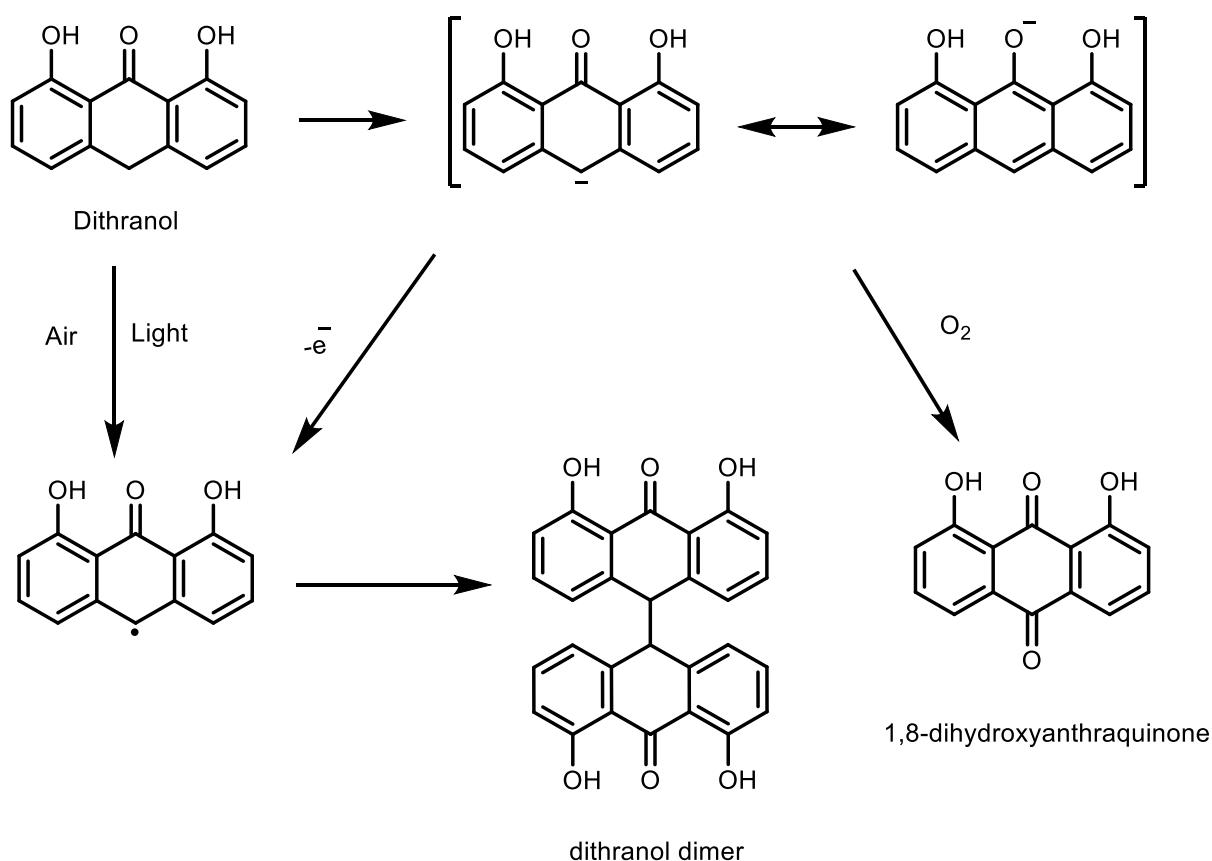
Scheme (5-5): The proposed synthetic route to **115**.

Finally, the last step of the procedure was to introduce the phosphate group into the 9 position of the enol form, **114**, but unfortunately the desired phosphorylation of the 9-position did not take place at all; instead after carrying out the reaction only starting material was recovered in addition to the oxidation product 1, 8-diaminoanthraquinone **112**. From ³¹P NMR, there were no signals to indicate a new phosphate compound, and only diethyl chlorophosphate was observed. A plausible explanation for this is that the conversion of the ketone form **113** to enol form **114** is not sufficient for reaction to occur. It is also possible that the NH₂ are sp²

hybridised and flat, which might hinder the carbonyl oxygen, and thus destabilising effect to the developing negative charge in the enol form when the proton is transferred from the methylene group of anthrone to the base and thus prevent the reaction.

5.1.3. Protection attempts of 1, 8-dipiperidine anthraquinone on position 10

It was proposed by *Muller* that dithranol is unstable and spontaneously oxidises to form multiple decomposition products, Scheme (5-6).¹⁰²⁻¹⁰³ Dithranol oxidation is enhanced by some factors, such as exposure to air, light, alkaline solution, temperature increase, the presence of trace metals, contact with proteins and lipids, and enzymes.

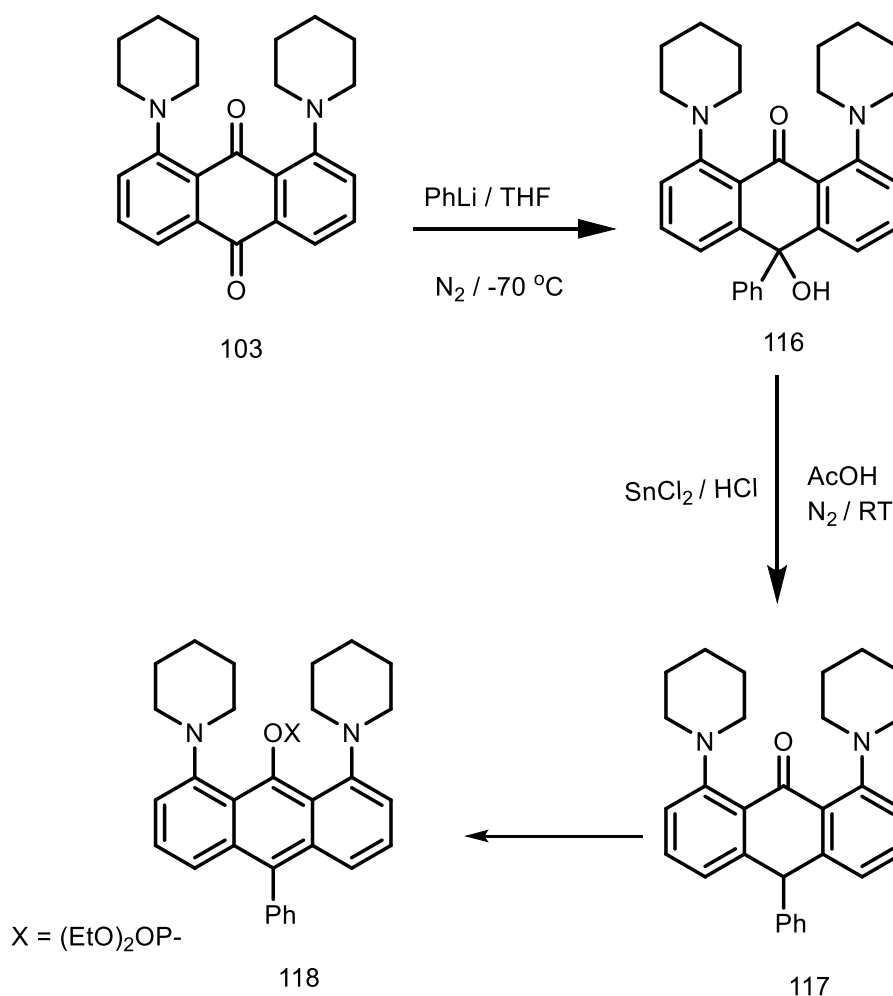


Scheme (5-6): The routes of decomposition of dithranol.¹⁰⁴

Several dithranol derivatives have been prepared and studied, involving modification at the C-10 methylene group with a phenyl ring with the aim of preventing oxidation of the central ring.¹⁰⁵ Another study revealed that an aromatic ring or phenyl alkylidene would be the best, as these substitutions made anthraline thoroughly stable. Moreover, they would have a small

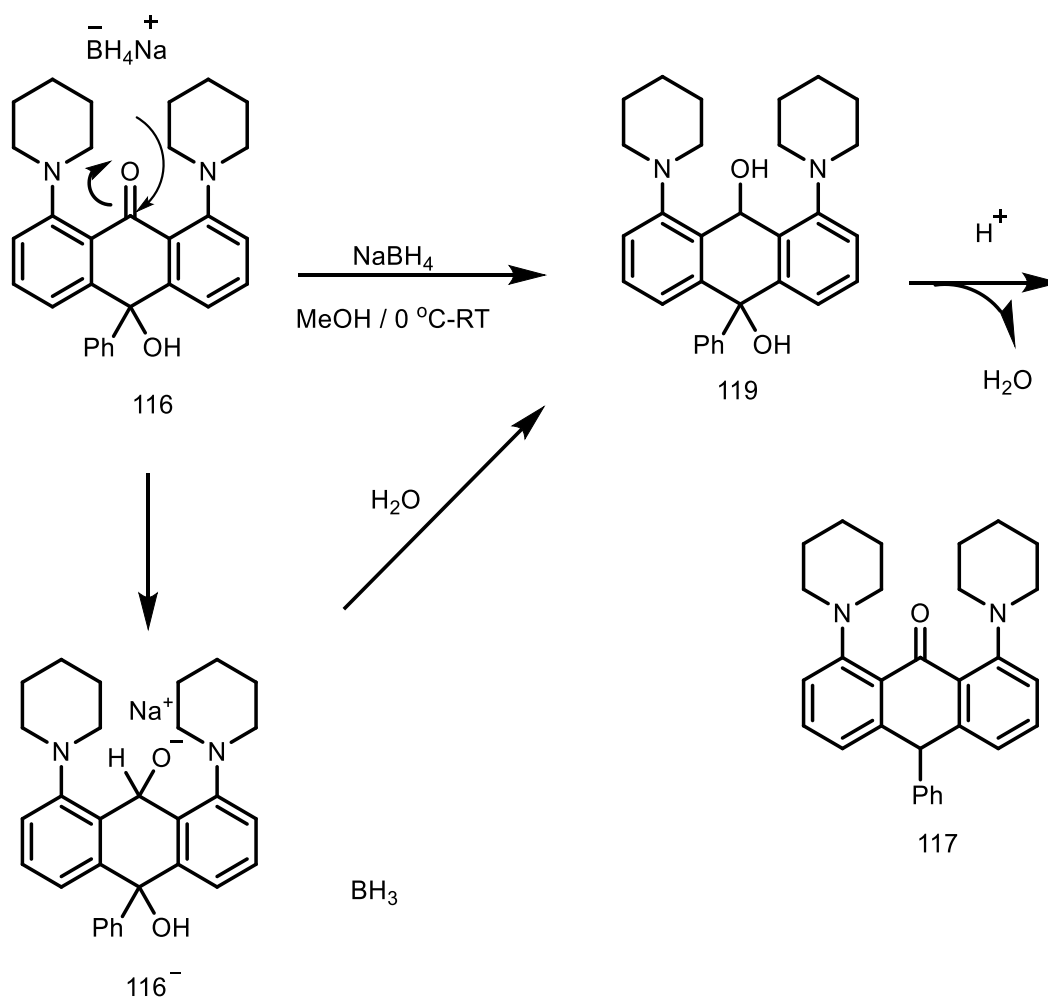
or no effect on the pK_a value of anthraline, and could provide an advantage for solubility issues.^{102, 106}

Thus, to overcome the oxidation problem, functionalisation of the 10-position of **103** was attempted, following the procedure illustrated in Scheme (5-7). Compound **103** was reacted with phenyl lithium to give anthrone **116** and then reducing anthrone **116** to give anthrone **117**, using a modified method described by Short.¹⁰⁴ The second step involved reduction of **116** with SnCl_2 in HCl to form **117** as described in the literature,¹⁰⁴ and then **117** reacts with diethyl chlorophosphate to form **118**. However, this reaction procedure was not attempted, due to the failure to reduce **116** to **117**. Alternative reducing agents, triethylsilane (Et_3SiH) was attempted, but the reaction did not succeed and only starting material was recovered.



Scheme (5-7): The proposed protection route of **117**.

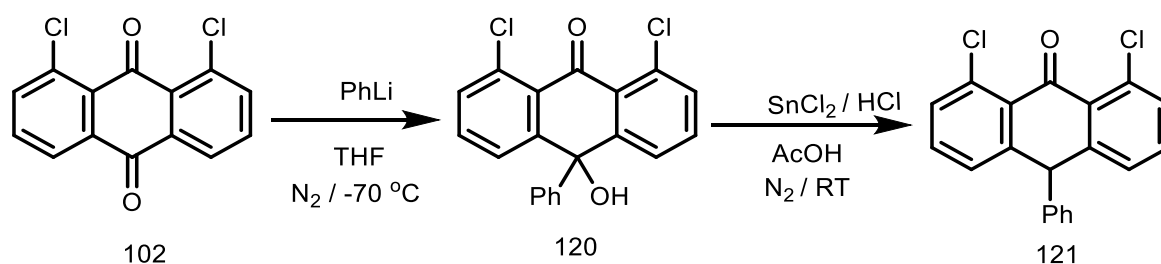
Use of Sodium borohydride: Another reduction attempt was examined with sodium borohydride, which could reduce the carbonyl group in the C-9 position to a hydroxyl group to give compound **119**, and then in the presence of acid, water will be lost to form **117**, Scheme (5-8). However, the desired product **117** was not detected, and the obtained product was the starting material, **116**. It could be that the piperidine substituents have a steric effect which hinders the addition of (H^-) from the borohydride to the carbonyl carbon, and thus no alkoxide ion **116⁻** will form.



Scheme (5-8): Proposed reduction of **116** by borohydride.

Functionalisation of 1,8-dichloro anthraquinone: Alternatively, it was thought that it might be possible to block **102** at the C-10 position to form **120**, and then reduce the hydroxyl group to give **121**, Scheme (5-9). The next step is the substitution of the chloride atoms with

piperidine to give **117**. The reaction with PhLi was carried out as described in literature,¹⁰⁴ but TLC indicated multiple products, which made the separation very challenging and did not lead to any pure fractions. Thus, due to the difficulty of separation, reduction of the crude reaction product with SnCl₂ was carried out in case subsequent separation becomes easier. After purification, a pure compound in small quantity amount and other crude fractions were separated. The pure compound was identified by ¹H NMR and mass spectrum to be compound **120**, which indicated that the reduction reaction did not possibly take place at all.



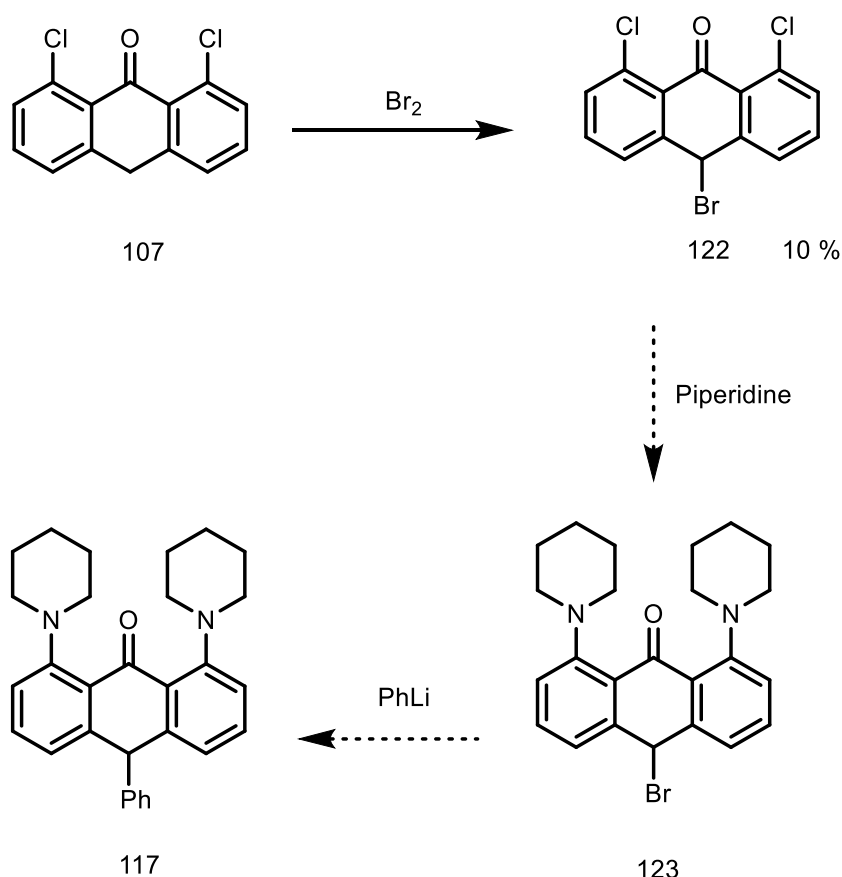
Scheme (5-9): The proposed synthesis route of the intermediate **121**.

Blocking the C-10 position with bromine: Another possible way to prevent oxidation in the C-10 position is the synthesis of 10-bromo-1,8-dichloroanthrone **122** as described in the literature¹⁰⁷ followed by replacing the bromine atom with another substituent. This procedure has been shown for the synthesis of 10-bromoanthralin, which is an interesting intermediary compound, due to the use in the synthesis of antipsoriatic drugs with clinical efficacy and reduced side effects.¹⁰⁸ Much work has been carried out to replace the substituted 10-bromo atom by many other substituents such as alkyl, acyl and ester groups. However, the synthesis of 10-bromoanthralin has been described as not simple or straightforward in literature, but results in the formation of a mixture of many other substituents on various positions of the anthracene backbone.¹⁰⁸

In this work, the procedure shown in Scheme (5-10) was proposed to synthesise anthrone **117**, involving the 10-bromo-1, 8-dichloroanthrone **122** as an intermediate, with the intention of

replacing the chlorine atoms with piperidine to make **123**. The substitution of 10-bromo atom of **123** can be replaced by phenyl ring to give **117**.

Bromination was carried out, and from the ^1H NMR spectrum the isolated product was identified as compound **122**, where the corresponding peak in C-10 position has been shifted from 4.2 to 5.3. However, the yield was not good (10% yield), on a scale where **100** mg of **107** gave about 10 mg of **122**. A larger scale was needed for the next step (substitution reaction), where the expected selective substitutions of chloride and bromide atoms is expected. However, although the reaction was tried over and over, this was to no avail; all resulted in the formation of the compound without improvement of the yield.

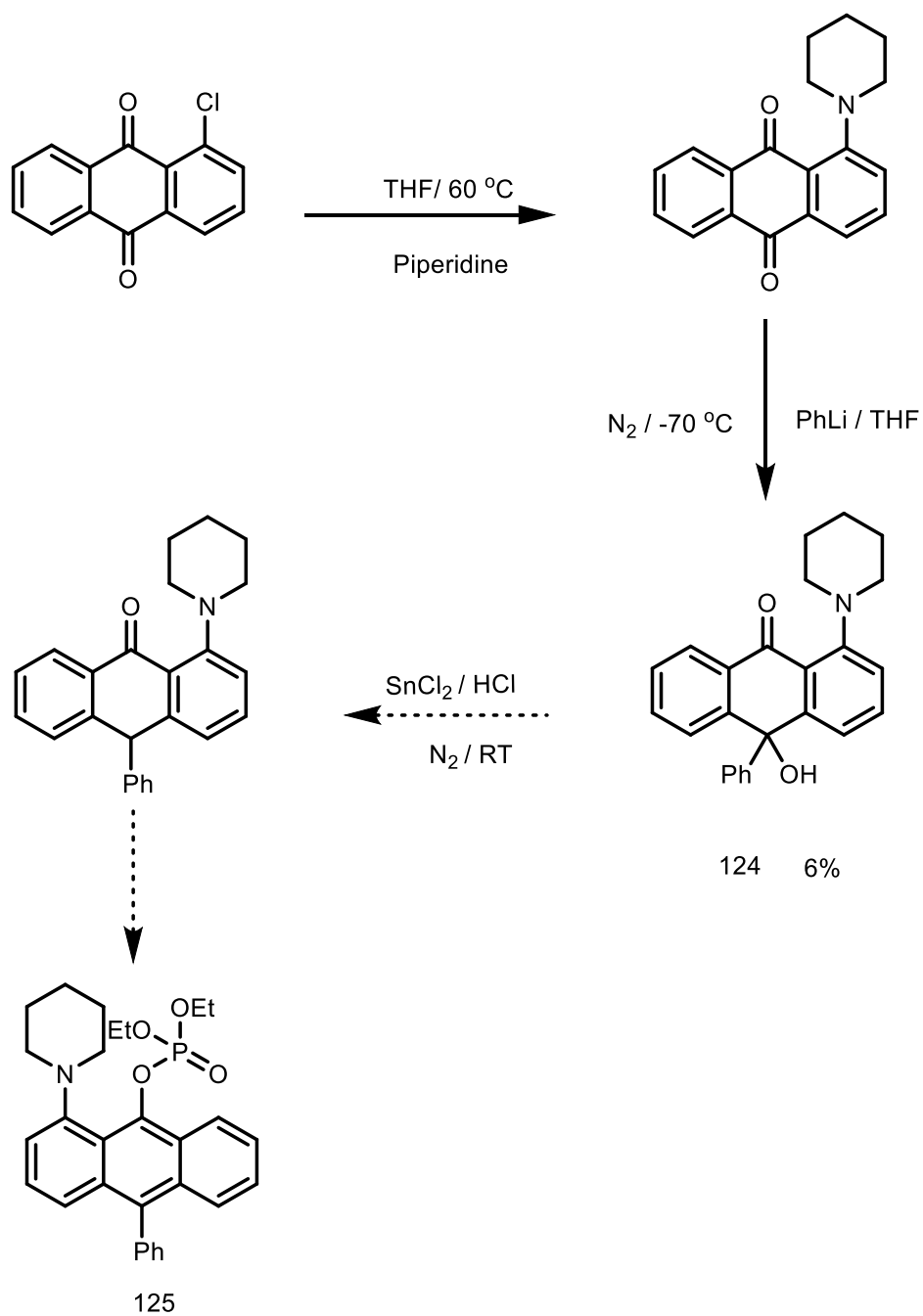


Scheme (5-10): The proposed synthesis of **117** by bromination of **107**.

5.2. Attempt to synthesis diethyl 1-piperidine 9-anthryl phosphate **125**

Triester phosphate **125**, which has one amine group as hydrogen bond donor, was chosen a control compound for comparison with **118**. Therefore, compound **125** is expected to exhibit a

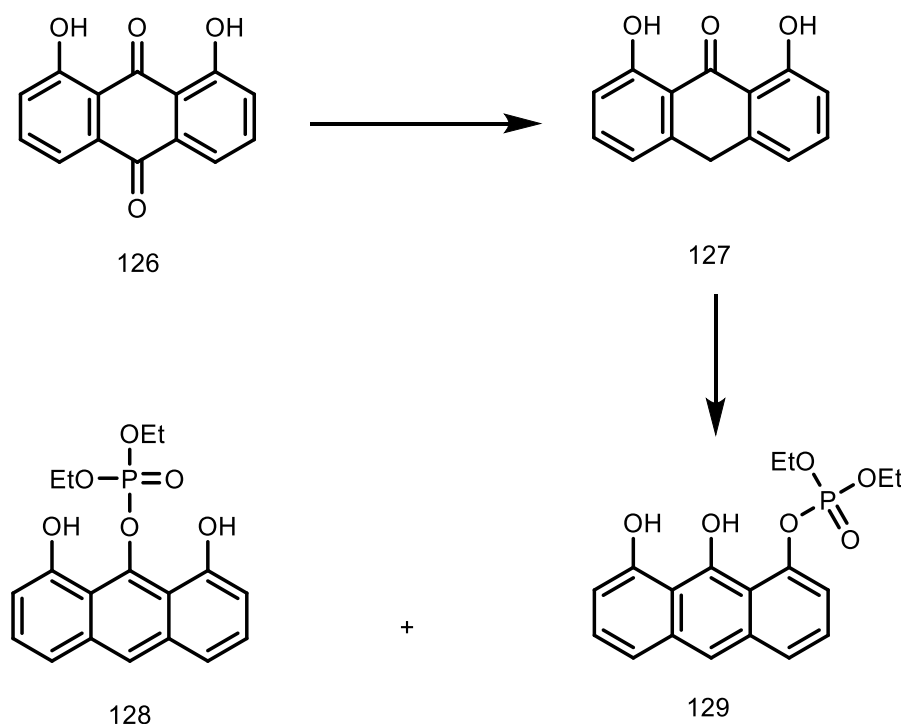
rate acceleration less than that in a presence of second hydrogen bond donor in **118**. Compound **125** was planned to be synthesised by a procedure similar to that of **118**, Scheme (5-11). The first and second steps were performed, but the yield of the phenyl lithium reaction (about 16 mg, 6% of **124**) was not high enough to be practical and due to the failure to synthesis the model **118**, no further attempts to optimise this reaction were made.



Scheme (5-11): The proposed synthesis route of **125**.

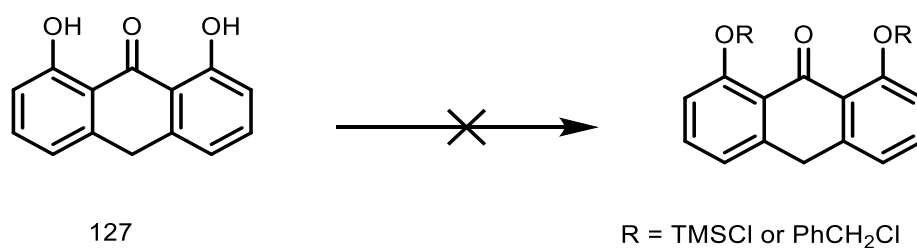
5.3. Synthesis of diethyl 1,8-dihydroxy anthracene-9-phosphate

First attempt to synthesis triester phosphate was carried out starting with reducing of 1,8-dihydroxy anthraquinone **126** to 1,8-dihydroxy anthrone **127** according to published procedure.⁹⁹ The second step is a direct phosphorylation of 1,8-dihydroxy anthrone to form one of the desired phosphate ester products, **128** and **129**, Scheme (5-12).



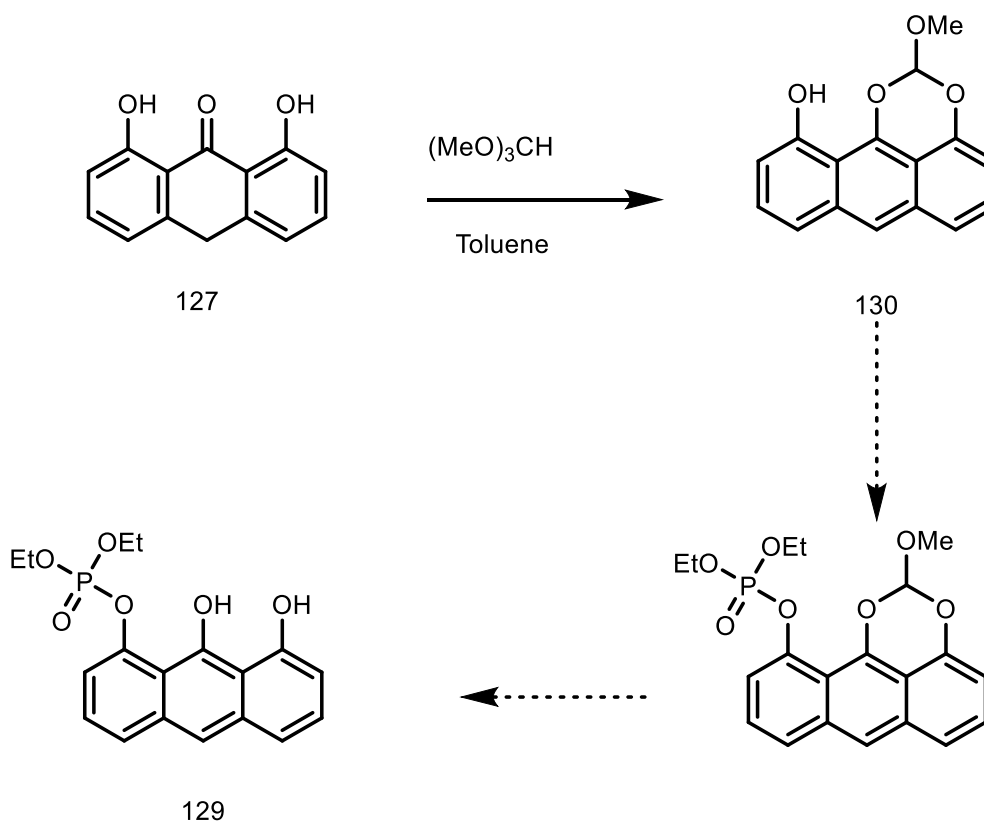
Scheme (5-12): The proposed synthesis route of **128** and **129** from anthraquinone **126**.

This route is apparently simple, but resulted in the formation of a mixture of phosphate triesters. ³¹P NMR of the crude reaction product revealed multiple signals attributed to triesters in the range of 0 ppm to -15 ppm. However, the purification was very difficult, and no pure fraction could be obtained. Due to this difficulty, an attempt to protect the hydroxyl groups in 1 and 8 position of anthraquinone **126** were carried out with different protecting groups. Reactions of trimethylsilyl chloride and benzyl chloride reaction with 1,8-dihydroxy anthrone **127** were tried, Scheme (5-13), but only starting material **127** was isolated along with the side products of oxidation 1,8-dihydroxyanthraquinone and dithranol dimer, Scheme (5-6).



Scheme (5-13): A protection attempt of **127**.

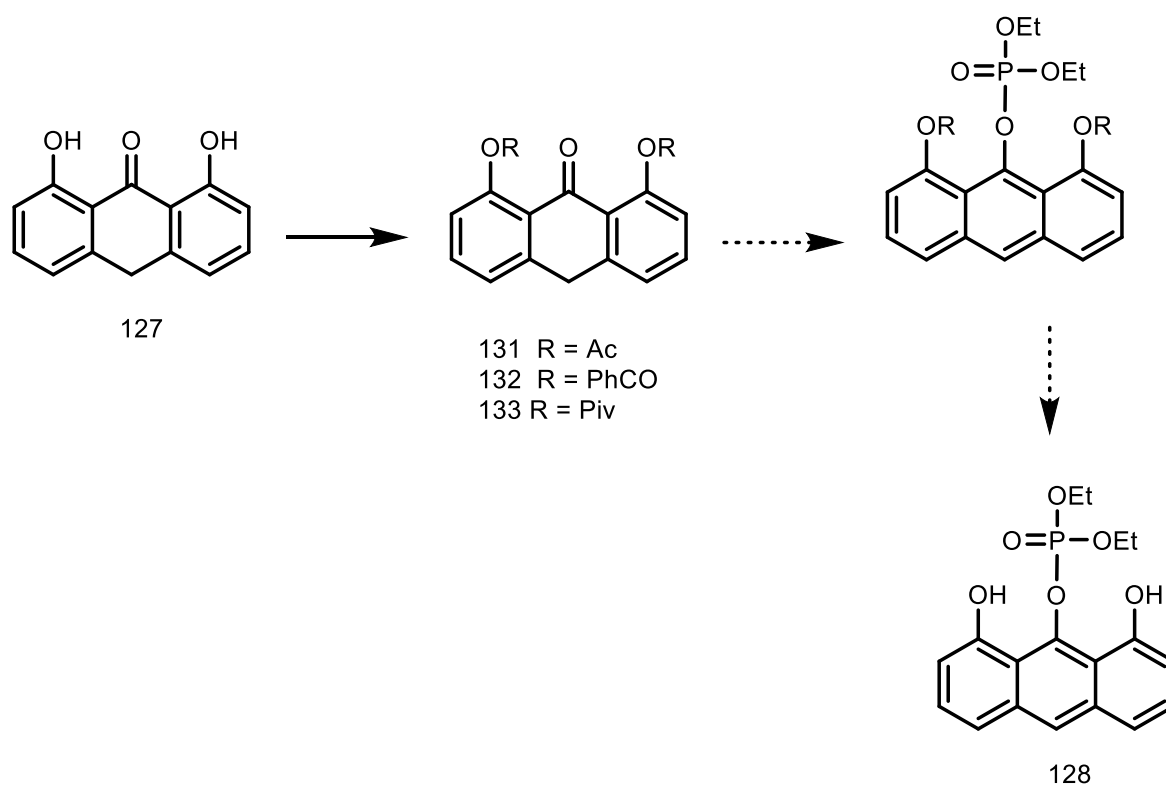
Alternatively, trimethyl orthoformate was used to protect the 1 and 9 positions of anthrone **127** giving cyclic orthoformate **130** to facilitate mono substitution to give **129** as shown in Scheme (5-14). However, although some reaction seemed to occur as shown by TLC, this was not efficient and the purification efforts led to decomposition of the product.



Scheme (5-14): A protection attempt of **127** by trimethylorthoformate.

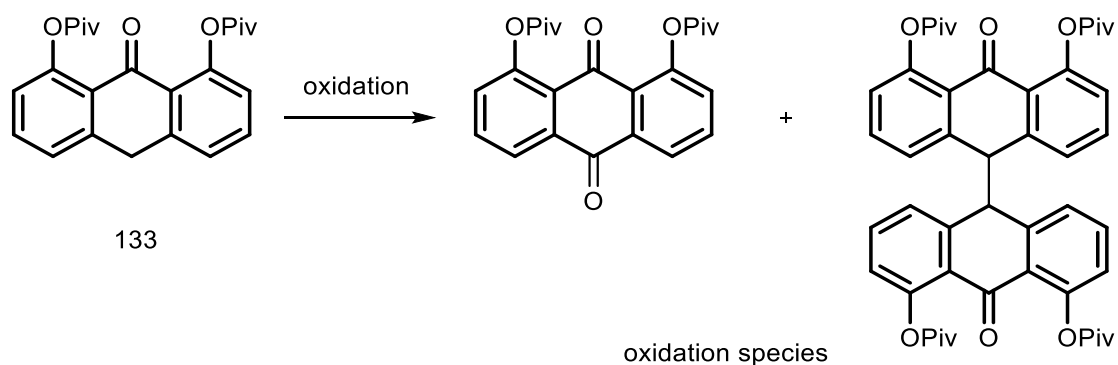
Reactions with acetyl chloride (AcCl), pivaloyl chloride (PivCl) or benzoyl chloride in the presence of triethylamine (Et₃N) in tetrahydrofuran (THF) at room temperature were also attempted. Repeating the O-acetylation of **1** following a literature procedure,¹⁰⁹⁻¹¹⁰ either by using AcCl or benzoyl chloride, always gave mixtures of 1-O-mono, 1, 8-O-di and 1,8 9-O-

triester products and side products. These side products are 1,8-dihydroxyanthraquinone and dithranol dimer Scheme (5-6), which were confirmed by comparing TLC and ^1H NMR of the crude reaction mixture with starting material under basic conditions. The only successful reaction was the protection by pivaloyl group, Scheme (5-15). Both hydroxyl groups were protected to give 1,8-bis-trimethylacetyloxy-anthracenone **133** in 80 % yield with small quantities of side products. It is worth noting that the expected 1,8,9-tripivaloyloxyanthracene derivative was not observed, probably due to the size of pivaloyloxy groups.



Scheme (5-15): Acylation reaction of dithranol **127** and proposed phosphate reaction.

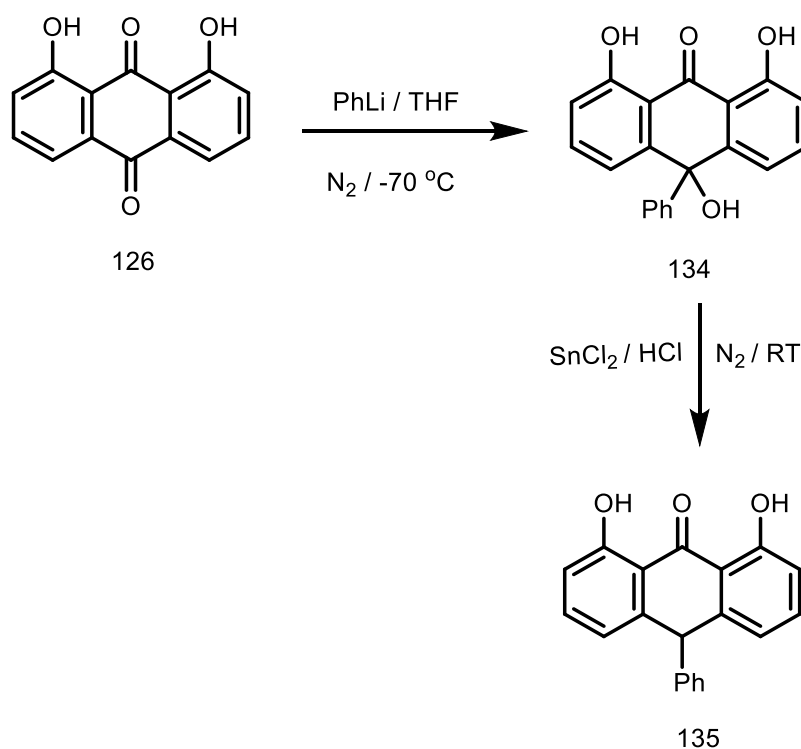
As the only 1,8-bis(trimethylacetyloxy)-9-antrone was obtained, it was used for the next step and reacted with diethyl chlorophosphate. After carrying out the reaction as presented in Scheme (5-15), TLC showed the presence of the starting material along with new compounds, expecting to be oxidised products Scheme (5-16), as shown in mass spectrum. ^{31}P NMR did not show any peak shifts related to the phosphate triester and the diethyl chlorophosphate at 4.06 were observed. A plausible explanation for this is that the steric congestion inhibits phosphorylation on the 9 position.



Scheme (5-16): The oxidation route of 1,8-dipivaloyl-9-anthrone.

Protection of position 10

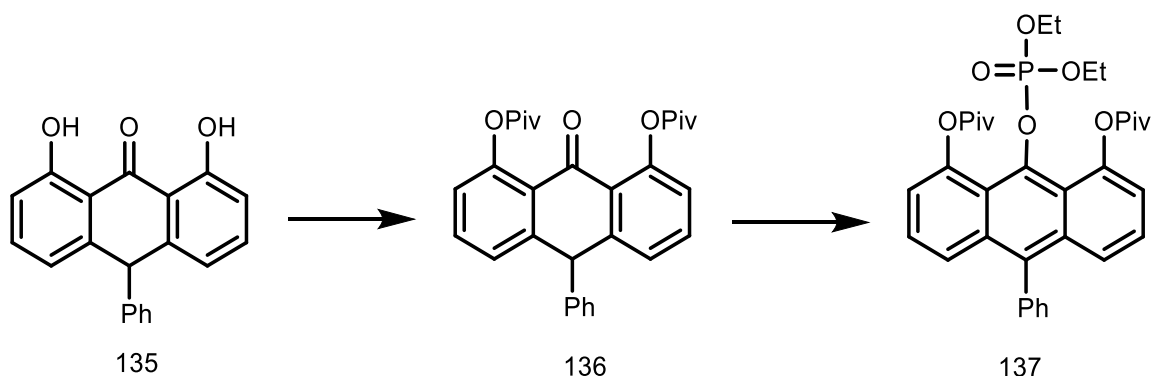
As in the reactions described above, there are side products formed in the protection reactions, which could decrease the possibility of forming of the desired product. Therefore, protection of the C-10 position with a phenyl ring to give **134** was carried out as described in the literature,¹⁰⁴ Scheme (5-17). Anthrone **134** was reduced to anthrone **135** in good yield.



Scheme (5-17): Protection of C-10 position of **126**.

This result suggested that it would be constructive to continue the work to protect the hydroxyl groups and then attempt the phosphorylation reaction. For the protection step, the same procedures described above for dithranol was carried out, but all failed due to similar issues;

all result were a mixture of products with purification difficulties. Again pivaloyl group was added successfully on position 1 and 8, but the next step involving addition of phosphate did not lead to the 9-phosphate ester **137**, Scheme (5-18).



Scheme (5-18): Protection of 1,8-O- positions of **135**.

Repeating these reactions with different solvents (THF, DCM, toluene) and bases (TEA, NaH, pyridine and *t*BuOK) did not succeed and the only starting material was recovered. At this point, working with these reactions to prepare these models was not continued due to the lack of time, and alternative, procedures, conditions and reagents need to be identified

6.1. Conclusion

1-O-mono-substituted and 9-O-mono-substituted phosphate esters have not been reported before. In this work, the preparation of acyclic triester anthryl phosphates was not as straightforward as expected due to the failure to synthesise key intermediates (protection steps), the stability of starting materials (due to the reactivity of the C-10 methylene group) and/or purification problems. Due to the stability issue, the reduction of anthraquinones to anthrones analogues did not always succeed, and only dithranol (**127**), 1,8-diamineanthrone (**113**) and 1,8-dipivaloyl (**133** and **136**) have been obtained. Although dithranol analogs modified at C-10 have been reported, in this research, the synthesis of 1,8-diamino-10-substituted 9-anthrone was not obtained under applying the same conditions, and the reduction step continued to be problematic. Only 1,8-dihydroxy-10-phenyl-9-anthrone **135** has been successfully prepared. The direct phosphorylation reaction of dithranol and its analogue **135** was not simple and did

not give the desired product and resulted in the formation of multiple products. Therefore, several general synthetic methods were proposed based on the protection of hydroxyl groups in dithranol, but these failed to yield the anticipated 1-O-mono-substituted and 1,8-O-disubstituted anthrone derivatives in our hands. The only key intermediates obtained were 1,8-divaloyl anthrone derivatives **133** and **136**, but unfortunately, these did not give the desired corresponding phosphate esters **128** and **137** respectively.

On the basis of these initial observations, the reduction step is very problematic. Thus, alternative preparative methods for dithranol phosphate esters models have to be investigated. In addition, the 1, 8-diaminoanthrone **39** was successfully prepared, thus it is worth to investigating different methods to synthesise the triester model **115**.

Overall, as the synthetic methods failed to yield the anthracene phosphate triesters in our hands, no kinetic study was carried out, and no more synthesis work on this section was undertaken due to time constraints.

Chapter Six: Future Work

6.1. Suggestions for future work

The hydrolysis of cyclic and acyclic phosphate triesters was enhanced in the presence of hydroxyl groups in specific position of anthryl and naphthyl rings. The effect of the hydroxyl groups is proposed to be due to hydrogen bond catalysis, thus it is of interest to compare its influence on the hydrolysis of other comparable species such as sulfate esters, Figure (6-1). Kinetic study of these compound could show if the hydroxyl group would provide a similar catalytic effect on a different reactions. In particular, sulfate monoesters have transition states in which bond cleavage to the leaving group is far advanced, and so the effect of stabilising the leaving group is predicted to have a maximal effect on the transition state.

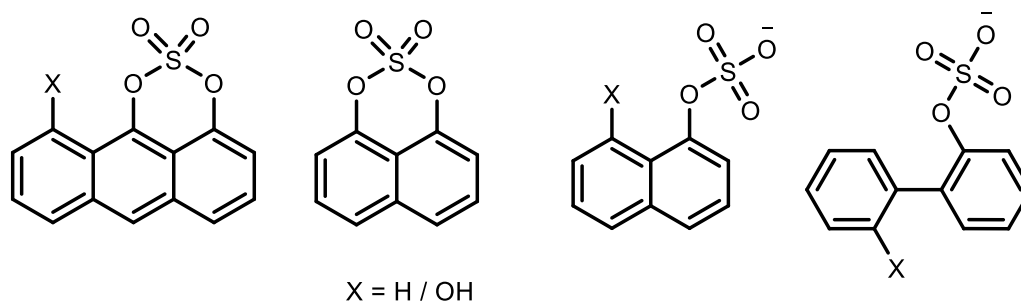


Figure (6-1): structures of sulfate di- and monoester.

8-Hydroxyl naphthyl phosphate triester **69** (pK_a of leaving groups is 6.6) showed high reactivity compared with biphenyl phosphate (pK_a of leaving groups is 7.5). The presence of electron-withdrawing groups was found to increase the acidity and thus increase the hydrogen bonding ability of the donor.^{95, 111} The question is how changing the pK_a of hydroxyl group could affect its ability as hydrogen bond donor, for example, compounds in Figure (6-2), would be used to be compared with triester **69**. In this case, proton transfer would be expected as part of the reaction, introducing general acid catalysis. If the leaving group is modified to create a better leaving group, then hydrogen bond donation would be the only mechanism that can operate. Comparison of the two systems may provide insights into any qualitative differences between these two pathways.

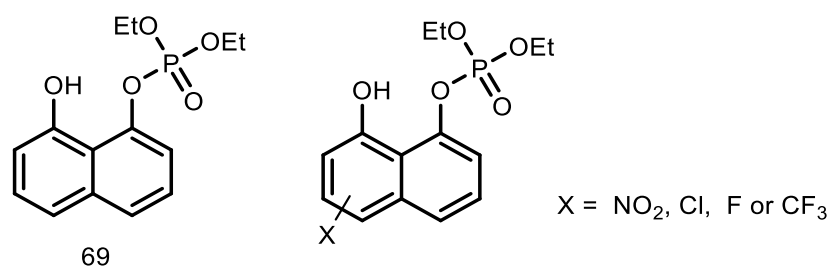


Figure (6-2): structure of naphthyl phosphate with different substituent.

As shown in chapter four, triesters phosphate of a substituted phenyl system underwent intramolecular nucleophilic catalysis by the hydroxyl group, so it would be useful to study phosphate monoester of this system, Figure (6-3), where no displacement of alkoxy group can be observed and the only reaction is P-O cleavage of aryl group. This would reveal the effect of multiple hydrogen bonds on the reactivity without competing reactions dominating the behaviour. As with sulfate monoesters, the transition state structure for phosphate monoesters has more advanced cleavage to the leaving group, and so larger effects from hydrogen bonding are likely to be evident.

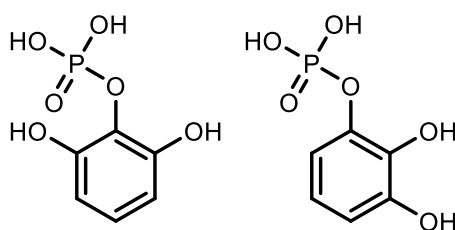


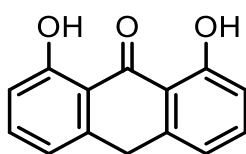
Figure (6-3): structure of phenyl phosphate mono ester with two hydrogen bond donors

Chapter Seven: Experimental Chapter

7.1. General material and instruments

Synthetic reactions were carried out under dry conditions using dry solvents and under a nitrogen or argon atmosphere. All starting materials and reagents were commercially obtained from Sigma Aldrich, Fisher Scientific, Fluorochem, Acros Organics and were used without further purification. All other chemicals were synthesised as described in chapter six. All reaction solvents were obtained from a Grubbs solvents purification system in the department. The ^1H NMR, ^{13}C NMR, ^{31}P NMR characterisation data were obtained from using a Bruker AV1-400 spectrometer; ^1H NMR were running at 400 MHz, ^{13}C NMR at 101 MHz and ^{31}P NMR at 162 MHz. All kinetic solutions were made up with twice distilled deionised water and Analar grade reagents. UV-Vis spectra were recorded on Cary 1 Bio spectrophotometer, and Cary 300 Bio spectrophotometer. Analytical high performance liquid chromatography (HPLC) was carried out using 150 mm \times 4.60 mm column in a HP 1100 Series HPLC. The HPLC method used for analytical and kinetics were applied using acetonitrile (MeCN) in water (both solvents containing 0.1 % TFA) over a period of 30 minutes, and analytical HPLC flow rate 1 ml/min.

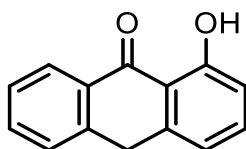
7.2. Synthesis of 1,8-dihydroxyanthracen-9(10 H)-one **51**



1,8-dihydroxyanthracen-9(10 H)-one **51** was synthesised according to published procedure.¹¹² To a mixture of the 1,8-dihydroxy anthraquinone (3.6 g, 15 mmol) in glacial acetic acid (150 mL) heated to reflux under N_2 , there was added dropwise over 3 h, a solution of $\text{SnCl}_2 \cdot 2\text{H}_2\text{O}$ (20.3 g, 90 mmol) in 37% HCl (40 mL). The solution was then cooled, and the resulting crystals were collected by filtration to provide a pure product; the 1, 8- dihydroxyanthracen-9(10 H)-one as yellow crystals in (3.15 g, 13.9 mmol, 93 %). mp 103-107 °C; ^1H NMR (400

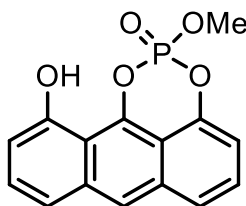
MHz, CDCl₃) δ 12.32 (s, 2H), 7.51 (t, $J = 7.9$ Hz, 1H), 6.88 (d, $J = 8.0$ Hz, 2H), 4.31 (s, 2H).
¹³C NMR (101 MHz, CDCl₃) δ 194.2, 163.0, 142.0, 136.3, 118.8, 115.9, 115.6, 32.9. ESI-MS positive ion mode m/z [(M+H)⁺]; calculated for C₁₄H₁₀O₃, 226.0624, found 226.0634. IR = 2980 (OH); 1597 (C=O) cm⁻¹.

7.3. Synthesis of 1-hydroxyanthracen-9(10 H)-one **53**



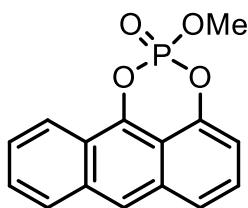
1-hydroxyanthracen-9(10 H)-one **53** was synthesised according to published procedure.¹¹² To a mixture of the 1-hydroxy anthraquinone (2 g, 8.9 mmol) in glacial acetic acid (85 mL) heated to reflux under N₂ was added dropwise over 3 h, a solution of SnCl₂·2H₂O (12 g, 53.5 mmol) in 37% HCl (23 mL). The solution was then cooled, and the resulting crystals were collected by filtration to provide a pure product; the 1-hydroxyanthracen-9(10 H)-one as pale orange solid in (1.5 g, 7.14 mmol, 80 %). mp = 130-131 °C. ¹H NMR (400 MHz, CDCl₃) δ 13.05 (s, 1H), 8.34 (dd, $J = 7.9, 1.4$ Hz, 1H), 7.63 (td, $J = 7.5, 1.5$ Hz, 1H), 7.45-7.51 (m, 3H), 6.94 (td, $J = 7.9$ Hz, 1H), 4.37 (s, 1H). ¹³C NMR (101 MHz, CDCl₃) δ 189.7, 163.2, 141.8, 140.7, 135.6, 133.4, 131.1, 128.3, 127.2, 127.1, 118.6, 116.6, 115.1, 32.5. ESI-MS positive ion mode m/z [(M+H)⁺]; calculated for C₁₄H₁₀O₂, 211.0754, found 211.0755. IR = 1634 (C=O), 3489 (OH) cm⁻¹.

7.4. Methyl 8-hydroxy-1,9-anthryl cyclic phosphate **46**



Methyl 8-hydroxy-1,9-anthryl cyclic phosphate **46** was synthesised according to a modified published procedure.¹¹³ 1,8-dihydroxy-9-anthrone (0.3 g, 1.33 mmol) and methyl dichlorophosphate (0.2 g, 1.33 mmol) were dissolved in dry THF (10 mL) under argon at 0 °C and in dark conditions. The reaction was stirred for 10 min then triethylamine (0.27g, 0.37 mL, 2.66 mmol) was added slowly and the solution stirred for 30 min at the same temperature. After 30 min, the solution was returned to room temperature. After 3h, the white precipitate, which formed, was filtered off and the solvent removed *in vacuo*. The crude product was purified over silica chromatography using 40 % ethylacetate (EtOAc) in petroleum ether, provided (36 mg, 0.12 mmol, 9 %) of methyl 8-hydroxy-1,9-anthryl cyclic phosphate as a yellowish solid. mp (decomposition) 179-180 °C; ¹H NMR (400 MHz, CDCl₃) δ 8.19 (s, 1H), 7.72 (d, *J* = 8.6 Hz, 1H), 7.52 (d, *J* = 8.1 Hz, 1H), 7.44 (m, 2H), 7.7 (d, *J* = 7.7 Hz, 1H), 6.10 (d, *J* = 8.0 Hz, 1H), 3.97 (d, *J* = 11.8 Hz, 3H). ¹³C NMR (101 MHz, CDCl₃) δ 152.2, 134.8, 131.7, 128.1, 126.3, 124.0, 122.7, 119.9, 111.5, 110.4, 55.5. ³¹P NMR (162 MHz, CDCl₃) δ -17.21 (q, *J* = 11.6); ³¹P NMR (162 MHz, CDCl₃) δ -17.21 (q, *J* = 11.6 Hz). ESI-MS positive ion mode *m/z* [(M+H)⁺]; HRMS (TOF mode) calculated for C₁₅H₁₁O₅P, 303.0417, found 303.0415. IR= 3500 (OH) cm⁻¹.

7.5. Methyl 1,9-anthryl cyclic phosphate **47**

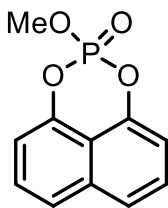


Methyl 1,9-anthryl cyclic phosphate **47** was synthesised according to a modified published procedure.¹¹³ 1-hydroxy-9-anthrone (0.5 g, 2.37 mmol) and methyldichlorophosphate (0.35 g, 2.37 mmol) were dissolved in dry THF (10 mL) under argon at 0 °C and in dark conditions. The reaction was stirred for 10 min then triethylamine (0.48 g, 0.7 mL, 4.75 mmol) was added slowly and the solution stirred for 30 min at the same temperature. After 30 min, the solution

was returned to room temperature. After 3h, the white precipitate, which formed, was filtered off and the solvent removed *in vacuo*. The crude product was purified over silica chromatography using 40 % ethylacetate (EtOAc) in petroleum ether (40 mg, 0.14 mmol, 6 %) of methyl 1,9-anthryl cyclic phosphate as a yellowish solid. mp = 118-119 °C

^1H NMR (400 MHz, CDCl_3) δ 8.35 (d, $J = 8.0$ Hz, 1H), 8.23 (s, 1H), 8.00 (d, $J = 8.0$ Hz, 1H), 7.77 (d, $J = 8.7$ Hz, 1H), 7.60 (m, 2H), 7.42 (t, $J = 8.0$ Hz, 1H), 7.10 (d, $J = 7.4$ Hz, 1H), 3.96 (d, $J = 11.7$ Hz, 3H). ^{13}C NMR (101 MHz, CDCl_3) δ 164.7, 164.6, 132.9, 131.7, 127.9, 127.0, 126.4, 125.9, 123.9, 121.6, 120.8, 110.9, 120.3, 110.4, 55.3. ^{31}P NMR (162 MHz, CDCl_3) δ -14.97 (q, $J = 11.8$ Hz). ESI-MS positive ion mode m/z [(M+H) $^+$]; calculated for $\text{C}_{15}\text{H}_{11}\text{O}_4\text{P}$, 287.0468, found 287.0477.

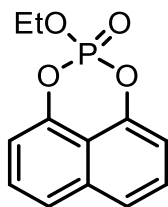
7.6. Methyl naphthyl 1,8-cyclic phosphate **48**



Methyl 1,8-naphthyl cyclic phosphate **48** was synthesised according to a modified published procedure.¹¹³ 1,8-dihydroxy-naphthalene (0.15 g, 0.93 mmol) and methyldichlorophosphate (0.14 g, 0.93 mmol) were dissolved in dry THF (10 mL) under argon at 0 °C. The reaction was stirred for 10 min then triethylamine (0.19 g, 0.26 mL, 1.86 mmol) was added slowly. The solution was stirred for 30 min at the same temperature, and then returned to room temperature. After 3h, the white precipitate formed was filtered off and the solvent removed *in vacuo*. The crude product was purified over silica chromatography using 50 % ethylacetate (EtOAc) in petroleum ether to yield (0.1 g, 0.423 mmol, 45 %) of methyl naphthyl 1,8-cyclic phosphate as a brown oil. ^1H NMR (400 MHz, DMSO) δ 7.83 (d, $J = 8.5$ Hz, 2H), 7.6 (t, $J = 7.8$ Hz, 2H), 7.33 (d, $J = 7.4$ Hz, 2H), 3.86 (d, $J = 11.6$ Hz, 3H). ^{13}C NMR (101 MHz, DMSO) δ 146.5,

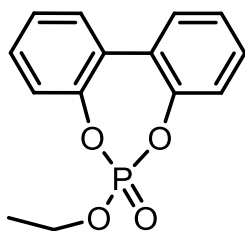
164.4, 135.2, 128.5, 124.3, 113.5, 113.4, 55.7. ^{31}P NMR (162 MHz, CDCl_3) δ -15.32 (s). ESI-MS positive ion mode m/z $[(\text{M}+\text{H})^+]$; HRMS (TOF mode) calculated for $\text{C}_{11}\text{H}_9\text{O}_4\text{P}$, 237.0311, found 237.0323.

7.7. Ethyl naphthyl 1,8-cyclic phosphate 49



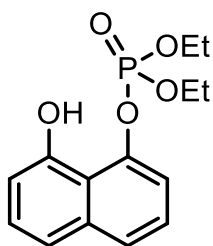
Ethyl 1,8-naphthyl cyclic phosphate **49** was synthesised according to a modified published procedure.¹¹³ 1, 8-dihydroxy-naphthalene (0.17 g, 1.1 mmol) and ethyldichlorophosphate (0.16 g, 1.1 mmol) were dissolved in dry THF (10 mL) under argon at 0 °C. The reaction was stirred for 10 min then triethylamine (0.22 g, 0.3 mL, 2.2 mmol) was added slowly. The solution was stirred for 30 min at the same temperature, and then returned to room temperature. After 3h, the white precipitate formed was filtered off and the solvent removed *in vacuo*. The crude product was purified over silica chromatography using 50 % ethylacetate (EtOAc) in petroleum ether to yield (0.1 g, 0.4 mmol, 40 %) of ethyl naphthyl 1,8-cyclic phosphate as a pale grey solid. mp = 64-65 °C. ^1H NMR (400 MHz, CDCl_3) δ 7.61 (d, J = 8.3 Hz, 2H), 7.44 (t, J = 7.9 Hz, 2H), 7.10 (d, J = 8.0 Hz, 2H), 4.29 (m, 2H), 1.30 (t, J = 7.2 Hz, 3H). ^{13}C NMR (101 MHz, CDCl_3) δ 146.8, 146.7, 135.1, 127.5, 123.4, 112.5, 77.3, 16.0. ^{31}P NMR (162 MHz, D_2O) δ -15.75 (s). ESI-MS positive ion mode m/z $[(\text{M}+\text{H})^+]$; HRMS (TOF mode) calculated for $\text{C}_{12}\text{H}_{11}\text{O}_4\text{P}$, 251.0468, found 251.0468.

7.8. Synthesis of Ethyl 2,2'-biphenyl cyclic phosphate 80



Ethyl 2,2'-Biphenylcyclic phosphate **80** was synthesised according to a modified published procedure.¹¹³ 2, 2'-Biphenol (0.5 g, 2.7 mmol) and ethyl dichlorophosphate (0.44 g, 2.7 mmol) were dissolved in dry THF (10 mL) under argon at 0 °C. The reaction was stirred for 10 min then triethylamine (0.54 g, 0.75 mL, 5.37 mmol) was added slowly. The solution was stirred for 30 min at the same temperature, and then returned to room temperature. After 3h, the white precipitate formed was filtered off and the solvent removed in vacuo. The crude product was purified over silica chromatography using 50 % ethylacetate (EtOAc) in petroleum ether to yield (0.45 g, 1.63 mmol, 60 %) of ethyl 2, 2'-biphenylcyclic phosphate as a colourless oil. ¹H NMR (400 MHz, CDCl₃) δ 7.55 (dd, *J* = 7.6, 1.8 Hz, 2H), 7.45 (m, 2H), 7.37 (t, *J* = 7.6 Hz, 2H), 7.31 (m, 2H), 4.41 (m, 2H), 1.45 (t, *J* = 7.1, 1.1 Hz, 3H). ¹³C NMR (101 MHz, CDCl₃) δ 147.8, 130.1, 129.9, 128.3, 126.4, 121.3, 66.0, 16.3. ³¹P NMR (162 MHz, CD Cl₃) δ 2.25 (s). ESI-MS positive ion mode *m/z* [(M+H)⁺]; HRMS (TOF mode) calculated for C₁₄H₁₃O₄P, 277.0624, found 277.0623.

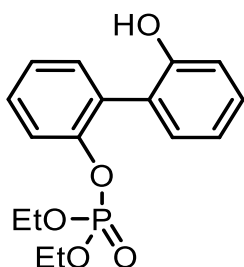
Synthesis of diethyl 8-hydroxy-1-naphthyl phosphate **69**



Diethyl 8-hydroxy-1-naphthyl phosphate **69** was synthesised according to a modified published procedure.¹¹³ 1,8-dihydroxy-naphthalene (0.2 g, 1.24 mmol) and diethylchlorophosphate (0.21 g, 1.24 mmol) were dissolved in dry THF (10 mL) under argon at 0 °C. The reaction was stirred for 10 min then triethylamine (0.25g, 0.35 mL, 2.5 mmol) was added slowly and the solution stirred for 10 min at the same temperature. After that, the solution was returned to room temperature. The reaction was monitored by TLC to avoid forming cyclic phosphate as major product. After 4 hr, the white precipitate which formed was filtered off and the solvent removed

in vacuo. The crude product was purified over silica chromatography using 40 % EtOAc in petroleum ether to yield (0.14 g, 0.472 mmol, 38 %) of diethyl 8-hydroxy-1-naphthyl phosphate as a grey solid. mp = 74-75 °C. ¹H NMR (400 MHz, CDCl₃) δ 8.14 (s, 1H), 7.64 (dt, *J* = 8.3, 0.9 Hz, 1H), 7.46 (dt, *J* = 7.8, 1.2 Hz, 1H), 7.42 – 7.32 (m, 3H), 6.99 (dd, *J* = 5.4, 3.3 Hz, 1H), 4.41 – 4.22 (m, 4H), 1.37 (td, *J* = 7.1, 1.1 Hz, 6H). ¹³C NMR (101 MHz, CDCl₃) δ 152.5, 146.6, 136.9, 127.7, 125.5, 125.3, 119.8, 114.0, 111.9, 65.4, 65.3, 16.1, 16.0. ³¹P NMR (162 MHz, CDCl₃) δ -6.61 (p, *J* = 8.8 Hz). ESI-MS positive ion mode *m/z* [(M+H)⁺]; HRMS (TOF mode) calculated for C₁₄H₁₇O₅P, 297.0886, found 297.0891. IR= 3132 (OH) cm⁻¹.

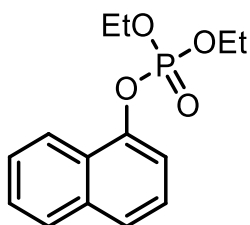
7.9. Synthesis of Diethyl 2-hydroxy-2'-biphenyl phosphate **71**



Diethyl 2-hydroxy-2'-biphenyl phosphate **71** was synthesised according to a modified published procedure.¹¹³ Biphenyl-2,2'-diol (0.3 g, 1.61 mmol) and diethyl dichlorophosphate (0.28 g, 1.61 mmol) were dissolved in dry THF (10 mL) under argon at 0 °C. The reaction was stirred for 10 min then triethylamine (0.32 g, 0.45 mL, 3.22 mmol) was added slowly and the solution stirred for 30 min at the same temperature. After that, the solution was returned to room temperature. After 5 h, the white precipitate, which formed, was filtered off and the solvent removed *in vacuo*. The crude product was purified over silica chromatography using 40 % EtOAc in petroleum ether to yield (0.28 g, 0.87 mmol, 55 %) of diethyl 2-hydroxy-2'-biphenyl phosphate as a white solid. mp = 72-73 °C. ¹H NMR (400 MHz, CDCl₃) δ 7.43 – 7.33 (m, 3H), 7.31 – 7.22 (m, 2H), 7.18 (dd, *J* = 7.6, 1.7 Hz, 1H), 6.97 (m, 2H), 6.36 (s, 1H), 4.02 – 3.82 (m, 4H), 1.21 (td, *J* = 7.1, 1.1 Hz, 6H). ¹³C NMR (101 MHz, CDCl₃) δ 153.7, 148.3, 132.3, 131.0, 130.0, 129.4, 125.5, 125.0, 120.5, 120.2, 117.1, 64.6, 15.9. ³¹P NMR (162 MHz, CDCl₃)

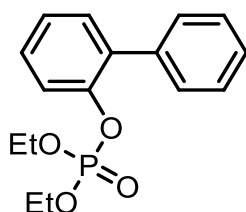
δ -6.07 (p, J = 8.8 Hz). ESI-MS positive ion mode m/z [(M+H)⁺]; HRMS (TOF mode) calculated for C₁₆H₁₉O₅P, 323.1043, found 323.1045. IR= 3169 (OH) cm⁻¹.

7.10. Synthesis of Diethyl 1-naphthyl phosphate **70**



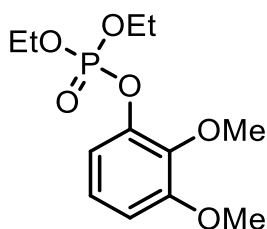
Diethyl 1-naphthyl phosphate **70** was synthesised according to a modified published procedure.¹¹³ 1-naphthol (0.5 g, 3.47 mmol) and diethyl dichlorophosphate (0.6 g, 3.47 mmol) were dissolved in dry THF (10 mL) under argon at 0 °C. The reaction was stirred for 10 min then triethylamine (0.7 g, 0.97 mL, 6.93 mmol) was added slowly and the solution stirred for 30 min at the same temperature. After that, the solution was returned to room temperature. After 3h, the white precipitate which formed was filtered off and the solvent removed *in vacuo*. The crude product was purified over silica chromatography using 50 % EtOAc in petroleum ether to yield (0.6 g, 2.14 mmol, 70 %) of diethyl 1-naphthyl phosphate as a light brown oil. ¹H NMR (400 MHz, CDCl₃) δ 8.16 (d, J = 8.0 Hz, 1H), 7.82 (dd, J = 7.9, 1.6 Hz, 1H), 7.64 (d, J = 8, 1.0 Hz, 1H), 7.56 – 7.45 (m, 3H), 7.39 (t, J = 7.9 Hz, 1H), 4.24 (m, 4H), 1.32 (t, J = 7.1 Hz, 6H). ¹³C NMR (101 MHz, CDCl₃) δ 146.6, 134.7, 127.7, 126.5, 126.3, 126.2, 125.4, 124.7, 121.5, 114.7, 64.6, 16.0. ³¹P NMR (162 MHz, CDCl₃) δ -6.03 (p, J = 8.3 Hz). ESI-MS positive ion mode m/z [(M+H)⁺]; HRMS (TOF mode) calculated for C₁₄H₁₇O₄P, 281.0937, found 281.093.

Synthesis of Diethyl 2-biphenyl phosphate **72**



Diethyl 2-biphenyl phosphate **72** was synthesised according to a modified published procedure.¹¹³ Biphenyl-2,2'-diol (0.5 g, 2.93 mmol) and diethyl dichlorophosphate (0.5 g, 2.93 mmol) were dissolved in dry THF (10 mL) under argon at 0 °C. The reaction was stirred for 10 min then triethylamine (0.6 g, 0.82 mL, 5.86 mmol) was added slowly and the solution stirred for 30 min at the same temperature. The solution was returned to room temperature, and stirred overnight. The white precipitate which formed was filtered off and the solvent removed *in vacuo*. The crude product was purified over silica chromatography using 50 % EtOAc in petroleum ether to yield (0.73 g, 2.38 mmol, 81 %) of diethyl 2-biphenyl phosphate as a colourless oil. ¹H NMR (400 MHz, CDCl₃) δ 7.44 (t, *J* = 8.4 Hz, 3H), 7.38 – 7.23 (m, 6H), 7.16 (tt, *J* = 7.5, 1.1 Hz, 1H), 3.95 – 3.80 (m, 4H), 1.13 (td, *J* = 7.1, 1.1 Hz, 6H). ¹³C NMR (101 MHz, CDCl₃) δ 147.6, 137.4, 133.5, 131.0, 129.4, 128.6, 127.9, 127.2, 125.1, 120.4, 64.2, 15.8. ³¹P NMR (162 MHz, CDCl₃) δ -6.93 (p, *J* = 8.1 Hz). ESI-MS positive ion mode *m/z* [(M+H)⁺]; HRMS (TOF mode) calculated for C₁₆H₁₉O₄P, 307.1094, found 307.1094.

7.11. Synthesis of Diethyl 1,2-dimethoxy-3-phenyl phosphate **85**

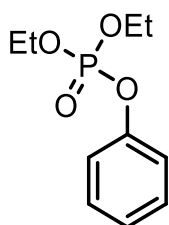


Diethyl 1,2-dimethoxy-3-phenyl phosphate **85** was synthesised according to a modified published procedure.¹¹³ 2,3-dimethoxyphenol (0.3 g, 1.95 mmol) and diethyl dichlorophosphate (0.33 g, 1.95 mmol) were dissolved in dry THF (10 mL) under argon at 0 °C. The reaction was stirred for 10 min then triethylamine (0.39 g, 0.55 mL, 3.9 mmol) was added slowly and the solution stirred for 30 min at the same temperature. After that, the solution was returned to room temperature, and stirred overnight. The white precipitate, which formed was filtered off and the solvent removed *in vacuo*. The crude mixture was washed with brine

and water and then extracted with DCM. The solvent evaporated, and the residue was purified over silica chromatography using 50 % EtOAc in petroleum ether to yield diethyl 1,2-dimethoxy-3-phenyl phosphate as a brown oil (0.48 g, 1.65 mmol, 85 %).

^1H NMR (400 MHz, CDCl_3) δ 7.03 – 6.94 (m, 2H), 6.76 (dd, $J = 7.7, 1.8$ Hz, 1H), 4.27 (m, 4H), 3.89 (d, $J = 9.2$ Hz, 6H), 1.38 (td, $J = 7.1, 1.1$ Hz, 6H). ^{13}C NMR (101 MHz, CDCl_3) δ 152.5, 149.5, 135.7, 124.0, 108.1, 104.1, 60.9, 55.8. ^{31}P NMR (162 MHz, CDCl_3) δ -6.25 (p, $J = 8.3$ Hz). ESI-MS positive ion mode m/z [(M+H) $^+$]; HRMS (TOF mode) calculated for $\text{C}_{20}\text{H}_{16}\text{O}_2\text{P}$, 291.0992, found 291.0995.

7.12. Synthesis of Diethyl phenyl phosphate **86**

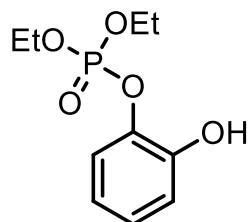


Diethyl phenyl phosphate **86** was synthesised according to a modified published procedure.¹¹³ phenol (0.5 g, 5.3 mmol) and diethyldichlorophosphate (0.91 g, 5.3 mmol) were dissolved in dry THF (10 mL) under argon at 0 °C. The reaction was stirred for 10 min then triethylamine (1.1 g, 1.5 mL, 10.6 mmol) was added slowly and the solution stirred for 30 min at the same temperature. After that, the solution was returned to room temperature, and stirred overnight. The white precipitate which formed was filtered off and the solvent removed *in vacuo*. The crude mixture was washed with brine and water and then extracted with DCM. The solvent evaporated, and the residue was purified over silica chromatography using 50 % EtOAc in petroleum ether to yield diethyl phenyl phosphate as a brown oil (1.06 g, 4.6 mmol, 87 %).

^1H NMR (400 MHz, CDCl_3) δ 7.29 – 7.19 (t, $J = 8.0$ Hz, 2H), 7.13 (d, $J = 7.8$ Hz, 2H), 7.09 – 7.03 (t, $J = 7.1$ Hz, 1H). ^{13}C NMR (101 MHz, CDCl_3) δ 150.6, 129.5, 124.8, 119.8, 119.7, 64.3,

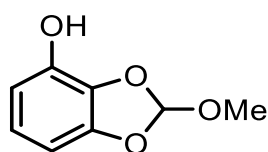
15.8. ^{31}P NMR (162 MHz, CDCl_3) δ -6.46 (p, $J = 8.4$ Hz). ESI-MS positive ion mode m/z $[(\text{M}+\text{H})^+]$; HRMS (TOF mode) calculated for $\text{C}_{10}\text{H}_{15}\text{O}_4\text{P}$, 231.0781, found 231.0791.

7.13. Synthesis of diethyl 2-hydroxy-1-phenyl phosphate **84**



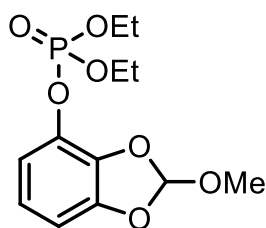
Diethyl 2-hydroxy-1-phenyl phosphate **84** was synthesised according to a modified published procedure.¹¹³ Catechol (0.5 g, 4.54 mmol) and diethyldichlorophosphate (0.78 g, 4.54 mmol) were dissolved in dry THF (10 mL) under argon at 0 °C. The reaction was stirred for 10 min then triethylamine (0.92 g, 1.3 mL, 9.08 mmol) was added slowly and the solution stirred for 30 min at the same temperature. After that, the solution was returned to room temperature. After 5h, the white precipitate which formed was filtered off and the solvent removed in vacuo. The crude product was purified over silica chromatography using 50 % EtOAc in petroleum ether to yield diethyl 2-hydroxy-phenyl phosphate as a yellowish solid (0.83 g, 3.37 mmol, 74 %). ^1H NMR (400 MHz, CDCl_3) δ 7.95 (s, 1H), 7.17 – 6.98 (m, 2H), 6.87 (t, $J = 8.0$ Hz, 2H), 4.39 – 4.18 (m, 4H), 1.36 (t, $J = 7.2$ Hz 6H). ^{13}C NMR (101 MHz, CDCl_3) δ 147.6, 138.4, 126.6, 121.3, 120.6, 119.2, 65.5, 15.9. ^{31}P NMR (162 MHz, CDCl_3) δ -3.07 (p, $J = 8.6$ Hz). ESI-MS positive ion mode m/z $[(\text{M}+\text{H})^+]$; HRMS (TOF mode) calculated for $\text{C}_{10}\text{H}_{15}\text{O}_5\text{P}$, 247.1073, found 247.0737. IR= 3192 (OH) cm^{-1} .

7.14. Synthesis of 2-Methoxybenzo[1,3]dioxol-4-ol **91**



2-Ethoxybenzo[1,3]dioxol-4-ol **91** was synthesised according to a modified published procedure.¹¹⁴⁻¹¹⁵ A mixture of pyrogallol (1 g, 7.93 mmol), and CH(OMe)₃ (2.524 g, 2.6 ml, 23.79 mmol, 3eq.), in dry toluene (25 ml) was refluxed for 22 h in a flask under N₂. The reaction mixture was cooled to 0 °C, filtered to remove the unreacted pyrogallol, and concentrated under vacuum. The residue was washed with cooled chloroform (3 × 50 ml), then filtered. The solvent was evaporated to give 2-ethoxybenzo[1,3]dioxol-4-ol (1.08 g, 6.42 mmol, 81 %). ¹H NMR (400 MHz, CDCl₃) δ 6.86 (s, 1H), 6.75 (t, *J* = 8.2 Hz, 1H), 6.51 (d, *J* = 8.2 Hz, 2H), 4.93 (br s, 1H), 3.42 (s, 3H). ¹³C NMR (101 MHz, CDCl₃) δ 147.1, 138.8, 132.8, 122.1, 119.3, 110.9, 101.4, 50.1. ESI-MS positive ion mode *m/z* [(M+H)⁺]; HRMS (TOF mode) calculated for C₈H₈O₄, 169.0495, found 169.0498. IR= 3391 cm⁻¹ (OH)

7.15. Synthesis of diethyl 2-methoxybenzo[1,3]dioxol-4- phosphate **92**

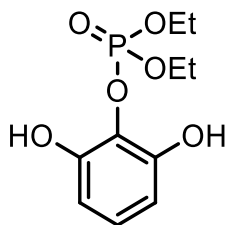


Diethyl 2-methoxybenzo[1,3]dioxol-4- phosphate **92** was synthesised according to a modified published procedure.¹¹³ 2-Methoxybenzo[1,3]dioxol-4-ol (19) (0.6 g, 3.57 mmol) and diethyl chlorophosphate (0.62 g, 3.57 mmol) were dissolved in dry THF (10 mL) under argon at 0 °C. The reaction was stirred for 10 min then triethylamine (0.72 g, 1 mL, 7.13 mmol) was added slowly and the solution stirred for 30 min at the same temperature. After that, the solution was returned to room temperature. After 6 hrs, the white precipitate which formed was filtered off and the solvent removed *in vacuo*. The crude product was purified over silica chromatography using 40 % EtOAc in petroleum ether to yield diethyl 2-methoxybenzo[1,3]dioxol-4-phosphate as a yellowish solid (0.48 g, 1.58 mmol, 45 %). ¹H NMR (400 MHz, CDCl₃) δ 6.92 (s, 1H), 6.89 (d, *J* = 8.4 Hz, 1H), 6.83 (t, *J* = 8.1 Hz, 1H), 6.74 (d, *J* = 8.0 Hz, 1H), 4.33 – 4.22

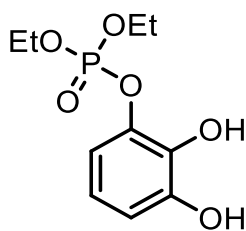
(m, 4H), 3.43 (s, 1H), 1.39 (t, $J = 7.1$ Hz, 6H). ^{31}P NMR (162 MHz, CDCl_3) δ -5.98 (p, $J = 7.9$ Hz). ^{13}C NMR (101 MHz, CDCl_3) δ 147.8, 136.4, 133.3, 121.8, 119.6, 114.9, 105.2, 64.8, 49.8, 16.0. ESI-MS positive ion mode m/z $[(\text{M}+\text{Na})^+]$; HRMS (TOF mode) calculated for $\text{C}_{12}\text{H}_{17}\text{O}_7\text{P}$, 327.0604, found 327.0616

7.16. Synthesis of Diethyl 1, 3-dihydroxy-2-phenyl phosphate and diethyl 1, 2-hydroxy-3-phenyl phosphate **82** and **83**

Diethyl 2,3-dihydroxy-1-phenyl phosphate and diethyl 1,2-hydroxy-2-phenyl phosphate were synthesised according to a modified published procedure.¹¹⁵ To a solution of diethyl 2-methoxybenzo[1,3]dioxol-4- phosphate (0.3 g, 0.986 mmol) in CHCl_3 (5 mL) was added *p*-toluenesulfonic acid (0.15%) as catalyst. The reaction mixture was stirred at room temperature overnight, then washed with saturated solution of NaHCO_3 , and dried over Na_2SO_4 . The solvent was removed and the crude was purified by flash column chromatography using (silica gel, EtOAc /petroleum ether 40:60) to yield 0.2 g, 0.76 mmol, 77 % of a mixture of **82** & **83** (in ratio 1:3) as a brown oil.

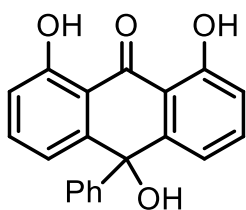


Diethyl 1, 3-dihydroxy-2-phenyl phosphate **82**: ^1H NMR (400 MHz, CDCl_3) δ 6.92 (s, 2H), 6.97 (dt, $J = 8.5, 1.1$ Hz, 1H), 6.62 (dd, $J = 2.3, 1.4$ Hz, 2H), 4.33 – 4.22 (m, 4H), 1.39 (t, $J = 7.1$ Hz, 6H). ^{31}P NMR (162 MHz, CDCl_3) δ -0.66 (p, $J = 8.9$ Hz). ^{13}C NMR (101 MHz, CDCl_3) δ 148.5, 127.2, 126.2, 109.7, 65.7, 16.9. ESI-MS positive ion mode m/z $[(\text{M}+\text{H})^+]$; HRMS (TOF mode) calculated for $\text{C}_{10}\text{H}_{15}\text{O}_6\text{P}$, 263.0679; found 263.0679.



Diethyl 1,2-dihydroxy-3-phenyl phosphate **83**: ^1H NMR (400 MHz, CDCl_3) δ 8.77 (s, 1H), 6.85 – 6.74 (m, 2H), 6.61 (t, $J = 8.1$ Hz, 1H), 5.96 (s, 1H), 4.33 – 4.22 (m, 4H), 1.39 (t, $J = 7.1$ Hz, 6H). ^{31}P NMR (162 MHz, CDCl_3) δ -2.29 (p, $J = 8.6$ Hz). ^{13}C NMR (101 MHz, CDCl_3) δ 147.6, 138.6, 135.2, 120.4, 112.7, 112.3, 65.7, 16.0. ESI-MS positive ion mode m/z [(M+H) $^+$]; HRMS (TOF mode) calculated for $\text{C}_{10}\text{H}_{15}\text{O}_6\text{P}$, 263.0679, found 263.0679.

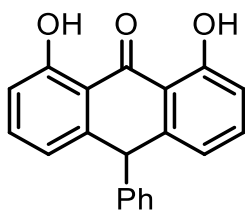
7.17. Synthesis of 10-phenyl, 1,8,10-trihydroxy-9- anthrone **134**



10-phenyl, 1,8,10-trihydroxy-9- anthrone **134**.¹⁰⁵ In a 500 ml round flask, there was added 1,8-dihydroxy anthraquinone (3 g, 12.5 mmol) and anhydrous tetrahydrofuran 200 mL. The reaction mixture is cooled to -70°C , then 4 equivalents of phenyllithium was added, with stirring, over a 30 minute period, This temperature was maintained throughout the addition between -60°C and -70°C . The reaction was monitored by TLC until the 1,8-dihydroxy anthraquinone has been transformed. The reaction mixture was acidified by adding acetic acid (40 mL) at the same temperature (60°C) and it is then permitted to return to ambient temperature. The solvent is removed under reduced pressure and the resulting oily product crystallised on stirring in water, and then filtered, washed with dichloromethane and dried, yielding yellow crystals (3.15 g, 9.9 mmol, 79 %) of 10-phenyl, 1,8,10-trihydroxy-9- anthrone, which were recrystallized in methanol. mp = $216\text{--}217^\circ\text{C}$ (lit. mp = 216°C). ^1H NMR (400 MHz, CDCl_3) δ 12.26 (s, 2H), 7.46 (t, $J = 8.0$ Hz, 2H), 7.36

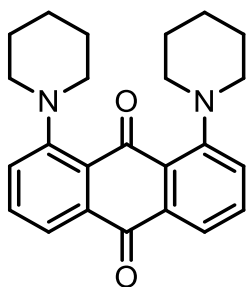
– 7.30 (m, 2H), 7.25 (dd, $J = 10.2, 4.9$ Hz, 2H), 7.22 – 7.15 (m, 1H), 7.13 (dd, $J = 7.7, 0.8$ Hz, 2H), 6.85 (dd, $J = 8.3, 0.8$ Hz, 2H), 3.15 (s, 1H). ^{13}C NMR (101 MHz, CDCl_3) δ 192.8, 162.3, 149.0, 146.0, 137.4, 128.4, 127.0, 124.8, 119.3, 117.2, 113.6, 73.3. ESI-MS negative ion mode m/z 317.1 [(M+H) $^+$]; HRMS (TOF mode) calculated for $\text{C}_{20}\text{H}_{14}\text{O}_4$, 317.0819, found 317.0823. IR = 1633 cm^{-1} (C=O), 3485.6 & 3033 (OH) cm^{-1} .

7.18. Preparation of 1,8-dihydroxy-10-phenyl-9-anthrone **135**



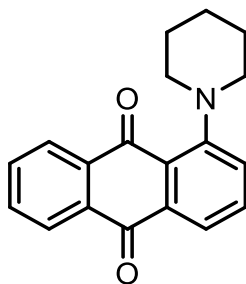
1,8-dihydroxy-10-phenyl-9-anthrone **135** was prepared according to the published procedure.¹⁰⁵ To 10 phenyl-1,8,10-trihydroxy-9-anthrone **134** (2 g, 6.28 mmol) under argon, there was introduced crushed tin chloride (8 g) and acetic acid (80 ml). The reaction mixture was stirred at ambient temperature, and then concentrated HCl (8 ml) was slowly added over a 30-minute period. The disappearance of the 10-phenyl 1,8,10-trihydroxy-9-anthrone was followed by TLC. After about 4 hours, the reduction reaction is terminated. The 1,8-dihydroxy-10-phenyl-9-anthrone, precipitated in the medium, is filtered, washed with water and dried, yielding light green solid (1.56 g, 5.16 mmol, 82 %). mp = 193-195°C (193-194 °C, lit). ^1H NMR (400 MHz, CDCl_3) δ 12.40 (s, 2H), 7.41 (t, $J = 8.0$ Hz, 2H), 7.33 – 7.27 (m, 2H), 7.24 (t, $J = 7.3$ Hz, 1H), 7.12 (d, $J = 7.0$ Hz, 2H), 6.90 (d, $J = 8.3$ Hz, 2H), 6.74 (d, $J = 7.6$ Hz, 2H), 5.37 (s, 1H). ^{13}C NMR (101 MHz, CDCl_3) δ 193.8, 162.6, 146.2, 145.8, 144.3, 136.6, 129.1, 128.4, 127.0, 120.3, 115.8, 114.9, 48.8. ESI-MS negative ion mode m/z [(M-H) $^-$]; HRMS (TOF mode) calculated for $\text{C}_{20}\text{H}_{14}\text{O}_3$, 301.087, found 301.0877. IR = 3035 & 1600 (C=O) cm^{-1} .

7.19. Synthesis of 1,8-dipiperidine anthraquinone **103**



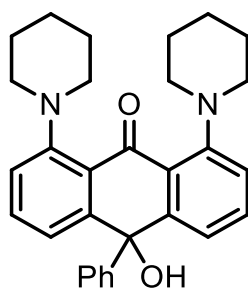
1,8-dipiperidine anthraquinone **103** was synthesised according to a modified published procedure¹¹⁶. In a flask fitted with a magnetic stirrer and condenser, a mixture of 1,8-dichloro anthraquinone (1 g, 3.6 mmol) in 8 ml of THF and 9 ml of piperidine (excess) was refluxed at 40 °C with stirring for 48 h. After cooling down to room temperature, water was added and the mixture was extracted with CHCl₃. The organic layer was separated then dried over anhydrous magnesium sulfate, filtered and then the solvent was evaporated *in vacuo*. The crude material was purified by column chromatography on silica (hexane:EtOAc, 80:20) to give 1,8-dipiperidine anthraquinone as a dark crimson solid (1.13 g, 3.02 mmol, 90 %). m.p. 182-184 °C. ¹H NMR (400 MHz, CDCl₃) δ 7.80 (d, *J* = 7.5 Hz, 2H), 7.53 (t, *J* = 8.0 Hz, 2H), 7.37 (d, *J* = 8.3 Hz, 2H), 3.14 (t, *J* = 5.2 Hz, 8H), 1.87 (q, *J* = 11.0, 5.6 Hz, 8H), 1.68 (q, *J* = 11.6, 5.9 Hz, 4H). ¹³C NMR (101 MHz, CDCl₃) δ 185.2, 183.6, 153.2, 135.1, 132.5, 127.3, 125.3, 119.4, 54.5, 26.3, 24.3. ESI-MS positive ion mode *m/z* [(*M*+*H*)⁺]; HRMS (TOF mode) calculated for C₂₄H₂₆N₂O₂, 375.2067, found 375.2083. IR = 1669 & 1647 (C=O) cm⁻¹.

7.20. Synthesis of 1-piperidine anthraquinone **109**



1-piperidine anthraquinone **109** was synthesised according to a modified published procedure¹¹⁶. In a flask fitted with a magnetic stirrer and condenser, a mixture of 1-chloroanthraquinone (1 g, 4.13 mmol) in THF (8 ml) and piperidine (5 ml) was refluxed at 40 °C with stirring for 48 h. After cooling down to room temperature, water was added and the mixture was extracted with CHCl₃. The organic layer was separated then dried over anhydrous magnesium sulfate, filtered and the solvent was then evaporated *in vacuo*. The crude material was purified by column chromatography on silica (hexane:EtOAc, 80:20) to yield 1-piperidine anthraquinone as a red solid: m.p. (1.06 g, 3.63 mmol, 88 %). m.p. 120_122 °C. ¹H NMR (400 MHz, CDCl₃) δ 8.3 (dd, *J* = 7.7, 1.2 Hz, 1H), 8.24 (dd, *J* = 7.6, 1.2 Hz, 1H), 7.90 (dd, *J* = 7.5, 1.2 Hz, 1H), 7.77 (td, *J* = 7.5, 1.5 Hz, 1H), 7.72 (td, *J* = 7.5, 1.5 Hz, 1H), 7.62 (dd, *J* = 8.4, 7.4 Hz, 1H), 7.42 (dd, *J* = 8.4, 1.2 Hz, 1H). 3.19 (t, *J* = 5.1 Hz, 8H), 1.87 (q, *J* = 11.3, 5.5 Hz, 8H), 1.68 (q, *J* = 11.4, 6.0 Hz, 4H). ¹³C NMR (101 MHz, CDCl₃) δ 184.3, 181.6, 154.1, 136.5, 135.5, 134.0, 133.9, 132.7, 132.3, 127.2, 126.3, 125.0, 122.2, 119.8, 53.9, 26.0, 24.1. ESI-MS positive ion mode *m/z* [(M+H)⁺]; HRMS (TOF mode) calculated for C₁₉H₁₇NO₂, 292.1332, found 292.1335. IR = 1663 & 1647 (C=O) cm⁻¹.

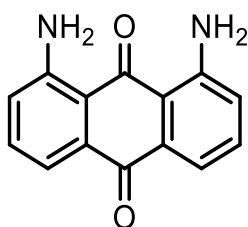
7.21. Synthesis of 1,8-dipiperidine-10-hydroxy-10-phenyl-9- anthrone **119**



1,8-dipiperidine-10-hydroxy-10-phenyl-9- anthrone **119** was synthesised according to a modified published procedure.¹⁰⁵ To (1g, 2.88 mmol) of 1,8-dipiperidine anthraquinone in 70 ml of anhydrous tetrahydrofuran in two neck flask fitted with a condenser under argon and at 70 °C, there was then added (4 eq.) of phenyl lithium over a 30 minute period. The reaction

was followed by TLC to confirm that all the 1,8-dipiperidine anthraquinone is transformed. The reaction mixture was acidified by adding acetic acid (16 ml) at this same temperature. The reaction mixture was returned to ambient temperature. The solvent was removed to dryness and the resulting oily mass, crystallizes by stirring in water. The resulting crystals are filtered, washed with diethylether and then dried, yielding 1,8-dipiperidine-10-phenyl-10-hydroxy-9-anthrone (0.17 g, 3.75 mmol, 14 %). mp = 152-153 °C. ^1H NMR (400 MHz, CDCl_3) δ 7.51 (dd, $J = 7.8, 1.1$ Hz, 2H), 7.42 (t, $J = 7.9$ Hz, 2H), 7.32 – 7.26 (m, 2H), 7.20 – 7.09 (m, 3H), 7.06 (dd, $J = 8.2, 1.1$ Hz, 2H), 3.22 (m, 4H), 2.91 (m, 4H), 2.75 (s, 1H), 1.83 (m, 8H), 1.62 (p, $J = 6.0$ Hz, 4H). ^{13}C NMR (101 MHz, CDCl_3) δ 186.2, 152.7, 147.6, 146.3, 132.09, 128.2, 127.5, 127.1, 125.7, 118.7, 117.9, 74.9, 55.0, 26.4, 24.4. ESI-MS positive ion mode m/z $[(\text{M}+\text{H})^+]$; HRMS (TOF mode) calculated for $\text{C}_{30}\text{H}_{32}\text{N}_2\text{O}_2$, 453.2537, found 453.2547. IR = 1667 cm^{-1} (C=O), 3429 cm^{-1} (OH).

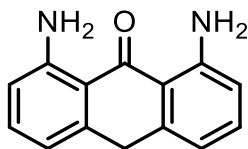
7.22. Synthesis of 1, 8-diamino anthraquinone 112



1,8-Diamino anthraquinone **112** was synthesised according to a published procedure¹¹⁷. A solution of $\text{Na}_2\text{S}\cdot 9\text{H}_2\text{O}$ (4.8 g, 20 mmol) in water (100ml) was added to a solution of 1,8-dinitroanthracene-9,10-dione (1.5 g, 5 mmol) in EtOH (30 mL) at RT. The reaction mixture was refluxed for 48 h, cooled to RT and then poured into an ice/water mixture with stirring. The resulting precipitate was collected by filtration, washed with water (2×15 mL) and dried *in vacuo*. Recrystallization from EtOH yielded 1, 8-diamino anthraquinone as red solid (1.08 g, 4.53 mmol, 90 %). ^1H NMR (400 MHz, DMSO) δ 7.86 (s,br, 4H), 7.45 (t, $J = 7.7$, Hz, 2H), 7.35 (d, $J = 7.3$, Hz, 2H), 7.16 (d, $J = 8.2$ Hz, 2H). ^{13}C NMR (101 MHz, DMSO) δ 188.1,

183.9, 152.0, 134.1, 133.9, 123.9, 115.3, 113.5. ESI-MS positive ion mode m/z $[(M+H)^+]$; HRMS (TOF mode) calculated for $C_{14}H_{10}N_2O_2$, 239.0815, found 239.0818. IR= 1652 (C=O) cm^{-1} .

Synthesis of 1, 8-diamino anthrone **113**



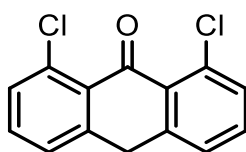
1,8-diamino anthrone **113** was synthesised according to a published procedure.⁹⁸ To a vigorously stirred suspension of (2.14 g, 9.0 mmol) of diamino anthraquinone in a mixture of aqueous ammonia (25%, 100 ml) and isopropyl alcohol (10 ml) at 90°C under argon, there was (8.0 g, 0.122 mol) of zinc dust was added in small portions during 1 h. Then the temperature was raised to 120°C for another 1 h. After cooling, the reaction mixture was extracted with diethyl ether (6 × 100 ml). The combined ethereal extracts were dried with anhydrous magnesium sulfate, the solvent was evaporated, and the residue was crystallized from toluene: (1.4 g, 6.24 mmol, 74%) of 1,8-diamino-9-anthrone as orange crystals. ¹H NMR (400 MHz, DMSO) δ 7.63 – 7.33 (br.s, 4H), 7.17 (t, J = 7.8 Hz, 2H), 6.64 (d, J = 8.3 Hz, 2H), 6.48 (d, J = 7.3 Hz, 2H), 4.14 (s, 2H). ¹³C NMR (101 MHz, DMSO) δ 190.5, 151.97, 141.7, 133.5, 115.1, 114.5, 114.3, 34.1. ESI-MS positive ion mode m/z $[(M+H)^+]$; HRMS (TOF mode) calculated for $C_{14}H_{12}N_2O$, 225.1022, found 225.1022. IR=1579 (C=O) cm^{-1} .

7.23. Synthesis of 1,8-dichloro- -9- anthrone **107**

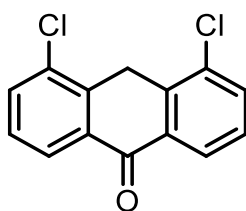
1,8-dichloro-9-anthrone **107** was synthesised according to a published procedure.¹¹² A solution of the 1,8-dichloroanthracene-9,10-dione (1g, 3.6 mmol) in glacial acetic acid (50 mL) was heated to reflux, then a solution of $SnCl_2 \cdot 2H_2O$ (7.5 g, 33.23 mmol) in Conc HCl (13.4 mL) was added dropwise over 3 h. The solution was returned to room temperature, and the resulting crystals were collected by filtration. Purification by column chromatography (hexanes: ethyl

acetate = 80:20) provided the 1, 8-dichloroanthracen-9(10H)-one (0.39 g, 1.48 mmol, 41 %) and 4,5-dichloroanthracen-9(10H)-one (0.51 g, 1.94 mmol, 54%).

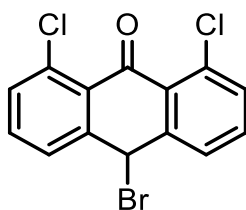
1.8-dichloro-9(10H)-anthrone **107**. ^1H NMR (400 MHz, CDCl_3) δ 7.44 (dd, $J = 7.8, 1.6$ Hz, 2H), 7.42 – 7.37 (m, 2H), 7.37 – 7.30 (m, 2H), 4.21 (s, 2H). ^{13}C NMR (101 MHz, CDCl_3) δ 183.5, 140.8, 133.4, 132.0, 131.7, 130.2, 126.3, 33.8. ESI-MS positive ion mode m/z [(M+H) $^+$]; HRMS (TOF mode) calculated for $\text{C}_{14}\text{H}_7\text{Cl}_2\text{O}$, 263.9919, found 263.9919. IR = 1677 (C=O) cm^{-1} .



1.8-dichloro-10(9H)-anthrone **108**. ^1H NMR (400 MHz, CDCl_3) δ 8.31 (d, $J = 7.9$ Hz, 2H), 7.72 (dd, $J = 7.8, 1.3$ Hz, 2H), 7.53 – 7.43 (m, 2H), 4.25 (s, 2H). ^{13}C NMR (101 MHz, CDCl_3) δ 182.70, 137.30, 134.15, 133.72, 132.78, 128.09, 126.36, 29.45. ESI-MS positive ion mode m/z ((M+H) $^+$); HRMS (TOF mode) calculated for $\text{C}_{14}\text{H}_7\text{Cl}_2\text{O}$, 263.9919, found 263.9919. IR = 1655 (C=O) cm^{-1} .

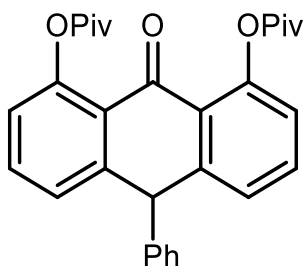


7.24. Synthesis of 1,8-dichloro-10-bromo-9-anthrone **122**



1,8-dichloro-10-bromo-9-anthrone **122** was synthesised according to a modified published procedure.^{108, 118} 1,8-Dichloride – anthrone (0.1 g, 0.36 mmol) was dissolved in freshly distilled carbon disulphide CS₂ (0.28 mL) at RT. Bromine (0.06 g, 0.75 mmol) was added dropwise over 20 minutes with stirring at RT. The solution was left stirring for 3 hours then, petroleum ether was added and the washed-out precipitate recrystallized from toluene to result (10 mg, 0.03 mmol, 8 %) of a white solid. ¹H NMR (400 MHz, CDCl₃) δ 7.45 (dd, J = 14.0, 5.4 Hz, 2H), 7.36 (t, J = 7.7 Hz, 2H), 7.25 – 7.14 (m, 2H), 5.33 (s, 1H). ¹H NMR (400 MHz, DMSO) δ 7.73 (d, J = 2.7 Hz, 1H), 7.72 (d, J = 2.7 Hz, 1H), 7.67 – 7.63 (m, 4H), 7.08 (s, 1H). ¹³C NMR (101 MHz, DMSO) δ 182.5, 142.8, 134.4, 132.6, 132.4, 131.5, 128.1, 55.3. ESI-MS positive ion mode m/z [(M+H)⁺]; HRMS (TOF mode) calculated for C₁₄H₇OBrCl₂, 342.9107; found 342.9107. IR = 1680.3 (C=O) cm⁻¹.

7.25. Synthesis of 1,8-dipivaloyl-10-phenyl-9-anthrone **136**

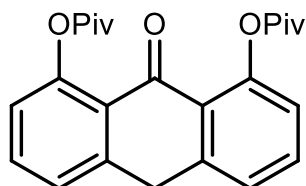


1,8-dipivaloyl-10-phenyl-9-anthrone **136** was synthesised according to a modified published procedure.¹⁰⁹ To a solution of anthrone **1** (1 g, 3.3 mmol) and PivCl (1.19 g, 9.9 mmol) in 10 mL of dry THF was added (0.67 g, 0.93 ml, 6.62 mmol) of Et₃N at 0 C° under Ar. After 10 min, the reaction mixture was returned to the room temperature. The reaction was monitored by TLC until the reaction was finished. The white precipitate formed was filtered. The filtrate was poured into water, then extracted with dichloromethane (3 × 10 mL). The combined organic layers were washed with 10% aq. NaHCO₃ solution, water, and brine, dried over anhydrous MgSO₄, filtered, and evaporated *in vacuo*. The resulting residue was purified by

column chromatography on silica gel eluting with 20 % EtOAc in hexane, to afford the corresponding product as pale yellow solid (1.1 g, 2.34 mmol, 70.6 %). mp = 156-57 °C

^1H NMR (400 MHz, CDCl_3) δ 7.45 (t, $J = 7.9$ Hz, 2H), 7.23 (m, 5H), 7.17 – 7.13 (d, $J = 8.0$ Hz, 2H), 6.95 (d, $J = 8.0$ Hz, 2H), 5.45 (s, 1H), 1.48 (s, 18H). ^{13}C NMR (101 MHz, CDCl_3) δ 181.7, 176.8, 150.4, 144.9, 143.6, 133.0, 129.1, 128.2, 127.0, 126.7, 125.6, 122.4, 49.5, 39.1, 27.3. ESI-MS positive ion mode m/z $[(M+H)^+]$; HRMS (TOF mode) calculated for $\text{C}_{30}\text{H}_{30}\text{O}_5$, 471.2166; found 471.2164. IR = 1745 & 1666 (C=O) cm^{-1} .

7.26. Synthesis of 1,8-dipivaloyl-9- anthrone **133**



1,8-dipivaloyl-9- anthrone **136** was synthesised according to a modified published procedure.¹⁰⁹ To a solution of **1** (1g, 4.42 mmol) and PivCl (1.6 g, 13.26 mmol) in 10 mL of dry THF was added (0.895 g, 1.2 ml, 8.84 mmol) of Et₃N at 0 C° and under Ar. After 10 min, the reaction mixture was returned to the room temperature. The reaction was monitored by TLC until the reaction was finished. The white precipitate formed was filtered. The filtrate was poured into water, then extracted with dichloromethane (3 X 10 mL). The combined organic layers were washed with 10% aq. NaHCO₃ solution, water, and brine, dried over anhydrous MgSO₄, filtered, and evaporated *in vacuo*. The resulting residue was purified by column chromatography on silica gel eluting with 30 % EtOAc in hexane to afford the corresponding product as pale yellow solid (1.02 g, 2.59 mmol, 58 %). mp = 164 °C. ^1H NMR (400 MHz, CDCl_3) δ 7.53 (t, $J = 7.8$ Hz, 2H), 7.32 (d, $J = 7.7$ Hz, 2H), 6.98 (d, $J = 8.0$ Hz, 2H), 4.34 (s, 1H), 1.46 (s, 19H). ^{13}C NMR (101 MHz, CDCl_3) δ 181.3, 177.0, 150.7, 141.2, 132.8, 126.1,

125.7, 122.2, 33.4, 27.3. ESI-MS positive ion mode m/z $[(M+H)^+]$; HRMS (TOF mode) calculated for $C_{24}H_{26}O_5$, 395.1853; found 395.1834. IR= 1745 & 1666 (C=O) cm^{-1} .

7.27. Kinetic experiments

7.27.1. Hydrolysis of phosphate triesters **46**, **47** and **48**

Reactions were followed spectrophotometrically by monitoring the absorbance of substrates; at 255 nm for **47**, 258 nm for **46** and 330 nm for triester **48**. The analyses employed an Agilent Cary 1 and 300 Bio-UV/Vis spectrophotometers, with a thermostabiliser to maintain the temperature at 25°C. The measurements of reaction rates were studied at 25 °C and ionic strength 1 M NaCl between pH = 3-10. Various buffer solutions (Formic acid, Acetic acid, MES, EPPS, CHES, CAPS) were using to keep the pHs of the solutions stabilised.

All the substrates (1-2 mM) were dissolved in acetonitrile as a stock solution. The reactions were initiated by adding 20 μ L of **46** and **47**, and 100 μ L of **48** to the suitable amount of 200 mM buffer solution to yield total volume 2.5 mL. This gives a 50 mM of the buffer, and 0.016 mM of triesters **46** and **47**, and (0.08 mM) of triester **48**. The k_{obs} was calculated from correlation between time and absorbance. All reactions were followed first order reactions.

7.27.2. The reaction of **46**, **47** and **48** with hydroxylamine

The reaction of **46**, **47** and **48** with the 0.5 M hydroxylamine was evaluated at different range pH 4-7. For pH 5 to 7, self-buffered solutions of hydroxylamine were used. Reactions were followed spectrophotometrically by monitoring signals of the triesters **46**, **47** and **48** at at 255 nm for **47**, 258 nm for **46** and 330 nm for triester **48** at 25 C° and ionic strength 1 M (NaCl) in aqueous solutions. Reactions were started by adding 20 μ L (triesters **46** and **47**) or 100 μ L (triesters **48**) of an acetonitrile stock solution to 2.5 mL of reaction mixture. This gives substrate concentration in the cuvette (0.016 mM) of **46** and **47** and (0.08 mM) of **48**. All observed first-order rate constants, k_{obs} , were calculated from correlation of absorbance against time.

7.27.3. The effect of hydroxylamine concentration on **46**, **47** and **48** degradation

For evaluate the effect of the concentration of hydroxylamine, different concentrations of $[\text{NH}_2\text{OH}]$ 0.01 -0.7 were used, and the reaction was investigated at pH 3-7 for triester **46** and pH 7 for triesters **47** and **48**. Reactions were followed spectrophotometrically by monitoring signals of the triesters **46**, **47** and **48** at an appropriate wavelength, at 25 °C and ionic strength 1 M (NaCl) in aqueous solutions. Second-order rate constants were calculated from plots of k_{obs} against $[\text{NH}_2\text{OH}]$.

7.27.4. The reaction of **46** with nucleophiles

The same procedure above was followed to evaluate the effect of fluoride, acetate and methoxyamine on the degradation of phosphate esters **46**. Different concentrations of the nucleophiles were used, and second-order rate constants were calculated from plots of k_{obs} against [nucleophile].

7.27.5. Product analysis for the hydrolysis of phosphate triesters **46**, **47**, **48** and **49** by ^{31}P NMR

The hydrolysis of **46**, **47**, **48** and **49** was followed in DMSO or D_2O at 25 °C, 1M ionic strength and pH 6 and 9 for triester **46**, pH 6 for triester **47** and pH 7 for triester **48** and **49**, using ^{31}P NMR. A solution of substrate (12 mg of triester 1 and 9, 8, and 2 mg for triester 7) in DMSO was added to the buffer solution in NMP tube to achieve 50 mM [buffer]. ^{31}P NMR experiments were performed on a 162 MHz spectrometer.

7.27.6. The effect of DMSO on the degradation of triesters **46**.

For evaluate the effect of DMSO on the hydrolysis of triester **46**, different concentrations of [DMSO] were used, and the reaction was investigated at pH 6. Reactions were followed spectrophotometrically by monitoring signals of the triester **46** at 258 nm, at 25 °C and ionic strength 1 M (NaCl) in aqueous solutions.

7.27.7. Product analysis for the hydrolysis of ethyl biphenyl cyclic phosphate by ^{31}P

NMR

The products of hydrolysis of cyclic phosphate **80** was analysed using ^{31}P NMR in D_2O at 25 °C, 1M ionic strength and pH 7.3. A solution of substrate (12 mg of triester **80**) in acetonitrile was added to the buffer solution in NMR tube to achieve 50 mM [buffer]. ^{31}P NMR experiments were performed on a 162 MHz spectrometer.

7.27.8. The reaction of diethyl 8-hydroxy-1-naphthyl phosphate **69 with hydroxylamine**

The reaction of **69** with the 0.5 M hydroxylamine was evaluated at different range pH 4-10. For pH 5 to 7, self-buffered solutions of hydroxylamine were used. Reactions were followed spectrophotometrically using an Agilent Cary 1 and 300 Bio-UV/Vis spectrophotometers, with a thermostabiliser to maintain the temperature at 60°C by monitoring signals of the triester at 343 nm and ionic strength 1 M (NaCl) in aqueous solutions. Reactions were started by adding 100 μL (2 mM) of an acetonitrile stock solution of the substrate to the reaction mixture to give total volume 2.5 ml. This yields substrate concentration in the cuvette 0.08 mM of **69**. All observed first-order rate constants, k_{obs} , were calculated from correlation of absorbance against time.

7.27.9. Effect of hydroxylamine concentrations on diethyl 8-hydroxy-1-naphthyl phosphate **69**

The effect of hydroxylamine concentration was evaluated using solutions prepared at concentrations between 0.1 and 1.0 M. The reactions were followed at 343 nm and monitored at pH 7.3, ionic strength 1 M (NaCl) and a constant temperature of 60°C. The reactions were initiated by adding 100 μL (2 mM) of an acetonitrile stock solution of the substrate to the reaction mixture to give total volume 2.5 ml. Second-order rate constants were calculated from plots of k_{obs} against $[\text{NH}_2\text{OH}]$.

7.27.10. The reaction of hydroxylamine with phosphate triesters 70, 71 and 72 using HPLC.

The degradations of triesters **70-71** and **82-84** were studied at different concentrations of hydroxylamine at 25 or 60 °C and pH 7.3 ± 0.1 . This allowed estimating the hydrolysis rate constants in absence of hydroxylamine, and evaluating the effect of hydroxylamine on the reactions. These reactions were monitored at appropriate wavelength of the substrates using 150 mm \times 4.60 mm column in a HP 1100 Series HPLC. The eluent system was 0.1% TFA in distilled water/0.1% TFA in acetonitrile as illustrated in Table (7-1). The substrates were dissolved in acetonitrile with concentrations (30 or 50 mM), and the injection volume 20 μ L. The total volume of the reaction mixture was 1.2 ml, yielding (0.5-4 mM) of the substrate.

Table (7-1): The Solvent system used in HPLC analysis to follow the hydrolysis of triesters studied here.

Time/min	0.1% TFA in CH ₃ CN %	0.1% TFA in D.W %	Flow rate mL/min
0	5	95	1
15	50	50	1
20	50	50	1
22	5	50	1
30	5	95	1

7.27.10.1. Hydrolysis of phosphate triesters 70-72.

Triesters **70-72** were dissolved in acetonitrile or DMSO with 50 mM concentration and added to the reaction mixture in water bath at 60 °C. Aliquots of the reaction mixtures were injected into HPLC by the automated sampler, and loaded into the column during a different time. The products were found to be the corresponding aryl diesters as a major product confirmed by mass spectrum, and corresponding phenol, as shown in Tables (6-2), (6-3) and (6-4).

Table (7-2): Structure and retention time of triester **71** and the corresponding products of hydrolysis.

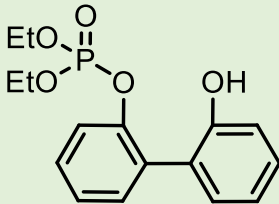
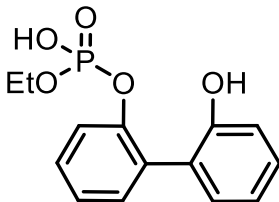
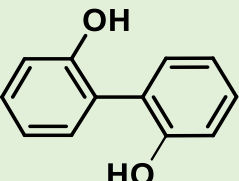
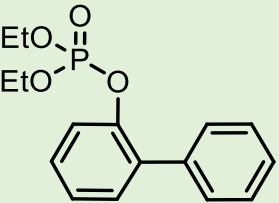
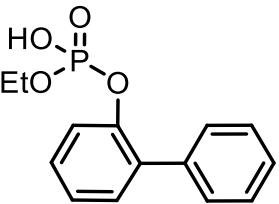
Compound	Structure	Retention time / min
Triester 71		19.1
Diester 78 (Main Product)		12.6
2, 2`-biphenyl-diol 73 (Second product)		21.1

Table (7-3): Structure and retention time of triester **72**, and the corresponding products of hydrolysis.

Compound	Structure	Retention time / min
Triester 72		19.1
Diester (Main Product)		19

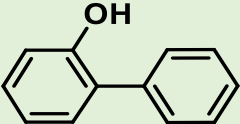
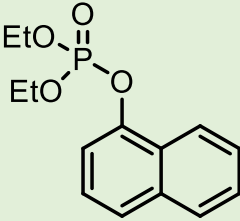
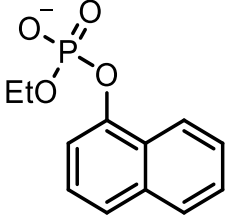
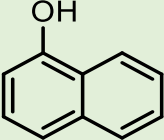
1-biphenol (Second product)		20
--	---	-----------

Table (7-4): Structure and retention time of triester **70**, and the corresponding products of hydrolysis.

Compound	Structure	Retention time / min
Triester 70		19.1
Diester (Main Product)		15
1-naphthol (Second product)		17.7

7.27.10.2. Hydrolysis of phosphate triesters **82-84**

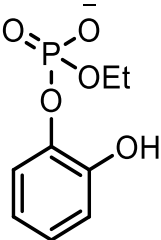
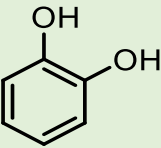
For triesters 1,2- and 1,3- dihydroxy phenyl diethyl phosphate **82** and **83**, and 1-hydroxy phenyl diethyl phosphate **84**. The reactions were studied at 25 °C and 1 M NaCl, and the samples were injected each 30 min. These esters were monitored at 270 nm for **82** and **83**, and at 275 for **84**, the wavelength of the substrates. The products of **82** and **83** were found to be diesters **93** and **94** and the pyrogallol, and the products of **84** were found to be diester **95** and catechol, Tables (6-5) and (6-6).

Table (7-5): Structure and retention time of triesters **82** and **83** and the corresponding products of hydrolysis.

Compound	Structure	Retention time / min
Triester 82 and 83		13.08 and 12.1
Diesters 93 and 94 (Main products)		6.2 and 7.5
Pyrogallol (Second product)		4.9

Table (7-6): Structure and retention time of triester **84** and the corresponding products of hydrolysis.

Compound	Structure	Retention time / min
Triester 84		15.03

<p>Diester 95 (Main Product)</p>		<p>8.03</p>
<p>Catechol (Second product)</p>		<p>8.4</p>

References

1. Pauling, L., Nature of Forces between Large Molecules of Biological Interest. *Nature* **1948**, *161* (4097), 707-709.
2. Pravda, L.; Svobodová Vařeková, R.; Sehnal, D.; Koča, J.; Berka, K.; Banáš, P.; Otyepka, M.; Laskowski, R. A., Anatomy of enzyme channels. *BMC Bioinformatics* **2014**, *15* (1).
3. Zhang, X.; Houk, K., Why enzymes are proficient catalysts: Beyond the Pauling paradigm. In *Accounts Chem. Res.*, 2005; Vol. 38, pp 379-385.
4. Lodish, H.; Berk, A.; Kaiser, C. A.; Krieger, M., *Molecular Cell Biology*. W. H. Freeman: 2007.
5. Arunan, E.; Desiraju, G.; Klein, R.; Sadlej, J.; Scheiner, S.; Alkorta, I.; Clary, D. C.; Crabtree, R. H.; Dannenberg, J.; Hobza, P.; Kjaergaard, H.; Legon, A.; Mennucci, B.; Nesbitt, D., Definition of the hydrogen bond (IUPAC Recommendations 2011). *Pure Appl. Chem.* **2011**, *83* (8), 1637-1641.
6. McAllister, M. A.; Chen, J.; Houk, J. K.; Lee, J. K., Short, Strong Hydrogen Bonds in the Gas Phase and in Solution: Theoretical Exploration of p K a Matching and Environmental Effects on the Strengths of Hydrogen Bonds and Their Potential Roles in Enzymatic Catalysis. *Journal of Organic Chemistry* **1998**, *63* (14), 4611-4619.
7. Anslyn, E. V.; Dougherty, D. A.; Dougherty, E. V.; Books, U. S., *Modern Physical Organic Chemistry*. University Science Books: 2006.
8. Cleland, W. W., Low-barrier hydrogen bonds and enzymatic catalysis. *Arch Biochem Biophys* **2000**, *382* (1), 1-5.
9. Cleland, W. W.; Kreevoy, M. M., Low-barrier hydrogen bonds and enzymic catalysis. *Science* **1994**, *264* (5167), 1887-90.
10. Cleland, M. M.; Kreevoy, M. M., Low- barrier hydrogen bonds and enzymic catalysis. *Science* **1994**, *264* (5167), 1887-1890.
11. Peter Guthrie, J., Short strong hydrogen bonds: can they explain enzymic catalysis? *Chemistry & Biology* **1996**, *3* (3), 163-170.
12. Gerlt, J. A.; Gassman, P. G., An Explanation for Rapid Enzyme-Catalyzed Proton Abstraction from Carbon Acids - Importance of Late Transition-States in Concerted Mechanisms. *Journal of the American Chemical Society* **1993**, *115* (24), 11552-11568.
13. Mock, W. L.; Chua, D. C. Y., Exceptional Active-Site H-Bonding in Enzymes - Significance of the Oxyanion Hole in the Serine Proteases from a Model Study. *Journal of the Chemical Society-Perkin Transactions 2* **1995**, (11), 2069-2074.
14. Schiott, B.; Iversen, B. B.; Larsen, F. K.; Bruice, T. C., On the Electronic Nature of Low- Barrier Hydrogen Bonds in Enzymatic Reactions. *Proceedings of the National Academy of Sciences of the United States of America* **1998**, *95* (22), 12799-12802.
15. Shan, S. O.; Herschlag, D., Energetic effects of multiple hydrogen bonds. Implications for enzymatic catalysis. *Journal of the American Chemical Society* **1996**, *118* (24), 5515-5518.
16. Tang, A. W.; Kong, X.; Terskikh, V.; Wu, G., Solid-State (17)O NMR of Unstable Acyl-Enzyme Intermediates: A Direct Probe of Hydrogen Bonding Interactions in the Oxyanion Hole of Serine Proteases. *J Phys Chem B* **2016**, *120* (43), 11142-11150.
17. Corey, D. R.; Craik, C. S., An Investigation into the Minimum Requirements for Peptide Hydrolysis by Mutation of the Catalytic Triad of Trypsin. *Journal of the American Chemical Society* **1992**, *114* (5), 1784-1790.
18. Carter, P.; Wells, J. A., Dissecting the catalytic triad of a serine protease. *Nature* **1988**, *332* (6164), 564-8.
19. Siau, W.-Y.; Wang, J., Asymmetric organocatalytic reactions by bifunctional amine-thioureas. *Catalysis Science & Technology* **2011**, *1* (8), 1298-1310.
20. Harris, T. K.; Abeygunawardana, C.; Mildvan, A. S., NMR studies of the role of hydrogen bonding in the mechanism of triosephosphate isomerase. *Biochemistry* **1997**, *36* (48), 14661-75.

21. Shokri, A.; Wang, Y.; Doherty, G. A.; Wang, X.-B.; Kass, S. R., Hydrogen- bond networks: strengths of different types of hydrogen bonds and an alternative to the low barrier hydrogen- bond proposal. *J. Am. Chem. Soc.* **2013**, *135* (47), 17919.
22. Samet, M.; Kass, S. R., Preorganized Hydrogen Bond Donor Catalysts: Acidities and Reactivities. *The Journal of organic chemistry* **2015**, *80* (15), 7727.
23. Dominelli-Whiteley, N.; Brown, J. J.; Muchowska, K. B.; Mati, I. K.; Adam, C.; Hubbard, T. A.; Elmi, A.; Brown, A. J.; Bell, I. A. W.; Cockroft, S. L., Strong Short-Range Cooperativity in Hydrogen-Bond Chains. *Angew Chem Int Ed Engl* **2017**, *56* (26), 7658-7662.
24. Tillett, J. G.; Wiggins, D. E., Neighbouring hydroxyl group catalysis in the hydrolysis of carbonate esters. *Tetrahedron Letters* **1971**, *12* (14), 911-914.
25. Hibbert, F.; Spiers, K. J., Kinetics of hydrolysis of 1-acetoxy-, 1-acetoxy-8-hydroxy-, and 1,8-diacetoxy-naphthalenes; intramolecular participation by a hydroxy group. *Journal of the Chemical Society, Perkin Transactions 2* **1988**, (4), 571.
26. Bromilow, R. H.; Kirby, A. J., Intramolecular general acid catalysis of phosphate monoester hydrolysis. The hydrolysis of salicyl phosphate. *Journal of the Chemical Society, Perkin Transactions 2* **1972**, (2), 149.
27. Hibbert, F.; Spiers, K. J., Intramolecular Catalysis of the Hydrolysis of an Acetal by an Internally Hydrogen-Bonded Hydroxy Group. *Journal of the Chemical Society-Perkin Transactions 2* **1989**, (4), 377-380.
28. Asaad, N.; Kirby, A. J., Concurrent nucleophilic and general acid catalysis of the hydrolysis of a phosphate triester. *Journal of the Chemical Society-Perkin Transactions 2* **2002**, (10), 1708-1712.
29. Bender, M. L.; Lawlor, J. M., Isotopic and kinetic studies of the mechanism of hydrolysis of salicyl phosphate. Intramolecular general acid catalysis. *Journal of the American Chemical Society* **1963**, *85* (19), 3010-3017.
30. Forconi, M.; Williams, N. H., Mimicking Metallophosphatases: Revealing a Role for an OH Group with No Libido. *Angewandte Chemie International Edition* **2002**, *41* (5), 849-852.
31. Khan, S. A.; Kirby, A. J.; Wakselman, M.; Horning, D. P.; Lawlor, J. M., Intramolecular catalysis of phosphate diester hydrolysis. Nucleophilic catalysis by the neighbouring carboxy-group of the hydrolysis of aryl 2-carboxyphenyl phosphates. *Journal of the Chemical Society B: Physical Organic* **1970**, (0), 1182-1187.
32. Abell, K. W. Y.; Kirby, A. J., Intramolecular General Acid Catalysis of Intramolecular Nucleophilic Catalysis of the Hydrolysis of a Phosphate Diester. *Journal of the Chemical Society-Perkin Transactions 2* **1983**, (8), 1171-1174.
33. Orth, E. S.; Brandao, T. A.; Souza, B. S.; Pliego, J. R.; Vaz, B. G.; Eberlin, M. N.; Kirby, A. J.; Nome, F., Intramolecular catalysis of phosphodiester hydrolysis by two imidazoles. *J Am Chem Soc* **2010**, *132* (24), 8513-23.
34. Gottlin, E. B.; Rudolph, A. E.; Zhao, Y.; Matthews, H. R.; Dixon, J. E., Catalytic mechanism of the phospholipase D superfamily proceeds via a covalent phosphohistidine intermediate. *Proc Natl Acad Sci U S A* **1998**, *95* (16), 9202-7.
35. Thompson, J. E.; Raines, R. T., Value of general Acid-base catalysis to ribonuclease a. *J Am Chem Soc* **1994**, *116* (12), 5467-8.
36. Orth, E. S.; Brandão, T. A. S.; Souza, B. S.; Pliego, J. R.; Vaz, B. G.; Eberlin, M. N.; Kirby, A. J.; Nome, F., Intramolecular catalysis of phosphodiester hydrolysis by two imidazoles. *Journal of the American Chemical Society* **2010**, *132* (24), 8513.
37. Rogers, G. A.; Bruice, T. C., Control of Modes of Intramolecular Imidazole Catalysis of Ester Hydrolysis by Steric and Electronic Effects. *Journal of the American Chemical Society* **1974**, *96* (8), 2463-2472.
38. Orth, E. S.; Brandão, T. A. S.; Milagre, H. M. S.; Eberlin, M. N.; Nome, F., Intramolecular acid-base catalysis of a phosphate diester: modeling the ribonuclease mechanism. *Journal of the American Chemical Society* **2008**, *130* (8), 2436.
39. Kirby, A. J.; Dutta-Roy, N.; Da Silva, D.; Goodman, J. M.; Lima, M. F.; Roussev, C. D.; Nome, F., Intramolecular general acid catalysis of phosphate transfer. nucleophilic attack by oxyanions on the PO₃ 2- group. *Journal of the American Chemical Society* **2005**, *127* (19), 7033-7040.

40. Kirby, A. J.; Rousev, C. D.; Lima, M. F.; Da Silva, D.; Nome, F., Efficient intramolecular general acid catalysis of nucleophilic attack on a phosphodiester. *Journal of the American Chemical Society* **2006**, *128* (51), 16944-16952.
41. Tossell, K. J. Catalysis of phosphate ester hydrolysis through hydrogen bonding. PhD Thesis, University of Sheffield, 2012.
42. Kirby, A. J.; Tondo, D. W.; Medeiros, M.; Souza, B. S.; Priebe, J. P.; Lima, M. F.; Nome, F., Efficient intramolecular general-acid catalysis of the reactions of alpha-effect nucleophiles and ammonia oxide with a phosphate triester. *J Am Chem Soc* **2009**, *131* (5), 2023-8.
43. Medeiros, M.; Wanderlind, E. H.; Mora, J. R.; Moreira, R.; Kirby, A. J.; Nome, F., Major mechanistic differences between the reactions of hydroxylamine with phosphate di- and tri-esters. *Org Biomol Chem* **2013**, *11* (37), 6272-84.
44. Lima, M.; da Cruz, P. A. U.; Fernandes, M.; Polaquini, C.; Miguel, E.; Pliego, J. R.; Scorsin, L.; Oliveira, B. S.; Nome, F., Cleaving paraoxon with hydroxylamine: Ammonium oxide isomer favors a Frontside attack mechanism. *Journal of Physical Organic Chemistry* **2019**, *32* (1).
45. Jencks, W. P., *Catalysis in chemistry and enzymology*. New York : Dover, 1987: New York, 1987.
46. Fernández, M. I.; Canle, M.; García, M. V.; Santaballa, J. A., A theoretical analysis of the acid–base equilibria of hydroxylamine in aqueous solution. *Chemical Physics Letters* **2010**, *490* (4), 159-164.
47. Kirby, A. J.; Souza, B. S.; Medeiros, M.; Priebe, J. P.; Manfredi, A. M.; Nome, F., Hydroxylamine as an oxygen nucleophile. Chemical evidence from its reaction with a phosphate triester. *Chemical Communications* **2008**, (37), 4428-4429.
48. Medeiros, M.; Souza, B. S.; Orth, E. S.; Brandao, T. A. S.; Rocha, W.; Kirby, A. J.; Nome, F., The reaction of hydroxylamine with aspirin. *Arkivoc* **2011**, *2011*, 461-476.
49. Kamerlin, S. C. L.; Sharma, P.; Prasad, R.; Warshel, A., Why nature really chose phosphate. *Quarterly reviews of biophysics (Print)* **2013**, *46* (1), 1-132.
50. Wolfenden, R.; Ridgway, C.; Young, G., Spontaneous hydrolysis of ionized phosphate monoesters and diesters and the proficiencies of phosphatases and phosphodiesterases as catalysts. *Journal of the American Chemical Society* **1998**, *120* (4), 833-834.
51. Barton, D.; Nakanishi, K.; Meth-Cohn, O., *Comprehensive Natural Products Chemistry: Enzymes, enzyme mechanisms, proteins, and aspects of NO chemistry*. Elsevier: 1999.
52. Munro, N., Toxicity of the organophosphate chemical warfare agents GA, GB, and VX: implications for public protection. *Environ Health Perspect* **1994**, *102* (1), 18-38.
53. Zheng, F.; Zhan, C.-G.; Ornstein, R. L., Theoretical studies of reaction pathways and energy barriers for alkaline hydrolysis of phosphotriesterase substrates paraoxon and related toxic phosphofluoridate nerve agents. *Journal of the Chemical Society, Perkin Transactions 2* **2001**, (12), 2355-2363.
54. Ghanem, E.; Raushel, F. M., Detoxification of organophosphate nerve agents by bacterial phosphotriesterase. *Toxicology and Applied Pharmacology* **2005**, *207* (2, Supplement), 459-470.
55. Katz, M. J.; Moon, S. Y.; Mondloch, J. E.; Beyzavi, M. H.; Stephenson, C. J.; Hupp, J. T.; Farha, O. K., Exploiting parameter space in MOFs: a 20-fold enhancement of phosphate-ester hydrolysis with UiO-66-NH₂. *Chem Sci* **2015**, *6* (4), 2286-2291.
56. Bigley, A. N.; Xiang, D. F.; Narindoshvili, T.; Burgert, C. W.; Hengge, A. C.; Raushel, F. M., Transition State Analysis of the Reaction Catalyzed by the Phosphotriesterase from *Sphingobium* sp. TCM1. *Biochemistry* **2019**, *58* (9), 1246-1259.
57. Wladkowski, B. D.; Ostazeski, P.; Chenoweth, S.; Broadwater, S. J.; Krauss, M., Hydrolysis of cyclic phosphates by ribonuclease A: a computational study using a simplified ab initio quantum model. *Journal of computational chemistry* **2003**, *24* (14), 1803-11.
58. Haake, P. C.; Westheimer, F. H., Hydrolysis and Exchange in Esters of Phosphoric Acid^{1a,b}. *Journal of the American Chemical Society* **1961**, *83* (5), 1102-1109.
59. Huttunen, K. M.; Mahonen, N.; Leppanen, J.; Vepsalainen, J.; Juvonen, R. O.; Raunio, H.; Kumpulainen, H.; Jarvinen, T.; Rautio, J., Novel cyclic phosphate prodrug approach for cytochrome P450-activated drugs containing an alcohol functionality. *Pharm Res* **2007**, *24* (4), 679-87.

60. Eto, M.; Oshima, Y., Syntheses and Degradation of Cyclic Phosphorus Esters Derived from Saligenin and Its Analogues. *Agricultural and Biological Chemistry* **1962**, *26* (7), 452-&.
61. Moss, R. A.; McKernan, B. A., Comparative nucleophilic reactivities in phosphodiester cleavage. *Tetrahedron Letters* **2002**, *43* (23), 4179-4182.
62. Moss, R. A.; Bose, S.; Ragunathan, K. G.; Jayasuriya, N.; Emge, T. J., An exceptionally reactive phosphotriester. *Tetrahedron Letters* **1998**, *39* (5-6), 347-350.
63. Kirby, A. J.; Dutta-Roy, N.; da Silva, D.; Goodman, J. M.; Lima, M. F.; Roussev, C. D.; Nome, F., Intramolecular general acid catalysis of phosphate transfer. nucleophilic attack by oxyanions on the PO₃²⁻ group. *J Am Chem Soc* **2005**, *127* (19), 7033-40.
64. Jencks, W. P., Requirements for General Acid-Base Catalysis of Complex Reactions. *Journal of the American Chemical Society* **1972**, *94* (13), 4731-&.
65. Ramasarma, T.; Rao, A. V. S.; Devi, M. M.; Omkumar, R. V.; Bhagyashree, K. S.; Bhat, S. V., New insights of superoxide dismutase inhibition of pyrogallol autoxidation. *Molecular and Cellular Biochemistry* **2015**, *400* (1), 277-285.
66. Wu, L.; Chladkova, B.; Lechtenfeld, O. J.; Lian, S.; Schindelka, J.; Herrmann, H.; Richnow, H. H., Characterizing chemical transformation of organophosphorus compounds by (13)C and (2)H stable isotope analysis. *Sci Total Environ* **2018**, *615*, 20-28.
67. Williams, N. H.; Williams, I. H., Advances in Physical Organic Chemistry Preface. *Adv Phys Org Chem* **2016**, *50*, ix-x.
68. McCann, G. M.; McDonnell, C. M.; Magris, L.; More O'Ferrall, R. A., Enol-keto tautomerism of 9-anthrol and hydrolysis of its methyl ether. *Journal of the Chemical Society, Perkin Transactions 2* **2002**, (4), 784-795.
69. Kageyama, T.; Koizumi, Y.; Igarashi, T.; Sakurai, T., 1-(Arylmethoxy) anthracenes: how substituents affect their photoreactivity and ability to initiate radical and cationic polymerizations. *Polymer Journal* **2012**, *44* (10), 1022-1029.
70. Machovina, M. M.; Ellis, E. S.; Carney, T. J.; Brushett, F. R.; DuBois, J. L., How a cofactor-free protein environment lowers the barrier to O₂ reactivity. *J Biol Chem* **2019**, *294* (10), 3661-3669.
71. Sellmer, A.; Terpetschnig, E.; Wiegrebe, W.; Wolfbeis, O. S., UV/Vis and fluorescence study on anthralin and its alkylated derivatives. *Journal of Photochemistry and Photobiology A: Chemistry* **1998**, *116* (1), 39-45.
72. Serjeant, E. P.; Dempsey, B., *Ionisation constants of organic acids in aqueous solution*, **IUPAC Chemical Data Series No. 23**. Pergamon, Oxford, 1979.
73. Rotkiewicz, K.; Grabowski, Z. R., Excited states of aminoanthracenes. An experimental approach to electron density distribution. *Transactions of the Faraday Society* **1969**, *65* (0), 3263-3278.
74. Shan, S.-o.; Herschlag, D., Energetic Effects of Multiple Hydrogen Bonds. Implications for Enzymatic Catalysis. *Journal of the American Chemical Society* **1996**, *118* (24), 5515-5518.
75. Shokri, A.; Wang, Y.; O'Doherty, G. A.; Wang, X. B.; Kass, S. R., Hydrogen-bond networks: strengths of different types of hydrogen bonds and an alternative to the low barrier hydrogen-bond proposal. *J Am Chem Soc* **2013**, *135* (47), 17919-24.
76. Leupold, I.; Musso, H., Über Wasserstoffbrücken, XI1). Einfluß von Substituenten auf die Acidität von 2.2'-Dihydroxybiphenylen. *Justus Liebigs Annalen der Chemie* **1971**, *746* (1), 134-148.
77. Gelsema, W. J.; de Ligny, C. L.; Visserman, M. G. F., Mesures de pH dans des Mélanges Eau-éthanol. *Recueil des Travaux Chimiques des Pays-Bas* **1965**, *84* (9), 1129-1154.
78. Perreault, D. M.; Anslyn, E. V., Unifying the Current Data on the Mechanism of Cleavage-Transesterification of RNA. *Angewandte Chemie International Edition in English* **1997**, *36* (5), 432-450.
79. Williams, N. H.; Cheung, W.; Chin, J., Reactivity of Phosphate Diesters Doubly Coordinated to a Dinuclear Cobalt(III) Complex: Dependence of the Reactivity on the Basicity of the Leaving Group. *Journal of the American Chemical Society* **1998**, *120* (32), 8079-8087.
80. Forconi, M.; Williams, N. H., Mimicking Metallophosphatases: Revealing a Role for an OH Group with No Libido We thank the Royal Society and Nuffield foundation for financial support, and the BBSRC for a studentship (M.F.). *Angewandte Chemie International Edition* **2002**, *41* (5), 849.

81. Kirby, A. J.; Medeiros, M.; Oliveira, P. S.; Orth, E. S.; Brandao, T. A.; Wanderlind, E. H.; Amer, A.; Williams, N. H.; Nome, F., Activating water: important effects of non-leaving groups on the hydrolysis of phosphate triesters. *Chemistry* **2011**, *17* (52), 14996-5004.
82. Kirby, A. J.; Medeiros, M.; Oliveira, P. S. M.; Brandão, T. A. S.; Nome, F., Activating Water: Efficient Intramolecular General Base Catalysis of the Hydrolysis of a Phosphate Triester. *Chemistry – A European Journal* **2009**, *15* (34), 8475-8479.
83. Khan, S. A.; Kirby, A. J., The reactivity of phosphate esters. Multiple structure–reactivity correlations for the reactions of triesters with nucleophiles. *J. Chem. Soc. B* **1970**, *0* (0), 1172-1182.
84. Lima, M.; Da Cruz, P. A. U.; Fernandes, M.; Polaquini, C.; Miguel, E.; Pliego, Jr.; Scorsin, L.; Oliveira, B. S.; Nome, F., Cleaving paraoxon with hydroxylamine: Ammonium oxide isomer favors a Frontside attack mechanism. *J. Phys. Org. Chem.* **2019**, *32* (1).
85. Serrano, L.; Kellis, J. T., Jr.; Cann, P.; Matouschek, A.; Fersht, A. R., The folding of an enzyme. II. Substructure of barnase and the contribution of different interactions to protein stability. *J Mol Biol* **1992**, *224* (3), 783-804.
86. Oakenfull, D. G.; Richardson, D. I., Jr.; Usher, D. A., Models of ribonuclease action. I. General species catalysis in the hydrolysis of a nucleotide diester analog. *J Am Chem Soc* **1967**, *89* (21), 5491-2.
87. Kosonen, M.; Oivanen, M.; Lonnberg, H., Hydrolysis and Interconversion of the Dimethyl Esters of 5'-O-Methyluridine 2'-Monophosphates and 3'-Monophosphates - Kinetics and Mechanism. *Journal of Organic Chemistry* **1994**, *59* (13), 3704-3708.
88. Kosonen, M.; Lönnberg, H., General and specific acid/base catalysis of the hydrolysis and interconversion of ribonucleoside 2'- and 3'-phosphotriesters: kinetics and mechanisms of the reactions of 5'-O-pivaloyluridine 2'- and 3'-dimethylphosphates. *J. Chem. Soc., Perkin Trans. 2* **1995**, (6), 1203-1209.
89. Kosonen, M.; Hakala, K.; Lönnberg, H., Hydrolysis and intramolecular transesterification of ribonucleoside 3'-phosphotriesters: the effect of alkyl groups on the general and specific acid–base-catalyzed reactions of 5'-O-pivaloyluridin-3'-yl dialkyl phosphates. *Journal of the Chemical Society, Perkin Transactions 2* **1998**, (3), 663-670.
90. Bromilow, R. H.; Khan, S. A.; Kirby, A. J., Intramolecular catalysis of phosphate triester hydrolysis. Nucleophilic catalysis by the neighbouring carboxyl group of the hydrolysis of dialkyl 2-carboxyphenyl phosphates. *Journal of the Chemical Society B: Physical Organic* **1971**, (0), 1091.
91. Kirby, A.; Manfredi, A.; Silveira de Souza, B.; Medeiros, M.; Priebe, J.; Brandão, T.; Nome, F., Reactions of alpha-nucleophiles with a model phosphate diester. *ARKIVOC: archive for organic chemistry* **2009**, *2009*.
92. Roussev, C. D.; Ivanova, G. D.; Bratovanova, E. K.; Vassilev, N. G.; Petkov, D. D., External transesterification of ribonucleotide esters naturally catalyzed by large ribozymes. *Journal of the American Chemical Society* **1999**, *121* (49), 11267-11272.
93. Musso, H.; Matthies, H.-G., Über Wasserstoffbrücken, IV: Acidität und Wasserstoffbrücken bei Hydroxy-biphenylen und Hydroxy-biphenylchinonen. *Chemische Berichte* **1961**, *94* (2), 356-368.
94. Jonsson, M.; Lind, J.; Merényi, G., Redox and Acidity Properties of 2,2'- and 4,4'-Biphenol and the Corresponding Phenoxyl Radicals. *The Journal of Physical Chemistry A* **2002**, *106* (18), 4758-4762.
95. Shokri, A.; Abedin, A.; Fattahi, A.; Kass, S. R., Effect of hydrogen bonds on pKa values: importance of networking. *J Am Chem Soc* **2012**, *134* (25), 10646-50.
96. Kaiser, E. T.; Kudo, K., Alkaline hydrolysis of aromatic esters of phosphoric acid. *Journal of the American Chemical Society* **1967**, *89* (25), 6725-6728.
97. Chowdhury, J. A.; Moriguchi, T.; Shinozuka, K., Pseudo-Dumbbell-Type Molecular Beacon Probes Bearing Modified Deoxyuridine Derivatives and a Silylated Pyrene as a Fluorophore. *Bull. Chem. Soc. Jpn.* **2015**, *88* (3), 496-502.
98. Staab, H. A.; Kirsch, P.; Zipplies, M. F.; Weinges, A.; Krieger, C., [3.3]Isoalloxazinophanes and Arene-Bridged Bis(Isoalloxazines) - Syntheses, Characterizations and Properties Related to Intramolecular Interactions. *Chemische Berichte* **1994**, *127* (9), 1653-1665.

99. Loh, C. C. J.; Fang, X.; Peters, B.; Lautens, M., Benzylic Functionalization of Anthrones via the Asymmetric Ring Opening of Oxabicycles Utilizing a Fourth-Generation Rhodium Catalytic System. *Chemistry – A European Journal* **2015**, *21* (40), 13883-13887.
100. Huang, H. S.; Chiu, H. F.; Lu, W. C.; Yuan, C. L., Synthesis and antitumor activity of 1,8-diaminoanthraquinone derivatives. *Chem Pharm Bull (Tokyo)* **2005**, *53* (9), 1136-9.
101. Dahan, A.; Ashkenazi, T.; Kuznetsov, V.; Makievski, S.; Drug, E.; Fadeev, L.; Bramson, M.; Schokoroy, S.; Rozenshine-Kemelmakher, E.; Gozin, M., Synthesis and Evaluation of a Pseudocyclic Trithiourea-Based Anion Host. *The Journal of Organic Chemistry* **2007**, *72* (7), 2289-2296.
102. Muller, K.; Gurster, D.; Piwek, S.; Wiegrebe, W., Antipsoriatic Anthrones with Modulated Redox Properties .1. Novel 10-Substituted 1,8-Dihydroxy-9(10h)-Anthracenones as Inhibitors of 5-Lipoxygenase. *Journal of Medicinal Chemistry* **1993**, *36* (25), 4099-4107.
103. Muller, K.; Wiegrebe, W.; Younes, M., Formation of active oxygen species by dithranol, III. Dithranol, active oxygen species and lipid peroxidation in vivo. *Arch Pharm (Weinheim)* **1987**, *320* (1), 59-66.
104. Shroot, B.; Lang, G.; Maignan, J.; Restle, S.; Hensby, C.; Colin, M., 10-aryl-1,8-dihydroxy-9-anthrones and their esters, process for preparing same, and use of same in human and veterinary medicine and in cosmetics. Google Patents: 1989.
105. Restle, S. M., J.; Lang, G.; Shroot, B, 10-Aryl-1,8-dihydroxyanthrones and their esters, the process for preparation thereof and pharmaceutical and cosmetic compositions containing them. *Google Patents* **1986**.
106. Müller, K. G., I; Wiegrebe, W, Acidity and Stability of 10-Substituted 1,8-Dihydroxy-9(10H)-anthracenones. *Arch. Pharm. (Weinheim)* **1995**, *328* (4), 359–362.
107. De Barry Barnett, E.; Wilt-shire, J. L., Über ms - Alkyl- anthracene und „ Transanellar-tautomerie“ □ (X- Mitteil. *Berichte der deutschen chemischen Gesellschaft (A and B Series)* **1930**, *63* (5), 1114-1123.
108. Ashnagar, A.; Bruce, J. M., Multi-bromination of 1,8-dihydroxy-9- anthrone, important intermediates in the synthesis of antipsoriatic drugs. *International Journal of ChemTech Research* **2011**, *3* (1), 1-10.
109. Liang, D. W. M.; Du, C. J., Potent antipsoriatic agents: A facile preparation of acylated derivatives from dithranol in a mild basic reaction. *Journal of the Chinese Chemical Society* **2004**, *51* (1), 115-118.
110. Van Duuren, B. L.; Segal, A.; Tseng, S. S.; Rusch, G. M.; Loewengart, G.; Mate, U.; Roth, D.; Smith, A.; Melchionne, S.; Seidman, I., Structure and tumor-promoting activity of analogs of anthralin (1,8-dihydroxy-9-anthrone). *Journal of Medicinal Chemistry* **1978**, *21* (1), 26-31.
111. Samet, M.; Kass, S. R., Preorganized Hydrogen Bond Donor Catalysts: Acidities and Reactivities. *J Org Chem* **2015**, *80* (15), 7727-7731.
112. Loh, C. C.; Fang, X.; Peters, B.; Lautens, M., Benzylic Functionalization of Anthrones via the Asymmetric Ring Opening of Oxabicycles Utilizing a Fourth-Generation Rhodium Catalytic System. *Chemistry* **2015**, *21* (40), 13883-7.
113. Kirby, A. J.; Percy, J. M., Synthesis of 8-Substituted 1-Naphthylamine Derivatives - Exceptional Reactivity of the Substituents. *Tetrahedron* **1988**, *44* (22), 6903-6910.
114. Alam, A.; Tsuboi, S., Total synthesis of 3,3',4'-tri-O-methylellagic acid from gallic acid. *Tetrahedron* **2007**, *63* (42), 10454-10465.
115. Cacciarini, M.; Cordiano, E.; Nativi, C.; Roelens, S., A tricatecholic receptor for carbohydrate recognition: synthesis and binding studies. *J Org Chem* **2007**, *72* (10), 3933-6.
116. Niedziałkowski, P.; Czaczyk, E.; Jarosz, J.; Wcisło, A.; Białobrzaska, W.; Wietrzyk, J.; Ossowski, T., Synthesis and electrochemical, spectral, and biological evaluation of novel 9,10-anthraquinone derivatives containing piperidine unit as potent antiproliferative agents. *Journal of Molecular Structure* **2019**, *1175*, 488-495.
117. Dahan, A.; Ashkenazi, T.; Kuznetsov, V.; Makievski, S.; Drug, E.; Fadeev, L.; Bramson, M.; Schokoroy, S.; Rozenshine-Kemelmakher, E.; Gozin, M., Synthesis and evaluation of a pseudocyclic trithiourea-based anion host. *J Org Chem* **2007**, *72* (7), 2289-96.

118. de Barry Barnett, E.; Wiltshire, J. L., Überms-Alkyl-anthracene und „Transanellar-tautomerie“ □ (X-Mittel.). *Berichte der deutschen chemischen Gesellschaft (A and B Series)* **1930**, 63 (5), 1114-1123.

Appendix: Chapter Two

Table (A-1): First-order rate constants for buffer catalysis of the hydrolysis of triester **46**, at 25 °C and ionic strength 1.0 M.

$k_{\text{obs}} / \text{s}^{-1}$					
[Buffer] / M	pH 3	pH 4	pH 5	pH 6	pH 7
50	1.13×10^{-3}	1.01×10^{-3}	1.3×10^{-3}	1.0×10^{-3}	1.41×10^{-3}
70					1.56×10^{-3}
100	1.31×10^{-3}	1.19×10^{-3}	1.68×10^{-3}	1.18×10^{-3}	1.84×10^{-3}
130					2.03×10^{-3}
140	1.50×10^{-3}	1.38×10^{-3}	2.04×10^{-3}	1.30×10^{-3}	
160				1.33×10^{-3}	2.25×10^{-3}
170	1.55×10^{-3}	1.5×10^{-3}	2.2×10^{-3}		
190	1.714×10^{-3}	1.52×10^{-3}	2.51×10^{-3}	1.43×10^{-3}	2.51×10^{-3}

Table (A-2): First-order rate constants for hydrolysis of triester **46**, at 25 °C and ionic strength 1.0 M.

pH	$k_{\text{obs}} / \text{s}^{-1}$	$\log k_{\text{obs}} / \text{s}^{-1}$
3.0	8.14×10^{-4}	-3.0893
4.0	7.29×10^{-4}	-3.1374
5.0	7.73×10^{-4}	-3.1120
6.1	7.73×10^{-4}	-3.1118
7.1	9.32×10^{-4}	-3.0306
9.8	1.017×10^{-3}	-2.9928

Table (A-3): First-order rate constants for the effect of DMSO on the hydrolysis of triester **46**, at pH 6, 25 °C and ionic strength 1.0 M

DMSO volume μL	Volume (DMSO) /volume (mixture) % (v/v)%	$k_{\text{obs}} / \text{s}^{-1}$
200	8	4.48×10^{-4}
300	12	5.35×10^{-4}
400	16	7.52×10^{-4}
600	24	8.39×10^{-4}
1030	41.2	9.36×10^{-4}
1230	49.2	9.61×10^{-4}

Table (A-4): First-order rate constants for hydrolysis of triester **47**, at 25 °C and ionic strength 1.0 M.

pH	$k_{\text{obs}} / \text{s}^{-1}$	$\log k_{\text{obs}} / \text{s}^{-1}$
4.01	2.26×10^{-5}	-4.6462
5.0	2.26×10^{-5}	-4.6448
6.0	2.29×10^{-5}	-4.6394
6.85	2.75×10^{-5}	-4.5601
7.97	4.21×10^{-5}	-4.3753
8.84	1.51×10^{-4}	-3.8223
9.8	4.37×10^{-4}	-3.3592

Table (A-5): First-order rate constants for hydrolysis of triester **48**, at 25 °C and ionic strength 1.0 M.

pH	$k_{\text{obs}} / \text{s}^{-1}$	$\log k_{\text{obs}} / \text{s}^{-1}$
3.0	9.18×10^{-6}	-5.037
4.0	1.05×10^{-5}	-4.979
5.0	8.92×10^{-6}	-5.0496
6.1	1.01×10^{-5}	-4.9958
7.1	1.81×10^{-5}	-4.7434
8.2	2.14×10^{-5}	-4.6702
8.9	1.18×10^{-4}	-3.9287
9.8	4.54×10^{-4}	-3.3432

Table (A-6): First-order rate constants for the reaction of triester **46** with hydroxylamine, at 25 °C and ionic strength 1.0 M.

pH	$k_{\text{obs}} / \text{s}^{-1}$	$\log k_{\text{obs}} / \text{s}^{-1}$
3.03	1.07×10^{-3}	-2.9705
4.01	1.18×10^{-3}	-2.9291
4.6	1.32×10^{-3}	-2.8797
5.0	1.98×10^{-3}	-2.7033
5.34	3.55×10^{-3}	-2.4497
5.8	7.59×10^{-3}	-2.1197
6.35	2.32×10^{-2}	-1.6337
6.67	2.95×10^{-2}	-1.5297
7.1	7.95×10^{-2}	-1.0997

Table (A-7): First-order rate constants for the reaction of triester **47** with hydroxylamine, at 25 °C and ionic strength 1.0 M.

pH	$k_{\text{obs}} / \text{s}^{-1}$	$\log k_{\text{obs}} / \text{s}^{-1}$
3.98	2.26×10^{-5}	-4.6462
4.8	8.1×10^{-5}	-4.0917
6.08	6.99×10^{-4}	-3.1553
6.7	1.49×10^{-3}	-2.8253
7.73	2.51×10^{-3}	-2.6011
8.18	2.59×10^{-3}	-2.5855
9.0	2.63×10^{-3}	-2.5803
9.75	2.78×10^{-3}	-2.5553

Table (A-8): First-order rate constants for the reaction of triester **48** with hydroxylamine, at 25 °C and ionic strength 1.0 M.

pH	$k_{\text{obs}} / \text{s}^{-1}$	$\log k_{\text{obs}} / \text{s}^{-1}$
3.03	9.18333E-06	-5.0370
3.89	1.05×10^{-5}	-4.9790
5.1	8.56×10^{-5}	-4.0676
6.01	2.79×10^{-4}	-3.5538
7.03	4.67×10^{-4}	-3.3301
8.13	8.39×10^{-4}	-3.0761
8.71	7.65×10^{-4}	-3.1163
8.84	7.6×10^{-4}	-3.1191
9.81	9.84×10^{-4}	-3.0070

Table (A-9): First-order rate constants for the reaction of triester **46** with vary concentration of hydroxylamine, at 25 °C and ionic strength 1.0 M.

$k_{\text{obs}} / \text{s}^{-1}$					
[NH ₂ OH]/M	pH 3	pH 4	pH 5	pH 6	pH 7
0.02	-	-	-	1.08×10^{-3}	1.40×10^{-3}
0.04	-	-	-	1.51×10^{-3}	3.16×10^{-3}
0.06	-	-	-	1.94×10^{-3}	4.10×10^{-3}
0.08	-	-	1.11×10^{-3}	2.67×10^{-3}	5.35×10^{-3}
0.1	1.09×10^{-3}	1.1×10^{-3}	1.16×10^{-3}	3.04×10^{-3}	7.26×10^{-3}
0.3	1.09×10^{-3}	1.25×10^{-3}	1.59×10^{-3}	1.02×10^{-2}	3.47×10^{-2}
0.5	1.2×10^{-3}	1.32×10^{-3}	2.22×10^{-3}	2.34×10^{-2}	8.08×10^{-2}
0.7	1.21×10^{-3}	1.43×10^{-3}	3.01×10^{-3}	4.27×10^{-2}	1.16×10^{-1}

Table (A-10): First-order rate constants for the reaction of triester **47** with vary concentration of hydroxylamine, at 25 °C and ionic strength 1.0 M at pH 7.

[NH ₂ OH] / M	$k_{\text{obs}} / \text{s}^{-1}$
0	2.78×10^{-5}
0.05	1.19×10^{-4}
0.1	2.1×10^{-4}
0.3	6.99×10^{-4}
0.5	1.5×10^{-3}
0.6	2.17×10^{-3}
0.7	2.8×10^{-3}

Table (A-11): First-order rate constants for the reaction of triester **48** with vary concentration of hydroxylamine, at 25 °C and ionic strength 1.0 M at pH 7.

[NH ₂ OH] / M	$k_{\text{obs}} / \text{s}^{-1}$
0	1.81×10^{-5}
0.05	4.68×10^{-5}
0.1	8.13×10^{-5}
0.12	9.57×10^{-5}
0.15	1.13×10^{-4}
0.17	1.25×10^{-4}
0.3	2.16×10^{-4}
0.5	4.32×10^{-4}
0.7	6.47×10^{-4}
0.9	8.92×10^{-4}

Table (A-12): First-order rate constants for the reaction of triester **46** with nucleophiles, at 25 °C and ionic strength 1.0 M at pH 6.

$k_{\text{obs}} / \text{s}^{-1}$			
[Nucleophile] / M	F ⁻	Acetate	MeONH ₂
0	7.73×10^{-4}	7.73×10^{-4}	7.73×10^{-4}
0.02	1.07×10^{-3}	9.81×10^{-4}	7.99×10^{-4}
0.04	1.25×10^{-3}	1.16×10^{-3}	8.26×10^{-4}
0.06	1.51×10^{-3}	1.38×10^{-3}	8.69×10^{-4}
0.08	1.69×10^{-3}	1.60×10^{-3}	8.88×10^{-4}
0.1	1.96×10^{-3}	1.82×10^{-3}	8.89×10^{-4}

Table (A-13): First order rate constants for the reaction of triester **46** with nucleophiles, at 25 °C and ionic strength 1.0 M at pH 6.

Nucleophile	pK_a	$k_2 \text{ M}^{-1} \text{ s}^{-1}$	$\log k_2 \text{ M}^{-1} \text{ s}^{-1}$
MeONH ₂	4.6	$1.3 \pm 0.1 \times 10^{-3}$	-2.8477
F ⁻	3.1	$1.16 \pm 0.03 \times 10^{-2}$	-1.8861
Acetate	4.81	$1.05 \pm 0.02 \times 10^{-2}$	-1.9318
NH ₂ OH	6.1	$1.7 \pm 0.4 \times 10^{-2}$	-1.7000

Appendix: Chapter Three

Table (B-1): First-order rate constants for the hydrolysis of triester **69** at 60 °C and ionic strength 1.0 M.

pH	$k_{\text{obs}} / \text{s}^{-1}$	$\log k_{\text{obs}} / \text{s}^{-1}$
5	3.98×10^{-4}	-3.4
6.1	1.09×10^{-3}	-2.96
6.6	2.09×10^{-3}	-2.68
7.5	2.48×10^{-3}	-2.60
7.9	2.2×10^{-3}	-2.65
8.97	2.88×10^{-3}	-2.54
9.7	3.23×10^{-3}	-2.49

Table (B-2): First-order rate constants for the reaction of triester **69**, **70** and **71** with vary concentrations of hydroxylamine, at pH 7.3, 60 °C and ionic strength 1.0 M.

	Triester 69	Triester 70	Triester 71
$[\text{NH}_2\text{OH}] / \text{M}$	$k_{\text{obs}} / \text{s}^{-1}$	$k_{\text{obs}} / \text{s}^{-1}$	$k_{\text{obs}} / \text{s}^{-1}$
0.1	5.5×10^{-4}	5.1×10^{-6}	5.31×10^{-6}
0.2	9×10^{-4}	-	-
0.3	1.27×10^{-3}	6.2×10^{-6}	6.7×10^{-6}
0.4	1.65×10^{-3}	8.07×10^{-6}	8.4×10^{-6}
0.5	2.2×10^{-3}	9.7×10^{-6}	9.9×10^{-6}

Appendix: Chapter Four

Table (C-1): First-order rate constants for the hydrolysis of triester **82** and **83** at pH 7.3, 25 °C and ionic strength 1.0 M.

	Triester 82		Triester 83	
pH	$k_{\text{obs}} / \text{s}^{-1}$	$\log k_{\text{obs}} / \text{s}^{-1}$	$k_{\text{obs}} / \text{s}^{-1}$	$\log k_{\text{obs}} / \text{s}^{-1}$
5	7.54×10^{-6}	-5.1226	7.5×10^{-6}	-5.1249
6.22	2.40×10^{-5}	-4.6189	2.42×10^{-5}	-4.6158
7.2	4.06×10^{-5}	-4.3915	4.17×10^{-5}	-4.3799
8	6.54×10^{-5}	-4.1844	6.88×10^{-5}	-4.1624
8.7	9.41×10^{-5}	-4.0263	9.34×10^{-5}	-4.0298
9.6	1.25×10^{-4}	-3.9006	1.28×10^{-4}	-3.8932

Table (C-2): First-order rate constants for the reaction of triester **82**, **83** and **84** with vary concentrations of hydroxylamine, at pH 7.3, 25 °C and ionic strength 1.0 M.

	Triester 82	Triester 83	Triester 84
$[\text{NH}_2\text{OH}] / \text{M}$	$k_{\text{obs}} / \text{s}^{-1}$	$k_{\text{obs}} / \text{s}^{-1}$	$k_{\text{obs}} / \text{s}^{-1}$
0	2.09×10^{-7}	3.03×10^{-7}	2.31×10^{-7}
0.1	6.2×10^{-6}	7.2×10^{-6}	6.65×10^{-6}
0.3	2.06×10^{-5}	2.3×10^{-5}	1.73×10^{-5}
0.5	4.06×10^{-5}	4.17×10^{-5}	2.87×10^{-5}
0.7	4.96×10^{-5}	5.17×10^{-5}	3.73×10^{-5}